

INFORMATION TO USERS

This manuscript has been reproduced from the microfilm master. UMI films the text directly from the original or copy submitted. Thus, some thesis and dissertation copies are in typewriter face, while others may be from any type of computer printer.

The quality of this reproduction is dependent upon the quality of the copy submitted. Broken or indistinct print, colored or poor quality illustrations and photographs, print bleedthrough, substandard margins, and improper alignment can adversely affect reproduction.

In the unlikely event that the author did not send UMI a complete manuscript and there are missing pages, these will be noted. Also, if unauthorized copyright material had to be removed, a note will indicate the deletion.

Oversize materials (e.g., maps, drawings, charts) are reproduced by sectioning the original, beginning at the upper left-hand corner and continuing from left to right in equal sections with small overlaps.

Photographs included in the original manuscript have been reproduced xerographically in this copy. Higher quality 6" x 9" black and white photographic prints are available for any photographs or illustrations appearing in this copy for an additional charge. Contact UMI directly to order.

**ProQuest Information and Learning
300 North Zeeb Road, Ann Arbor, MI 48106-1346 USA
800-521-0600**

UMI[®]

University of Alberta

Apoptosis in Early Heart development

by



William Michael Keyes

A thesis submitted to the Faculty of Graduates Studies and Research in partial fulfillment
of the requirements for the degree of **Doctor of Philosophy**

Department of Physiology

Edmonton, Alberta

Spring 2002



**National Library
of Canada**

**Acquisitions and
Bibliographic Services**

**395 Wellington Street
Ottawa ON K1A 0N4
Canada**

**Bibliothèque nationale
du Canada**

**Acquisitions et
services bibliographiques**

**395, rue Wellington
Ottawa ON K1A 0N4
Canada**

Your file Votre référence

Our file Notre référence

The author has granted a non-exclusive licence allowing the National Library of Canada to reproduce, loan, distribute or sell copies of this thesis in microform, paper or electronic formats.

The author retains ownership of the copyright in this thesis. Neither the thesis nor substantial extracts from it may be printed or otherwise reproduced without the author's permission.

L'auteur a accordé une licence non exclusive permettant à la Bibliothèque nationale du Canada de reproduire, prêter, distribuer ou vendre des copies de cette thèse sous la forme de microfiche/film, de reproduction sur papier ou sur format électronique.

L'auteur conserve la propriété du droit d'auteur qui protège cette thèse. Ni la thèse ni des extraits substantiels de celle-ci ne doivent être imprimés ou autrement reproduits sans son autorisation.

0-612-68589-6

Canada

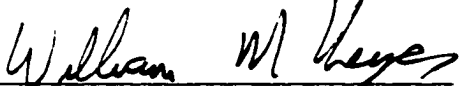
University of Alberta

Library Release Form

Name of Author William Michael Keyes
Title of Thesis Apoptosis in Early Heart Development
Degree Doctor of Philosophy
Year this Degree Granted: 2002

Permission is hereby granted to the University of Alberta Library to reproduce single copies of this thesis and to lend or sell such copies for private, scholarly or scientific research purposes only.

The author reserves all other publication and other rights in association with the copyright in the thesis, and except as herein before provided, neither the thesis nor any substantial portion thereof may be printed or otherwise reproduced in any material form whatever without the author's prior written permission.


William M. Keyes

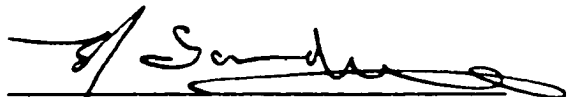
Meelick,
Portlaoise,
Co. Laois,
Ireland

January 29 2002
Date submitted to FGSR

University of Alberta

Faculty of Graduate Studies and Research

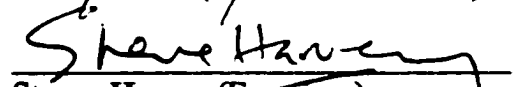
The undersigned certify that they have read, and recommend to the Faculty of Graduate Studies and Research for acceptance, a thesis entitled **Apoptosis in Early Heart Development** submitted by *William Michael Keyes* in partial fulfillment of the requirements for the degree of Doctor of Philosophy


Esmund J. Sanders (Supervisor)


Joy M. Richman (External examiner)


Warren J. Gallin (Committee member)


John J. Greer (Committee member)


Steven Harvey (Examiner)

Jan 29 2002

Date approved by committee

*I'm a dweller on the threshold
And I'm waiting at the door
And I'm standing in the darkness
I don't want to wait no more*

*I have seen without perceiving
I have been another man
Let me pierce the realm of glamour
So I know just what I am*

**“Dweller on the Threshold”
Van Morrison**

Dedicated to the memory of Frances Keyes

Abstract

Heart development involves complex morphogenetic processes that result in the remodeling of a simple tubular structure into the mature four-chambered form. Intrinsic to this process is the proper growth and alignment of the cardiac valves and septa. Deregulation of the normal growth of these structures contributes to the majority of congenital heart defects.

The endocardial cushions are mesenchymal tissue masses that contribute to the mature valves and septa of the adult heart. During the normal development of the endocardial cushions, specific foci of cell death are known to occur. The work presented here focuses on the distribution, regulation and role of cell death in the endocardial cushions. A reassessment of the distribution of dying cells was made using specific techniques for programmed cell death. This was correlated with an assessment of the contribution of cell proliferation and of dying neural crest cells in heart development. Evidence for the involvement of the main regulators and effectors of programmed cell death were examined using immunolabeling techniques and functional studies on primary cell cultures, which show differential distribution and expression patterns suggestive of involvement in apoptosis in the endocardial cushions. Immunostaining and retroviral overexpression studies implicate members of the bone morphogenetic protein (BMP) family as stimulators of apoptosis in the cushions. Attempts were also made at addressing the role of cell death in the cushions via overexpression of anti-apoptotic bcl-2 using retroviral micro-injection and DNA electroporation studies. In summary, these results contribute to the understanding of apoptosis in early heart development, provide evidence for the involvement of the main families of regulators and effectors, implicate members

of the BMP family as stimulators, and provide a basis for future studies to address the developmental significance of endocardial cushion cell death in heart morphogenesis.

Acknowledgements

I would like to thank my supervisor Dr. Esmond Sanders, for giving me the opportunity of coming to Canada for my graduate studies, but also for the guidance and opportunities he has given me during my time in his lab. I would also like to convey a huge thank you to Ewa Parker for her constant help and friendship in the lab over the last number of years.

Dr. Cairine Logan at the University of Calgary, whose lab I had the good fortune of visiting a couple of times, provided much valuable assistance with the retroviral studies. My committee members, Dr. John Greer and Dr. Warren Gallin also deserve my thanks for their help during my time here. Thanks also to Dr. Keith Bagnell, who has always been available to me whenever I asked for help, and Dr. Peter Nguyen, for his support and postdoc advice.

I have the pleasure of thanking many dear friends who made my time here so much more enjoyable, and each is not done justice by mere mention of their names. Karen, Stuart, Gayle and Rob, who made all of this so much better in many ways you do and do not know about – I'm forever indebted. Newton, Jennie and Marc, not only provided me with lots of help in the lab, but a lot of friendship too. Rebecca, for making the worst so much better. And the other graduate students in the department for always being there. Further afield, David and John, thanks for the semi-regular empathy.

But most of all, I owe a huge debt of thanks to my family, a constant source of support throughout all of this. To Siobhan, Kieran and Catriona, thank you so much for everything. To my Dad, also thank you so much for everything you have done for me – I'm forever grateful.

Table of Contents

Chapter 1	Introduction	1
	INTRODUCTION	2
Chapter 2	Literature Review	4
	HEART DEVELOPMENT	5
	Heart Induction	5
	Heart Looping	7
	Heart Septation	10
	ENDOCARDIAL CUSHION GROWTH	14
	Transforming Growth Factor- β family	16
	Valve Development	20
	NEURAL CREST	21
	CONGENITAL HEART DEFECTS	24
	APOPTOSIS	26
	Morphological Features of Apoptosis	26
	Biochemical Features of Apoptosis	27
	APOPTOSIS IN DEVELOPMENT	29
	Apoptosis in Heart Development	32
	MECHANISMS OF APOPTOSIS	34
	Caspase Activation	35
	<i>Caspase activation by cell-surface receptors</i>	36
	<i>Caspase activation by mitochondria</i>	38
	Caspase Activity	39
	Genetic Knockout Studies on Caspases	41
	Apoptosis Regulators: the Bcl-2 Family	42
	<i>Bcl-2 family regulation at the mitochondrial membrane</i>	47
	Genetic Knockout Studies on the Bcl-2 Family	48
	AIMS OF THE RESEARCH	49

Chapter 3	Materials and Methods	50
	EMBRYO DISSECTION AND PREPARATION	51
	IMMUNOCYTOCHEMISTRY	51
	Antibodies	52
	TUNEL LABELING	53
	POLYACRYLAMIDE GEL ELECTROPHORESIS (PAGE) AND WESTERN BLOTTING	55
	Antibodies	56
	PRIMARY CUSHION CELL CULTURE	57
	CUSHION CULTURE IMMUNOCYTOCHEMISTRY	60
	Antibodies	61
	CUSHION CULTURES WITH CASPASE INHIBITORS	61
	CUSHION CULTURES WITH CONDITIONED MEDIUM	62
	DiI LABELING	62
	RETROVIRAL OVEREXPRESSION	63
	Plasmid Amplification and Purification	63
	Chick Embryo Fibroblast Culture	64
	Transfection of Chick Embryo Fibroblasts	65
	Viral Collection and Concentration	65
	CUSHION CULTURES WITH RETROVIRUS	66
	VIRAL MICROINJECTION	67
	ELECTROPORATION	68
Chapter 4	Distribution of Cell Death and Proliferation in the Endocardial Cushions	70
	DISTRIBUTION OF DYING CELLS IN THE DEVELOPING HEART	71
	DISTRIBUTION OF TUNEL POSITIVE CELLS IN THE ENDOCARDIAL CUSHIONS	71

	DISTRIBUTION OF PROLIFERATING CELLS IN THE ENDOCARDIAL CUSHIONS	79
	CELL DEATH LEVELS IN EXPLANT CUSHION CULTURES	81
	EFFECT OF CONDITIONED MEDIUM ON CELL DEATH LEVELS IN CUSHION CULTURES	85
	DII LABELING OF NEURAL CREST CELLS	86
Chapter 5	Regulation of Apoptosis in the Endocardial Cushions	92
	EXPRESSION OF BCL-2 FAMILY MEMBERS IN THE EMBRYONIC HEART	93
	Immunoblot Analysis of Bcl-2 Family Members	93
	Immunocytochemical Localisation of Bcl-2 Family Members	97
	Sub-Cellular Distribution of Bcl-2 Family Members in Cushion Cells	102
	CASPASE EXPRESSION AND ACTIVITY IN THE EMBRYONIC HEART	116
	Immunoblot Analysis of Caspase-9 and the Caspase Substrate PARP	116
	Caspase Inhibitors on Serum-Starved AV Cushion Cultures	119
Chapter 6	Expression and Function of Bone Morphogenetic Proteins in the Endocardial Cushions	121
	EXPRESSION OF BONE MORPHOGENETIC PROTEINS IN THE EMBRYONIC HEART	122
	Immunocytochemical Localisation of Bone Morphogenetic Protein 2	122
	Immunocytochemical Localisation of Bone Morphogenetic Protein 4	126
	RETROVIRAL OVEREXPRESSION OF BONE MORPHOGENETIC PROTEIN RECEPTORS IN CUSHION CULTURES	132

	Overexpression of BMP-Receptors 1A and 1B in Endocardial Endothelial Cells	140
Chapter 7	Bcl-2 Overexpression in the Endocardial Cushions	144
	VIRAL-MEDIATED BCL-2 OVEREXPRESSION	145
	Virus Production and Controls	145
	Viral Bcl-2 Overexpression <i>in vitro</i>	148
	Viral Bcl-2 Overexpression <i>in vivo</i>	150
	DNA OVEREXPRESSION VIA ELECTROPORATION	156
	Bcl-2 and GFP DNA Electroporation	157
	FUTURE APPROACHES: TIMP-2 / TAT STUDIES	161
Chapter 8	Discussion	169
	DISCUSSION	170
	Are members of the bcl-2 family involved in the regulation of apoptosis in the endocardial cushions?	171
	Are members of the caspase family of enzymes involved in apoptosis in the endocardial cushions?	174
	What is the cell type dying in the cushions?	177
	Are similar processes of cell death in effect in both sets of cushions?	179
	Are the dying cells neural crest in origin?	179
	What are the species differences in distribution?	181
	Why is there a more limited distribution of apoptotic cells than initially described?	183
	What is the stimulus for the cells to die?	184
	What is the role of apoptosis in the endocardial cushions?	187
	What are the possible reasons for lack of viral infection?	188
	FUTURE DIRECTIONS	192
	References	194

List of Figures

Chapter 2

Figure 2-1	Schematic diagram of heart formation during the first week of chick embryo development	8
Figure 2-2	Planes of section of the developing heart, showing the location of the endocardial cushions	11
Figure 2-3	Cardiac defects resulting from varying degrees of cardiac neural crest ablation	22
Figure 2-4	Pathways of caspase activation	37
Figure 2-5	Structural classification of the bcl-2 family members	44

Chapter 3

Figure 3-1	Schematic diagram showing site of viral injection	69
Figure 3-2	Schematic diagram showing site of DNA injection for Electroporation	69

Chapter 4

Figure 4-1	TUNEL labeling of apoptotic cells in the ED4 chick outflow tract	72
Figure 4-2	TUNEL labeling of apoptotic cells in the ED5 chick outflow tract	73
Figure 4-3	TUNEL labeling of apoptotic cells in the ED6 atrioventricular cushions	74
Figure 4-4	TUNEL labeling of apoptotic cells in the ED7 atrioventricular cushions	75
Figure 4-5	TUNEL labeling in the embryonic heart	77
Figure 4-6	Quantification of TUNEL positive cells in the endocardial cushions	78
Figure 4-7	Immunocytochemical localisation of proliferating nuclear cell antigen (PCNA) in the endocardial cushions	80
Figure 4-8	Culture of atrioventricular cushion explants	83
Figure 4-9	Levels of apoptosis in AV explant cultures over time, measured by TUNEL and Annexin-V labeling	84
Figure 4-10	Effect of conditioned medium on apoptosis levels in dissociated cushion cultures	87
Figure 4-11	DiI labeling of migratory neural crest cells	90

Figure 4-12	DAPI and DiI labeling in the outflow tract	91
Chapter 5		
Figure 5-1	Bcl-2 expression in dissected AV cushions and outflow tract	94
Figure 5-2	Bax expression in dissected AV cushions and outflow tract	95
Figure 5-3	Bak expression in dissected AV cushions and outflow tract	96
Figure 5-4	Immunocytochemical localisation of bcl-2 in the endocardial cushions	99
Figure 5-5	Immunocytochemical localisation of bax in the endocardial cushions	100
Figure 5-6	Immunocytochemical localisation of bak in the endocardial cushions	101
Figure 5-7	Immunodetection of bax in the ventricle of the embryonic heart	103
Figure 5-8	Examples of immunohistochemistry negative controls	104
Figure 5-9	Confocal image of healthy AV cushion culture stained for endogenous bcl-2	106
Figure 5-10	Confocal image of serum starved AV cushion culture stained for endogenous bcl-2	107
Figure 5-11	Confocal image of serum starved AV cushion culture, with a general caspase inhibitor, stained for endogenous bcl-2	108
Figure 5-12	Confocal image of healthy AV cushion culture stained for endogenous bax	110
Figure 5-13	Confocal image of serum starved AV cushion culture stained for endogenous bax	111
Figure 5-14	Confocal image of serum starved AV cushion culture, with a general caspase inhibitor, stained for endogenous bax	112
Figure 5-15	Immunoblotting with the I-19 bax polyclonal antibody	115
Figure 5-16	Caspase-9 cleavage fragment expression in dissected AV cushions and outflow tract	117
Figure 5-17	Poly (ADP)-ribose polymerase (PARP) cleavage fragment expression in dissected AV cushions and outflow tract	118
Figure 5-18	Effect of caspase inhibitors on the incidence of apoptosis in serum starved AV cushion cultures	120

Chapter 6

Figure 6-1	Immunocytochemical localisation of BMP2 in the ED5-6 chick heart	123
Figure 6-2	Immunocytocheical localization of BMP2 in the ED10.5 mouse heart	124
Figure 6-3	Immunocytochemical localisation of BMP2 in the ED12.5 mouse heart	125
Figure 6-4	Immunocytochemical localisation of BMP4 in the ED5-6 chick heart	127
Figure 6-5	Immunocytochemical localisation of BMP4 in the ED10.5 mouse heart	128
Figure 6-6	Immunocytochemical localisation of BMP4 in the ED12.5 mouse heart	129
Figure 6-7	Dissociated AV cushion cultures overexpressing dominant-negative BMP receptors	133
Figure 6-8	Immunocytochemistry for PCNA on AV cushion cultures, overexpressing constitutively active BMP receptors	134
Figure 6-9	Comparison of TUNEL counts on serum-starved cushion cultures overexpressing BMP receptors	136
Figure 6-10	Uninfected control serum-starved AV cushion cultures	137
Figure 6-11	Serum-starved AV cushion cultures, overexpressing constitutively-active BMP receptor 1A	138
Figure 6-12	Serum-starved AV cushion cultures, overexpressing constitutively-active receptor 1B	139
Figure 6-13	Overexpression of BMP receptors in endocardial endothelial cells	142
Figure 6-14	Effects of BMPR on endocardial cell cultures	143

Chapter 7

Figure 7-1	Immunocytochemical controls on RCASBP(B) transfected chick embryo fibroblasts	146
Figure 7-2	Immunoblotting on chick embryo fibroblasts for human bcl-2	147
Figure 7-3	Retroviral bcl-2 overexpression in dissociated AV endocardial cushion cultures	149
Figure 7-4	Immunocytochemistry for viral coat and human bcl-2 in RCASBP(B)-bcl-2 infected heart	152
Figure 7-5	Immunocytochemistry for viral coat and human bcl-2 in	

	RCASBP(B)-bcl-2 infected heart	154
Figure 7-6	Immunocytochemistry for viral coat and human bcl-2 in RCASBP(B)-bcl-2 infected heart	155
Figure 7-7	Brightfield and fluorescence views of embryonic heart following GFP electroporation	158
Figure 7-8	Examples of green fluorescent protein in the embryonic chick heart following electroporation	160
Figure 7-9	Immunostaining for human bcl-2 following electroporation of RCASBP(B)-bcl-2 into the embryonic chick heart	162
Figure 7-10	Immunostaining for human bcl-2 following electroporation of RCASBP(B)-bcl-2 into the embryonic chick heart	163
Figure 7-11	TIMP-2-TAT-FITC transduces into primary cultures of endocardial cushion cells in a concentration-dependant manner	167
Figure 7-12	Injection of TIMP-2-TAT into the circulation of the chick embryo	168

List of Tables

Table 5-1.	Summary of bcl-2 and bax sub-cellular distribution in healthy, serum-starved and apoptotic cushions in culture	114
Table 6-1	Summary of the distribution pattern for BMP2 and BMP4 immunocytochemistry in the chick and mouse heart	131
Table 7-1	Summary of electroporation experiments, for RCASBP(B)-gfp and RCASBP(B)-bcl-2.	164

List of Abbreviations

$\Delta\psi_m$	change in permeability transition
aa	aortic arches
ADP/dADP	adenosine diphosphate / deoxy-adenosine diphosphate
AEC	3-amino-9-ethylcarbazole
ANOVA	analysis of variance
ANT	adenine nucleotide translocator
ANT	adenine nucleotide translocator
ANZ/PNZ	anterior / posterior necrotic zone
AP	anterior / posterior
apaf	apoptotic protease activating factor
APS	aorticopulmonary septum
ATP/dATP	adenosine triphosphate / deoxy-adenosine triphosphate
AV	atrioventricular
AVC	atrioventricular cushions
BH	bcl-2 homology
BMP	bone morphogenetic protein
BMPR	bone morphogenetic protein receptor
bp	base pairs
BSA	bovine serum albumin
CAD/DFF	caspase activated deoxyribonuclease / DNA fragmentation factor
CARD	caspase recruitment domain
CEF	chick embryo fibroblasts
CFLIP	cellular Fas-associated death domain-like IL-1-converting enzyme-inhibitory protein
CMF	calcium/magnesium free
COTC	conal outflow tract cushions
CS	chick serum
DAPI	diamidino-phenylindole
DD	death domain

DDW	double distilled water
DED	death effector domain
DiI	1,1 -dioctadecyl-3,3,3 ,3 -tetramethylindocarbocyanine perchlorate
DISC	death inducing signaling complex
DMSO	dimethyl sulfoxide
DNA	deoxyribonucleic acid
DNA'se	deoxyribonucleic acidase
DR	death receptor
dUTP	deoxy-uridine triphosphate
ECL	enhanced chemiluminescence
ED	embryonic day
EDTA	ethylenediamine-tetraacetic acid
EMT	epithelial-mesenchymal transformation
ER	endoplasmic reticulum
ES	EDTA soluble
FADD	Fas-associated protein with death domain
FBS	foetal bovine serum
FGF	fibroblast growth factor
FITC	fluorescein isothiocyanate
GFP	green fluorescent protein
HH	Hamburger and Hamilton stage
IAS	interatrial septum
ICAD/DFP45	inhibitor of CAD / DNA fragmentation factor-45
Ig	immunoglobulin
INZ	interdigital necrotic zone
IVS	interventricular septum
kbp	kilo base pairs
kDa	kilo Daltons
LB	Lurian and Burrous
MMP	matrix metalloproteinase
mRNA	messenger ribonucleic acid

NC	neural crest
NCAM	neural cell adhesion molecule
NGF	nerve growth factor
OT	outflow tract
OTC	outflow tract cushions
P0-P1	passage zero-passage one
PAGE	polyacrylamide gel electrophoresis
PARP	poly(ADP-ribose) polymerase
PBS	phosphate buffered saline
PCD	programmed cell death
PCNA	proliferating cell nuclear antigen
PFA	paraformaldehyde
PMSF	phenylmethanesulphonyl fluoride
PTS	phosphatidylserine
PS	primitive streak
PT	permeability transition
PTA	persistent truncus arteriosus
RAIDD	RIP-associated ICH-1/CED-3-homologous protein with a death domain
RCASBP(B)	replication-competent, <u>A</u> LV LTR, <u>s</u> plice acceptor, <u>B</u> ryan-RSV <i>pol</i> , envelope subgroup <u>B</u>
rpm	revolutions per minute
RV/LV	right ventricle / left ventricle
SREBP's	sterol regulatory binding proteins
SSC	saline sodium citrate
TBS	tris-buffered saline
TdT	terminal deoxynucleotide transferase
TGFβ	transforming growth factor beta
TIMP	tissue inhibitor of matrix metalloproteinase
TNF	tumour necrosis factor
TNFR	tumour necrosis factor receptor
TRADD	TNF-receptor associated death domain

TRAIL	TNF-related apoptosis-inducing ligand
TRAMP	TNF-related apoptosis-mediating protein
TTBS	TBS with tween
TUNEL	terminal deoxynucleotide transferase mediated dUTP-biotin nick-end labeling
Tween	polyoxyethylenesorbitan monolaurate
VDAC	voltage dependent anion channel
VT	ventricular trabeculae

Chapter 1
INTRODUCTION

INTRODUCTION

The heart is the first functional organ to develop in the vertebrate embryo. Beginning with the induction and clustering of cardiogenic cells, the heart initially forms as a primitive tubular structure that undergoes complex remodeling to achieve the mature shape. Externally, the heart undergoes looping and fusion processes that bring the different regions of the heart into correct alignment. Internally, the remodeling process involves the development of the valves and septa that divide the primitive structure into the four-chambered organ capable of maintaining two independent circulatory systems.

Congenital heart defects are among the most common birth defects in humans, occurring in almost one percent of live births, ten percent of stillbirths, and possibly up to twenty percent of spontaneous abortions (Ya *et al*, 1997). The majority of congenital heart defects involve abnormal development of the valves and septa of the heart. During development, mesenchymal tissue masses, called endocardial cushions form the main contribution to the valves and septa, arising by the process of an epithelial to mesenchymal transformation from the inner endocardium, under the influence of the outer myocardium. Cell death has been shown to be an intrinsic part of the normal development of the endocardial cushions.

Programmed cell death, or apoptosis, is a distinct mode of cell death, characterized by specific morphological and biochemical features, that results in the demise of the cell without the incurrence of an immune response. This type of cell death is known to be involved in many developmental and physiological processes, with deregulation of this process implicated in many diseases. The regulation of apoptosis involves intricate signaling systems, with a number of different regulators involved. The main family of regulators of the apoptotic pathway is the bcl-2 family of molecules,

which act in an either pro- or anti-apoptotic manner, to influence downstream signaling mechanisms. The apoptotic pathway results in the activation of a downstream family of cysteine protease enzymes called caspases. These enzymes, when activated, cleave distinct sub-cellular targets that result in the organized destruction of the cell.

The work of Pexieder (1975) has stood as an authority on programmed cell death in the developing heart. Previously, cell death has been shown to have a widespread distribution throughout the early remodeling stages, in a number of species, with the highest incidence occurring in the endocardial cushions. The recent surge of interest in apoptosis has led to the development of a number of techniques specific for this mode of cell death, and a better understanding of the mechanisms involved.

The objective of the work presented here was to provide a better understanding of the significance of cell death in the developing heart. A reassessment of the distribution of cell death in early heart development was made using techniques specific for apoptosis. Attempts were made to understand the regulatory processes involved in this cell death, concentrating on the expression and distribution of members of the bcl-2 family of regulators and the caspase family of enzymes, using *in vivo* and *in vitro* studies. The involvement of the bone morphogenetic family of growth factors as stimulators of apoptosis was also investigated, by overexpression of BMP receptors. Finally, attempts were made to disrupt the normal patterns of cell death, to investigate the roles played by this process in cushion morphogenesis. An understanding of the normal occurrence and regulation of cell death in the endocardial cushions is essential to the understanding of heart development, and will hopefully contribute to a better understanding of the underlying causes of congenital heart defects.

Chapter 2
LITERATURE REVIEW

HEART DEVELOPMENT

The heart is the first functional organ to develop during embryogenesis (Romanoff, 1960; Olson and Srivastava, 1996). It undergoes a complex series of morphogenetic changes in attaining the adult structure with four chambers, capable of maintaining two circulatory systems. Heart formation begins with induction and clustering of cardiogenic cells, forming a heart tube, which is remodeled by looping and septation to achieve the adult structure with two atria and two ventricles, inflow veins and outflow arteries.

Heart Induction

In chick development, prior to Hamburger and Hamilton (HH) stage 3, pre-cardiac cells are found in the area of the epiblast, lateral to the midportion of the primitive streak (PS; Rosenquist and DeHaan, 1966). During gastrulation, as they involute through the PS, the prospective mesodermal cells become committed to become prospective myocardial cells, under the influence of signals, such as bone morphogenetic protein (BMP)-2, from the anterior endoderm (Schultheiss *et al*, 1995; Fishman and Chien, 1997; Schultheiss and Lassar, 1997). However, some reports suggest that even prior to gastrulation, a hypoblast-derived signal, such as activin may induce cardiac myogenesis (Yatskievych *et al*, 1997). The cardiac precursors are found in a broad zone of the PS, but are absent from the most anterior and posterior regions. At the 3-4 somite stage (HH stage 6), the pre-cardiac cells condense in bi-lateral areas of splanchnic mesoderm in the anterior embryonic pole; an area known as the heart-field (Schultheiss *et al*, 1995; Fishman and Chien, 1997). This region is defined by the expression of the

earliest known marker of cardiogenic lineage, *nkx-2.5* (Lints *et al*, 1993; Ehrman and Yutzey, 1999), a homeobox gene homologous to the *Drosophila tinman* gene which is necessary for cardiac specification. However, recent findings have suggested the presence of an extra anterior heart-forming field of mesoderm, anterior to the initial heart tube, which contributes to the development of the outflow region of the heart (Mjaadvedt *et al*, 2001).

During formation of the head fold and anterior intestinal portal, the cardiac precursors are brought together passively by the movements of the developing foregut. The cardiac precursors, consisting of premyocardial cells and presumptive endocardial cells, then fuse in the embryonic midline, under the foregut, and form the primitive tubular heart by HH stage 10 (Icardo, 1996; Schultheiss and Lassar, 1999). An essential role in heart tube formation has been shown for the GATA family of transcription factors, with GATA4-deficient embryos failing to form a functioning heart tube (Kuo *et al*, 1997; Molkenin *et al*, 1997). The simple tubular heart consists of two epithelial layers: the inner endocardium and the outer myocardium which together consist of three cell types: endocardial endothelia, ventricular myocytes and atrial myocytes (Mikawa, 1999). The area between the double layers of the tubular heart is occupied by an acellular extracellular matrix, called the cardiac jelly. Although it appears transparent under the light microscope, it is a complex basement membrane, consisting of many different molecules, including, various glycosaminoglycans, collagen type I and IV, tenascin and fibronectin (Hurle *et al*, 1980; Little *et al*, 1989). Initially it was thought that the cardiac jelly contributed to cardiac looping through its ability to create an internal osmotic pressure (Nakamura and Manasek, 1981), but looping is now known to involve an axial

signaling system, that includes the morphogens Sonic hedgehog and Nodal, a transforming growth factor-beta (TGF β) family member (Levin *et al*, 1995). The looping of the heart, with the cardiac jelly lining the heart also functions to maintain an anterograde blood flow, prior to valve formation.

Heart Looping

As fusion of the primitive tubular heart continues in a caudal direction, the heart tube bulges to the right in a loop around HH stage 10, initially bringing the tubular heart into U-shaped tube (Majumder and Overbeek, 1999). By the end of looping stage, the different regions of the heart can be clearly recognized (Figure 2-1). Blood flows in series through the venous inflow and the sinus venosus, into the primitive single chambered atrium. The through a constriction of the atrioventricular (AV) canal between the atrium and primitive left ventricle. Then into the presumptive right ventricle, and to the outflow tract of the heart, which is composed of a proximal conal region and a distal truncal region. Blood flow then continues from the outflow tract, to the aortic sac and aortic arches, before reaching the dorsal aorta (Romanoff, 1960). This process of looping is necessary to bring the primary segments of the heart tube, which are in a linear array, into proper alignment (Majumder and Overbeek, 1999). The conal septum is repositioned to overlie the future left and right ventricles, and the AV canal is aligned with the primitive right ventricle. This process also brings the inlet and outlet regions of the heart together, developing the inner curvature of the U-shaped heart (Mjaatvedt *et al*, 1999; Manner, 2000).

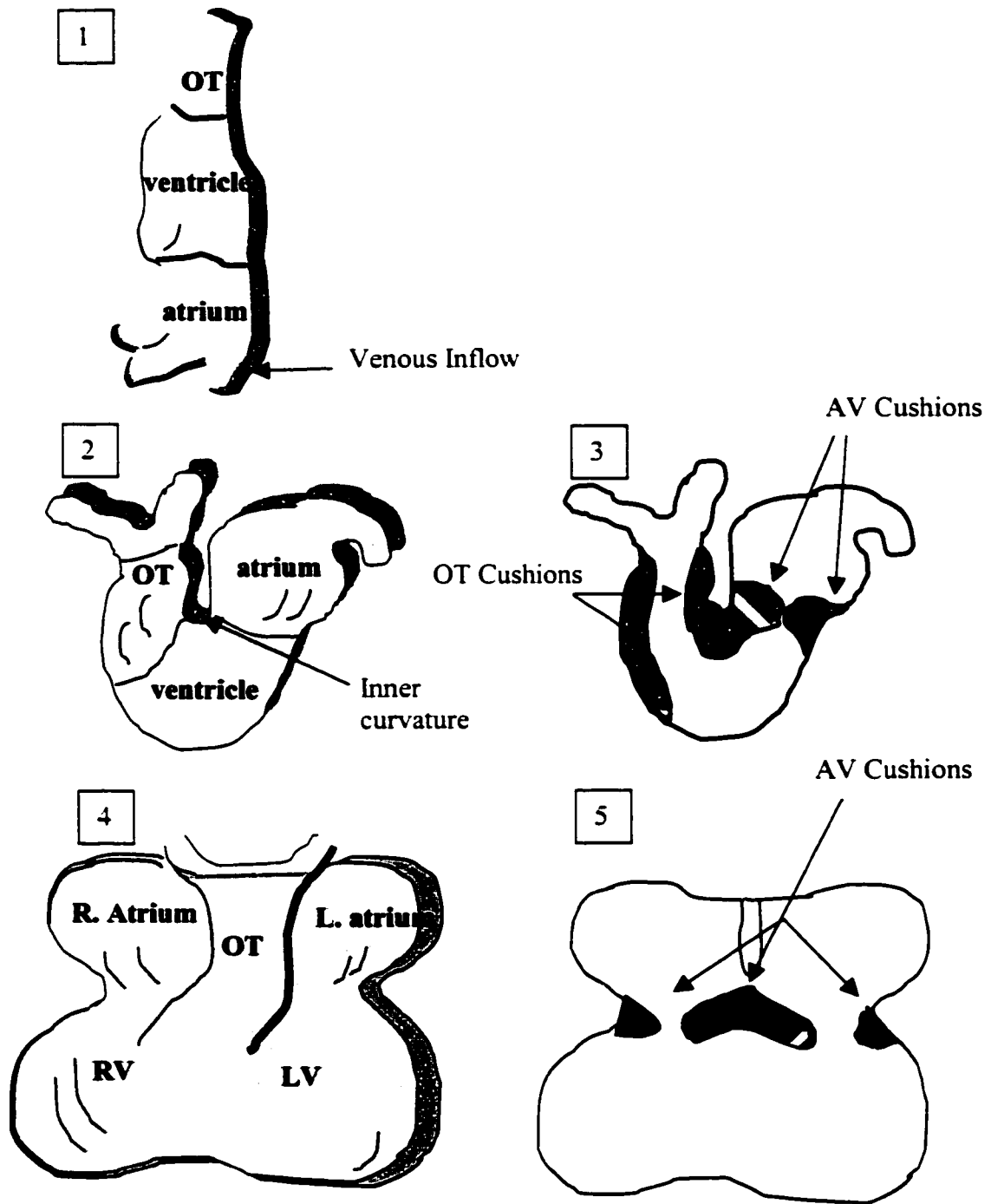


Figure 2-1. Schematic diagram of lateral views of heart formation during the first week of chick embryo development. 1. The primitive heart develops initially as a tubular structure, with slight demarcation of the regions. 2. The heart tube undergoes looping in the rightward direction at HH 10, bringing the different regions into correct alignment. 3. The sectional image shows the location of the OT and AV cushions during looping. 4. The U-shaped tube rotates such that the OT and the venous inflow regions come together, and the right and left chambers are formed. RV, right ventricle; LV, left ventricle 5. The sectional diagrams show the internal location of the central and lateral AVendocardial cushions.

Although the regions of the heart are not morphologically distinguishable until after looping, they are genetically programmed from a much earlier stage. Each chamber possesses different contractile properties and patterns of gene expression (Christoffels *et al*, 2000; Srivastava and Olson, 2000). Chamber-specific isoforms of the myosin light and heavy chain genes show restricted expression in the ventricles and atria prior to chamber demarcation, and are specified before looping (Yutzey and Bader, 1995). The future right and left ventricles in the mouse, have restricted expression of the basic helix-loop-helix (bHLH) transcription factors dHAND and eHAND respectively (Srivastava *et al*, 1997), and a ventricle-specific homeobox gene *irx4* can activate ventricle-specific gene expression (Bao *et al*, 1999). The MEF-2 family of transcription factors has also been shown to be necessary for chamber formation, with null-mutations displaying weak atrial contractions and no future right ventricle (Lin *et al*, 1997). In the atrio-ventricular (AV) and OT regions, there is restricted expression of members of the TGF β family, including TGF β -1 and -2, and bone morphogenetic protein-4 (BMP4) (Eisenberg and Markwald, 1995). In the endocardium and mesenchyme of the AV and OT endocardial cushions, there is restricted expression of the homeobox genes *msx-1*, *msx-2* and *mox-1* (Eisenberg and Markwald, 1995). The T-box family of transcription factors (*Tbx*) (Bollag *et al*, 1994) has also been shown to be involved in heart development. *Tbx-2*, -3 and -5 have all been shown to be present during different times of chick cardiac development (Yamada *et al*, 2000), and are suggested to lie downstream of BMP signaling. The *Tbx-5* gene displays asymmetric expression during heart looping (Bruneau *et al*, 1999) and has been implicated as one of the main factors in Holt-Oram syndrome, a developmental disease

with many heart defects (Li *et al*, 1997). Knockout mice lacking *Tbx5* also display cardiac defects characteristic of Holt-Oram syndrome (Bruneau *et al*, 2001).

Heart Septation (Figure 2-2)

After looping the heart undergoes a series of profound changes that remodels the simple tubular structure into the four-chambered organ. Internally, the single atrium and single ventricle are divided into their left and right sides by the growth of septa. The AV canal and the OT are divided by lateral outgrowth of proliferations of cells called endocardial cushions, which respectively separate the atrium from the ventricle and divide the single OT into two vessels. The septa and endocardial cushions meet internally, dividing the heart into four chambers. Externally, the inner curvature of the looped heart is removed and incorporated into the heart, with the result that the posterior wall of the OT and the anterior wall of the AV canal share a common wall (Webb *et al*, 1998; Mjaatvedt *et al*, 1999)

The atrial septum forms from two different septa. The septum primum grows downward from the roof of the atrium, towards the developing AV cushions (Figure 2-2a). The opening between the two outgrowths is known as the foramen primum, before the septum meets and fuses with the cushions (Hay *et al*, 1984). However, a second opening, the foramen secundum develops cranially in the septum primum, to allow blood to pass from the right to the left atrium. To the right of this, a second septum develops as a myocardial flap that prevents back flow of blood, by closing over the foramen secundum. This structure differs slightly in the chick embryo compared to the

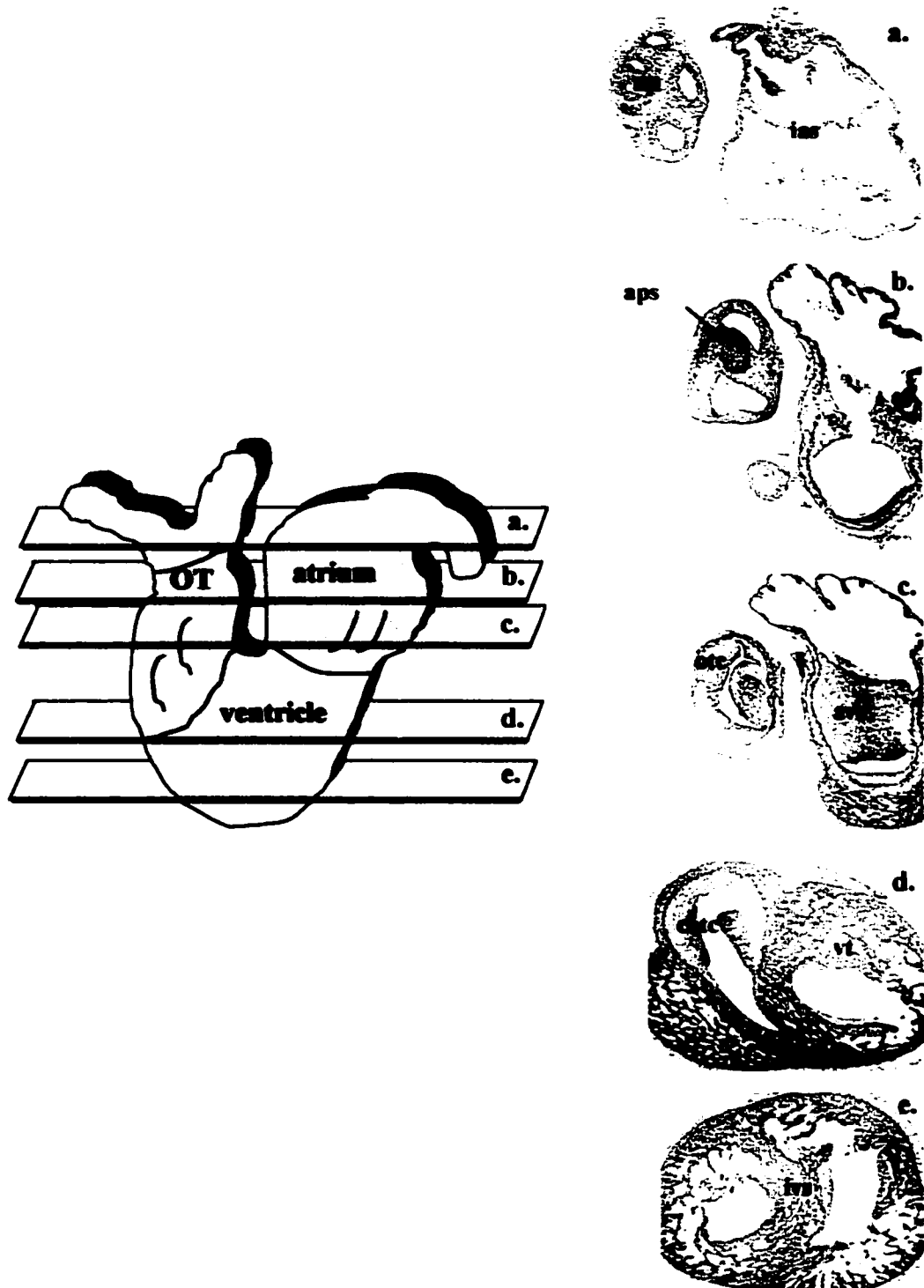


Figure 2-2. Planes of section of the developing heart, HH 27, showing the location of the endocardial cushions. Figures a-e show different levels through the developing heart, as seen in the cartoon on the left. (a) The interatrial septum (ias) is seen to separate the single atrium into its left and right sides, while the aortic arches (aa) are at the distal outlet end. (b) The condensed mesenchyme of the aorticopulmonary septum (aps) is seen to separate the outflow tract (ot). (c) The proliferations of outflow tract and atrioventricular cushions (otc; avc) are clearly seen. (d) The conal OT cushions (cotc) are seen to continue to the level of ventricular trabeculae (vt). (e) The interventricular septum (ivs) separates the left and right chambers of the ventricle.

mammalian heart, with only a single septum forming, that develops fenestrations throughout, to allow blood to flow through (Romanoff, 1960; Hay *et al*, 1984).

After looping, the single ventricle is divided into its left and right components, while developing a sponge-like trabecular appearance (Figure 2-2d). The trabeculae develop only in the ventricle, as ingrowths of the endocardium into the cardiac jelly, concurrently with increased proliferation in the compact myocardium, which gives the characteristic appearance of large intercellular spaces between the myocytes (Icardo and Fernandez-Teran, 1987; Sedmera *et al*, 1997). The trabeculae function to allow oxygenated blood to diffuse through to the inner layers, a function that will be replaced with the development of the coronary vasculature, as well as functioning as contractile elements in the beating heart (Sedmera *et al*, 1997). The single primitive ventricle is divided into its left and right components by the growth and apposition of trabeculae, toward the developing AV cushions, forming the interventricular septum (IVS) (Figure 2-2e), and with the concomitant increase in size of the left and right chambers (Hay *et al*, 1984; Leatherbury and Waldo, 1995). The posterior horn of the IVS makes contact with the right side of the developing dorsal AV cushion, which is necessary for correct alignment of the left ventricle with the aorta (Icardo, 1996). The anterior horn remains separated until a later stage when it will fuse with the AV cushions.

The AV canal is divided by two outgrowths of endocardial cushions, which separate the single cavity into its left and right sides (Figure 2-2c). These initially grow from either side, forming the dorsal and ventral AV cushions (Hay and Low, 1972; de la Cruz *et al*, 1983), which grow, meet and fuse in the middle of the AV canal, forming the central mass of cushion tissue (Los and van Eijndthoven, 1973). The cushions also grow

to line the adjacent myocardial layer, forming the lateral aspects of the cushions (Webb *et al.*, 1998). Both the central mass and lateral cushions initially serve to separate the bloodflow into the two developing ventricular chambers, but will also contribute to the leaflets of the mitral and tricuspid valves (Wessels *et al.*, 1995).

The outflow tract, or conotruncus, which at this stage appears as a single tube abutting the rest of the heart, is divided into two sections; the proximal region is known as the conus, or conal region, and the distal section, the truncal region (Bartelings and Gittenberger-de Groot, 1989). The OT is divided internally by the development of two spiraling masses of endocardial cushion tissue, called the conotruncal ridges, or the OT cushions (Figure 2-2c). The cushions meet in the middle of the OT and fuse, separating the single tube into the precursors of the aorta and pulmonary artery of the adult heart. The distal truncal cushions are fused by the downward movement of a condensed spur of mesenchymal tissue, known as the aortico-pulmonary septum (APS; Figure 2-2b). This is a neural crest-derived structure, that projects downward in two prongs into the truncal cushions (Kirby *et al.*, 1983). As the condensed mesenchyme of the APS moves downward to the level of the semilunar valves, it fuses the truncal cushions together in the middle, forming the truncal septum. Continued fusion of the truncal cushions brings the conal cushions together, which subsequently fuse, forming the conal septum (Bartelings and Gittenberger-de Groot, 1989). The fused conal cushions meet at the top of the ventricular foramen, and continued growth brings the fused conal septum to the top of the IVS, effectively separating the left and right ventricles with the aorta and pulmonary artery respectively. The conal region becomes incorporated into the ventricles,

while the truncal regions contribute to the main arteries (Hay *et al*, 1984; Bartelings and Gittenberger-de Groot, 1989).

Effectively, the development of the interatrial and interventricular septa, and the concurrent development of the AV and OT cushions divides the primitive heart form into a four chambered structure, being completed by approximately HH 34. Correct alignment and fusion of these structures is crucial to normal heart development, with the majority of congenital heart defects arising from impaired alignment.

ENDOCARDIAL CUSHION GROWTH

Along the AP axis of the developing heart tube, restricted swellings of the cardiac jelly develop in the AV and OT regions. The cardiac jelly is rich in hyaluronic acid and glycosaminoglycans, enabling it to become a highly hydrated matrix, and swell. In the AV canal, these swellings are restricted to the dorsal and ventral sides. Following the swelling, the areas are invaded by mesenchymal cells, beginning at approximately HH stage 16-17. The cells differentiate into the endocardial cushion cells. The cushion cells arise by the process of epithelial-mesenchymal transformation (EMT) from the inner layer of the heart tube, the endocardium (Bolender and Markwald, 1979; Fitzharris, 1981; Markwald *et al* 1996).

Much of the information on the biology of endocardial cushion growth has come from the use of an *in vitro* culture model. In culture, the transformation of endothelium to mesenchyme can be replicated in a 3-dimensional collagen gel (Bernanke and Markwald, 1982). Tissue explants from the AV and OT regions of the heart are placed on a gel prior to the stage of *in vivo* transformation. The endothelial cells transform and migrate along

the top, and into, the collagen gel. However, the EMT only occurs in tissue from the AV and OT regions and only in endocardial tissue from these areas that has the myocardium still attached. Ventricular myocardium will not undergo a similar transformation (Runyan and Markwald, 1983). This is similar to the events *in vivo*, in that only cushion tissue will develop in the AV and OT regions, but not in the ventricle, and the presence of the adjacent myocardium is necessary for transformation to occur.

Prior to cushion formation *in vivo*, particulates of 0.1 to 0.5 μ m in diameter have been shown to accumulate in the cardiac jelly of the AV and OT regions. These complexes have been called adherons (Markwald *et al*, 1990). They have been shown to be released by the myocardium and their components are known as ES (EDTA soluble) antigens, which include fibronectin, transferrin and a novel protein termed ES/130 (Eisenberg and Markwald, 1995). Isolated adherons have been shown to induce EMT in culture explants of both the AV and OT endothelium (Krug *et al*, 1985).

The activated endocardial cells undergo a number of characteristic changes, including, endothelial hypertrophy, loss of cell-cell contacts, lateral mobility, formation of migratory appendages, an increased expression of ECM molecules and invasion into the cardiac jelly (Markwald *et al*, 1977; Krug *et al* 1985; Boyer *et al*, 1999).

During EMT, there are changes in the cell-cell and cell-substrate adhesion of the endothelial cells. The expression of the cell-adhesion molecule N-CAM (neural cell adhesion molecule) ceases at the onset of EMT (Crossin and Hoffman, 1991). At present, there are no specific markers of transformed cushion mesenchyme. One cushion specific antigen, JB3 (Wunsch *et al*, 1994) has since been shown to be the extracellular matrix molecule fibrillin-2 (Rongish *et al*, 1998). Several ECM molecules have been shown to be

associated with the EMT of the endocardial cells in cushion formation, including laminin, fibronectin, vitronectin, fibulin-1 and fibulin-2 (Loeber and Runyan, 1990; Spence et al, 1992; Zhang et al, 1995; Tsuda *et al*, 2001), and the homeodomain transcription factor *msx-1* has also been shown to be associated with the transforming endothelial and mesenchymal cells (Chan-Thomas *et al*, 1993).

Transforming Growth Factor- β family

The regulatory factors involved in the process of cushion formation is an area of much investigation, with numerous studies indicating that the TGF β family of signaling molecules is involved in the EMT. During mouse cardiogenesis, TGF β 1 mRNA is seen in the endocardial layer of the heart tube, but becomes restricted to AV and OT endothelial cells that undergo EMT, with expression continuing in the endothelia of the heart valves (Akhurst *et al*, 1990). During cushion tissue formation, TGF β 2 is regionally restricted to the AV and OT myocardium, and TGF β 3 is not seen until the cushion tissue has formed (Milan *et al*, 1991; Dickson *et al*, 1993). In the chick, TGF β 2 mRNA is expressed in the endocardium and myocardium prior to and after EMT (Boyer *et al*, 1999). Also in the chick, TGF β 3 mRNA has been shown to be expressed in the endocardium and myocardium in the AV and OT regions at the onset of EMT, and in the cushion mesenchyme during migration (Nakajima *et al*, 1998; Yamagishi *et al*, 1999a). Using the cushion culture model, it has been shown that neutralizing antibodies to TGF β 2 and β 3 inhibit mesenchymal formation (Ramsdell and Markwald, 1997; Boyer *et al*, 1999), while TGF β 2 and β 3 protein can initiate changes characteristic of EMT in chick endocardial cultures (Nakajima *et al*, 1998; Boyer *et al*, 1999). Antisense oligonucleotides to TGF β 3

have been shown to inhibit EMT in the cushion culture model (Potts *et al*, 1991). Thus, there appear to be many similarities and some minor differences in TGF β expression patterns between the chick and mouse heart development (Akhurst *et al*, 1994; Yamagishi *et al*, 1999a), with TGF β 1 and 2 mRNA being predominant in the mouse heart, and TGF β 2 and 3 in the chick (Boyer *et al*, 1999).

One member of the TGF β superfamily of growth factors is the bone morphogenetic subfamily of dimeric peptides. Over 20 different BMP's have been identified in many species (Hogan, 1996). BMP's are expressed at many sites during embryogenesis, and often at sites of EMT (Zhang and Bradley, 1996; Nakajima *et al*, 2000). BMP's may also exhibit differences in expression patterns between the chick and mouse embryos (Dudley and Robertson, 1997; Abdelwahid *et al*, 2001b). Bone morphogenetic proteins are involved at many stages of heart development. They play a role in the induction stages in cardiac myogenesis (Schultheiss *et al*, 1997), and at later stages, there is evidence that they also play roles in endocardial cushion development (Nakajima *et al*, 2000), with most studies investigating mRNA expression.

During mouse cardiogenesis, BMP 2 mRNA is expressed in the myocardium of the AV and OT regions prior to and during endocardial cushion development (Lyons *et al*, 1990; Jones *et al*, 1991). Recent evidence suggests that BMP2 transcripts are also present in the mouse AV endocardial cushions, increasing in level with the differentiation of the cushions (Abdelwahid *et al*, 2001b). The message for BMP6 is expressed in the mesenchymal cushion tissue (Jones *et al*, 1991), while BMP3, -5 and -7 are all also expressed in the heart (Dudley and Robertson, 1997; Nakajima *et al*, 2000). In the chick, BMP2 mRNA has been shown in the myocardium adjacent to the cushion regions during

EMT, but with no observed expression in the endocardial cushion tissues (Yamagishi *et al.*, 1999b). In the rat, BMP2 mRNA expression has also been shown in the AV region (Ikeda *et al.*, 1996). Functionally, BMP2 has been shown to act synergistically with TGF β 3 during EMT in the chick heart (Yamagishi *et al.*, 1998; 1999b) and has been suggested that BMP2 is one of the myocardially derived inductive signals for initiation of EMT (Nakajima *et al.*, 2000), in combination with other signals.

The transcript for BMP4 has been detected in the myocardium of the AV and OT regions in the mouse heart (Jones *et al.*, 1991), and in the atrium of the rat heart (Ikeda *et al.*, 1996). Recent evidence also shows evidence of BMP4 message in the AV and OT cushions of the mouse heart (Abdelwahid *et al.*, 2001b). Both BMP6 and BMP7 are expressed in the embryonic mouse heart, including the endocardial cushions, with double mutant BMP6; BMP7 mice exhibiting cardiac defects (Kim *et al.*, 2001), while BMP10 has restricted expression to the developing heart (Neuhaus *et al.*, 1999).

Bone morphogenetic proteins, along with the TGF β family in general, exert their signalling effects through cell-surface receptors with serine/threonine kinase activity, which in turn phosphorylate members of a downstream family of intracellular proteins called Smads (Massague, 1996). The BMP ligand binds to a type II receptor, which activates one of three type I receptors, BMPR-1A, BMPR-1B or ActR-1 (Hogan, 1996; Massague and Weis-Garcia, 1996). To date, there has been little work on the expression or activity of the BMP receptors in the developing heart, but there is known expression of Smads 2,3,4 and 5 in the atrial and ventricular myocardium, and Smad 6 in the atrium (Flanders *et al.*, 2001), with the Smad 6 knockout mouse displaying cardiac defects, in the AV and OT regions (Galvin *et al.*, 2000). The distribution of the receptor subtypes in

heart development is unknown, but it is now known that there are redundant functions between receptor subtypes (Yi *et al*, 2000). During cartilage formation and differentiation, there is evidence that BMPR-1A may regulate chondrocyte differentiation (Zou *et al*, 1997). Whereas BMPR-1B had previously been implicated in the regulation of apoptosis of chondrocytes in the developing limb (Zou *et al*, 1997; Zhang *et al*, 2000), knockout mice for the BMPR1B receptor show an essential role for this receptor in proliferation of prechondrogenic cells of the limb (Yi *et al*, 2000), with the absence of signaling through this receptor resulting in increased apoptosis of the prechondrogenic mesenchyme only at later stages of limb development (Baur *et al*, 2000).

Knowledge of the BMP receptors function has been greatly aided by the development of retroviral vectors encoding constitutively-active (CA) or dominant-negative (DN) receptor variants (Varley *et al*, 1997). Infection of cells with one of these receptors respectively results in constitutive activation of the receptor signaling pathway, or inhibition of the endogenous signaling pathway, enabling assessment of phenotypic effects of the signaling pathways on the cell in the presence (DA) or absence (CA) of the protein.

Bone morphogenetic proteins have been shown to induce apoptosis in a number of cell types. Although the exact pathways are not completely understood, some interactions are becoming evident. Bone morphogenetic protein 4 has been shown to induce apoptosis and the expression of the transcription factor *Msx-2* and the cyclin-dependent kinase inhibitor p21, simultaneously with apoptosis in sympathetic neurons (Gomes and Kessler, 2001). Bone morphogenetic protein 2 has been shown to increase the expression of the anti-apoptotic Bcl-X_L, and the activity of caspases-3, -6, -7 and -9

(Hay *et al*, 2001; Izumi *et al*, 2001) through both Smad-dependent and -independent pathways. Bone morphogenetic protein 2 also has been shown to induce apoptosis through activation of TGF β -activated kinase and subsequent phosphorylation of p38 stress activated protein kinase (Kimura *et al*, 2000).

Valve Development

The endocardial cushions of the heart function initially to separate the bloodflow in the AV canal and in the OT. However, they also provide the framework for the valves and septa of the mature heart. The AV cushions contribute to the mitral and tricuspid valves (sometimes called the AV-valves) (Chin *et al*, 1992), as well as the IVS. The OT cushions ultimately contribute to the semilunar valves of the pulmonary artery and aorta, as well as the muscular outlet septum separating the pulmonary artery and the aorta, and in part to the IVS. Proper development and alignment of the endocardial cushions is critical for normal septation of the heart. Less is known about the later stages of endocardial cushion development, than is known about their formation. In the mature heart, the valves and septa are composed of myocytes and fibrous connective tissue, that have replaced the cushion mesenchyme . It is known that a number of steps are involved in this process. The cushion mesenchyme has been shown to differentiate into the fibrous connective tissue of the valves and septa (Lamers *et al*, 1995). However, the cushion mesenchyme is also invaded by myocardial cells from the adjacent myocardium, in a process called myocardialization, which occurs in the OT between HH stages 28-38 (van den Hoff *et al*, 1999), and is probably under the control of the cushion mesenchyme. Conditioned medium from the non-myocardial cushion regions was shown to promote

myocyte migration using a culture model (van den Hoff *et al*, 1999). It has been suggested that the endocardial cushion and myocardial cells contribute equally to valve formation, at least in the mitral and tricuspid valves, as to the membranous atrioventricular and ventricular septa (Lamers *et al*, 1995; Wessels *et al*, 1996). The transcription factor NF-ATc has been shown to be essential for cardiac valve formation, with null mutants lacking the semilunar valves of the OT, resulting in the embryos dying *in utero* (de la Pompa *et al*, 1998; Ranger *et al*, 1998)

NEURAL CREST

The heart receives a number of populations of extracardiac cells, including the epicardial cells, which ultimately contribute to the coronary vasculature, and neural crest cells, which contribute to the septation of the heart and to the cardiac ganglia (Kirby, 1999; Jiang *et al*, 2000). The neural crest is a population of cells that arises in the dorsal region of the neural tube, forming at all axial levels of the embryo. Neural crest cells contribute to a variety of ectodermal and mesodermal cell types, including cells of the sympathetic and parasympathetic nervous systems, the adrenergic cells of the adrenal medulla, melanocytes, skeletal and connective tissue components of the head and the aortic arches and OT of the heart. The neural crest can be divided into four main domains; the cephalic, the trunk, the vagal/sacral, and the cardiac neural crest. The fate of some individual neural crest cells is determined prior to migration from the neural tube, while that of others depends on their final site of migration (Kirby, 1999). However, when the cardiac population of neural crest cells is replaced with other crest-derived

cells, heart defects are seen, suggesting that cardiac neural crest cells are committed prior to migration (Kirby, 1989).

The cardiac neural crest cells, emanating from the hindbrain region at the level of rhombomeres 6, 7 and 8 (midotic placode to somite 3), migrate to the three caudal pharyngeal arches (Kirby, 1997). The aortic arches develop in the pharyngeal arch region, and the cardiac population of neural crest cells supports their development and maintenance, along with development of the thymus and parathyroid glands derived from this region (Kirby and Waldo, 1995). The derivatives of aortic arches 3, 4 and 6 are the arch of the aorta, the common carotid and subclavian arteries and the ductus arteriosus, with the neural crest-derived cells ultimately contributing to the smooth muscle cells of the tunica media of these arteries (Le Lievre and Le Dourain, 1975; Kirby and Waldo, 1990). A sub-population of neural crest cells continues its migration from the pharyngeal arches into the outflow tract of the heart, forming the aortopulmonary septum of the OT (Figure 2-2 b) (Kirby *et al*, 1983). The ingrowth of this mesenchymal septum fuses the truncal cushions of the OT. The APS projects into the truncal cushions in two prongs or columns, to the level of the semilunar valves. Some neural crest cells then continue past the level of the valves, and by way of sub-endocardial migration, reach the proximal conal cushions and the site of closure of the interventricular septum (Waldo *et al*, 1998).

Much of the understanding of the contribution of cardiac neural crest to heart development has come from ablation studies, where the premigratory neural crest population of cells is eliminated, or from chimeric studies using transplanted quail neural crest tissue in chick embryos. Deletion of the cardiac neural crest results in a range of

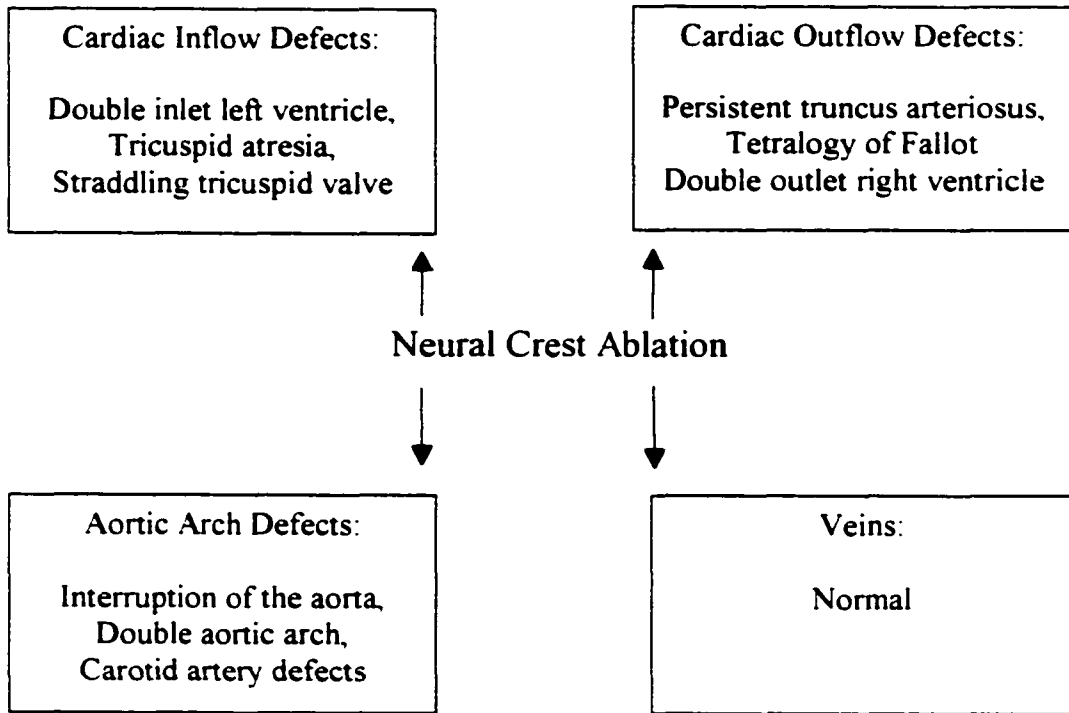


Figure 2-3. Cardiac defects resulting from varying degrees of cardiac neural crest ablation (Adapted from Kirby, 1999).

heart defects, dependant on the completeness of ablation. However, all have been shown to affect the development of the outflow septum of the heart and the patterning of the great arteries (Kirby, 1999), and are referred to as the neural crest ablation model of defective heart development (Creazzo *et al*, 1998). The most common heart defect associated with neural crest ablation is persistent truncus arteriosus (PTA), which occurs when a threshold level of neural crest cells fails to reach the OT and divide the single vessel into the aorta and pulmonary artery (Creazzo *et al*, 1998). Other common defects include double-outlet right ventricle, ventricular septal defect, overriding aorta and Tetralogy of Fallot (Kirby, 1999). The better-characterised anomalies resulting from neural crest ablation are summarized in figure 2-3.

CONGENITAL HEART DEFECTS

Congenital defects of the heart are of relatively high incidence, occurring in almost one percent of live births and ten percent of still births (Ya *et al*. 1997). Anomalies of the septa and valves occur in the majority of heart defects, with ventricular septal defects being the most common (Todd *et al*, 1994). Ventricular septal defects occur when incorrect fusion of the interventricular septum occurs with the conal cushions of the OT and the AV endocardial cushions. This defect results in the incorrect communication between the two ventricles. Endocardial cushion defects constitute a large percentage of congenital heart defects. They usually include an atrial septal defect, in which correct alignment and closure of the interatrial septum fails, and fusion with the AV cushion is incomplete. Endocardial cushion defects may also contain a ventricular

septal defect. Deformities of the mitral and tricuspid valves also occur with impaired cushion development (Todd *et al*, 1994).

The early stages of formation and transformation during cushion morphogenesis can also be affected by retinoic acid (RA). Quail embryos deficient in RA develop cardiac defects, including cardia bifida and underdeveloped endocardial layers (Heine *et al*, 1985), while mice embryo cushion explants have reduced EMT following treatment with RA (Nakajima *et al*, 1996). Mice deficient for the RA receptor RXR α also display a variety of defects in OT cushion morphogenesis (Gruber *et al*, 1996). Retinoic acid also plays a role in the contribution of neural crest to OT septation, with RA deficiency resulting in a spectrum of defects of the derivatives of NC, in the aortic arches and OT (Kubalak and Sucov, 1999).

APOPTOSIS

Apoptosis is a specific mode of cell death, distinct from necrosis, which is characterized by specific morphological and biochemical features (Kerr *et al*, 1972; Majno and Joris, 1995; Allen *et al*, 1997). Originally described by Kerr *et al*, (1972) with reference to physiological and pathological situations, this type of cell death is now known to be crucial to many processes, including normal embryonic development (Sanders and Wride, 1995; Jacobson *et al*, 1997), the immune system (Krammer, 2000), and in homeostatic physiology (Renehan *et al*, 2001). Deregulated apoptosis is also known to contribute to, or cause, pathological damage, including developmental defects (James, 1997), cancer (Parton *et al*, 2001; White and McCubrey, 2001), neurodegenerative disease (Mattson, 2000; Mattson *et al*, 2001), and autoimmune disease (Lorenz *et al*, 2000; Eguchi, 2001), and has also been shown to occur after trauma in many situations, such as cardiovascular (Kang and Izumo, 2000) or central nervous system damage (Barinaga, 1988).

Morphological features of apoptosis

Apoptosis as a distinct mode of programmed cell death (PCD), is defined by typical morphological and biochemical features that occur in an orderly sequence, and differ significantly from those occurring during necrosis (Wyllie *et al*, 1980a; Allen *et al*, 1997; Lincz, 1998). Some of the characteristic features of necrosis include swelling of the cytoplasm, ER and mitochondria, random chromatin dispersal and DNA fragmentation, rupture and lysis of the cell membrane, and an inflammatory response by the surrounding tissue (Walker *et al*, 1988; Allen *et al*, 1997). During apoptosis, the earliest observable

event, as seen ultrastructurally, is the condensation of the chromatin to form dense masses at the edge of the nuclear envelope. The nucleolar chromatin also forms osmiophilic aggregates in the nucleus (Wyllie *et al*, 1981). At the same time as nuclear condensation, cell shrinkage is seen, which results in loss of cell-cell contact (Kerr, 1971). At this stage, the cell now appears smaller, with a pyknotic nucleus. Then, blebbing of the cell membrane occurs, with convolutions forming in the nuclear and plasma membranes, and the blebs detach from the cell (Kerr *et al*, 1972; Walker *et al*, 1988). Subsequently, the nucleus breaks into discrete fragments that are enclosed in a double-layered nuclear envelope. These fragments are found within larger cytoplasmic blebs, and are called apoptotic bodies (Kerr *et al*, 1972; Allen *et al*, 1997). These bodies are spherical or oval in shape and vary considerably in size, contain intact closely packed organelles, and only remain visible in tissues for a few hours (Wyllie *et al*, 1980b; Walker *et al*, 1988). These apoptotic bodies are phagocytosed rapidly by macrophages or neighbouring cells, yet the organelles remain intact within them (Kerr *et al*, 1972). The engulfment of the apoptotic bodies occurs without an inflammatory response, which is another hallmark of apoptosis. Apoptotic cells in culture undergo what is called secondary necrosis, where the apoptotic bodies disintegrate and burst.

Biochemical features of apoptosis

Cells undergoing apoptosis can display a number of cell-surface markers, with the externalization of phosphatidylserine being the best known (Saville and Fadok, 2000). Phosphatidylserine (PTS) is normally found on the inner surface of the plasma membrane but is flipped to the outside early in the apoptotic cycle (Allen *et al*, 1997). Its

translocation plays a role in the recognition of the dead cell by macrophages. (Fadok *et al.*, 1992). Phosphatidylserine externalization is probably mediated by interactions between translocase and scramblase enzymes, normally involved in maintaining cell integrity (Fadok *et al.*, 1998), which can be inhibited by apoptosis inhibitors, e.g. bcl-2, and provides a mechanism for identifying early stage apoptotic cells. Annexin-V, a calcium-dependent phospholipid-binding protein with a high affinity for PTS, binds to PTS on the external surface of the cell, and can therefore be used as a marker for dying cells (Vermes *et al.*, 1995).

One of the earliest biochemical changes is fragmentation of the nuclear DNA, by Ca^{2+} dependent endonucleases (Wyllie, 1980; Walker and Sikorska, 1997), which probably starts at the sites of DNA attachment to the nuclear matrix. There is an initial cleavage of DNA into large fragments of ~300kbp and ~50kbp, usually followed by cleavage of the DNA into oligonucleosomal fragments of ~180 - 200bp (Walker and Sikorska, 1997). It is these smaller fragments that give the characteristic ladder-pattern when apoptotic DNA is run on an agarose gel. It is also this internucleosomal fragmentation that is utilized in one of the key techniques for recognizing apoptosis, i.e. TUNEL (terminal deoxynucleotide transferase mediated dUTP-biotin nick-end labeling), which labels the fragmenting DNA. The TUNEL technique uses the enzyme terminal deoxynucleotide transferase (Tdt) to add labeled deoxynucleotide triphosphates (dUTP) to the free 3' OH ends of single- or double- stranded DNA generated during apoptotic cleavage (Gavrieli *et al.*, 1992). However, because of the rapid uptake and elimination of apoptotic cells, *in vivo* staining of sections can underestimate the total number of dying

cells (Kerr *et al*, 1972). During the apoptotic process, mitochondrial DNA does not appear to be cleaved.

APOPTOSIS IN DEVELOPMENT

It has long been known that cell death is an important aspect of animal development (Glucksmann, 1951; Saunders, 1966; Clarke and Clarke, 1996; Hirata and Hall, 2000). However, even with the seminal paper from Kerr *et al*, (1972) outlining the process of apoptosis in homeostasis, pathology and development, it was much longer before the significance of cell death in development was examined in detail (Clarke, 1990; Sanders and Wride, 1995; Vaux and Korsmeyer, 1999; Ranganath and Nagashree, 2001). Programmed cell death is now known to have many different functions in development, in different areas of the embryo. Some general roles and function may be assigned to developmental cell death, which basically involve removal of cells to achieve specific functions. These include the sculpting and shaping of structures, removing structures that are not needed, and the regulation of cell numbers (Jacobson *et al*, 1997; Meier *et al*, 2000).

In sculpting structures, the removal of the cells in the developing limb are probably the best characterized. The limbs initially develop as paddle-shaped outgrowths, in which interdigital spaces are subsequently sculpted out by massive cell death in regions called the interdigital necrotic zones (INZs) and the anterior and posterior necrotic zones (ANZ/PNZ). This cell death is responsible for forming the individual digits and limb shape (Garcia-Martinez *et al*, 1993; Tone *et al*, 1994). Cell death is also important for fusion or invagination of epithelia during development, as in the neural tube

and palate (Jacobson et al, 1997, Weil et al, 1997; Martinez-Alvarez *et al*, 2000). During development, apoptosis is also involved in the removal of vestigial structures that were needed by an ancestral species, and structures required at one stage of development but not later. Examples of this include the pronephric tubules, which are eliminated in mammals, but not in fish and amphibia (Ellis and Youson, 1990), and the tail bud in *Xenopus*, in which the tail is removed by apoptosis at metamorphosis (Sachs *et al*, 1997). The vertebrate nervous system is one of the best examples where cell numbers are regulated by apoptosis (Nijhawan *et al*, 2000). Between 15 and 85% of the initial number of neurons that are initially produced are removed by PCD, (Oppenheim, 1991), matching the final number of cells to the total number of target sites available. Also, during development certain cells undergo an apoptotic-like event in achieving a terminally differentiated state. Examples include the lens epithelia, where the cell does not die, but apoptotic-like events remove the cell organelles and the cell persists in a differentiated state (Wride *et al*, 1999), and skin keratinocytes (Jacobson *et al*, 1997), where the cell does die, but remains as a squame on the outer layer. Along with these examples, there are also many examples of developmental cell death where the exact role is not known. Cell death during heart development can be included here, with many regions of cell death observed, but with little agreement on a precise role, as is discussed below (Pexieder, 1975; Fisher *et al*, 2000).

Much of developmental cell death is controlled by external signals (Raff, 1992). This may entail the removal of an external signal triggering the cells to die, or the presence of an external signal inducing apoptosis. In the developing nervous system, the cells normally require survival signals, in the form trophic factors that are derived from

the potential target of the cell. Failure to make contact with the target or with the trophic factor, through competition with other cells, induces apoptosis (Barde, 1989; Oppenheim, 1991). In certain other situations, contact with the cell matrix is necessary to provide external signaling to the cell. This is probably mediated via integrin signaling, and removal of this results in an apoptotic event termed anoikis, as seen in many cell types, including fibroblasts and epithelia (Frisch and Ruoslahti, 1997; Frisch and Screaton, 2001). In many cases, the cell receives an external signal that induces the cell to enter the apoptotic pathway. In the developing limb mesenchyme, apoptosis is mediated by interactions between the BMP's and fibroblast growth factor-4 (FGF4; Yokouchi *et al*, 1996; Zou and Niswander, 1996; Montero *et al*, 2001). In the developing rhombencephalon, BMP4 induces apoptosis in neural crest cells (Graham *et al*, 1994).

Much of our understanding of apoptosis has come from genetic studies in developing *Caenorhabditis elegans* (Horvitz, 1999). During development of this nematode, of the total 1090 somatic cells, 131 of these die, leaving the adult comprised of 959 cells. Genetic analysis of mutants that are defective in the death of these 131 cells has led to the discovery of specific genes involved in the regulation and execution of apoptosis (Ellis and Horvitz, 1986). Four of these genes are necessary for the removal of cells, *egl-1*, *ced-3*, *ced-4* and *ced-9*. Loss of function of *egl-1*, *ced-3* or *ced-4* results in survival of the 131 cells, implicating these genes in cell death induction, whereas loss of *ced-9* results in death of the animal due to excess cell death, implicating this gene as a suppressor of cell death. It was the analysis of these genes that led to the discovery of the homologous mammalian counterparts, and discovery of the complex apoptosis pathways (Yuan and Horvitz, 1992; Horvitz, 1999; Hengartner, 2000).

Ced-3 encodes a protease homologous to members of the caspase family of enzymes in vertebrates (Yuan *et al*, 1993). *Ced-4* is an adaptor protein, which activates *ced-3* protease activity, and is now known to be homologous to vertebrate apaf-1 (apoptotic protease activating factor), an adaptor protein involved in regulation of mitochondrial-activated apoptosis (Yuan and Horvitz, 1992; Zou *et al*, 1997). *Ced-9*, the death repressor gene, is homologous to the vertebrate *bcl-2* family, and can bind *ced-4*, thus inhibiting activation of the death pathway (Hengartner and Horvitz, 1992). *Egl-1* can displace *ced-9* from *ced-4*, thereby unmasking the inhibition, and allowing the protease activity of *ced-3* to occur (Conradt and Horvitz, 1998). The vertebrate homologues of *egl-1* are the BH3 proapoptotic members of the *bcl-2* family.

Apoptosis in heart development

Interest in apoptosis in heart development has dramatically increased in recent years (Fisher *et al*, 2000; Poelmann *et al*, 2000; van den Hoff *et al*, 2000). Much of this recent work has concentrated on the distribution and occurrence of apoptotic cells, with a reassessment of the detailed work of Pexieder (1975), using more modern techniques.

In his exhaustive study on the subject, Pexieder identified 31 different foci of cell death in the developing chick heart, between ED4-8 (Pexieder, 1972; 1975), with the highest incidence occurring at ED4 in the bulbar cushions. This work was performed mostly using vital dyes such as Nile blue sulphate, and cell morphology assessment at the light and electron microscope level as indicators of cell death. This work also compared the levels and incidences of cell death in other species, with the human embryonic heart having 16 foci and the rat heart having 21 at corresponding periods of development. The

foci of cell death common to each species include the AV cushions, the OT cushions, the walls of the aorta and pulmonary aorta, the semilunar valves and the interventricular septum (Pexieder, 1975).

With the advent of more specific methods for assessing cell death, such as TUNEL labeling (Gavrieli *et al.*, 1992), and an understanding of the factors involved in the regulation of apoptosis, the application of these techniques to heart development seem to be pointing to a more localized distribution of dying cells than previously thought, with a smaller number of main foci of cell death (Fisher *et al.*, 2000; Poelmann *et al.*, 2000). Most of the recent work has used the chick embryo, with some correlative studies in the mouse and rat. In the chick heart, atrial and ventricular tissues seem to have little documented cell death in early development. In the OT, apoptotic cells have been shown in the prongs of the AP septum below semi-lunar valve level, and scattered throughout the OT cushions (Poelmann *et al.*, 1998). Levels of apoptosis were highest around HH27-31 (ED5-6) and some of these cells were shown by retroviral and TUNEL labeling to be derived from a subpopulation of cardiac neural crest cells. Another subpopulation of cardiac neural crest cells, that enters the heart via the venous pole and targets the prospective cardiac conduction system and the AV cushions, has also been shown to undergo apoptosis on reaching these sites at approximately HH 31 (Poelmann and Gittenberger-de Groot, 1999), as seen by retroviral and TUNEL labeling. In the muscle wall of the OT, myocytes have been shown to be eliminated by apoptosis in large numbers between ED4-8 (Watanabe *et al.*, 1998), as seen with concomitant adenoviral and TUNEL labeling, with peak numbers of dying cells seen around ED 6 (HH stage 31). A large number of dying cells are also reportedly seen in the superior aspect of the

interventricular septum, at the site of its fusion with the atrial septum and OT septum (Fisher *et al*, 2000; van den Hoff *et al*, 2000). This area includes the sites of formation of the AV node, the bundle of His and the left and right bundle branches. It is worth noting here also, that this site is also the final destination of some of the cardiac neural crest cells. Cell death is also seen between HH 29-35 in the coronary artery orifices of the chick heart (Velkey and Bermanke, 2001).

Apoptotic cells have also been described in the embryonic mouse heart. In the ventricle of the heart, dying cells have been shown between ED 11-16, with greater number of dying cells in the compact myocardial regions as opposed to the less-dense trabeculae (Abdelwahid *et al*, 1999), but at very low levels. Some evidence has been shown for apoptosis in the endocardial cushions of the mouse heart, but at lower levels and with a more restricted distribution than in the chick (Abdelwahid *et al*, 2001a; 2001b). In the mouse, apoptotic cells were not seen in areas that were positive for PCNA, which may differ from the findings in the chick. In the embryonic rat heart, some dying cells were seen in the OT during ED 14-16, which corresponds to the equivalent time that apoptosis is seen in the chick OT. However, the total number of dying cells was again much lower than that seen in the chick (Takeda *et al*, 1996).

MECHANISMS OF APOPTOSIS

Most of the morphological changes seen in apoptosis are brought about by a family of cysteine proteases called caspases (cysteine aspartic acid specific proteases (Alnemri *et al*, 1996; Martins and Earnshaw, 1997; Earnshaw *et al*, 1999), that are activated in apoptotic cells. These enzymes are highly conserved throughout evolution

(Hengartner, 2000), with at least 14 members of the caspase family having been found in vertebrate cells at the time of writing (Wang and Lenardo, 2000). Caspases are constitutively present in most cells (Weil et al, 1996), residing in the cytosol as an inactive single chain proenzyme (Green, 1998). Caspases are among the most specific of proteases with a requirement for cleavage at an aspartic acid residue. The diversity in their biological functions is the result of significant differences in the preferred tetrapeptide recognition motifs, as well as a necessity for the correct tertiary structural elements being present (Thornberry and Lazebnik, 1998). Caspases function as both proapoptotic initiators, at the start of the apoptotic signaling pathway and as effectors of cell disassembly. Caspases belong to one of two categories, pro-inflammatory or cytokine-maturing caspases and pro-apoptotic caspases. Caspases -1 and -11 belong to the first group and the others belong to the second group (Wang and Lenardo, 2000).

Caspase activation

All caspases are expressed as proenzymes, with 3 domains - an NH₂-terminal prodomain, a large subunit (~20kDa) and a small subunit (~10kDa) (Thornberry and Lazebnik, 1998). Caspases may have either long or short prodomains (Villa *et al*, 1997). Those with long prodomains, such as caspases -8, -10, -1, -2, -4, -9, are believed to be upstream initiator caspases, while those with short prodomains, such as -3, -6, -7, are activated predominantly through the action of other proteases (Wang and Lenardo, 2000). Caspases may be activated by proteolytic cleavage at two sites: one between the large and small subunits and another by the enzyme itself to remove its own prodomain. There are a number of possible mechanisms of caspase activation. The induced proximity model of

activation entails ligand binding to death receptors e.g. CD95, which results in aggregation of the receptor, and signaling which recruits several procaspase 8 molecules. This high local concentration of the zymogen possesses intrinsic protease activity of procaspase 8, sufficient to allow autoprocessing to the active protease (Muzio *et al*, 1998; Salvesen and Dixit, 1999). Most caspase activation occurs as result of proteolytic cleavage. However, all these cleavage sites are at caspase recognition sites, resulting in autocatalytic activation, which results in a caspase cascade activation of the key downstream caspases -3, -6 and -7 (Thornberry *et al*, 1997). Activation may also be the result of association of the procaspase with a regulatory subunit. This scenario applies to the upstream caspase 9, which requires association with the protein co-factors, apaf-1, cytochrome c and dATP, resulting in the formation of an apoptosome (Zou *et al*, 1999; Hengartner, 2000).

Caspase activation by cell surface receptors

The death receptor pathway is used by cytotoxic T lymphocytes to activate the death pathway in infected cells (Figure 2-4A; Krammer, 2000). Currently, there are six cell surface receptors known to transduce death signals (Daniel *et al*, 2001). These receptors are members of the tumour necrosis factor / nerve growth factor (TNF / NGF) receptor superfamily (Wallach, 1997; Schmitz *et al*, 2000), including Fas/APO-1/CD95, TNF receptor-1 (TNFR1), TNF receptor-related apoptosis-mediating protein (TRAMP; DR3/Apo-3), the TNF-related apoptosis-inducing ligand (TRAIL) receptor (Muhlenbeck *et al*, 1998), and death-receptor-6 (DR6; Wallach, 1997; Budihardjo *et al*, 1999; Daniel *et al*, 2001). With ligand binding to the receptor, there are 3 distinct steps to apoptosis

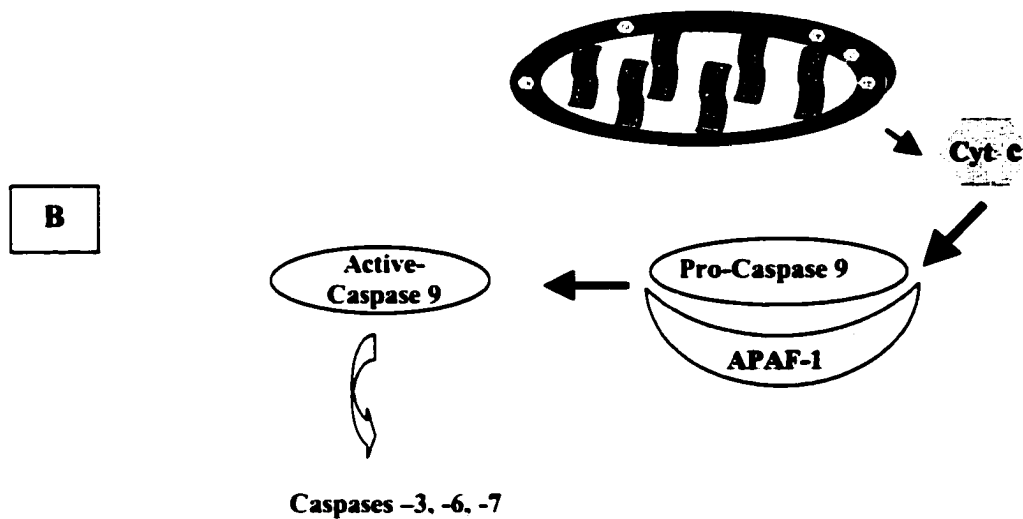
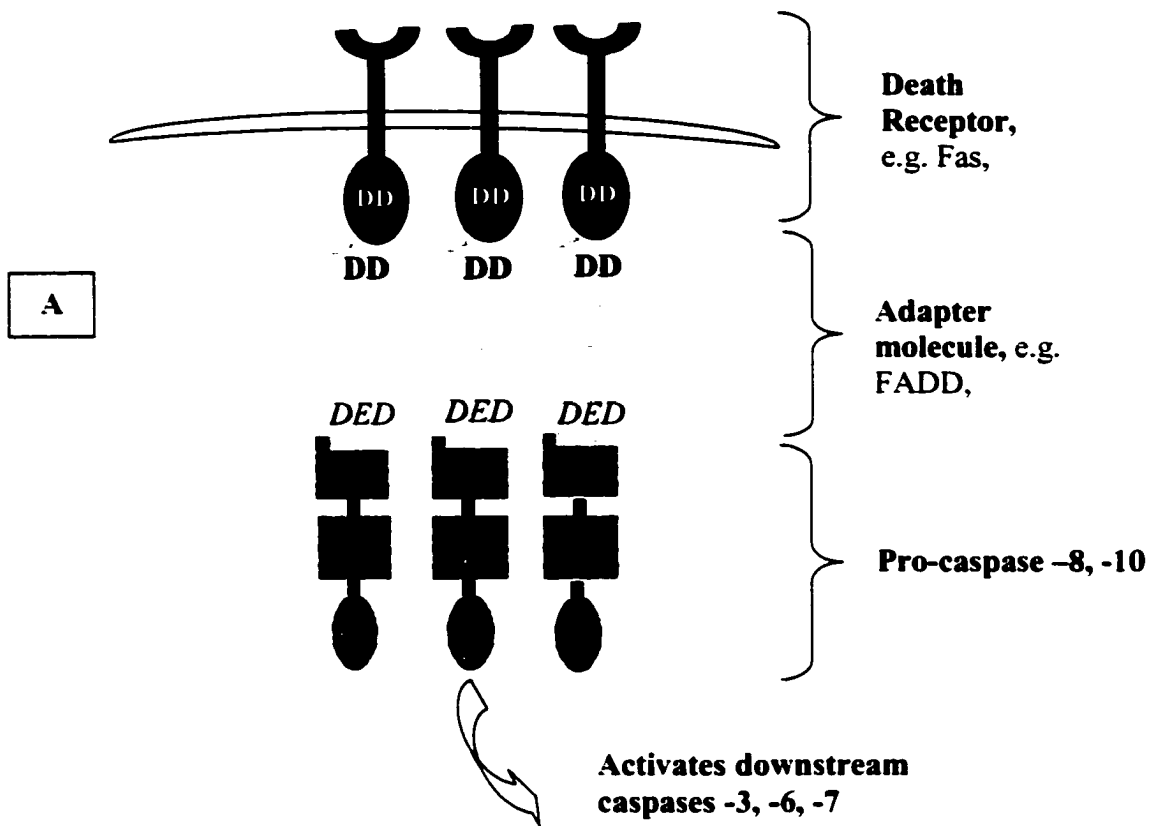


Figure 2-4. Pathways of caspase activation. (A) A schematic diagram showing the components of the cell-surface mediated caspase activation pathway. (B) A schematic diagram showing the main components of the mitochondrial-mediated caspase pathway.

activation; the first is ligand-induced receptor trimerization, then the recruitment of intracellular receptor-associated proteins, and finally, the initiation of caspase activation. The transmembrane receptors contain a conserved protein-protein interaction sequence called the death domain (DD) in their cytoplasmic region (Budihardjo *et al*, 1999). Ligand binding induces trimerization of the receptor, which also results in recruitment of a number of DD-containing intracellular adapter molecules. These include, among others, FADD (Fas-associated protein with death domain; Yeh *et al*, 1998), TRADD (TNF-receptor associated death domain; Hsu *et al*, 1995), and RAIDD (Duan and Dixit, 1997), each of which the receptor binds through interaction with its own DD (Budihardjo *et al*, 1999). The ligand-bound death receptor, with its intracellular receptor associated proteins is called the DISC (death-inducing signaling complex). The N-terminus of FADD also contains a shared sequence called the death effector domain (DED), which binds the upstream procaspases (Wallach, 1997). These procaspases e.g. caspase -8 and -10, contain two tandem repeats of the DED within their own prodomain (Budihardjo *et al*, 1999; Hengartner, 2000). Interaction between the DED's of the adaptor proteins and the upstream procaspases, results in caspase activation by induced proximity (Muzio *et al*, 1996, 1998).

Caspase activation by mitochondria

The other upstream initiator caspases with long prodomains, including caspases -1, -2, -4 and -9 contain a caspase recruitment domain (CARD) within their prodomain (Wang and Lenardo, 2000). The DED and CARD share some sequence similarity, and their 3-dimensional structures are very similar (Chou *et al*, 1998). Apaf-1 is a 130kDa

protein with 3 domains (Zou *et al*, 1997). Its N-terminus functions as a CARD, which binds caspases with a similar CARD (Hofmann *et al*, 1997). However, only caspase 9 is activated by apaf-1. During the apoptotic process, cytochrome c is released from the intermembrane space in the mitochondria (Figure 2-4B; Liu *et al*, 1996; Zou *et al*, 1999). In the presence of cytochrome c, apaf-1 hydrolyses ATP/dATP to ADP and dADP, and in so doing, forms an apaf-1/cytochrome c complex, called an apoptosome, which is fully functional in recruiting and activating caspase 9 through autocatalysis (Zou *et al*, 1999). Active caspase 9 is then released to activate at least six downstream caspases (-2, -3, -6, -7, -8 and -10) by proteolytic activation in a hierarchical cascade (Budihardjo *et al*, 1999; Slee *et al*, 1999). Only cytochrome c that has been assembled in the mitochondria, with an attached heme can activate apaf-1 (Green, 1998). Cytochrome c is also referred to as apaf-2, the caspase 9 proenzyme is apaf-3, and the vertebrate homolog of ced-4 is apaf-1 (Li *et al*, 1997; Kuida *et al*, 1998).

Caspase activity

Caspases contribute to the demise of the cell in a number of ways, involving both activation and inactivation of cellular proteins (Villa *et al*, 1997; Hengartner, 2000). One example of protein activation by a caspase results in one of the more recognizable features of apoptosis, the cleavage of DNA into nucleosomal fragments (Wyllie, 1980; Zhang and Xu, 2000). The activation of CAD/DFF (caspase activated deoxyribonuclease / DNA fragmentation factor), the main enzyme responsible for DNA fragmentation during apoptosis by downstream caspases, occurs by cleavage of its inhibitory subunit ICAD/DFF45, and results in the release of the active nuclease (Liu *et al*, 1997; Enari *et*

al, 1998; Tang and Kidd, 1998). DFF itself may not directly cleave the DNA, but instead it probably activates downstream $\text{Ca}^{2+}/\text{Mg}^{2+}$ endonucleases that reside in the nuclei, which result in internucleosomal cleavage (Liu *et al*, 1997). Other acidic enzymes, activated by a decrease in intracellular pH may also be involved (Walker and Sikorska, 1997). Other proteins that are activated by caspases include the sterol regulatory binding proteins (SREBP's) (Wang *et al*, 1996) and as mentioned, some of the caspases themselves. Also, the removal of inhibitory domains or subunits are also involved in gain of increased biological activity of cleaved proteins e.g. the truncation of pro-apoptotic bid (Li *et al*, 1998; Hengartner, 2000).

Caspase activity may also lead to inactivation of numerous vital cellular proteins by cleavage, such as DNA-dependent protein kinase (Song *et al*, 1996) and the retinoblastoma tumour suppressor protein. Caspases also cleave antiapoptotic bcl-2 family members, resulting in their inactivation or possibly conversion to pro-apoptotic molecules (Cheng *et al*, 1997). Caspase enzymes also directly or indirectly disassemble cell structures by cleavage of structural proteins of the nucleus and cytoskeleton (Villa *et al*, 1997). Direct cleavage of the nuclear lamins results in chromatin condensation and nuclear budding (Orth *et al*, 1996; Takahashi *et al*, 1996). Indirect effects are mediated by cleaving and deregulating proteins involved in the maintenance of the cytoskeleton, such as gelsolin and poly (ADP-ribose) polymerase (PARP). Gelsolin is an actin-regulatory protein that may suppress apoptosis by acting upstream of the caspases, but cleavage of gelsolin results in constitutive activation of this protein that severs actin filaments, leading to apoptosis (Ohtsu *et al*, 1997; Kamada *et al*, 1998). PARP is among the first target proteins to be specifically cleaved during apoptosis, at a very early stage of

apoptotic cell death (Kaufmann 1989; Tewari *et al*, 1995). PARP is an enzyme that aids in DNA repair. When the DNA of a cell is damaged, polymers of poly (ADP-ribose) are synthesized by PARP (Lindahl, 1995). These polymers function in reorganizing chromatin at the lesion site (Sato and Lindahl, 1992). Cleavage of PARP is one of the hallmarks of apoptosis. PARP is normally present as a 113kDa protein. But during apoptosis, it is cleaved into 89 and 24kDa fragments (Duriez and Shah, 1997). The 89kDa fragment is a catalytic unit, whereas the 24kDa fragment is the DNA binding unit. The 24 kDa fragment may also block DNA repair at the strand breaks, as it has 2 zinc fingers that bind the DNA strand breaks. PARP cleavage has been shown to occur very early in the apoptotic cycle, at approximately 15-30 min. (Duriez and Shah, 1997). This is much earlier than DNA degradation or degradation of other proteins (Greidinger *et al*, 1997). Because of this, PARP cleavage is now used as a sensitive and relatively simple assay for apoptosis.

Genetic knockout studies on caspases

Knockouts of the different caspase enzymes do not result in a total suppression of apoptosis, but a cell- and tissue-specific or stimulus-dependent inhibition of apoptosis (Kuida *et al*, 1998). Both caspase-9 and caspase-3 knockout mice display severe defects in the CNS, and are born at a lower frequency than normal. The caspase-9 knockout phenotype is more severe than the caspase-3 knockout, which suggests that it lies upstream of other caspases (Wang and Lenardo, 2000). In caspase-9 knockout mice, the majority of homozygotes die perinatally due to an enlarged cerebrum, caused by reduced apoptosis (Kuida *et al*, 1998). In the apaf-1 knockout mouse (Yoshida *et al*, 1998),

defects are found in practically all those tissues that undergo developmental cell death e.g. limbs, palate, nervous system, lens and retina, suggesting that developmental cell death is dependent on mitochondrial release of cytochrome c. In tissues susceptible to other forms of apoptosis e.g. Fas mediated, the apoptotic pathway was still intact and no defects were seen (Green, 1998). However, the caspase-9 and apaf-1 knockout mice were not identical in their defects, suggesting that apaf-1 may work through different pathways, or may have other non-apoptotic roles (Green, 1998). In caspase-8 deficient embryos, the ventricular musculature of the heart was thin, and the trabeculae were thin and disorganized (Varfolomeev *et al*, 1998), while in normal hearts, whole-mount and histological *in situ* hybridization showed elevated levels of caspase 8 transcript in the heart, especially the ventricle. PARP knockout mice develop normally, with no differences in apoptosis in different tissues when compared to healthy mice. This is probably due to the redundancy among signaling molecules in the pathway (Wang *et al*, 1995).

Apoptosis regulators: the bcl-2 family

The main, and best characterized, family of apoptosis regulators is the bcl-2 family of molecules (Gross *et al*, 1999; Tsujimoto and Shimizu, 2000a). The prototype member, bcl-2 itself, was discovered to be structurally and functionally homologous to the anti-apoptotic *ced-9* gene in *C. elegans* (Hengartner and Horvitz, 1992). Bcl-2 itself has since been shown to be anti-apoptotic, and is capable of protecting many cell types from various insults, including γ -irradiation, serum-withdrawal, cytotoxic drug treatment and staurosporine (Adams and Cory, 1998; Susin *et al*, 1998). The number of bcl-2 family

members is constantly increasing, with new homologues discovered regularly. At least fifteen members of the bcl-2 family have been identified (Adams and Cory, 1998) and these have been classified in a number of ways. Initially, they are subdivided on the basis of being either pro- or anti-apoptotic, and the ratio between the expression of these two subsets helps, in part, to determine the susceptibility of cells to a death signal (Susin *et al*, 1998). Members of the bcl-2 family can be further classified into three groups, based on structural similarities and functional criteria (Hengartner, 2000). Structurally, all bcl-2 family members contain at least one of four conserved bcl-2 homology (BH) domains, termed BH1-BH4 (Figure 2-5; Tsujimoto and Shimizu, 2000a). Most anti-apoptotic members of the family possess at least BH1-2, and those most similar to bcl-2, possess all four BH domains. These include the mammalian bcl-2, bcl-X_L, bcl-W, mcl-1, the viral protein E1B and the *C. elegans* gene *ced-9* (Kelekar and Thompson, 1998). Some of the pro-apoptotic members of the family possess only the BH1-BH3 domains, and closely resemble bcl-2 in structure. These include bax, bak and bok. Other pro-apoptotic members of the family possess only the BH3 domain and include mammalian bik, bad, bid, and the *C. elegans* egl-1 protein (Kelekar and Thompson, 1998). One feature of the protein family is the ability to form homo- and hetero-dimers between themselves, and between pro- and anti-apoptotic family members, which is thought to inhibit the biological activity of the dimerized partner (Tsujimoto and Shimizu, 2000a). This is mediated by interactions between the BH domains. In some anti-apoptotic family members, the BH1-BH3 domains form a hydrophobic cleft, into which a BH3 domain from an pro-apoptotic protein can be inserted (Sattler *et al*, 1997). A further sub-classification of the pro-apoptotic family members based on sequence and structural

Anti-apoptotic



Pro-apoptotic



Figure 2-5. Structural classification of the bcl-2 family members. Each family member is classified according to the number of bcl-2 homology (BH) domains it possesses. Anti-apoptotic members similar to bcl-2 possess BH1-4. Pro-apoptotic members possess wither BH1-3 or BH3 only. Some members also possess transmembrane (TM) binding domains.

analysis, suggests that the BH3 domains may be “buried” or “exposed” (Gross *et al*, 1999; McDonnell *et al*, 1999). If the BH3 domain is buried, the protein may either be an anti-apoptotic molecule, or an inactive pro-apoptotic molecule. If the BH3 domain is exposed, the protein may have been activated or undergone a conformational change to expose the BH3 domain (McDonnell *et al*, 1999). Anti-apoptotic members of the bcl-2 family are known to reside on the membranes of certain cell organelles, including the mitochondria, the endoplasmic reticulum (ER) and the nuclear membranes (Hockenberry *et al*, 1990; Krajewski *et al*, 1993; Hacki *et al*, 2000). Here, they can prevent the release of apoptotic factors, such as cytochrome c, into the cytosol (Yang *et al*, 1997). Anti-apoptotic members may also function downstream of the mitochondria, as bcl-X_L has been shown to bind to downstream apaf-1, and prevent caspase-9 association and activation (Hu *et al*, 1998).

In contrast to the anti-apoptotic molecules, most pro-apoptotic family members reside in the cytosol or on the cytoskeleton, and translocate to the membranes, particularly the mitochondrial outer membrane, upon receiving an activation signal (Gross *et al*, 1998). Most BH1-BH3 family molecules are thought to interact with the membrane-associated anti-apoptotic molecules, such as bcl-2, following activation (Cheng *et al*, 2001). However, BH3-only molecules can insert into the membranes, independent of interaction with other molecules. Once in the membrane, the proapoptotic molecules are thought to aid in, or cause, the release of apoptotic factors, such as cytochrome c (Hengartner, 2000). At present the mitochondrial association of the bcl-2 family molecules, and their involvement in the regulation of cytochrome c release is better understood than their association with other membranes, such as the ER and nuclear membranes. Although,

evidence for communication between the mitochondria and the ER has been shown (Hacki *et al.*, 2000), with ER-specific effects possibly mediating Ca^{2+} mobilization (Ichimiya *et al.*, 1998; Foyouzi-Youssefi *et al.*, 2000). In the nucleus, bcl-2 and bax have been shown to be associated with the nuclear matrix (Wang *et al.*, 1999; Gajowska *et al.*, 2001), prior to appearance of an apoptotic morphology, and inhibition of bax expression blocks lamin A cleavage in the nucleus (Ho *et al.*, 1999).

Pro-apoptotic family members have been shown to be activated under a number of situations. Pro-apoptotic bax is mostly found in the cytosol in a monomeric form. Upon activation, it translocates and inserts into the mitochondrial membrane as an integral membrane protein, and may dimerise in the process (Wolter *et al.*, 1997; Gross *et al.*, 1998). Bax translocation may also be induced by a number of factors, including integrin-mediated signaling (Gilmore *et al.*, 2000) and a rise in intracellular pH (Khaled *et al.*, 1999). Bax insertion into the mitochondrial membrane is thought to facilitate the release of cytochrome c (Antonsson *et al.*, 2000). However, bax activation may be inhibited by anti-apoptotic family members, such as bcl-2 and bcl-X_L. A similar model of activation is in place for pro-apoptotic bak (Chittenden *et al.*, 1995; Kiefer *et al.*, 1995). It too is thought to translocate to the mitochondria on activation, which also may involve a conformational change, and interaction with bax (Griffiths *et al.*, 1999; Nechushtan *et al.*, 2001). Pro-apoptotic bad is dephosphorylated by serum withdrawal, and is released from its cytosolic sequestering-molecule 14-3-3 (Zha *et al.*, 1996). Upon dephosphorylation, bad is activated and is found to associate with anti-apoptotic bcl-2 and bcl-X_L, via its BH3 domain (Zha *et al.*, 1997). Cleavage by caspases is another method of activation of pro-apoptotic family members. Pro-apoptotic bid, a BH3-only molecule, may be cleaved

by caspase-8 (Li *et al*, 1998), and the truncated form can then translocate and insert into the mitochondrial membrane (Gross *et al*, 1999). Both pro- and anti-apoptotic members of the bcl-2 family may also be transcriptionally upregulated following a death signal. Examples include bax upregulation following p53 induction (Miyashita and Reed, 1995), and upregulation of bcl-2 by Akt/protein kinase B (Pugazhenti *et al*, 2000) and bcl-X_L by CD28 signaling (Boise *et al*, 1995).

Bcl2-family regulation at the mitochondrial membrane

There are a number of theories as to how exactly the bcl-2 family members control apoptosis at the mitochondrial membrane. One theory is that the proteins themselves may form channels, or regulate existing ones, in the outer-mitochondrial membrane (Reed, 1997). Evidence for the ability of bcl-2 family members to form channels has mostly come from *in vitro* studies where bcl-2, bax and bcl-X_L have been shown to form channels in lipid bilayers (Antonsson *et al*, 1997; Green and Reed, 1998), and from the structural similarity of anti-apoptotic bcl-X_L to the membrane insertion domains of bacterial toxins (Muchmore *et al*, 1996). Other studies suggest that bcl-2 family members may alter existing channels. One characteristic of apoptosis is the occurrence of a mitochondrial membrane permeability transition (PT), which is characterized by a membrane potential change ($\Delta\psi_m$) (Kroemer *et al*, 1997; Susin *et al*, 1998). The release of the apoptotic factor cytochrome c may or may not involve a PT. The $\Delta\psi_m$ is brought about by the opening of a pore in the mitochondrial membrane, the PT pore (Kroemer *et al*, 1997), which is a large conductance pore that forms after a necrotic or apoptotic signal (Gross *et al*, 1999). It is composed of a voltage-dependent

anion channel (VDAC) on the outer mitochondrial membrane and an adenine nucleotide translocator (ANT) on the inner membrane. Opening of the PT pore results in mitochondrial depolarization and uncoupling of oxidative phosphorylation (Gross *et al*, 1999). Members of the bcl-2 family have been shown to interact with the VDAC and regulate the release of cytochrome c (Shimizu *et al*, 2000; Tsujimoto and Shimizu, 2000b). Addition of bax or bak to isolated mitochondria results in cytochrome c release and $\Delta\psi_m$ (Jurgensmeier, *et al*, 1998), and bax has been shown to interact with VDAC and its component ANT (Shimizu *et al*, 1999). Bax and bak have also been shown to induce cytochrome c release in wild-type, but not VDAC-deficient yeast mitochondria (Shimizu *et al*, 1999). However, BH3-only family members, such as bid and bik, do not interact with VDAC (Shimizu and Tsujimoto, 2000). The VDAC is known to be an essential component in cytochrome c release, as well as $\Delta\psi_m$ (Shimizu *et al*, 1999), and once in the cytosol, mitochondrial-released cytochrome c is capable of activating some of the caspase family of enzymes, as described above.

Genetic knockout studies on the bcl-2 family

Knockout studies on members of the bcl-2 family seem to suggest that different members of the family are associated with different organ systems (Adams and Cory, 1998). Mice deficient for bcl-2 develop normally, and only later show increased lymphoid apoptosis, impaired melanocytes and intestinal epithelium and develop terminal kidney disease, pointing to a role of the protein in an antioxidant pathway (Veis *et al*, 1993). Mice deficient for anti-apoptotic bcl-x die *in utero* around ED 13, with extensive apoptosis of the developing neurons of the brain, spinal cord and dorsal root ganglia

(Motoyama *et al*, 1995). Knockout mice bearing the deletion of anti-apoptotic bcl-w develop normally, but spermatogenesis is abolished in these animals by cell death of germ cells (Ross *et al*, 1998). Deletion of pro-apoptotic bax results in viable animals, but with increased numbers of B-cells and thymocytes, and excess follicles in the ovaries (Knudson *et al*, 1995).

AIMS OF THE RESEARCH

The work presented here is aimed at understanding the mechanisms and developmental significance of apoptosis that occurs during early heart development. The chick embryo is an ideal model for studying heart development, possessing similar developmental processes to mammalian species, and providing a system that enables relatively easy accessibility to, and manipulation of, the developing heart. The working hypothesis of this thesis, based on the findings of Pexieder (1975), is that apoptosis is a significant process necessary for proper development of the heart. Apoptosis is known to occur during heart development, but relatively little else is known about the process. This work was aimed at answering the following questions: using techniques specific for apoptosis, when and where in the heart is programmed cell death occurring; are some of the main protein regulators of the apoptotic pathway involved specifically in apoptosis in the heart; is the bone morphogenetic protein family involved in the stimulation of cell death; and what functional role does the cell death play in the development of the embryonic heart? Answering these questions will give a better understanding of the role of apoptosis in heart development, and possibly lead to a better understanding of congenital heart defects.

Chapter 3

MATERIALS AND METHODS

EMBRYO DISSECTION AND PREPARATION

Fertilized White Leghorn hens' eggs were incubated at 37°C for 4 – 8 days and the resulting embryos were staged according to Hamburger and Hamilton (1951). The embryos were removed and washed in Tyrode's saline (CaCl₂, MgCl₂, 6H₂O, KCl, NaHCO₃, NaCl, NaH₂PO₄H₂O, Glucose, pH 7.4). For immunocytochemistry, the heads were removed and the embryos immersed in 4% paraformaldehyde (PFA) in 0.1M phosphate-buffered-saline (PBS) at 4°C, for 4-15 hours, with later stages requiring longer fixation time. After fixing, the embryos were washed in PBS and stored at 4°C. For western blotting and cell culture, the hearts were removed to Tyrode's saline on ice. Using electrolytically sharpened tungsten needles, the AV endocardial cushions and the entire OT were dissected free from the heart.

Mouse embryos were also used for immunocytochemistry. Timed-pregnant CD1 mice were obtained from Charles River. The day of the appearance of the vaginal plug was considered day 0. Embryos from embryonic day (ED) 9.5 – 12.5 were used. The females were sacrificed by cervical dislocation, in accordance with the ethical guidelines of the university, and the embryos were dissected to ice cold Tyrode's saline. After rinsing, the embryos were fixed overnight in 4% PFA in PBS at 4°C. The embryos were then rinsed and stored in PBS at 4°C.

IMMUNOHISTOCHEMISTRY

After fixing, the embryos were washed in PBS, dehydrated through a graded series of ethanol, and cleared in Hemo-De (Fisher Scientific). The embryos were then embedded in paraffin wax, sectioned at 8µm and mounted on glass slides. Sections were

cleared in Hemo-De (2 x 10 min), rehydrated in graded ethanol and washed in double distilled water (DDW). To quench endogenous peroxidase, sections were treated with 0.3% H₂O₂ in DDW for 30 min, followed by washing in DDW. Antigenic sites were blocked in 10% serum (goat or rabbit) with 0.5% Tween 20 (Fisher Scientific) for 1 h at room temperature. Excess solution was removed and sections were incubated with primary antibodies diluted in 1% serum at 4°C overnight. Sections were washed 3 x 5 min in PBS, and then incubated with a biotinylated secondary antibody, at a dilution of 1:200 in 1% serum, for 1 h at room temperature. Following another wash, 3 x 5 min in PBS, sections were incubated with the Vecstatin ABC (Vector Laboratories) reagent according to manufacturers instructions for 1 h at room temperature. Following another wash, sections were stained using 3,3' -diaminobenzidine (Sigma) with ammonium nickel sulphate. Sections were washed in PBS, dehydrated through graded ethanol, cleared in Hemo-De and mounted with permount (Fisher Scientific Inc.). Negative controls consisted of either preincubating the primary antibody with the suppliers blocking peptide when available, or incubation in serum alone, minus the primary antibody.

ANTIBODIES

The primary antibodies used were; bcl-2 rabbit polyclonal (N-19, 1:200; mouse, rat and human reactive), bax rabbit polyclonal (I-19, 1:200; mouse, rat and human reactive) and bak rabbit polyclonal (G-23 1:100; mouse, rat and human reactive), all from Santa Cruz. A monoclonal antibody to proliferating cell nuclear antigen (PCNA), clone PC10 (Sigma) was used, at a dilution of 1:200. Antibodies to bone morphogenetic

proteins (BMP's) used were BMP2 goat polyclonal (n-14; mouse, rat and human reactive) and BMP4 goat polyclonal (n-16; mouse, rat and human reactive) (Santa Cruz) both at a dilution of 1:200. The secondary antibodies used, at a concentration of 1:200 were, biotinylated goat anti-rabbit IgG or biotinylated goat anti-mouse IgG (both from Vector Laboratories) or biotinylated rabbit anti-goat IgG (Sigma).

TUNEL LABELING

Cell death was assayed using a modification of the TUNEL method as described previously (Gavrieli *et al*, 1992). This technique identifies nuclei containing DNA that is undergoing internucleosomal cleavage. Sections of paraffin embryos were cleared in Hemo -De (2 x 10 min), rehydrated through graded ethanol and washed in DDW. Sections were then immersed in 2x SSC buffer (0.3M sodium chloride, 30mM sodium citrate, pH 7.0) at 60°C for 20 min and then washed in DDW. Sections were then immersed in Tris-HCl (10mM, pH 8.0) at room temperature, before being treated with proteinase K (15µg/ml in 10mM Tris-HCl, pH 8.0) at room temperature to aid in DNA exposure, followed by thorough washing in DDW. To quench endogenous peroxidase, sections were treated with 3% H₂O₂ in DDW with 0.5% Tween 20 for 15 minutes at room temperature, followed by a wash in DDW. To prepare the sections for the enzymatic reactions, sections were incubated with TdT buffer (30mM Trizma base, 140mM sodium cacodylate, 1mM cobalt chloride; pH 7.2) for 5 min at room temperature. The reaction mixture was prepared as follows, using components from the terminal transferase kit by Roche Molecular Biochemicals, using a volume of approximately 100µl per slide: DDW, 81µl; TdT buffer, 6.5µl; cobalt chloride, 3.26µl; biotin-16-dUTP

stock (1nmol/ μ l), 1.86 μ l; dUTP, 5.5 μ l; and TdT (10 units/ μ l), 2 μ l. The sections were coverslipped and were incubated with the reaction mixture for 90 min at 37°C in a humid chamber. The reaction was terminated by immersion of the slides in 2X SSC for 15 min at room temperature. After washing in PBS, the sections were covered with 3% skimmed milk in PBS with 0.5% Tween 20 for 15 min at room temperature, to block non-specific binding. After this, excess solution was removed and the slides were incubated with Extra-avidin-peroxidase (Sigma) at a dilution of 1:50 in 3% skimmed milk in PBS with 0.5% Tween 20 at room temperature for 30 min. After another wash in PBS, sections were stained with 3-amino-9-ethylcarbazole (AEC; Pierce). A stock solution was prepared by dissolving AEC at a concentration of 4mg/ml in dimethyl formamide. To prepare the reaction concentration, 670 μ l of stock AEC was added to 0.1M sodium acetate buffer (pH 5.2), and 10 μ l of 30% H₂O₂. This solution was filtered onto the sections and the staining process was monitored under a microscope to obtain optimal colour reaction. Sections were washed again in PBS and mounted in Crystal Mount (Fisher Scientific Inc.). Both positive and negative controls were also performed. Positive controls entailed treating the sections with DNase I buffer (30mM Trizma base, 140mM sodium cocodylate, 4mM magnesium chloride, 0.1mM dithiothreitol) for 5 min at room temperature, following the quenching of endogenous peroxidase. Then sections were treated with DNase I (Roche Molecular Biochemicals) in buffer at a concentration of 25 μ g/ml for 10 min at room temperature, followed by washing in DDW. Negative controls involved omitting TdT from the reaction mixture.

To perform the TUNEL procedure on cultures, cells were treated similarly, but without the proteinase K pretreatment. A final volume of 20 μ l reaction mixture was used

on each culture, and the final fluorochrome Streptavidin-FITC (Calbiochem) was used at a concentration of 1:200, for 1 h at room temperature. Cultures were again washed 3×5 min in PBS and were treated with diamidino-phenylindole (DAPI; Sigma) at a concentration of 0.25µg/ml in PBS at room temperature for 4 min in the dark, to label all the nuclei. Following more washes, the coverslips were mounted on slides with Vectashield (Vector Laboratories Inc.) mounting medium.

POLYACRYLAMIDE GEL ELECTROPHORESIS (PAGE) AND WESTERN BLOTTING

The dissected AV endocardial cushions and the OT were homogenized in protease inhibitor buffer, containing 15µg/ml aprotinin, 1µg/ml leupeptin, 5µg/ml pepstatin, and 1.74mg/ml phenylmethylsulphonyl fluoride (PMSF), and the protein concentration was determined using the Bradford-based Bio-Rad protein assay, with bovine serum albumin (BSA) as a concentration standard. Samples were loaded at a concentration of 10-15µg per lane and run on a 10% polyacrylamide gel for 45 min at 150V, using a Power Pac 200 power supply (BioRad Inc.). The separated proteins were transferred to nitrocellulose membranes, at 100 V for 2 h. The membranes were stained initially with Ponceau red dye (Sigma) to aid in visualisation of even loading of lanes and a successful transfer. The membranes were then subjected to blocking in 5% skimmed milk in TTBS buffer (150mM Tris, 50mM NaCl, 0.1% Tween 20) for 1 h at room temperature. The membranes were probed with primary antibodies diluted in 5% skimmed milk in TTBS overnight at 4°C. The membranes were washed for 3×5 min in 5% skimmed milk and probed with biotinylated secondary antibodies for 1.5 h at room

temperature. After another washing step, the membranes were incubated with the Vectastain ABC (Vector Laboratories) kit for 1.5 h at room temperature, washed again and developed using enhanced chemiluminescent reagent (ECL, Amersham Ltd.). Immunoblots were visualized by exposure to Hyperfilm-ECL (Amersham Ltd.). Immunoblots were scanned to computer with a Microtek Scanmaker X6, and were quantified by densitometric analysis on SigmaGel 1.0 software (Jandel Scientific Inc.). The intensities of each pixel in the band were measured and integrated to give a total value for band density.

ANTIBODIES

The following primary antibodies were used for immunoblotting: Bcl-2 B46620 monoclonal (1:200, Transduction Laboratories; rat, mouse and chick reactive); Bax B-9 monoclonal (1:50, Santa Cruz Biotechnologies Inc; mouse, rat and human reactive); Bak Ab-2 monoclonal (1:50, Oncogene Research Products, Calbiochem); PARP A-20 goat polyclonal (1:50, Santa Cruz; mouse, rat and human reactive); Caspase-9 AAP-109 rabbit polyclonal (1:500, StressGen Biotechnologies Corp). The secondary antibodies used, at a concentration of 1:1000-1:2000, were biotinylated goat anti-rabbit IgG or biotinylated goat anti-mouse IgG (both from Vector Laboratories) or biotinylated rabbit anti-goat IgG (Sigma).

PRIMARY CUSHION CELL CULTURE

Three types of primary cell cultures were made from dissected AV and OT cushions; dissociated cushion cell culture, cushion explant culture, or endocardial cell culture.

For dissociated cushion cell cultures, AV or OT cushions were dissected to ice cold Tyrode's saline, from HH stage 24 hearts (2 dozen/experiment) using electrolytically sharpened tungsten needles. Cells were then dissociated in 2% trypsin/EDTA (Sigma) in calcium/magnesium-free (CMF) Tyrode's saline (6H₂O, KCl, NaHCO₃, NaCl, NaH₂PO₄H₂O, Glucose, pH 7.4) for 10 min at 37°C. Trypsinization was stopped with the addition of 1 ml medium 199 with 10% fetal bovine serum (FBS) (Gibco, BRL). Cells were spun in a benchtop centrifuge for 5 min and the supernatant discarded. The cells were washed in 1ml medium 199 and re-centrifuged for 3 min. Cells were then re-suspended in 100µl complete medium (medium 199 with 10% FBS and 1:1000 gentamycin (Gibco BRL), counted using a hemocytometer slide, and re-suspended in complete medium, for a final volume of 100µl/coverslip. Coverslips for culturing cells were prepared by sonication in DDW for 2-4 h, cleaned with Kimwipes and were sterilised by autoclaving. They were then coated with 10µl type I rat tail collagen working solution, (Gibco, BRL). A 1mg/ml stock solution of collagen was prepared by dissolving collagen (5mg; Sigma) in 5ml of 1:500 acetic acid:DDW overnight at 4°C. For the working solution, this was re-suspended 1:20 with 60% EtOH, and NaOH added to a final concentration of 15mM. The collagen coated coverslips were exposed to ultraviolet light overnight. 100µl of the cell suspension was added to each and the cultures were incubated overnight at 37°C in a 5% CO₂ incubator. Cultures were given fresh complete

medium every second day for 4-6 days. Serum starved cultures were treated in the same way, with FBS absent from the medium. Following treatment, the cultures were stained with TUNEL, as outlined. As each dissociated cushion culture was seeded with the same cell number, in the same volume, the total number of TUNEL positive cells per culture were counted using a fluorescence microscope and compared. Statistical analysis using one-way Anova and Tukey's multi comparison post test was performed on the total number of positive cells.

For primary cultures of cushion and ventricle explants, the dissected tissue was placed directly onto collagen gels that had been pre-soaked with complete medium and the medium removed. The explant was allowed to attach for 4-6 hours at 37°C in a 5% CO₂ incubator, and 1ml complete medium was added. The cultures were grown for 18, 24 or 30 h. and were then stained with TUNEL or Annexin-V. TUNEL staining was performed as described. Annexin-V staining using the Annexin-V-FITC labeling kit (Clontech Laboratories) was performed as outlined by the manufacturers instructions. The cultures were rinsed with PBS. The labeling solution was prepared by mixing 10µl Annexin-V-FITC with 200µl binding buffer. To each explant culture, 10µl of the labeling mixture was added for 10 min at room temperature. The cultures were then fixed in 4% PFA in PBS for 15 min at room temperature. They were then rinsed and mounted using Vectashield mounting medium.

Primary cultures of the endocardial cell layer that lines the heart were also made, according to the method of Runyan and Markwald (1983). Collagen-coated coverslips were prepared as described. The endocardial cushions were dissected and placed on the collagen, with the endocardial endothelium facing the collagen, at 37°C in a 5% CO₂

incubator. After four hours, the cushion explant was removed, leaving endocardial endothelial cells on the surface of the collagen. The cultures were infected with RCAS virus containing transcripts for BMP receptors as described below. Measurements of the cell area and aspect ratio were made after capturing the cell image using Image Pro software. For cell area measurements, the outline of the cell was traced and the area calculated using an arbitrary scale. Measurements were made on ten cells in each treatment. The aspect ratio was measured by dividing the long axis of the cell by the short axis, with values closer to one representing rounder cells, and elongated cells having higher numbers. Values were on an arbitrary scale, for ten cells in each treatment. For both cell area and aspect ratio measurements, the results were analyzed and compared to the uninfected control with one-way ANOVA and Tukey's post-test.

For cell death measurements in the culture experiments, the total number of cells and the total numbers staining with TUNEL or Annexin-V were counted using a MTI CCD camera connected to a Leica DMRBE fluorescence microscope. The cells counted were spread on the collagen layer and images of a set field of view on the camera were captured on computer. For counts of the total number of cells / culture, the total number of stained cells were counted in every second field of view, such that the entire culture area was covered and the resulting counts doubled to give an estimate of the total number of cells per culture. For counts of apoptotic cells, the total number of cells staining with TUNEL in each culture were counted. For the dissociated cell cultures, the results were expressed as the total number of TUNEL-positive cells per culture compared to the untreated control. For the explant cultures, the results were expressed as the percentage of the total cells staining with TUNEL or Annexin-V.

CUSHION CULTURE IMMUNOCYTOCHEMISTRY

Primary cell cultures were prepared as described above. For mitochondrial labeling, MitoTracker Red® CMXRos (Molecular Probes Inc.) was used, by addition of 5µl of 10µM MitoTracker® to 1ml of medium. Cultures were incubated in this reagent for 45 min at 37°C, then washed in warm Tyrode's solution and fixed with 4% paraformaldehyde in PBS, for 45 min at room temperature. Cultures were washed 3×5 min in PBS, and treated with blocking solution of 10% serum (goat or rabbit) in PBS with 0.5% Tween 20 for 30 min at room temperature. Cultures were incubated with the primary antibodies overnight at 4°C in 1% serum with 0.5% Tween 20. Cells were then washed 3×5 min in PBS. Biotinylated secondary antibodies were added for 1 h at room temperature, and then washed three times in PBS. Cells were then fluorescently labeled with streptavidin-FITC at a concentration of 1:200 in 1% serum with 0.5% Tween 20, for 1 h at room temperature in the dark. The cultures were washed again 3×5 min in PBS, and stained with DAPI for 4 min at room temperature. Cells were washed 3×5 min in PBS and mounted on slides with Vectashield mounting medium. Specimens were examined using a Zeiss LSM510 confocal microscope equipped with argon, helium/neon and ultraviolet lasers. For immunocytochemical / TUNEL double labeling, the TUNEL technique was performed first, as described, to the step of fluorochrome addition. Then the immunocytochemistry protocol was followed to the stage of secondary antibody addition. The Streptavidin-FITC (for TUNEL detection) and a Texas-red conjugated secondary antibody were mixed in 1% serum with 0.5% Tween 20 and added together for 1 h at room temperature, and the staining protocol followed as described.

ANTIBODIES

Primary antibodies used were as described for immunohistochemistry for bcl-2 and bax at a concentration of 1:200, and the monoclonal AMV-3C2 anti-viral coat protein antibody supernatant (University of Iowa Developmental Studies Hybridoma Bank) was used undiluted. The secondary antibodies used, at a concentration of 1:200 were, biotinylated goat anti-rabbit IgG or biotinylated goat anti-mouse IgG (both from Vector Laboratories). For fluorescence double labeling, Texas-red conjugated anti-rabbit IgG (Calbiochem) was used at a concentration of 1:200.

CUSHION CULTURES WITH CASPASE INHIBITORS

Primary dissociated cushion cultures were prepared as described and serum starved to induce apoptosis. The cultures were then treated with specific peptide caspase inhibitors. The following peptide caspase inhibitors were used: caspase-3 inhibitor II (Z-DEVD-FMK); caspase-9 inhibitor I (Z-LEHD-FMK), (both from Calbiochem). A universal caspase inhibitor (BOC-Asp(OME)-FMK) (Enzyme Systems Products Inc. Livermore, CA) was also used to inhibit all caspases. All inhibitors were dissolved in dimethyl sulfoxide (DMSO) at a concentration of 50mM, aliquoted and stored at -20°C. Caspase inhibitors were added to fresh medium 199 without serum, which was added to cultures every other day, at a final concentration of 50µM. After 4-6 days, cells were washed in PBS and fixed in 4% paraformaldehyde in PBS and stained with TUNEL and DAPI. Cultures were then mounted with Vectashield mounting medium. The total number of cells staining with both TUNEL and DAPI were counted and the results were analyzed using one-way Anova and Tukey's multiple comparison post test.

CUSHION CULTURES WITH CONDITIONED MEDIUM

Conditioned medium was prepared from various regions of the developing heart, for addition to dissociated cushion culture. The different regions of the heart dissected were: the atrioventricular cushions, the outflow tract cushions, the atrioventricular cushions with myocardium, the outflow tract cushions with myocardium, and the ventricle. Each region was dissected, dissociated and cultured as described previously, for a period of 5-7 days in collagen-coated 24-well tissue culture plates (Nunc). At the end of the culture period, the medium was collected from each well and like samples were pooled. The freshly collected medium was added to 24 hr cultures of either dissociated AV and OT cushions, for a period of 12 hours. Following this incubation, the cushion cultures were washed 3 times in PBS, fixed and stained with TUNEL and DAPI. The total number of TUNEL positive cells and the total number of cells were counted and were analyzed statistically using Anova and Tukey's multiple comparison post-test.

DiI LABELLING

To label premigratory neural crest cells, *in ovo* microinjection of the fluorescent lipophilic dye DiI (Molecular Probes, Inc.) was used. The dye was prepared by dissolving 3mg of DiI in 0.1ml of 100% ethanol. This was then diluted with 1.1ml of 3% bovine serum albumin (BSA) in PBS (Bagnall, 1992). Eggs were windowed and the dye was injected into the lumen of the neural tube of HH stage 9-11, using a Picospritzer (General Valve Corp.). Subblastodermal injection of India ink was used as a contrast agent (prepared by mixing 3 drops of ink in 5ml egg yolk). Following the injection, the eggs were sealed with Scotch tape and were reincubated for 3-4 days. After this time, the

embryos were dissected and the heads removed from the body. They were then fixed in 4% paraformaldehyde in 0.1 M PBS overnight at 4°C and then were embedded in OCT compound. The specimens were then frozen and sectioned at 10µm. The frozen sections were stained with DAPI for 4 min at RT and mounted with Vectashield mounting medium. The slides were examined using a Zeiss LSM510 confocal microscope equipped with argon, helium/neon and ultraviolet lasers.

RETROVIRAL OVEREXPRESSION

PLASMID AMPLIFICATION AND PURIFICATION

The retroviral vectors pRCASBP(B)-*bcl2* and pRCASBP(B) plasmids (donated by Dr. S.H. Hughes, Frederick Cancer Research and Development Centre, Maryland) were amplified as follows. 50µl aliquots of frozen E.coli (XL1-Blue) were thawed on ice. To this, 2.5µl of plasmid (either *bcl-2* or negative control) DNA was added, mixed and left on ice for 30 min. The mixtures were then heat shocked in a circulating water bath at 42°C for exactly 1 min. The mixtures were then placed back on ice for 4 min. To each, 450µl prewarmed LB broth (BBL, Becton Dickinson) was added and the mixtures were then placed in a shaking incubator at 37°C for 1 h at 220-250 rpm. The mixtures were plated on LB agar (BBL, Becton Dickinson) plates, with 50µg ampicillin (Gibco BRL), and incubated overnight at 37°C. Following incubation, individual colonies were selected and inoculated into 10ml LB broth containing 50µg ampicillin. The cultures were then incubated for 12-16 h in a shaking incubator at 37°C at 220-250 rpm and were then centrifuged at 3000 rpm for 10 min to collect the bacterial cells. The Qiagen plasmid mini-prep kit was used to isolate the plasmid DNA from the bacterial pellet, according to

the manufacturers instructions. The absorbance of the final solution was read at a wavelength of 260nm to determine the isolated plasmid DNA concentration.

CHICK EMBRYO FIBROBLAST CULTURE

Primary cultures of chick embryo fibroblasts (CEF's), compatible with subgroup B retrovirus were made from specific pathogen free line 0 embryos (Hyvac, Adel, Iowa). The embryos were removed from ED 10 eggs, the head and viscera removed and the trunk tissue from 3-4 embryos was placed a petri dish. The tissue was minced with a sterile spatula, 10ml sterile Tyrode's solution was added and the tissue was pipetted to dissociate it. To this, 2ml 1X Trypsin/EDTA (Sigma) at 37°C was added, pipetted for 1 min to dissociate the tissue and allowed to stand to let the clumps settle. The supernatant was then transferred to a sterile 50ml conical tube on ice, with 10ml ice cold CEF medium (Medium 199 (Gibco, BRL), 10% FBS, 2% chick serum (CS; Gibco, BRL) and 1% penicillin/streptomycin). To the remaining undissociated clumps of tissue, another 10ml Tyrode's saline and 2ml 1X Trypsin/EDTA was added, dissociated as before, and allowed to settle. The supernatant was transferred to the conical tube with the other supernatant and the suspension was centrifuged at 1000 rpm for 10 min. The supernatant was discarded and the pellet was resuspended in 20 ml fresh CEF medium. From this, 3ml was added to 10cm tissue culture plates (Greiner), and each volume was brought to 10ml with CEF medium. The cultures were incubated at 37°C in 5% CO₂ and were passaged when confluent.

TRANSFECTION OF CHICK EMBRYO FIBROBLASTS

CEF cultures were transfected with the retroviral vectors pRCASBP(B)-*bcl2* and pRCASBP(B) using Cytofectin GS transfection reagent (Glen Research Inc.) For transfection of each 10ml tissue culture plate, 10µl cytofectin reagent was mixed with 200µl serum free Opti-MEM medium (Gibco BRL) for a final concentration of 10µg/ml cytofectin. Plasmid DNA (*bcl-2* or the negative insert) was diluted in 200µl Opti-MEM medium to give a final concentration of 2µg/ml. The cytofectin/Opti-MEM solution and the DNA/Opti-MEM suspension were mixed and left to stand at room temperature for 20 min. Then, 3.6ml Opti-MEM with 10% FBS and 1% penicillin/streptomycin was added to each. The medium was removed from P0-P1 CEF cultures that were 60-70% confluent and the DNA / transfection mixture was added for 5 h at 37°C in 5% CO₂. Following this, another 4ml Opti-MEM with 10% FBS and 1% penicillin/streptomycin was added and the culture incubated at 37°C in 5% CO₂. The cells were passaged 2-3 times with a 1:5 split over 2-3 weeks. Cells were passaged in complete CEF medium supplemented with 8 µg/ml polybrene (Sigma), which aids in the infection of cells by virus with subgroup B envelope receptors.

VIRAL COLLECTION AND CONCENTRATION

Following the final split, when the cells reached 70-80% confluence, the medium was removed and replaced with reduced serum medium (M199, 2% FBS, 0.2% CS) overnight. This medium was removed, stored at 4°C, and replaced with a second batch of reduced serum medium overnight. Following this, the two batches of medium were combined and the cells discarded. The combined media was filtered using a Nalgene

150ml 0.45µm filter. The media was divided into polyallomer SW28 tubes (Beckman Instruments Inc.) and was centrifuged for 2.5 h at 25,000 rpm at 4°C. Immediately after centrifuging, the supernatant was poured off and the pellet was allowed to air dry. To each tube, 100µl Opti-MEM was added. The tubes were placed in an ice bucket and put in a cold room overnight to allow the pellet to resuspend. The next day, the viral suspensions were pooled and separated into 25µl aliquots. The aliquots were frozen on dry ice and transferred to a -80°C freezer for storage. Viral titer was obtained by serial dilution and infection of CEF's for 48 h. Cells were immunostained for the viral coat protein and the number infectious virions calculated as 5.0×10^7 per ml.

CUSHION CULTURES WITH RETROVIRUS

Dissociated primary cushion cultures were prepared as described. Cells were infected with virus after the first overnight incubation. For infection with RCASBP(B)-*bcl-2* / RCASBP(B), the initial 100µl medium was removed and replaced with fresh 100 µl complete medium containing 5µl concentrated virus with 8µg/ml of the polycationic polymer polybrene overnight. Then 1ml of medium with no serum was added every other day for 4-6 days. No other virus was added during the subsequent medium changes, but fresh polybrene was included in each medium change. Following the culture period, cultures were stained with DAPI, Mitotracker Red, and an antibody to *bcl-2* or the viral coat protein. The total number of TUNEL positive cells per culture was counted and analysed using Anova and Tukey's multiple comparison post test.

Retroviral overexpression *in vitro* was also performed using RCAS vectors containing constructs for BMP receptors. The RCASBP(A) vectors contained transcripts

for each of BMPR-IA and IB constitutively-active and dominant-negative receptor isoforms. These were supplied by Dr. C. Logan, University of Calgary, as unconcentrated viral supernatant that had been tested for insert stability. For infection of cultures, the culture medium was removed and was replaced with unconcentrated viral supernatant with 5% FBS added, for 24 h. This was replaced with fresh medium without serum every other day, for 4-5 days. No polybrene was used for subgroup A virus. Following the culture period, the cultures were stained with DAPI, TUNEL and an antibody to the viral coat, and the total numbers of TUNEL staining cells were compared. Preliminary staining with PCNA was also performed.

VIRAL MICROINJECTION

Eggs were windowed at stage HH 12-16. Viral supernatant was prepared by adding 1/10 vol. fast green and methylcellulose to the viral concentrate. Polybrene was added to give a final concentration of 8µg/ml. The solution was loaded into pulled glass micropipettes, which were then loaded into a Picospritzer (General Valve Corp.). The viral supernatant was injected into the pericardial sac, as shown in Figure3-1. If possible in some embryos, the pipette was placed into the heart and viral solution injected into the cushion regions. After injection, 300µl of a 1% penicillin/streptomycin solution was added. The windows were sealed with Scotch tape and the embryos re-incubated for 3-5 days. The embryos were then dissected, fixed in 4% paraformaldehyde and processed for immunohistochemistry.

ELECTROPORATION

High concentration DNA was generated by transformation of *E.coli* and large-scale plasmid purification by Cs-Cl gradient (performed by Dr. C. Logan, University of Calgary). The initial pRCASBP(B)-*bcl-2* plasmid was used for amplification, as well as RCASBP(B)-GFP as a control. The resulting DNA was further concentrated to give a final concentration of 1mg/ml. Fast green was added at a volume of 1/10 the total volume. Eggs were windowed at HH stages 9-16, for various treatments. The concentrated DNA was loaded into pulled glass micropipettes and connected to a pneumatic pico pump (PV820, WPI). The concentrated *bcl-2* DNA was used at a concentration of 1mg/ml and the GFP DNA at a concentration of 820µg/ml. The loaded pipette was lowered near the heart. The electrodes of the electroporator (ECM830, BTX) were placed either side of the embryo, parallel to the heart region. Then, 300µl of ice-cold Ringer's solution with 1% penicillin/streptomycin was added to temporarily stop the heart. While the heart was stopped, the loaded pipette was pushed through the outflow tract and the lumen was filled with DNA. The electroporator was activated to pulse the DNA. Various pulse numbers and durations were tried, to optimize delivery of both DNA samples. These were; 5 x 25 ms pulses, 25V; 10 x 50 ms pulses, 25V; 8 x 25 ms pulses, 25V, or 10 x 25 ms pulses, 25V. Following electroporation, the eggs were sealed with scotch tape and re-incubated. Following another 3-5 day's incubation, the embryos were then dissected, fixed in 4% paraformaldehyde and processed for immunohistochemistry.

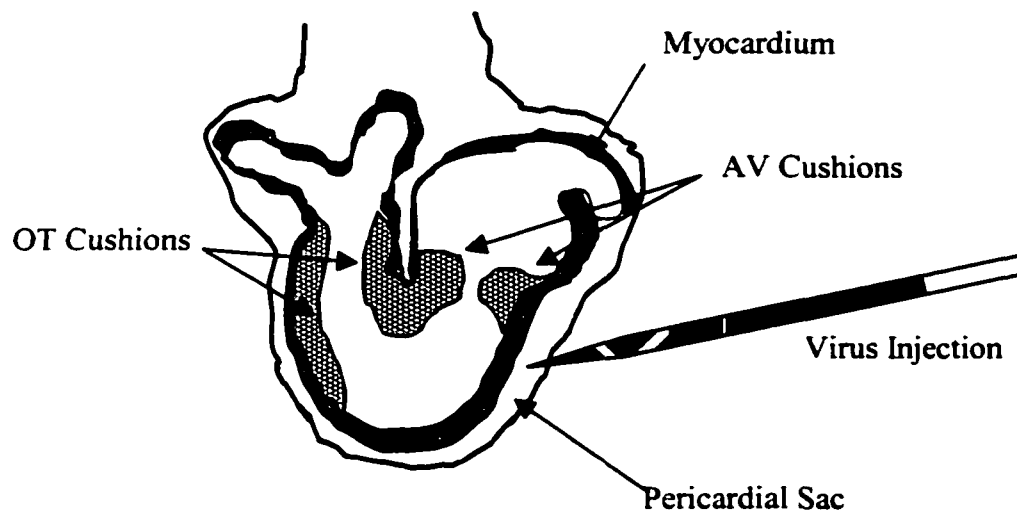


Figure 3-1. Schematic diagram showing site of viral injection

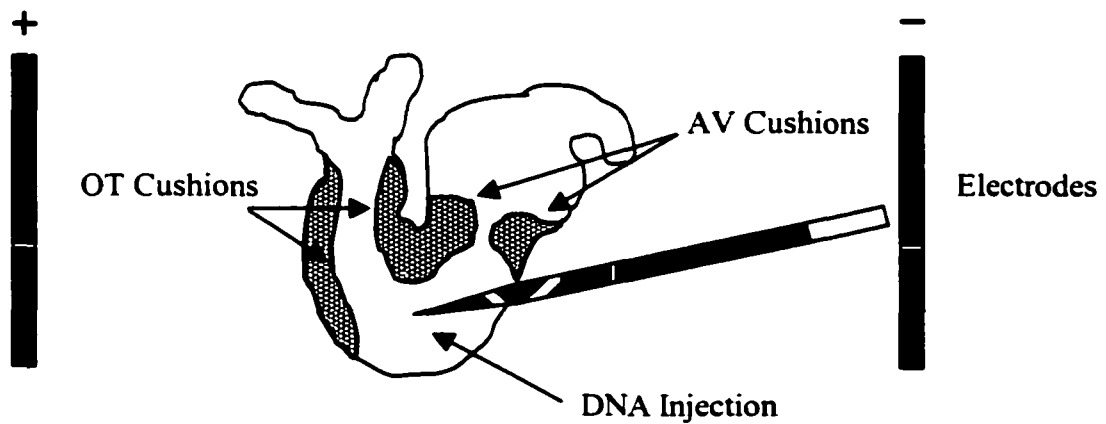


Figure 3-2. Schematic diagram showing site of DNA injection for electroporation

Chapter 4

**DISTRIBUTION OF CELL DEATH AND PROLIFERATION
IN THE ENDOCARDIAL CUSHIONS**

DISTRIBUTION OF DYING CELLS IN THE DEVELOPING HEART

To assess the distribution of cell death during early heart development, staining for the fragmenting DNA of apoptotic cells was performed on heart sections. This was correlated with staining for proliferating cells, and the use of a cell culture model to attempt to determine the pattern and source of the signal for apoptosis in these cells. As it is speculated that some of the dying cells may be of neural crest origin, fluorescent labeling of premigratory neural crest cells was performed to identify if any of these cells were dying.

DISTRIBUTION OF TUNEL POSITIVE CELLS IN THE ENDOCARDIAL CUSHIONS

Sections of the embryonic chick heart were stained using the TUNEL technique to label apoptotic cells. from ED 4 – 8 chick embryos . TUNEL-positive cells first appeared in the chick embryo heart in the endocardial cushions of the outflow tract (OT) at stage HH 25 (ED4) (Figure 4-1). Positive cells were present throughout the length of the OT, from the more distal truncal cushions (Figures 4-1 a and b) to the proximal conal cushions, where the OT joins the primitive ventricle (Figures 4-1c and d). Labeled cells were present throughout the cushions, with no apparent localisation to any particular region. The OT cushions appeared more cellularised at this stage than the AV cushions (not shown). At stage 27 (ED5) the dying cells appeared throughout the cushions (Figure 4-2a). However no cell death was seen in the condensed mesenchyme of the aorticopulmonary septum (Figure 4-2b). Cell death persisted from the distal regions, through to the proximal cushions (Figure 4-2c) and into the inner curvature of the rotating

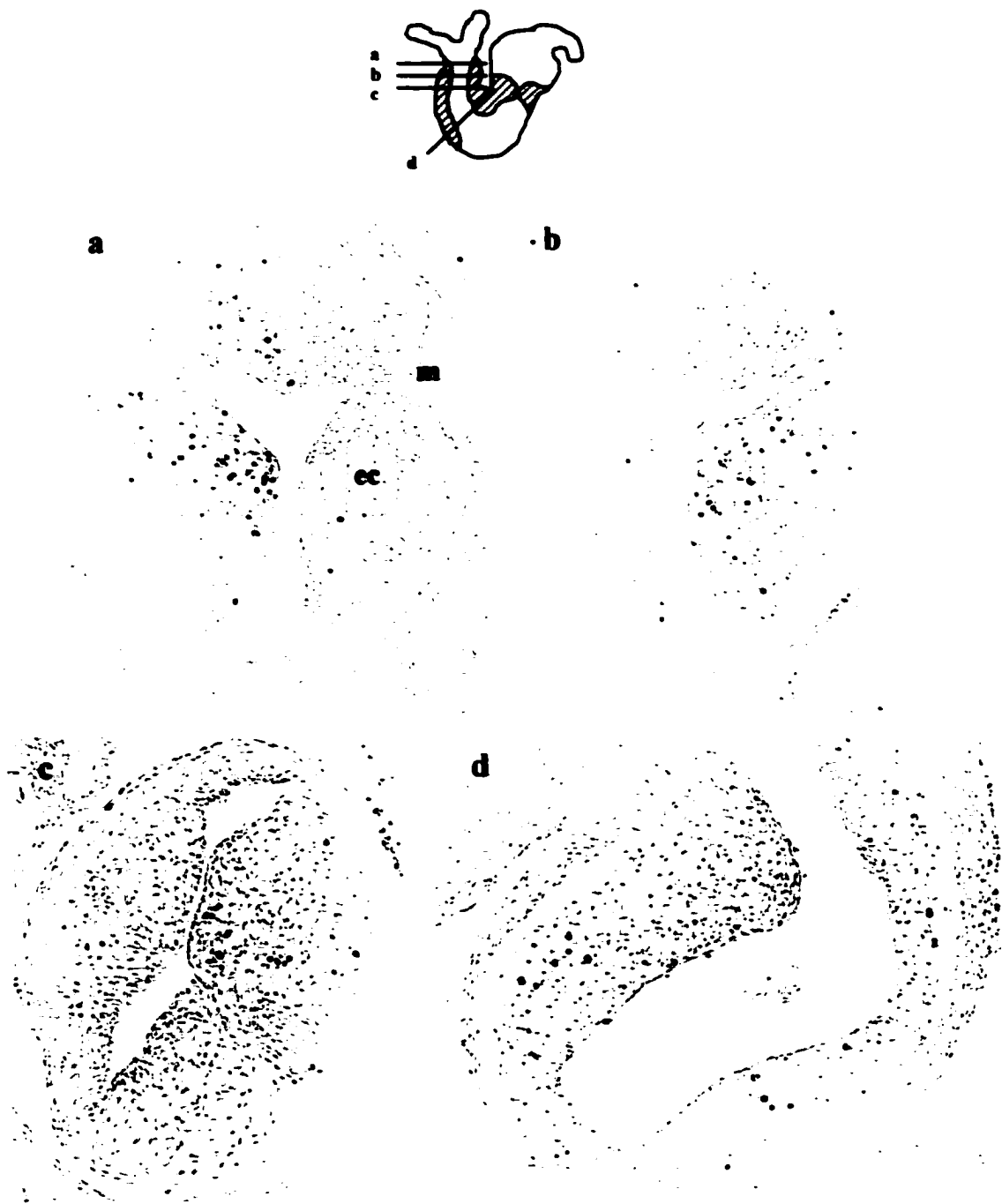


Figure 4-1. TUNEL labeling of apoptotic cells in ED4 chick outflow tract (OT). (a) Scattered TUNEL positive cells in the endocardial cushions (ec) of the distal truncal OT, with few positive cells in the myocardium (m). (b) More TUNEL positive cells in the distal OT. (c) TUNEL positive cells are also found in the more proximal OT cushions. (d) TUNEL positive cells are seen in both ridges of the proximal conal OT cushions. Mag. x140, a-d.

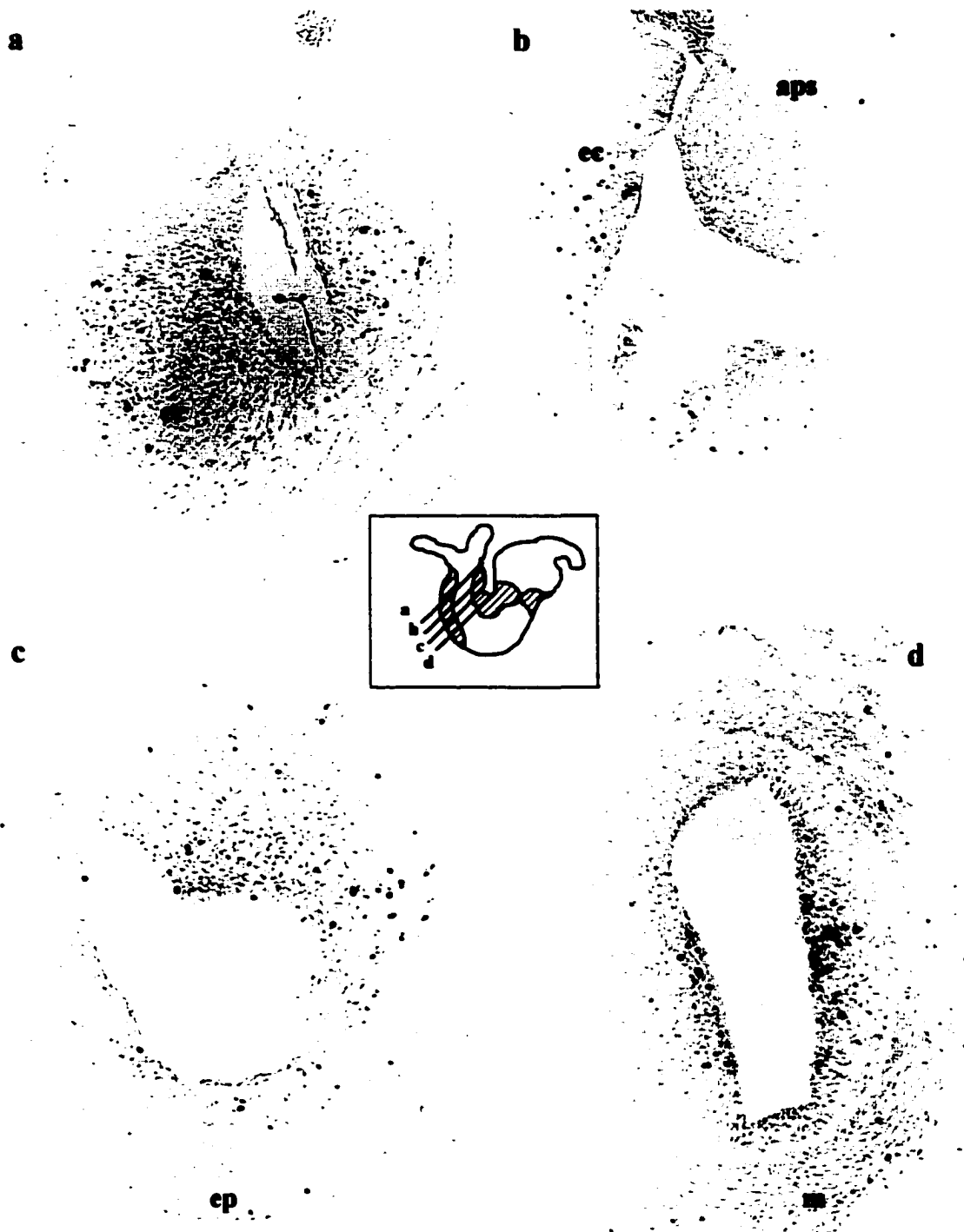


Figure 4-2. TUNEL labeling of apoptotic cells in the ED5 chick outflow tract (OT). (a) TUNEL positive cells are seen scattered throughout the endocardial cushions (ec) of the OT. (b) Positive cells are seen in the endocardial cushions (ec), but with no apparent association with the aorticopulmonary septum (aps). (c) TUNEL positive cells are seen throughout all levels of the OT cushion, and occasional positive cells are seen in the epicardial layer (ep). (d) Dying cells continue in expression in the cushions of the inner curvature of the developing heart, and occasionally are seen in the OT myocardium (m). Mag. x140, a-d.

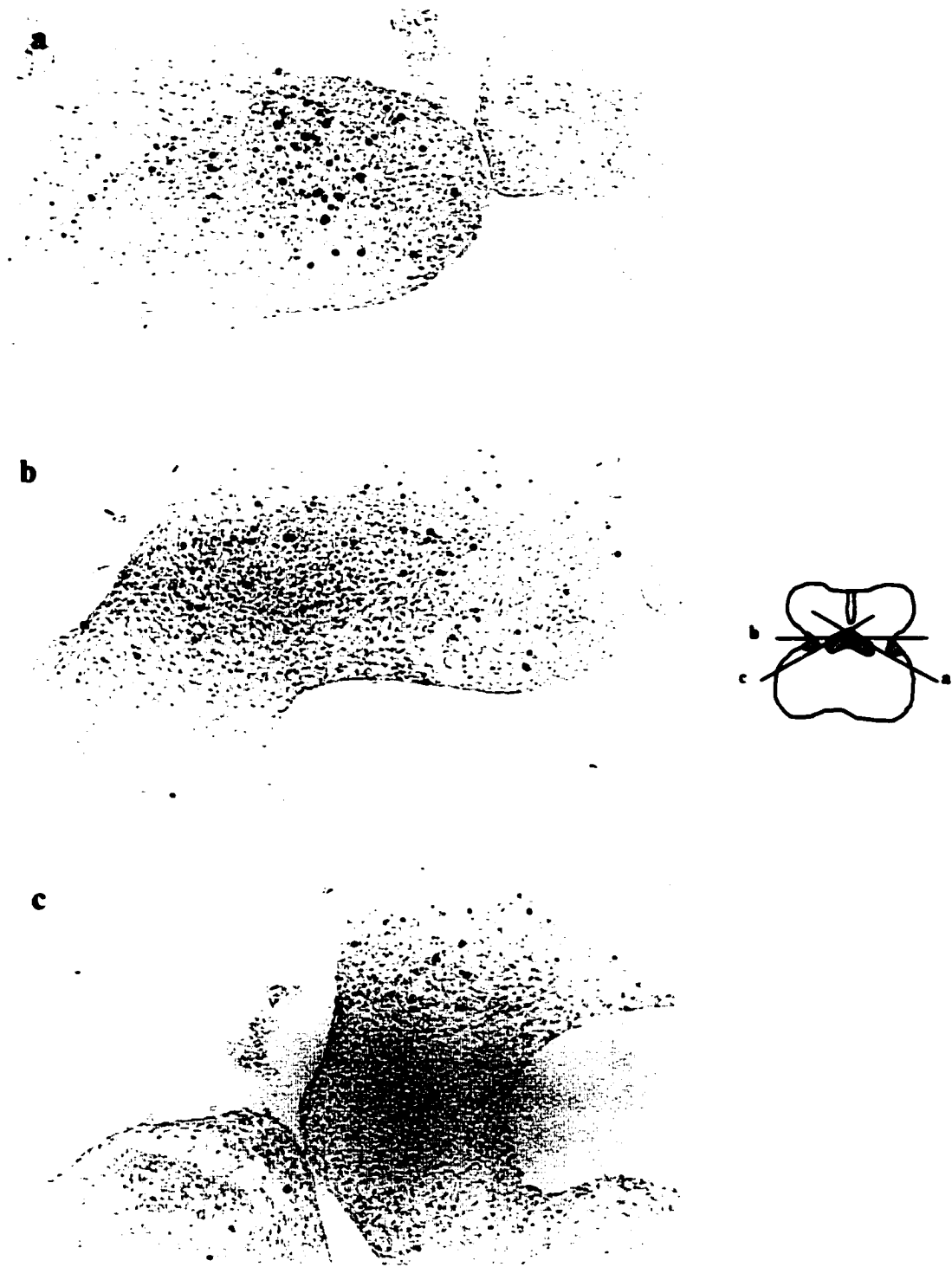


Figure 4-3. TUNEL labeling of apoptotic cells in the ED6 chick atrioventricular cushions. Scattered TUNEL positive cells can be seen in the left (a), central (b) and right (c) aspects of the central mass of AV cushions. Mag. x140 a-c.

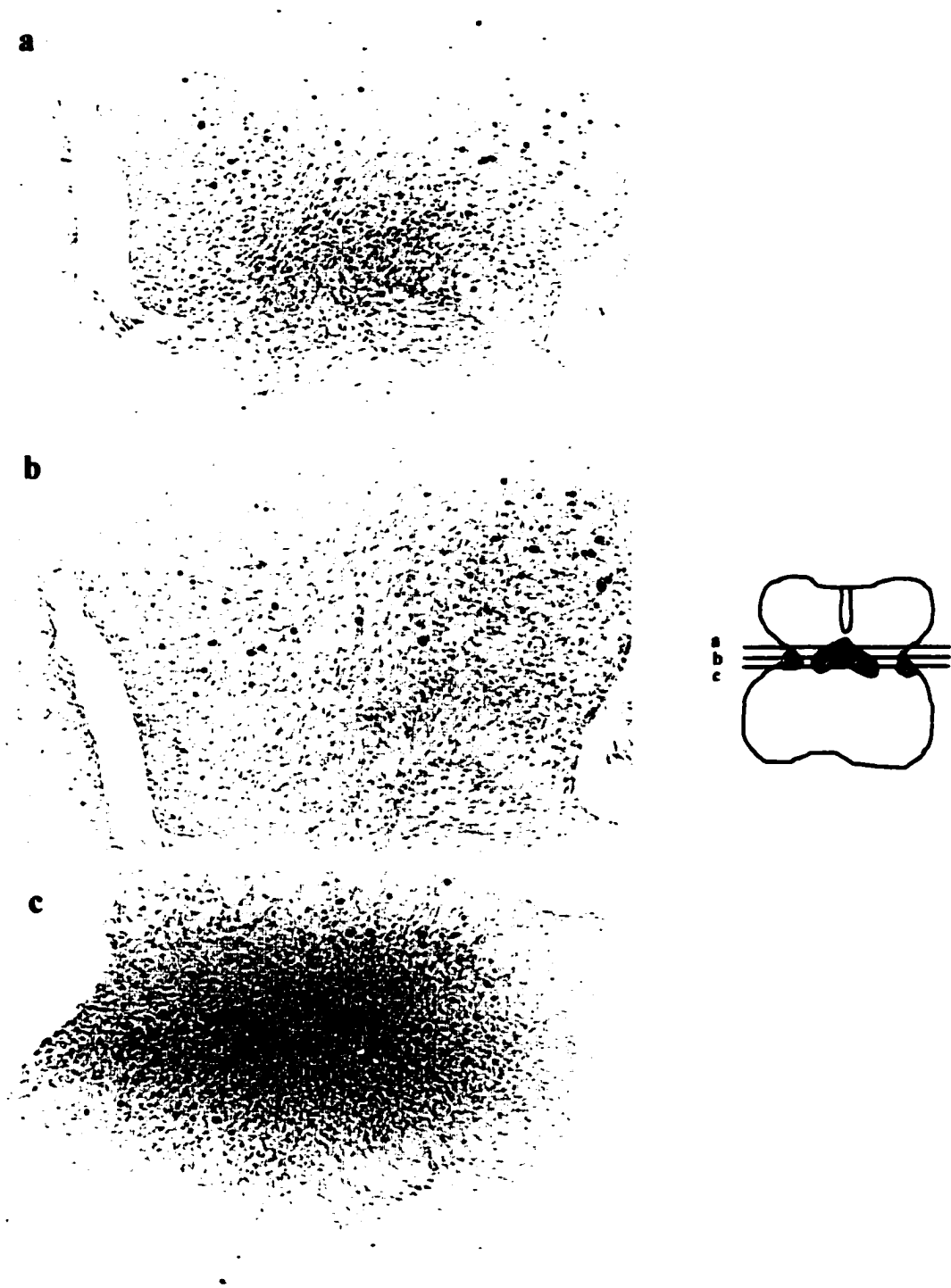


Figure 4-4. TUNEL labeling of apoptotic cells in the ED7 chick atrioventricular cushions. Scattered TUNEL positive can be seen in the developing valve leaflets, through the rostral (a), central (b) and caudal (c) levels of the central mass of AV cushions. Mag. x140, a-c.

OT, where the conal cushions meet with the ventricle (Figure 4-2d). At stage 29-30 (ED6), in the OT cushions, a significant number of dying cells were still present below the level of the semilunar valve and at the junction of the ventricle (not shown). By stage 31 (ED6), the OT was well differentiated and separated into the aorta and pulmonary trunk in the distal regions, with a reduction in the levels of dying cells that were seen. In the most proximal regions of the OT, however, where the cushions were not completely cellularised, some positive stained cells remained.

In the AV cushions, at stage 26, the dorsal and ventral cushions are in the early phases of fusion, but no apoptotic cells were present in the incipient fusion seam. By stage 27, in the central fused AV cushions, a few TUNEL positive cells were present, but there were none in the region of active fusion. By stage 29-30 (ED6) (Figure 4-3 a-c) foci of intense cell death were observed from the left through to the right aspects of the fused central mass of AV cushions. However, no apoptotic cells stained in the lateral cushions, which also contribute to the leaflets of the mitral and tricuspid valves. By stages 31-32 (ED7) (Figure 4-4), valve structure was also now obvious, with cell death persisting from the more rostral regions of the cushions, through to the tips of the developing valve leaflets which projected into the ventricular cavity (Figure 4-4 a-c). Again, only the central AV cushions contained positive cells. It should be stressed that only individual isolated apoptotic cells were ever seen in the ventricle, atrial walls or epicardial cushions (as in Figure 4-2 c and d), and these were not consistently located between different specimens.

When examined at a higher magnification, the TUNEL technique was shown to label both fragmenting nuclei, with the characteristic blebs of the apoptotic cells visible,

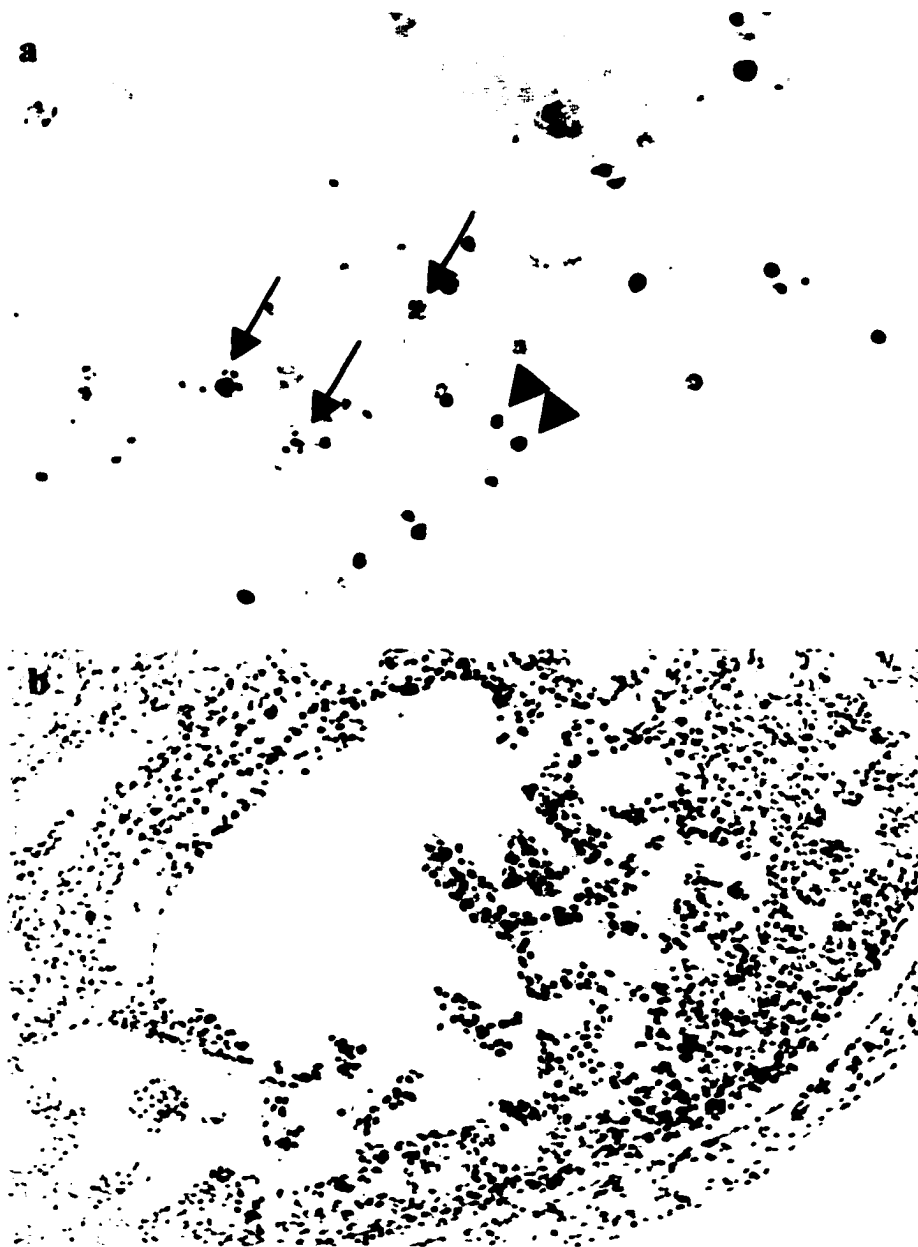


Figure 4-5. TUNEL labeling in the embryonic heart. (a) High magnification of TUNEL positive cells in the AV endocardial cushions showing the characteristic blebs of apoptotic cells (arrows) and the condensed nuclei of early stage apoptotic cells (arrowheads). Mag. x560. **(b)** A positive control for TUNEL in the heart ventricle showing positive labeling of all the cells after treatment with DNA'se. Mag x280.

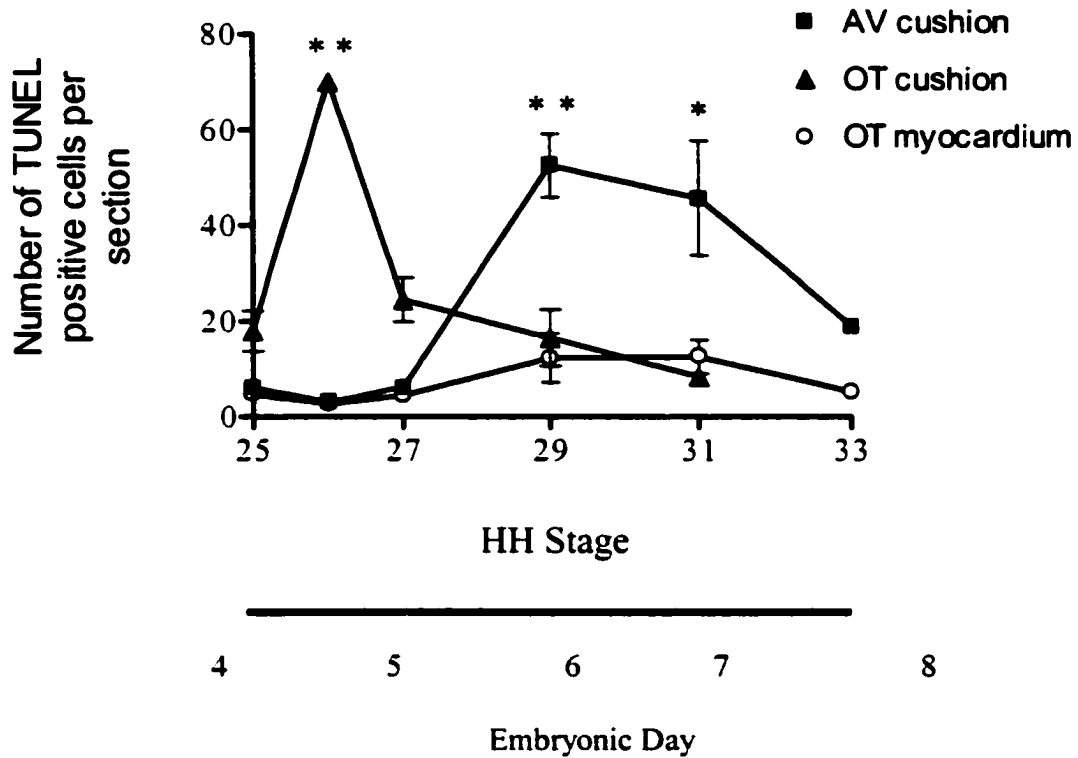


Figure 4-6. Quantification of TUNEL positive cells in endocardial cushion sections. The total number of TUNEL positive cells per section in the areas of the OT and AV cushions and the OT myocardium were counted from HH stages 25 – 33. A range of 8-12 sections per embryo, for 2-3 embryos per stage were counted in total. The data shown represents the mean number of TUNEL-positive cells per section \pm SEM, at each developmental stage, analysed using one way ANOVA and Tukey's post test. Peak cell death is observed in the OT cushions at ED 4-5 (**= $p < 0.01$ compared to each stage), while peak cell death is seen in the AV cushions at ED 6-7 (**= $p < 0.01$; *= $p < 0.05$, compared to each stage). A more prolonged but lower level of dying cells is seen from ED 4 – 8 in the OT myocardium.

and pyknotic nuclei of earlier stage apoptotic cells (Figure 4-5a). The positive control for the TUNEL technique entailed treating the sections with DNA'se, to cleave the DNA in every cell, which subsequently stained positively (Figure 4-5b).

Quantification of the total number of TUNEL positive cells in both the AV and OT cushions is shown in Figure 4-6. Quantification of TUNEL staining on sections involved counting the number of TUNEL-positive cells per 8 μ m section, in the areas of the AV and OT cushions, and the OT myocardium. The sectional tissue area counted was similar for each stage. The average number of TUNEL-positive nuclei was determined for each area and plotted for HH stages 25-33. For each stage, two to four embryos were counted with a range of eight to twelve sections per embryo.

This graph shows that apoptosis occurs in two waves; first, in the OT cushions from HH stages 25 – 31, peaking at stage 26 (ED 4-5), and second in the AV cushions, from HH stage 27 – 33, peaking at stage 29 (ED 6). A lower level of cell death was seen in the myocardium of the OT, lasting from around HH stage 25 to around stage 33 (ED 4 – 8) (example in Figure 4-2d).

DISTRIBUTION OF PROLIFERATING CELLS IN THE ENDOCARDIAL CUSHIONS

Sections of the embryonic chick heart were stained using a monoclonal antibody to proliferating cell nuclear antigen (PCNA), to label proliferating cells. At HH stage 26, in the distal and mid-levels of the OT cushions, only a few PCNA immunoreactive cells were present, dispersed in the cushions (Figure 4-7a). In the proximal cushions and at the fusion of the cushions with the ventricle, there were not as many cells as in the more

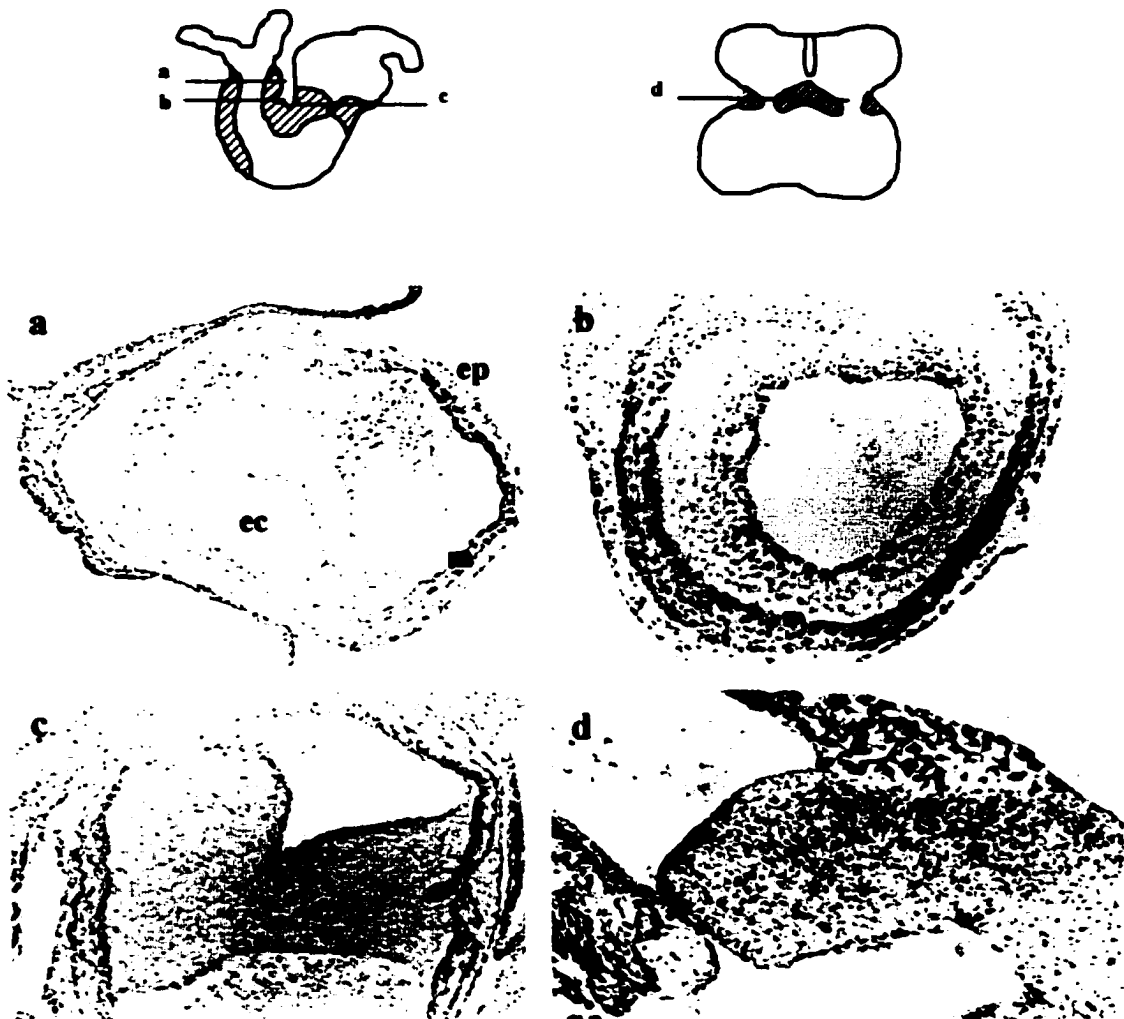


Figure 4-7. Immunocytochemical localization of proliferating cell nuclear antigen (PCNA) in the endocardial cushions. (a) Stage 26 outflow tract stained for PCNA shows positive staining in the myocardium (m) and epicardium (ep), but with only a few positive cells in the endocardial cushions (ec). (b) Stage 27-28 OT stained for PCNA shows strong staining in the myocardium and epicardium. The staining in the endocardial cushions is localized towards the endocardium. (c) Stage 26 in the fusing AV cushions shows a concentration of proliferating cells at the fusion points. (d) By stage 29, extensive PCNA immunoreactivity is seen throughout the AV cushions. Mag x140, a-d.

advanced distal regions, and here positively stained cells were located towards the endocardial layer of the cushions (not shown). The myocardium of the OT at this stage stained uniformly positively for proliferating cells throughout its length (Figure 4-7a). The AV cushions are fusing at this stage, and showed cells which were immuno-positive for PCNA at the fusion points (Figure 4-7c). In the unfused areas of these cushions, cell proliferation was seen in the tips of the dorsal and ventral cushions. At all stages examined, the atrial wall and ventricular trabeculae were immunolabelled throughout, as were cells in the narrow epicardial cushion layer (not shown).

At stage 27-28, the OT cushions were more cellularised than before, and positively stained cells predominantly appeared in, and adjacent to, the endocardial layer (Figure 4-7b), with staining diminishing towards the myocardium, where there was less cellularisation. Again, the myocardial layer was stained throughout, as was the epicardium. In the AV cushions, proliferating cells persisted at the growing tips of the developing leaflets, but remained sparse within the cushions.

By stage 29, the OT cushions were fully cellularised and the valve structure was becoming apparent. A uniform distribution of positively stained proliferating cells was present throughout the length of the OT, the cushions, the valves, myocardium and epicardium (not shown). The cells of the AV cushions (Figure 4-7d) were also now stained throughout.

CELL DEATH LEVELS IN EXPLANT CUSHION CULTURES

To determine if apoptosis occurred in a time-dependent programmed manner in the endocardial cushions, cultures were made of explanted AV cushion tissue grown for

different times. The levels of cell death in the cultures were measured by TUNEL and Annexin-V staining. Cultures were made from ED 4 and ED 5 AV cushions, at a time that precedes the onset and peak levels of cell death *in vivo*. The cultures were grown for 18, 24 or 30 hours, at which point the cells are at a stage that corresponds to the timing of *in vivo* apoptosis. Figure 4-8A shows an example of an AV cushion explant by phase contrast microscopy, after 12 hours in culture and also stained by TUNEL. The outgrowing cells can be seen spreading from the explant onto the collagen gel. When stained by TUNEL, the explant contains some positive apoptotic cells at the edge of the explant (Figure 4-8Aii-arrows). The cultures were left for the specified periods of time and stained using TUNEL (Figure 4-8B) or Annexin-V. The total number of cells staining with each label and the total number of cells in the outgrowth area of each culture in each culture was counted. The cells analysed using this technique were the cells that migrated away from the initial explant that had been placed on the coverslip. Dying cells in or attached to the initial explant were not included. It was subsequently concluded that the migrating cells may not be representative of the cells that were actually dying *in vivo*, so future culture experiments used dissociated cushions in culture as described. To allow for variation in the size of the initial explant, and the resulting culture outgrowths, the number of apoptotic-staining cells was expressed as a percentage of the total number of cells for each time-period, with each stain.

In the AV explant cultures, when the total number of TUNEL staining apoptotic cells is expressed as a percentage of the total number of cells, there is an increase in levels of cell death when the ED4 cushions are cultured for 24 hours (Figure 4-9A). Similar cultures were also stained using Annexin-V, to label early stage apoptotic cell

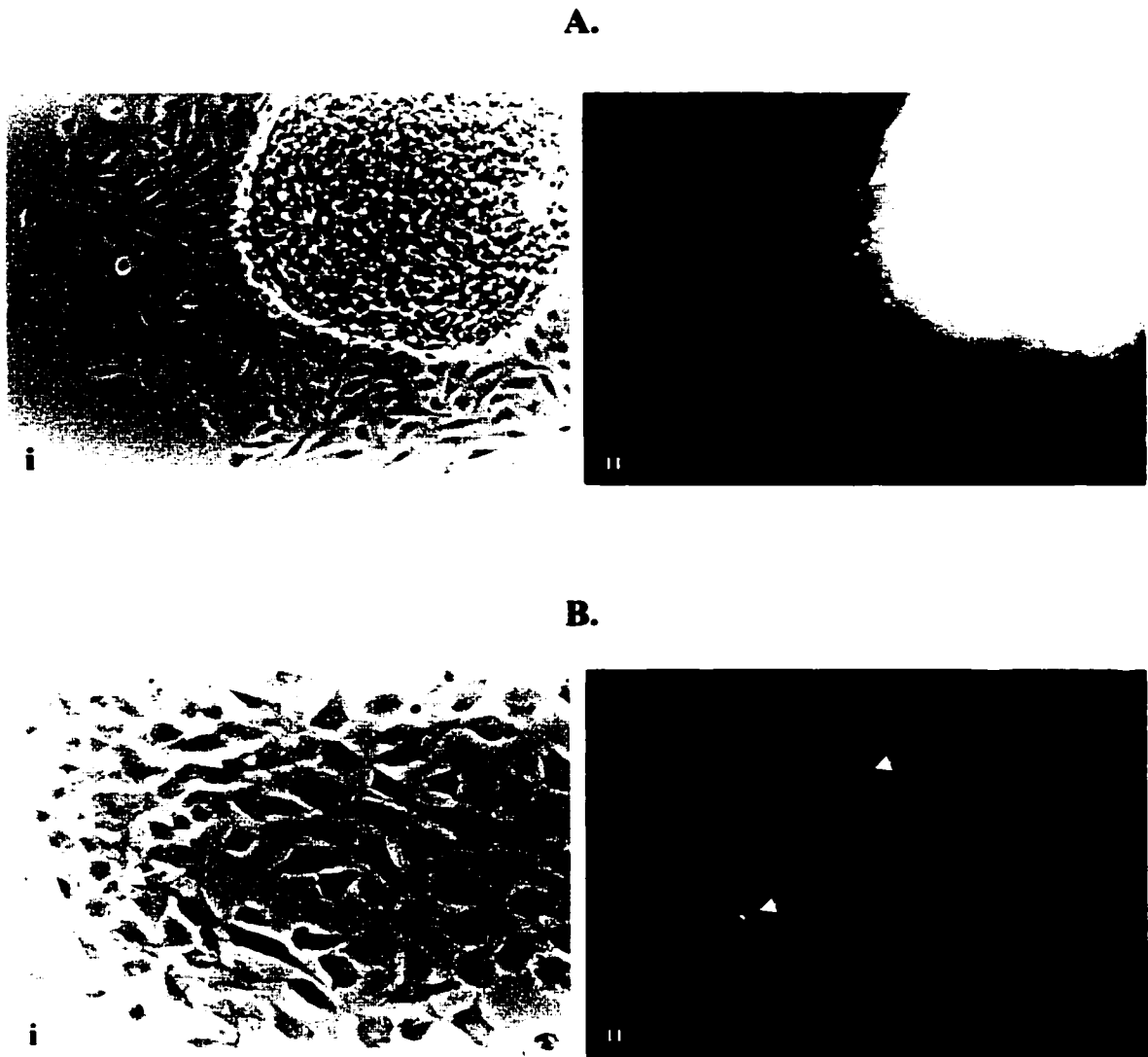
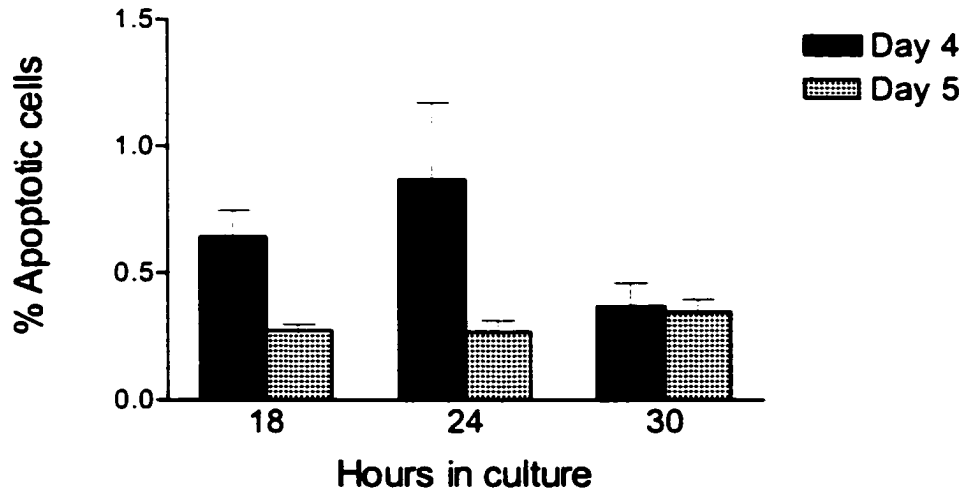


Figure 4-8. Examples of cultures of atrioventricular cushion explants. (A) Representative 12 h AV cushion explant cultures seen in phase contrast view (i), and TUNEL staining (ii) of the same field of view with positive apoptotic cells at the edge of the explant (arrows). Mag. x140. **(B)** The outgrowth of a 12 h AV cushion explant seen in a phase contrast view (i) and TUNEL staining on the same culture. The arrows point to the same apoptotic cells in each view. Mag. x560.

A. TUNEL staining



B. Annexin-V staining

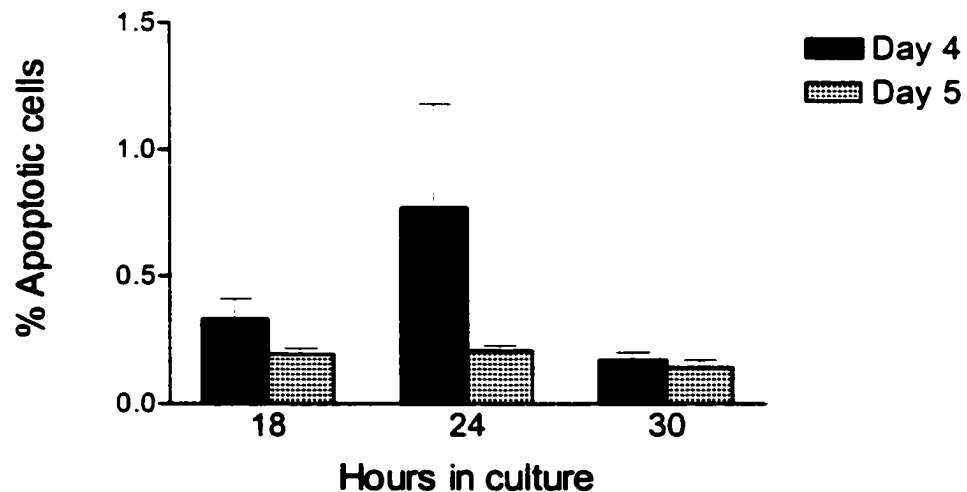


Figure 4-9. Levels of apoptosis in AV explant cultures over time, measured by TUNEL and Annexin-V labeling. Only the cells that migrated away from the initial explant were included in the cell counts. (A) When the total number of TUNEL positive cells is expressed as a percentage of the total number of cells per culture, ED 4 – 24 h had the highest incidence of cell death. (n=11). (B) In similar cultures, stained with Annexin-V, a similar pattern of cell death is seen, with an increase in levels of apoptosis in the ED4 – 24h culture (n=5).

membrane changes. When the total number of positive cells per culture is expressed as a percentage of the total number of cells per culture, there is also an increase in cell death levels when the ED 4 cultures are grown for 24 hours (Figure 4-9B). This increase in levels of apoptosis in cultures precedes levels seen *in vivo* by 24 h, possibly due to some intrinsic factor in the explant that induces cell death, or increased proximity of the culture cells to the signal compared to that *in vivo*.

EFFECT OF CONDITIONED MEDIUM ON CELL DEATH LEVELS IN CUSHION CULTURES

To determine the source of the signal for apoptosis in the endocardial cushions, dissociated cushion cultures were treated with conditioned medium derived from primary cultures of different parts of the heart, and were assayed for differing levels of cell death. Conditioned medium was prepared from the following different regions of the heart; AV cushions. OT cushions. AV cushions with myocardium, OT cushions with myocardium, and the ventricle.

Cultures of dissociated cushions were then treated with the conditioned medium; dissociated AV cushions received AV-derived conditioned medium, and dissociated OT cushions received OT-derived or ventricle-derived conditioned medium. Controls involved treating the cultures with non-conditioned medium 199. Also, as ventricle tissue exhibits no apoptosis *in vivo*, ventricle cultures were also treated, as a control, with OT-derived myocardium- or ventricle-conditioned medium. After treatment with the conditioned medium, the cultures were stained with TUNEL and the total numbers of positively staining cells per culture were counted.

In AV cushion cultures, comparison of the number of TUNEL positive cells per culture after each treatment, revealed that treatment of dissociated AV cushion cultures with AV cushion-conditioned medium significantly increased the levels of cell death ($P < 0.01$) when compared to the control (Figure 4-10A).

In dissociated OT cushion cultures, comparison of the number of TUNEL positive cells per culture showed that the level of cell death was significantly increased by OT cushion conditioned medium ($P < 0.01$) and more significantly by ventricle-conditioned medium ($P < 0.001$) when compared the control (Figure 4-10B). Treatment of ventricle cultures yielded similar results to the control, with no significant increase in levels of cell death when treated with OT-derived myocardium conditioned medium or ventricle-conditioned medium (Figure 4-10B). The results of these culture experiments suggests that in the AV cushions, apoptosis is induced by some factor present in the cushions themselves, while in apoptosis in the OT cushions, factors in the OT cushions themselves and in the ventricle may be involved.

DiI LABELING OF NEURAL CREST CELLS

To investigate if neural crest cells were undergoing apoptosis in the endocardial cushions, double labeling was performed for neural crest cells and fragmenting nuclei. The premigratory neural crest cells were labeled by flushing the neural tube, prior to closure and cardiac neural crest migration at HH stage 9-11, with a solution of the fluorescent dye DiI. This dye is readily taken up into the plasma membrane of the cells it comes into contact with. All the cells of the neural tube subsequently fluoresce red. On leaving the neural tube to go to various body sites, the migratory NC cells carry the dye

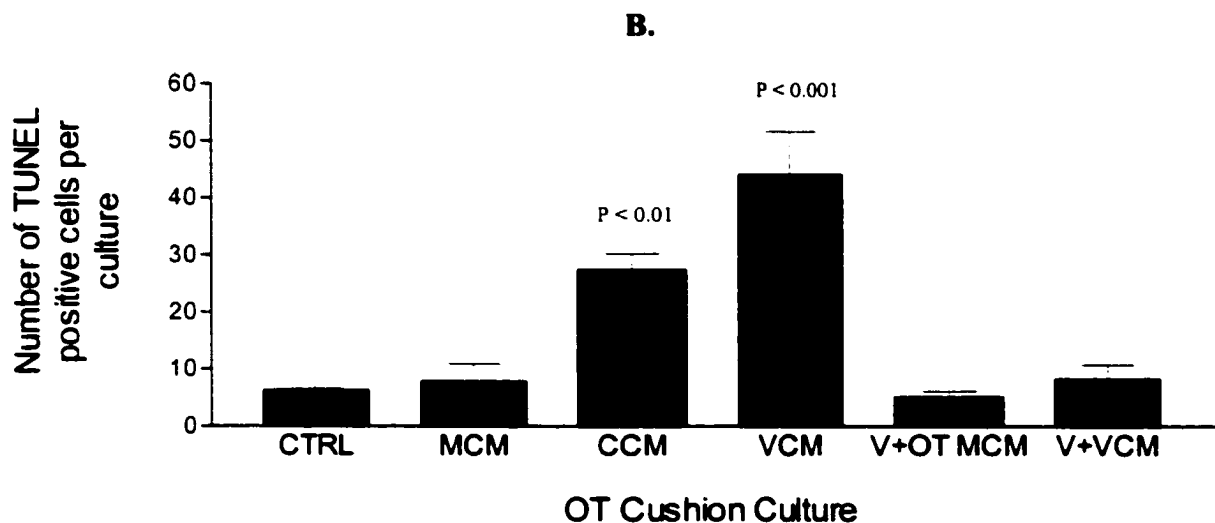
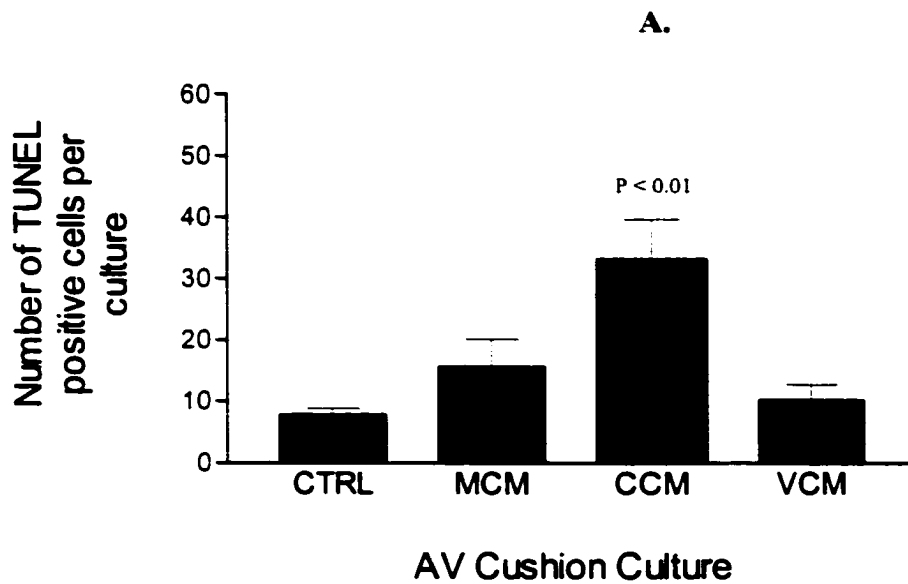


Figure 4-10. Effect of conditioned medium on apoptosis levels in dissociated cushion cultures. (A) Cultures of AV cushions were treated with AV-myocardium conditioned medium (MCM), AV-cushion conditioned medium (CCM), ventricle conditioned medium (VCM) and control medium 199 (CTRL). (B) Cultures of OT cushions were treated with OT-myocardium conditioned medium (MCM), OT-cushion conditioned medium (CCM), ventricle conditioned medium (VCM) and control medium 199 (CTRL). Ventricle cultures (V) were treated with conditioned medium from OT myocardium (OT MCM) and ventricle conditioned medium (VCM). In each case, equal numbers of cells were initially seeded. The total number of apoptotic cells per culture was compared to the control. Statistical analysis was performed on the total number of TUNEL positive cells, using one way ANOVA and Tukey's post-test (AV, n=7; OT, n=5).

with them. The migratory pathways of NC cells have been well studied and documented with the cardiac NC cells being the focus of much ongoing attention (Creazzo *et al*, 1998; Waldo *et al*, 1999; Jiang *et al*, 2000). Among the better-characterized NC derivatives are the dorsal root ganglia (DRG) and melanocytes of the trunk NC. These can be seen to have taken the fluorescent label to their destination sites (Figure 4-11a) acting as an internal positive control. The cardiac NC cells enter the distal OT by way of the pharyngeal arches and form the AP septum and contribute to the conal septum. Fluorescent labeling of clusters of cells can be seen in the septum of the distal OT, indicating that labeled NC cells are reaching the heart (Figure 4-11b). The sections were stained with DAPI to label the nuclei and examined using a confocal microscope, looking for fragmenting nuclei of apoptotic cells. In the OT cushions, many apoptotic cells were seen, as evidenced by the characteristic fragmenting nuclei (Figure 4-12a). In the condensed mesenchyme of the AP septum, neural crest cells were seen, as evidenced by DiI labeling, but these were not apoptotic (Figure 4-12b). In the prongs of the AP septum that project into the OT cushions, which are also known to contain NC cells, there was some overlap with DiI labeling and DAPI staining of fragmented nuclei (Figure 4-12c), indicating that some of the NC cells were dying. In the OT cushions also, there was also some overlap of DiI neural crest labeling with fragmenting nuclei (Figure 4-12d), suggesting that in the cushions, the NC cells may also undergo apoptosis. When DiI has been in the embryo for a number of days, its appearance within the cell changes from brightly labeled membranes to a granular cytoplasmic appearance (Bagnall, 1992). It is this granular appearance that is seen in the heart regions. Overall, these findings further

support the fact that some NC cells may undergo apoptosis in the cushions and distal tips of the AP septum.

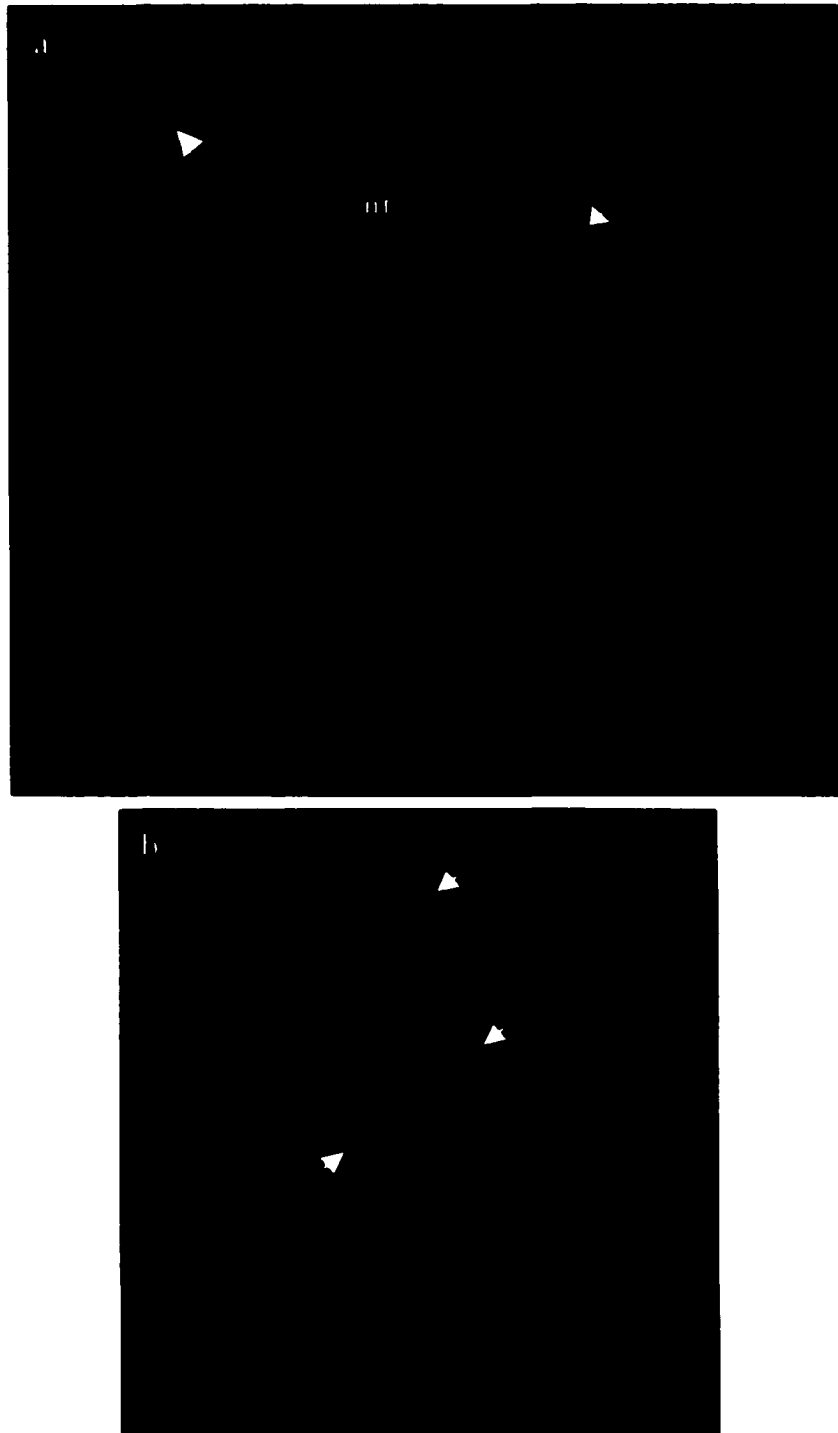


Figure 4-11. DiI labeling of migratory neural crest cells. (a) DiI labeling of the neural tube (nt), and the neural crest derivatives in the dorsal root ganglia (arrow) and the melanocytes (arrowhead) show that neural crest cells were correctly labeled. Mag x140. (b) In the distal OT, fluorescently labeled neural crest cells can be seen in lining the vessels and in the intermediary septum (arrows), showing that cardiac neural crest cells were indeed labeled with the dye. Mag. x280.

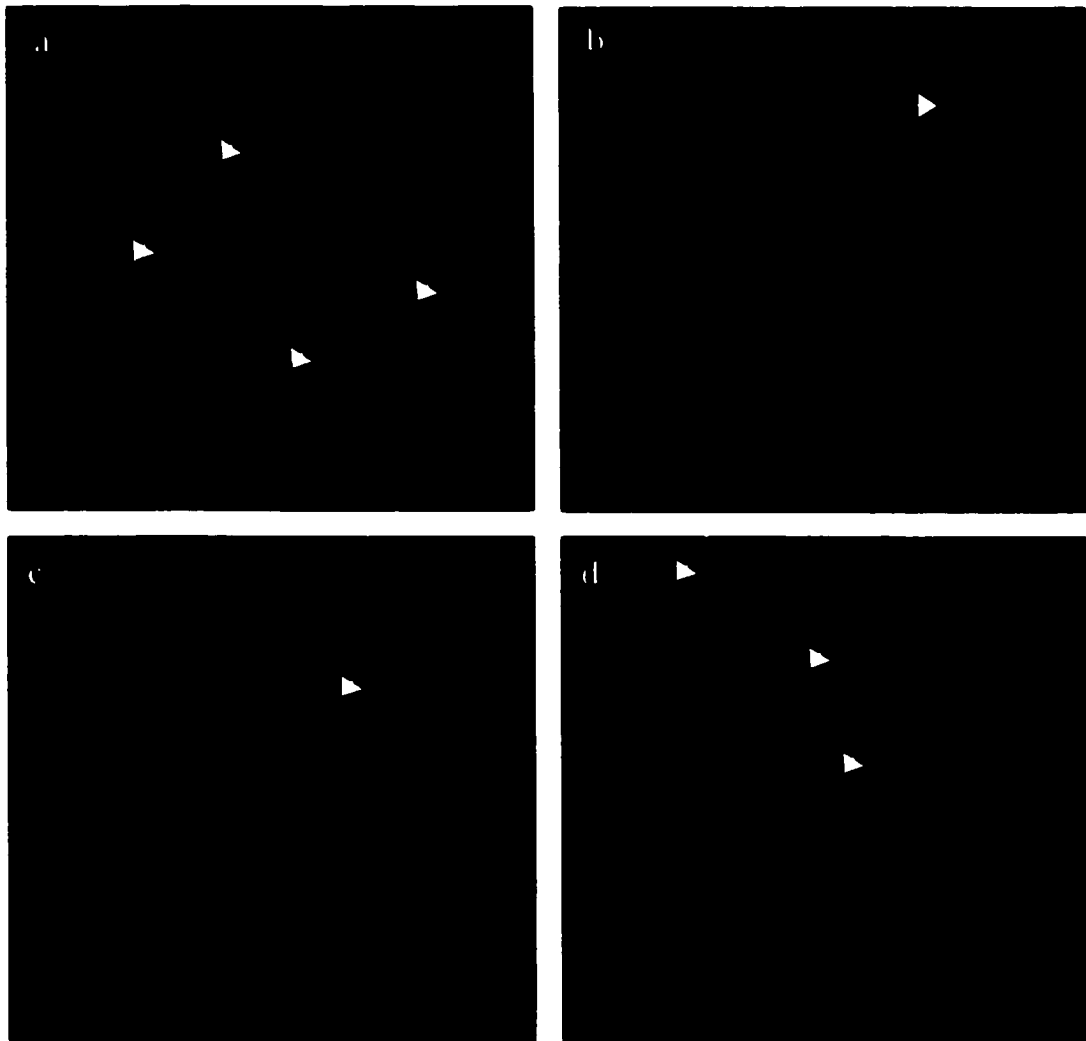


Figure 4-12. DAPI and DiI labeling in the outflow tract. (a) DAPI labeling of the OT cushions, showing many fragmenting apoptotic cells (arrows). (b) DAPI and DiI labeling of the condensed mesenchyme of the AP septum. A fluorescently labeled neural crest cell is shown (arrow). (c) In the prongs of the AP septum, DiI labeling overlaps with some of the fragmenting DAPI stained nuclei (arrows). (d) In the OT cushions, some overlap is seen, with DiI and DAPI labeling (arrows). Mag x560, a-d.

Chapter 5

**REGULATION OF APOPTOSIS IN THE ENDOCARDIAL
CUSHIONS**

EXPRESSION OF BCL-2 FAMILY MEMBERS IN THE EMBRYONIC HEART

The bcl-2 family of proteins are known regulators of the apoptotic pathway, acting in either a pro- or anti-apoptotic pathway. It is generally considered that it is the ratio of levels of both subtypes that decides whether a cell will live or die. Embryonic hearts were examined for some of the bcl-2 family members by western blotting and immunocytochemistry, to test if members of this family are present in these tissues, and if so, to assess if they have a differential distribution.

Immunoblot analysis of bcl-2 family members

Immunoblotting was carried out on extracts of dissected AV cushions and whole OT to determine if members of the bcl-2 family were present, and to assess if expression patterns changed throughout the timecourse during which cell death is seen. Immunoblotting with a monoclonal antibody to anti-apoptotic bcl-2 showed the 26 kDa band to be present throughout E.D. 4-7 in both the AV cushions (Figure 5-1a) and in the OT (Figure 5-1b). This same band was present in the Jurkatt cell positive control. The antibody also consistently recognized a lower ~23 kDa band, which corresponds to another bcl-2 isoform (Tsujiimoto and Croce, 1986). As this band was present at much lower levels in the positive control, this may suggest a role for this isoform in heart development. Densitometric analysis of the blots showed that bcl-2 levels decreased significantly at ED 5, compared to ED7 in the AV cushions (Figure 5-1c) while in the OT, bcl-2 protein levels were lower at ED 4 in comparison with the other days examined, although the decrease was not statistically significant (Figure 5-1d). The

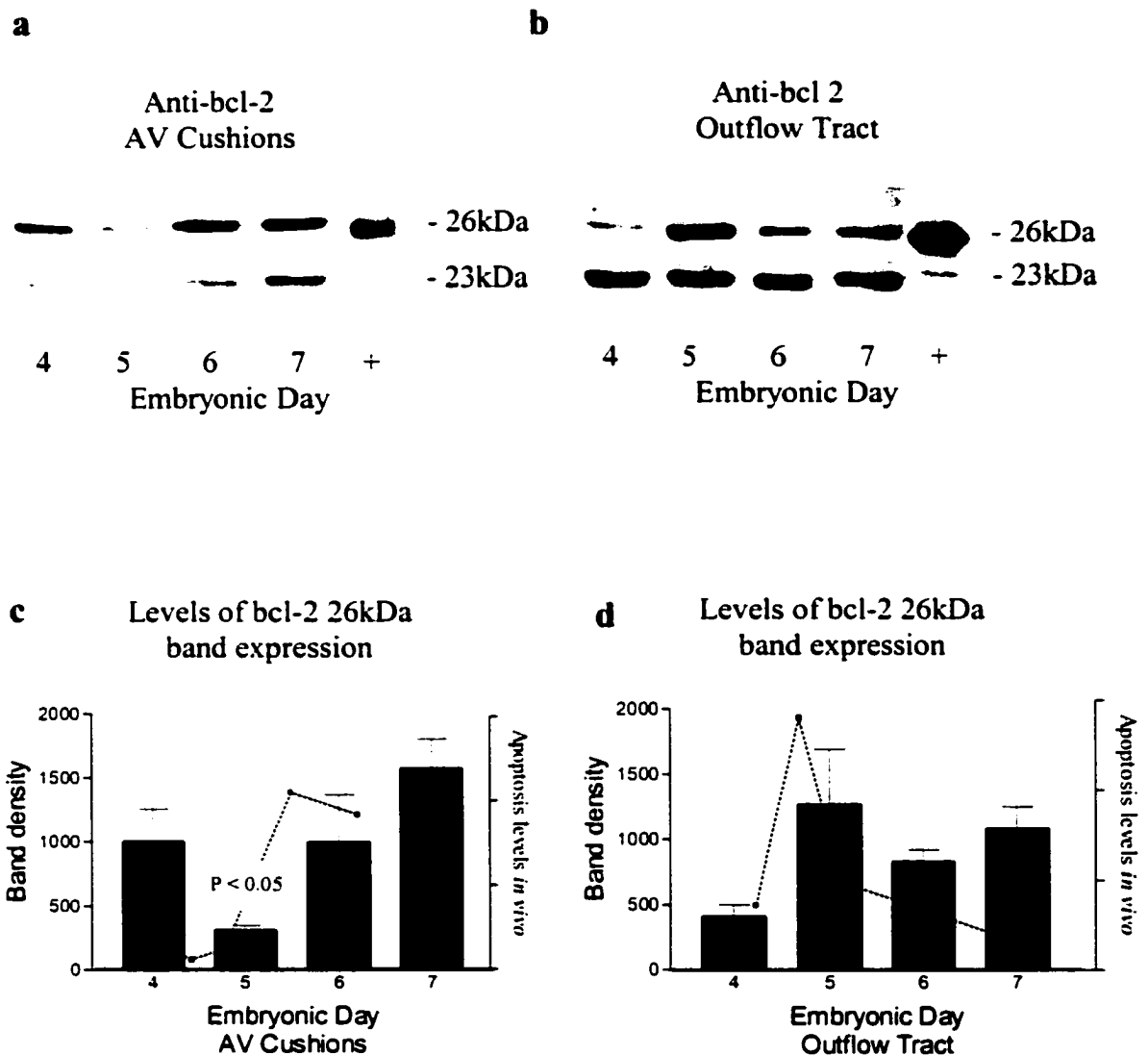


Figure 5-1. Bcl-2 expression in dissected AV cushions and outflow tract. (a) Dissected atrioventricular (AV) cushion extracts immunoblotted with monoclonal anti-bcl-2. The 26kDa band is present throughout embryonic days 4-7 and in the Jurkatt cell positive control (+), with a decrease in expression at ED5. The lower 23kDa band represents another isoform of bcl-2. (b) Dissected outflow tract immunoblotted with monoclonal anti-bcl-2, showing the same 26 and 23kDa bands, with a decrease in expression at ED4. (c) Average densitometric scans for the 26kDa band in AV bcl-2 blots (n=3), with a significant decrease in expression at ED 5 compared to ED7. (d) Average densitometric scans for the 26kDa band in outflow tract bcl-2 blots (n=3) showing a decrease in expression at ED4. Data shown represents the mean band density for each day \pm SEM. Statistical analysis was performed using one way ANOVA and Tukey's post-test. The dashed lines show the pattern of apoptosis seen *in vivo*.

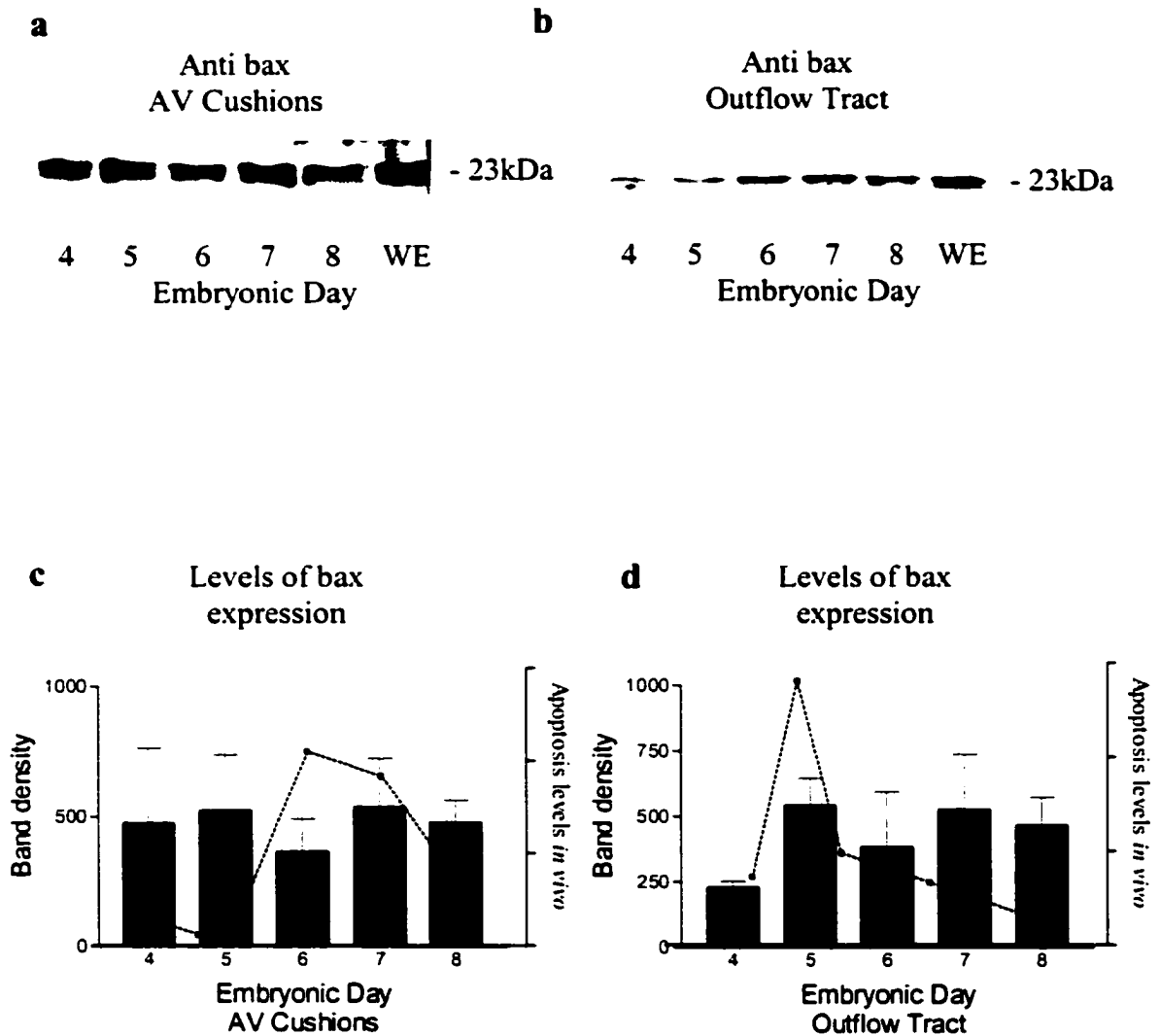


Figure 5-2. Bax expression in dissected AV cushions and outflow tract. (a) Dissected atrioventricular (AV) cushions immunoblotted with monoclonal anti-bax. The 23kDa band is consistently expressed in the AV cushions from ED 4-8, in similar levels to the whole embryo (WE) positive control. (b) Dissected outflow tract immunoblotted with monoclonal anti-bax, showing the 23kDa band throughout ED 4-8. (c) Average densitometric scans for the 23kDa band in AV bax blots (n=3), showing consistent expression levels throughout ED 4-8. (d) Average densitometric scans for the 23kDa band in outflow tract bax blots (n=2), showing a reduced expression at ED 4. Data shown represents the mean band density for each day \pm SEM. Statistical analysis was performed using one way ANOVA and Tukey's post-test. No significant differences were seen between days. The dashed lines show the pattern of apoptosis seen *in vivo*.

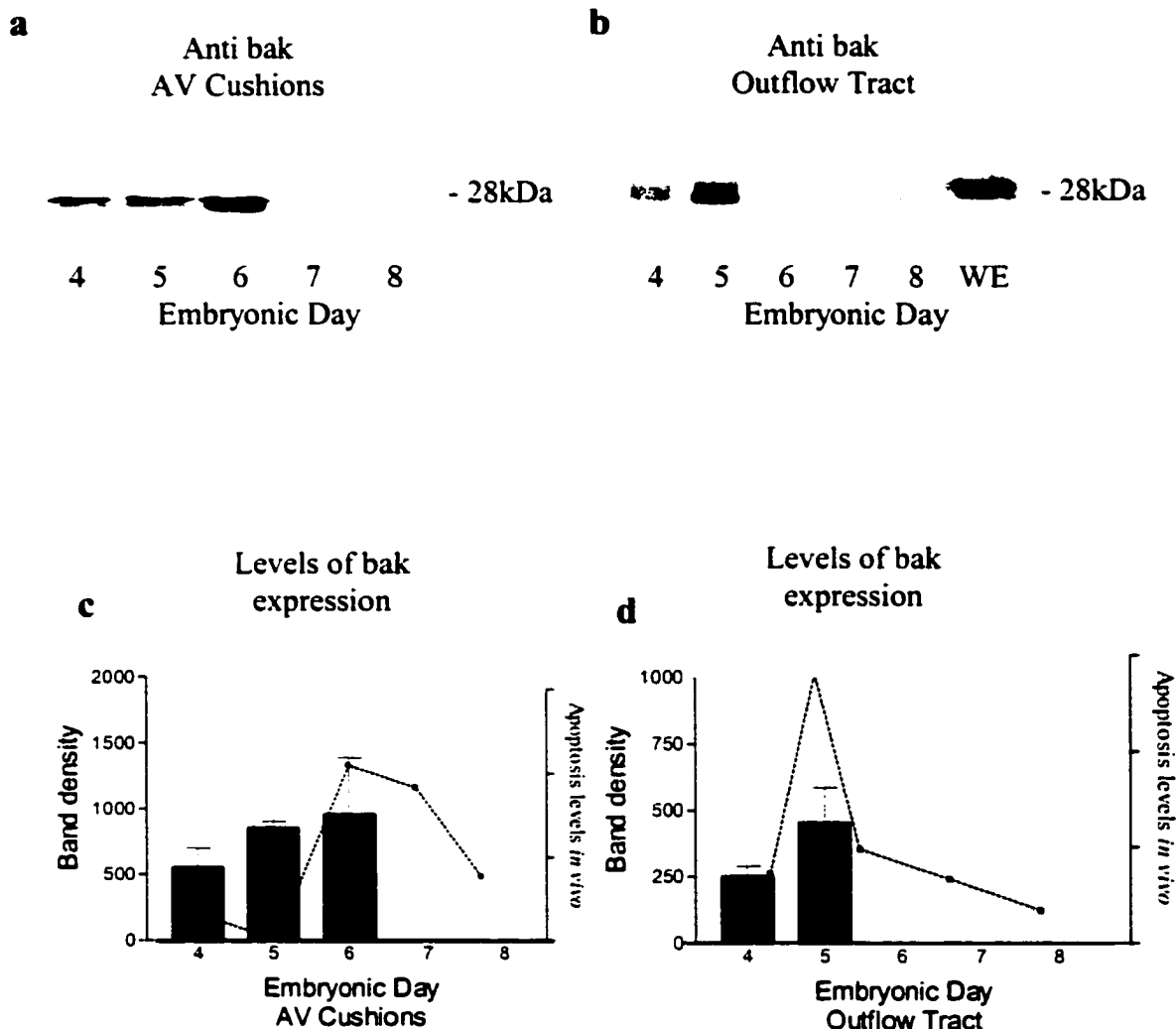


Figure 5-3. Bak expression in dissected AV cushions and outflow tract. (a) Dissected atrioventricular (AV) cushions immunoblotted with monoclonal anti-bak. The 28kDa band is only present during ED 4-6. (b) Dissected outflow tract immunoblotted with monoclonal anti-bak, showing the 28kDa band in ED 4-5, and the whole embryo (WE) positive control. (c) Average densitometric scans for the 28kDa band in AV bak blots (n=3), showing protein expression during ED 4-6, with an absence of protein at later stages examined. (d) Average densitometric scans for the 28kDa band in outflow tract blots (n=3) showing expression in ED 4-5, with an absence of protein at later stages examined. Data shown represents the mean band density for each day \pm SEM. The dashed lines show the pattern of apoptosis seen *in vivo*.

antibody used did not detect any protein in ventricular tissue (not shown). Immunoblotting was also performed on dissected AV cushions and the OT for pro-apoptotic bax, using a cross reactive monoclonal antibody. The 23kDa band was present throughout ED 4-8 in the AV cushions and in the whole embryo positive control (Figure 5-2a). In the outflow tract, the 23kDa band was also present throughout ED 4-8 and in the positive control (Figure 5-2b). Densitometric analysis of bax expression in the AV cushions (Figure 5-2c) showed similar levels of the protein throughout ED 4-8. In the outflow tract, densitometric analysis also revealed constitutive expression throughout ED 4-8, with no significant differences seen between days. (Figure 5-2d). Immunoblotting with a monoclonal antibody to pro-apoptotic bak revealed the 28kDa bands in ED 4-6 in dissected AV cushions (Figure 5-3a), while in the dissected outflow tract, the band was present in ED 4-5 (Figure 5-3b). Densitometric analysis of the bands in the AV cushions supported these results, revealing expression of the protein from ED 4-6 in the AV cushions (Figure 5-3c) and from ED 4-5 in the outflow tract (Figure 5-3d). Interestingly, the protein was absent from both regions at later stages, after the time of peak cell death. Extracts of whole embryo tissue serve as a positive control when the protein of interest is known to be present during the developmental stages examined, and with immunoblotting serves to show the band is present at the correct molecular weight.

Immunocytochemical localisation of bcl-2 family members

To visualise the localisation of bcl-2 family members, sections of the developing heart were stained for various members of the bcl-2 family at times when peak cell death is observed in the AV and OT regions. At ED 4, in the distal OT (Figure 5-4a) bcl-2

protein was present in individual cells of the endocardial cushion cells (arrows) but with only background staining in the APS. In the more proximal cushions (Figure 5-4, c and d), the protein was expressed in the majority of cushion cells (arrows) as evidenced by darker staining of the cell bodies and cytoplasmic processes, compared to the background staining in non-positive cells (arrowheads) and the myocardium. A similar pattern was seen in the AV cushions at ED 4 and 6 (Figure 5-4, f and e respectively), with high *bcl-2* expression in most cushion cells (arrows), but less in the adjacent myocardium. Heart sections were also stained for *bax*, a pro-apoptotic family member. At ED 4, in the distal OT (Figure 5-5a), the *bax* protein was absent from the centre of the condensed mesenchyme of the AP septum, but was present in some of the adjacent cushion and myocardial cells, and at the edges of the condensed mass (Figure 5-5a, arrow). *Bax* was also seen in the fusing cushions of the distal OT, adjacent to the AP septum (Figure 5-5b). In the more proximal cushions (Figures 5-5, c and d) *bax* expression appeared to associate strongly with the prongs of the AP septum that protrude into the endocardial cushions, but was also present in individual cells in the surrounding cushions and in the myocardium. In the AV cushions (Figure 5-5e) *bax* appeared to be scattered throughout the central cushion mass at ED 6, when peak cell death is occurring. Pro-apoptotic *bak*, was also examined for in sections at times when peak cell death is occurring. In the OT at ED 4, *bak* appeared to strongly localise to the prongs of the AP septum (Figure 5-6, a and b), and was also present in some parts of the endocardial cushions and the myocardium. In the AV cushions at ED 6, *bak* also appeared to have a specific distribution in regions that normally show extensive apoptosis (Figure 5-6c), but with little staining in the adjacent myocardium.

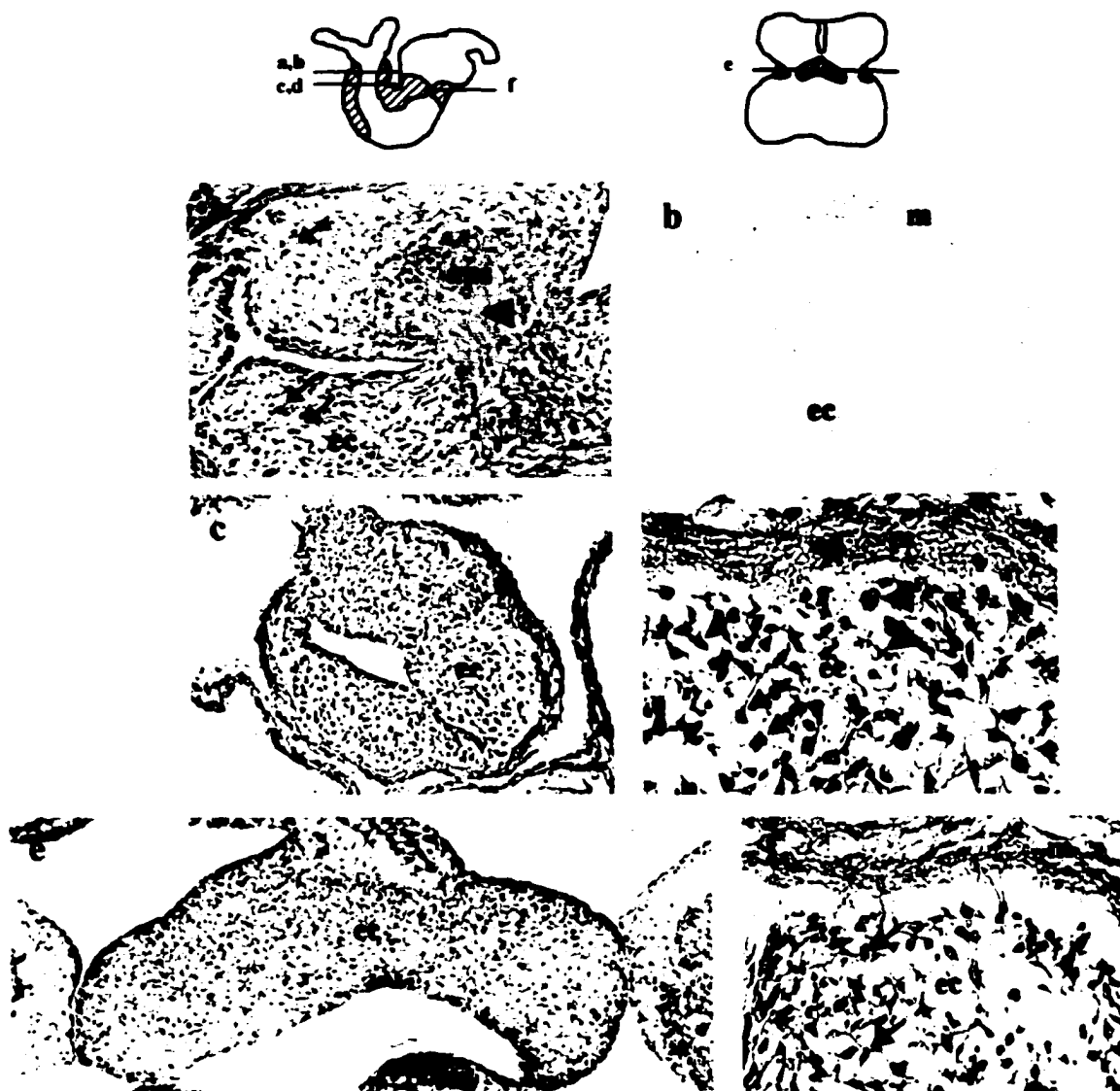


Figure 5-4. Immunocytochemical localisation of bcl-2 in the endocardial cushions. (a) The distal outflow tract, ED 4, stained for bcl-2, showing the endocardial cushions (ec) and the aorticopulmonary septum (aps). Staining appears more prominent in individual cells in the cushions (arrows), compared to background staining in the condensed mesenchyme of the aps (arrowhead) (b) A pre-absorbed negative control of the OT shows no staining in the endocardial cushions (ec) or the myocardium (m). (c) In the proximal outflow tract, positive staining can be seen throughout the endocardial cushions. At a higher magnification (d), many positive cells are seen (arrows), as evidenced by darker staining of the cell bodies and cytoplasmic processes, with background staining in the adjacent myocardium (m) and some cushion cells (arrowheads). (e) In the AV cushions, bcl-2 is seen throughout the central mass of cushions (ec) at the time of peak cell death (ED 6). (f) At an earlier stage (ED 4), bcl-2 is also seen throughout the AV cushions, again with less staining in the adjacent myocardium (m). Mag. x140, c,e; x280, a; x560, d,f.

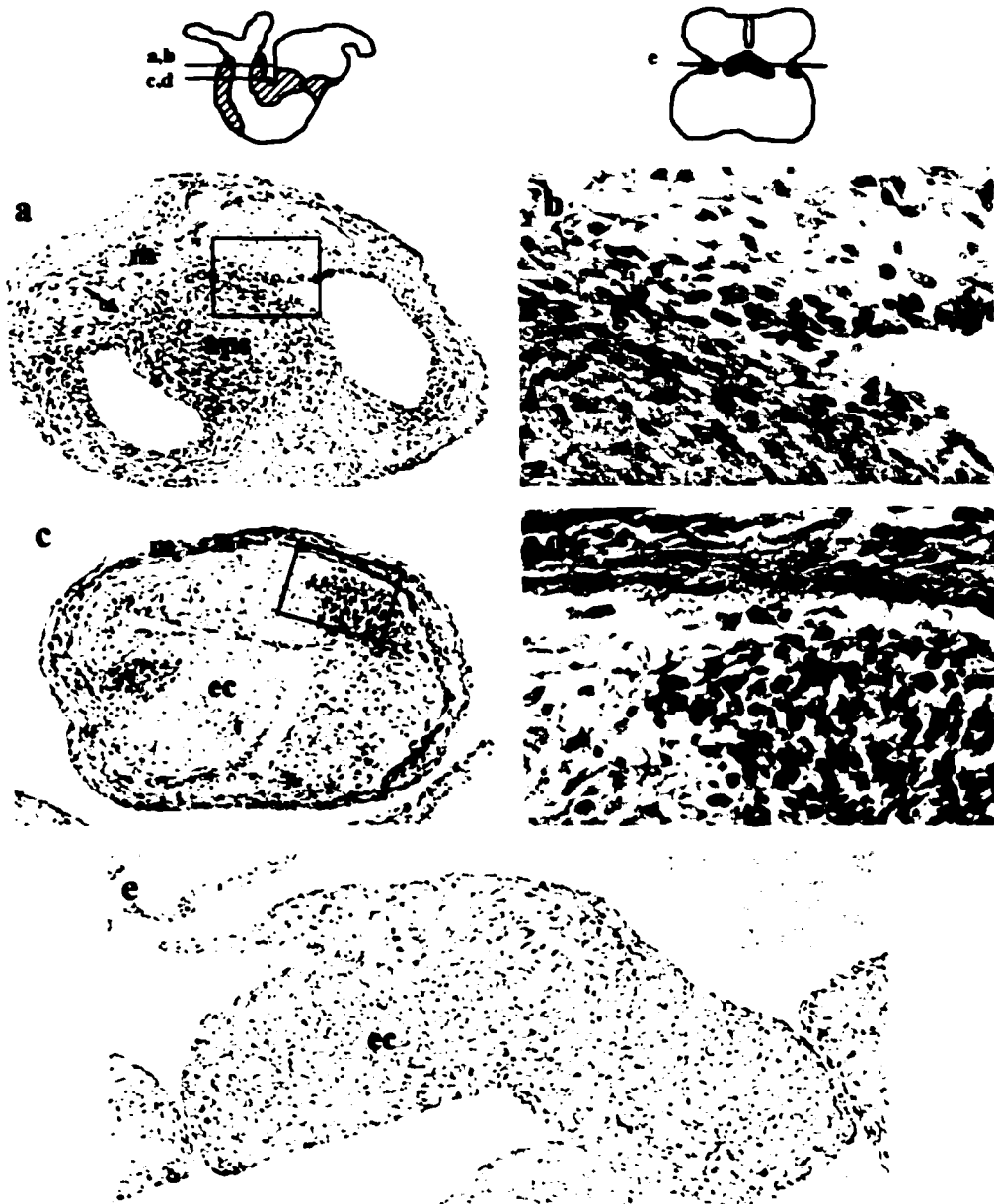


Figure 5-5. Immunocytochemical localisation of bax in the endocardial cushions. (a) The distal outflow tract, ED 4, stained for pro-apoptotic bax, shows the condensed mesenchyme of the aorticopulmonary septum (APS). Staining is absent from the central mass but is present in the adjacent cells (arrow) and is scattered throughout the surrounding myocardium (m). **(b)** At a higher magnification of the boxed area in a, bax immunoreactivity can be seen in individual cells in the fusing endocardial cushions. **(c)** The proximal outflow tract, showing a strong association of staining with the prongs of the APS and with individual positive staining cells scattered throughout the endocardial cushions (ec) and the myocardium (m; arrows). **(d)** A higher magnification of the boxed area in figure c shows the association of bax staining with the APS. **(e)** Individual bax stained cells scattered throughout the central mass of AV cushions, ED 6, at the time of peak cell death occurrence. Mag. x140, a,c,e; x280, b,d.



Figure 5-6. Immunocytochemical localisation of bak in the endocardial cushions. (a) The outflow tract, ED 4, stained for pro-apoptotic bak shows the protein present in some of the endocardial cushions (ec) and myocardium (m) of the outflow tract and with a strong association with the aorticopulmonary septum (aps). (b) A higher magnification of the aorticopulmonary septum (aps). (c) Bak immunoreactivity is seen in the endocardial cushions (ec) in the AV region, with no obvious staining in the adjacent myocardium (m). Mag. x140, a,c; x280, b.

Expression of bax was also seen in the ventricle of the heart. Western blotting on ventricular tissue for the 23kDa bax protein revealed expression throughout ED 4 – 8 (Figure 5-7a) at levels equal to or greater than the whole embryo positive control. Immunostaining on ventricular sections revealed widespread immunoreactivity throughout the ventricular myocardium (Figure 5-7b) and at a higher magnification (Figure 5-7c) throughout the trabeculae. In all procedures involving immunostaining, negative controls were performed that entailed pre-incubation of the antibody with a blocking peptide, or incubation of the sample in serum alone, minus the primary antibody. This resulted in absence of staining in all cases, with examples shown in figure 5-8.

Sub-Cellular distribution of bcl-2 family members in cushion cells

The sub-cellular dynamics of the bcl-2 family members bcl-2 and bax were examined in the cushion cells in culture to determine if translocation occurred between cellular compartments in ways which suggest the activation of apoptotic pathways in these cells. Dissociated cultures of AV cushions were either maintained with serum or were serum-starved, which is known to induce the cells to undergo apoptosis. The cultures were then stained for anti-apoptotic bcl-2 or pro-apoptotic bax, with concomitant staining for the nuclei with DAPI and the mitochondria with Mitotracker Red ® CMXRos, and the images were combined to determine the cellular localisation of the bcl-2 family members in healthy and dying cells. Some serum-starved cultures were also treated with a general caspase inhibitor to determine if bcl-2 family involvement may be downstream of caspase activity.

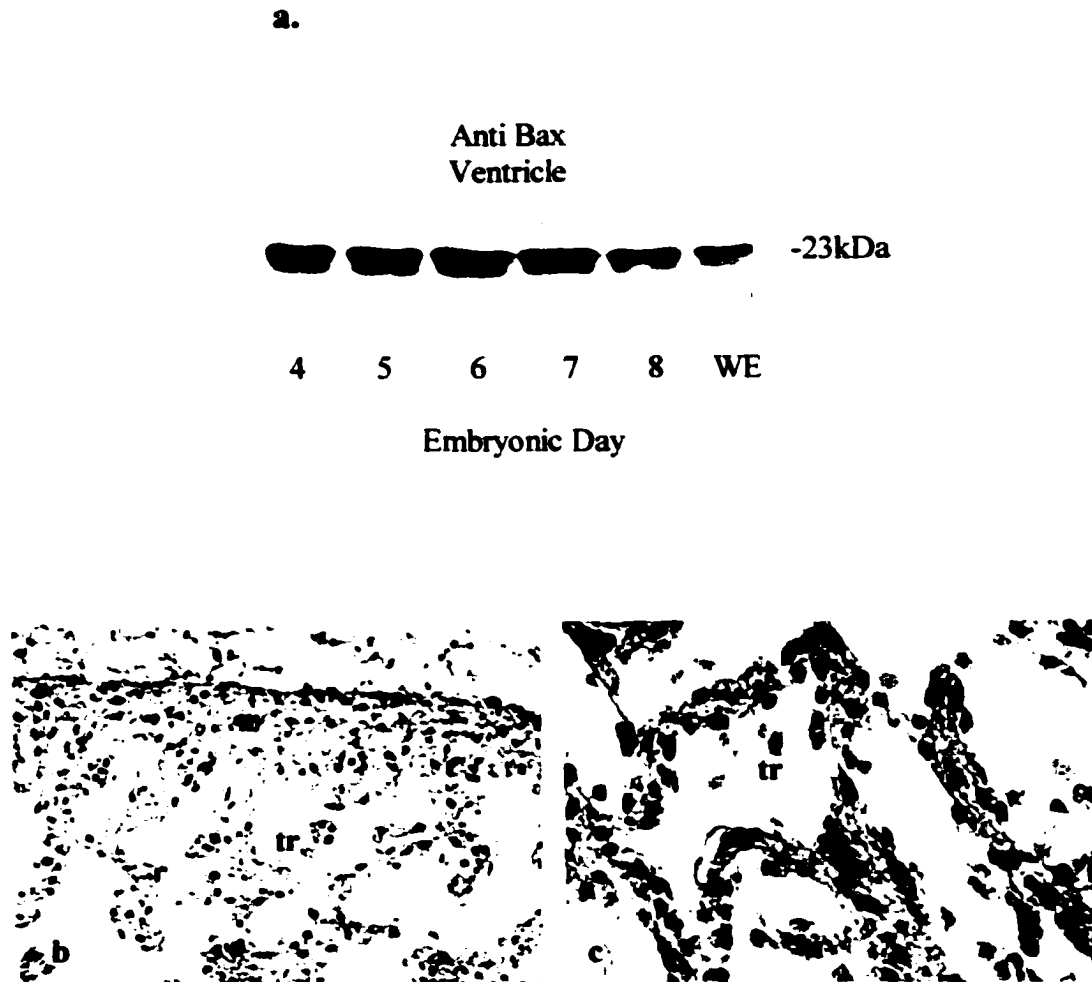
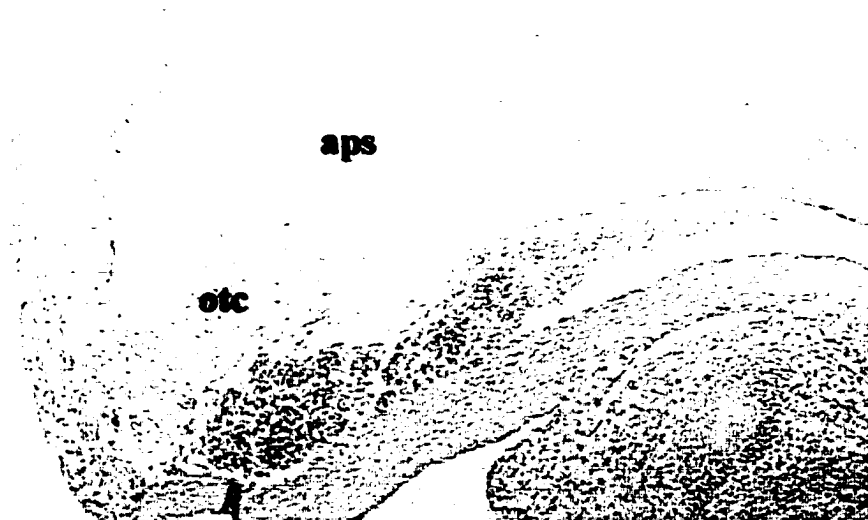


Fig 5-7. Immunodetection of bax in the ventricle of the embryonic heart. (a) Dissected ventricular tissue immunoblotted with monoclonal anti-bax. The 23kDa band is present throughout ED 4-8, at levels equal to or greater than the whole embryo (WE) positive control. (b) Immunocytochemical detection of bax in the ventricular tissue (B and at a higher magnification in C) shows bax to be expressed in the myocardium (m) and the trabeculae (tr). Mag. x280, b; x560, c.

a.



b.



Figure 5-8. Examples of immunohistochemistry negative controls. In all immunohistochemical procedures, negative controls were performed that consisted of pre-incubating the antibody with a blocking peptide, or incubation in serum without the primary antibody. (a) Negative control in the area of the distal outflow tract, showing the aorticopulmonary septum (aps) and the OT cushions (otc). (b) Negative control in the AV cushions (avc). Mag. x140, a; x280, b.

In healthy cultures stained for bcl-2 (Figure 5-9), DAPI staining shows large, healthy nuclei (Figure 5-9a) with mitochondria dispersed throughout the cells (Figure 5-9b). With concurrent staining for endogenous bcl-2, the protein was seen throughout the cytoplasm, and in specific immunoreactive clusters in each cell (Figure 5-9c). When the images were combined (Figure 5-9d), there was some overlap of the bcl-2 stain with the mitochondria, and the positive staining clusters appeared to lie adjacent to or in the nuclei. In direct overlap of the blue and green staining, the resulting colour would appear as pale-blue in colour. Other cultures were serum starved to induce apoptosis and were also stained for bcl-2 (Figure 5-10). In these illustrations, the nuclear DAPI staining shows an intact nucleus beside a fragmenting nucleus of an apoptotic cell (Figure 5-10a). With mitochondrial labeling in the same cells (Figure 5-10b), the intact cell has dispersed mitochondria, possibly beginning to encircle the nucleus, while in the fragmenting cell, the mitochondria have clustered around the fragmenting nucleus. Staining for bcl-2 (Figure 5-10c) shows some similar expression patterns between bcl-2 staining and the mitochondrial staining in the intact cell (arrows). In the apoptotic cell, the pattern of bcl-2 expression is similar to the DAPI staining of the fragmenting nucleus in the same cell. In the combined image (Figure 5-10d), the areas of overlap of bcl-2 and the mitochondria appear orange/yellow, confirming the mitochondrial association of bcl-2 in the serum-starved cell, while in the dying cell, bcl-2 expression overlaps with the fragmenting nucleus, as evidenced by the combined pale-blue appearance of the bcl-2 stain with DAPI. Some of the serum starved cultures were treated with a general caspase inhibitor and stained for bcl-2 (Figure 5-11). These cultures resembled the healthy cultures in that

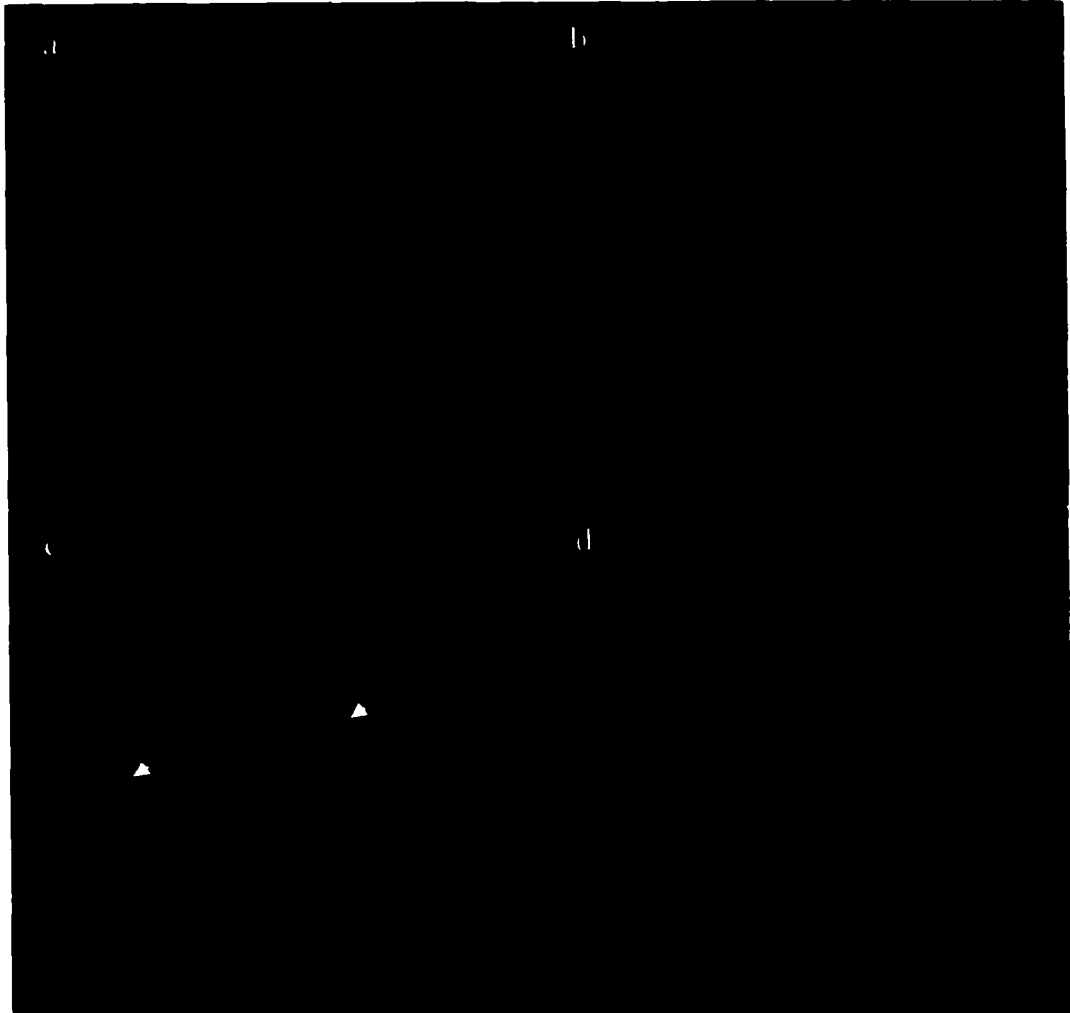


Figure 5-9. Confocal image of healthy AV cushion culture stained for endogenous bcl-2. (a) DAPI staining on healthy dissociated primary cultures of AV cushion cells showing the healthy nuclei. (b) Staining of the mitochondria with Mitotracker Red in the same field of view showing the dispersed mitochondria. (c) Staining for bcl-2 (green) showing a cytoplasmic distribution of the protein, with immunoreactive clusters in each cell (arrows). (d) In the combined image, the positive clusters appear to lie adjacent to the nuclei, with cytoplasmic protein distribution and some overlap with the mitochondria. Mag. x560.

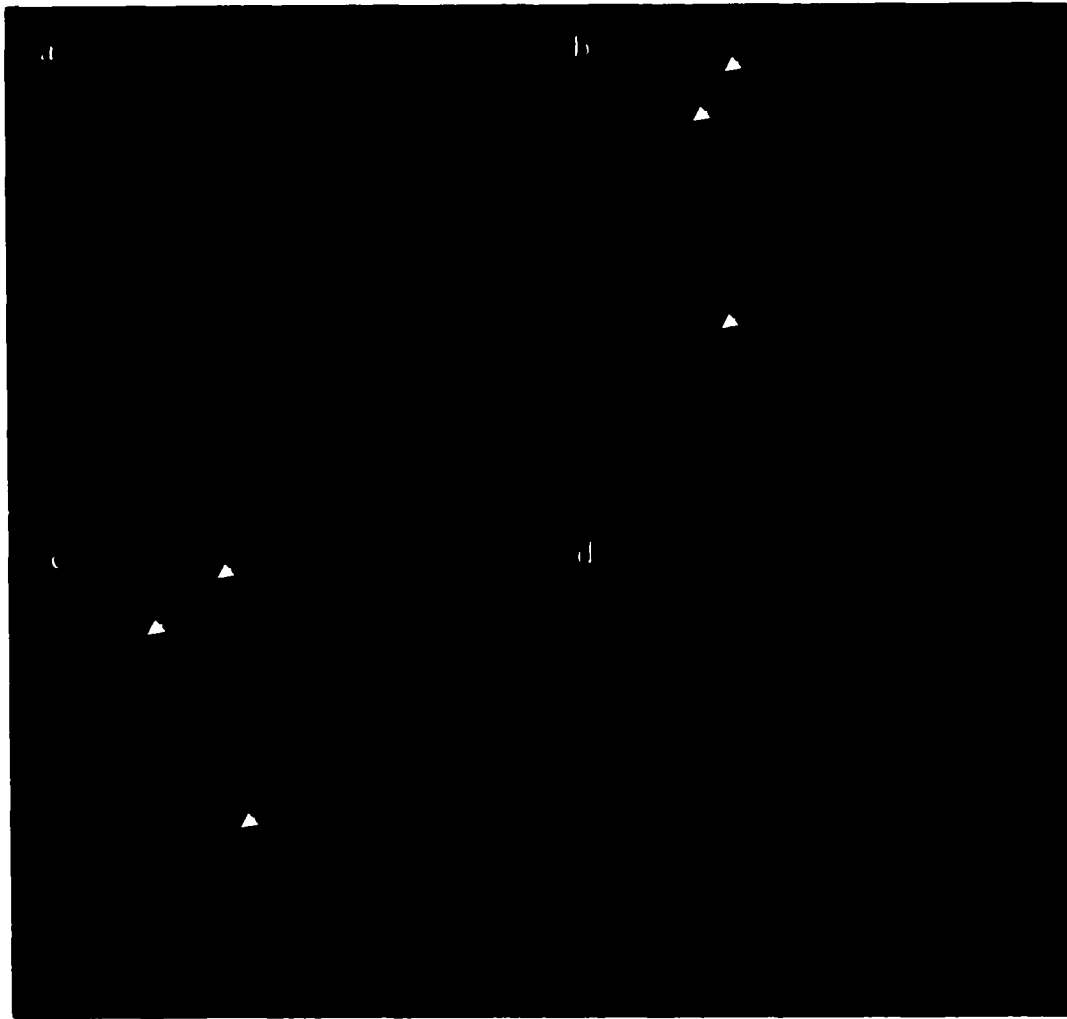


Figure 5-10. Confocal image of serum starved AV cushion culture stained for endogenous bcl-2. (a) DAPI staining on serum starved dissociated primary cultures of AV cushion cells showing an intact nucleus on the left, adjacent to a fragmenting nucleus of an apoptotic cell. (b) Staining of the mitochondria with Mitotracker Red in the same field of view showing the dispersed mitochondria in the intact cell and the clustered mitochondria in the dying cell. (c) Staining for bcl-2 (green) shows widespread distribution throughout the intact cell, with overlap of areas positive for mitochondria (arrows in b and c). In the apoptotic cell, bcl-2 appears to overlap with regions of the fragmenting nucleus. (d) In the combined image, regions of overlap between mitochondria and bcl-2 appear orange/yellow, while areas of overlap of nucleus and bcl-2 appear pale blue. Mag. x560.

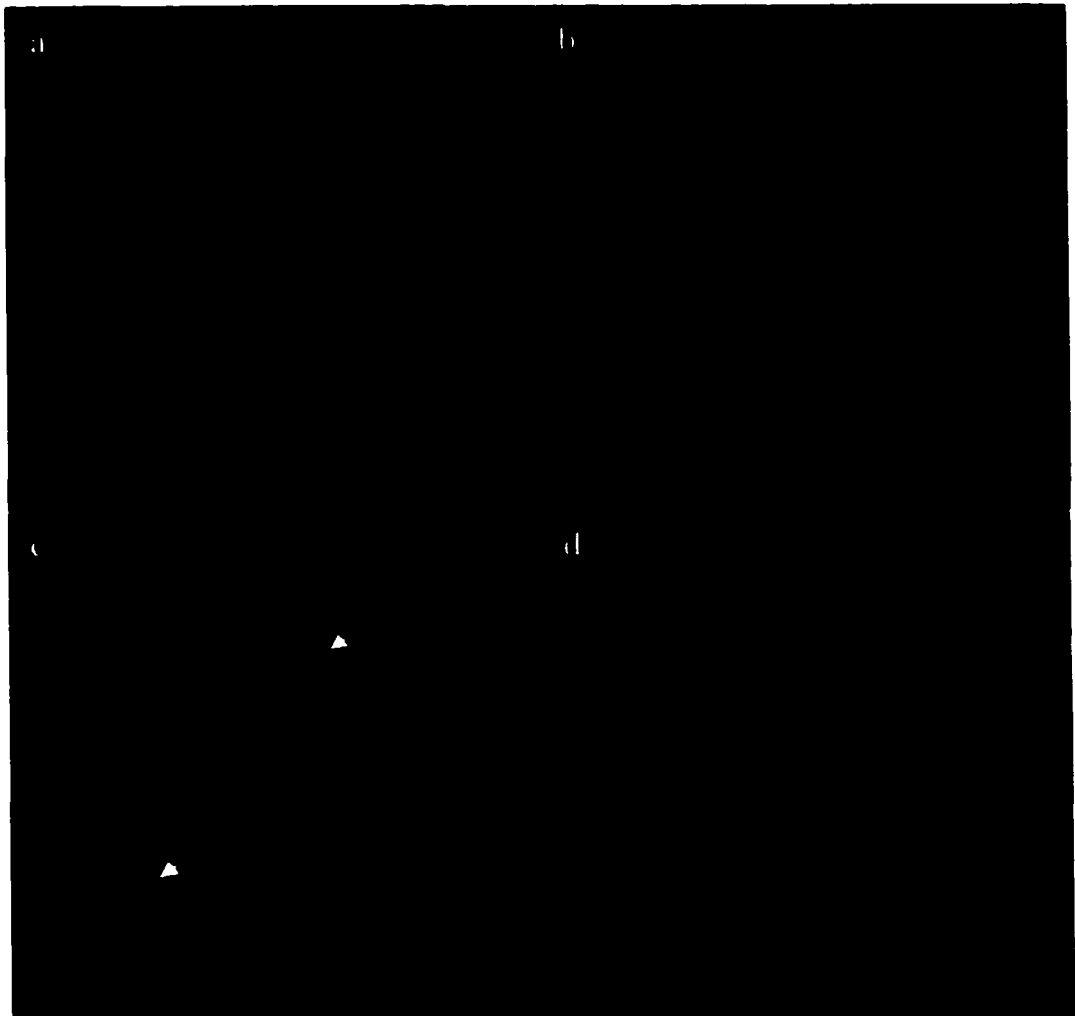


Figure 5-11. Confocal image of serum-starved AV cushion culture with a general caspase inhibitor, stained for endogenous bcl-2. (a) DAPI staining on healthy dissociated primary cultures of AV cushion cells showing a healthy nucleus beside a probable mitotic nucleus. (b) Staining of the mitochondria with Mitotracker Red in the same field of view showing the dispersed mitochondria. (c) Staining for bcl-2 (green) showing a cytoplasmic distribution of the protein, with immunoreactive clusters in each cell (arrows). (d) In the combined image, the positive clusters appear to lie adjacent to the nuclei, with cytoplasmic protein distribution and some mitochondrial overlap. Mag. x560.

the clustered immunoreactivity persisted in the nuclear region (Figure 5-11c), and again there was some overlap between the mitochondria and bcl-2 (Figure 5-11d).

Dissociated AV cushion cultures were also stained for pro-apoptotic bax (Figure 5-12). In these cultures, the DAPI labeling stained the healthy nuclei (Figure 5-12a) and Mitotracker Red showed the mitochondria to be dispersed throughout the cell (Figure 5-12b). Staining for bax showed expression of the protein throughout the cytosol, with some specific focal points (Figure 5-12c). When the images were combined, there was no apparent overlap of bax with either the nuclei or the mitochondria (Figure 5-12d). In serum starved cultures stained for bax, the DAPI labeling (Figure 5-13a) shows the shrunken nucleus of an early stage apoptotic cell, between two intact cells. The mitochondrial labeling (Figure 5-13b) shows the widespread distribution of the mitochondria in the intact cells, while in the dying cells, the mitochondria surround the shrunken nucleus. With the staining for bax (Figure 5-13c), the characteristic blebs of the apoptotic cell are apparent, with bax localizing to these areas. In the non-apoptotic cells, bax distribution appears to be scattered throughout the cytoplasm, and with immunoreactivity in the nucleus. When the images are combined (Figure 5-13d), in the apoptotic cell, there is no apparent association between bax and the mitochondria or the nucleus, whereas in the intact cells, the association of bax with the nuclei and cytoplasm is evident. When serum starved cultures were treated with caspase inhibitors and stained for bax (Figure 5-14), the pattern of distribution resembled that of healthy cells in that there was still little overlap of bax with the mitochondria (Figure 5-14d), but more interestingly, the nuclear immunoreactivity of bax was absent (Figure 5-14c), which may suggest bax activity is downstream of caspase activity.

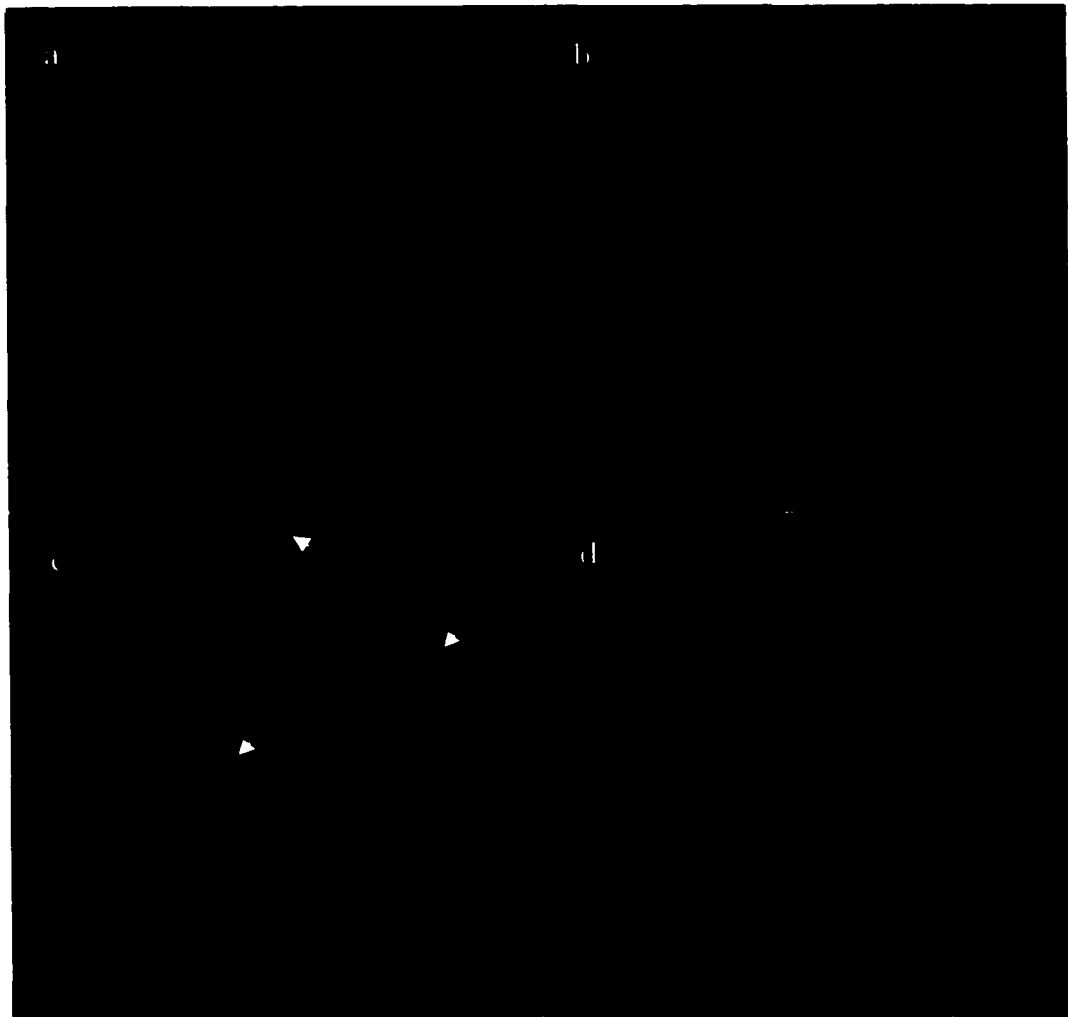


Figure 5-12. Confocal image of healthy AV cushion culture stained for endogenous bax. (a) DAPI staining on dissociated primary cultures of AV cushion cells, labeling the healthy nuclei. (b) Staining of the mitochondria with Mitotracker Red in the same field of view, showing the dispersed mitochondria in the healthy cells. (c) Staining for bax (green) shows a cytoplasmic distribution of the protein, with some focal points (arrows). (d) In the combined image, there appears to be little overlap of bax with the mitochondria and none with the nuclei. Mag. x560.

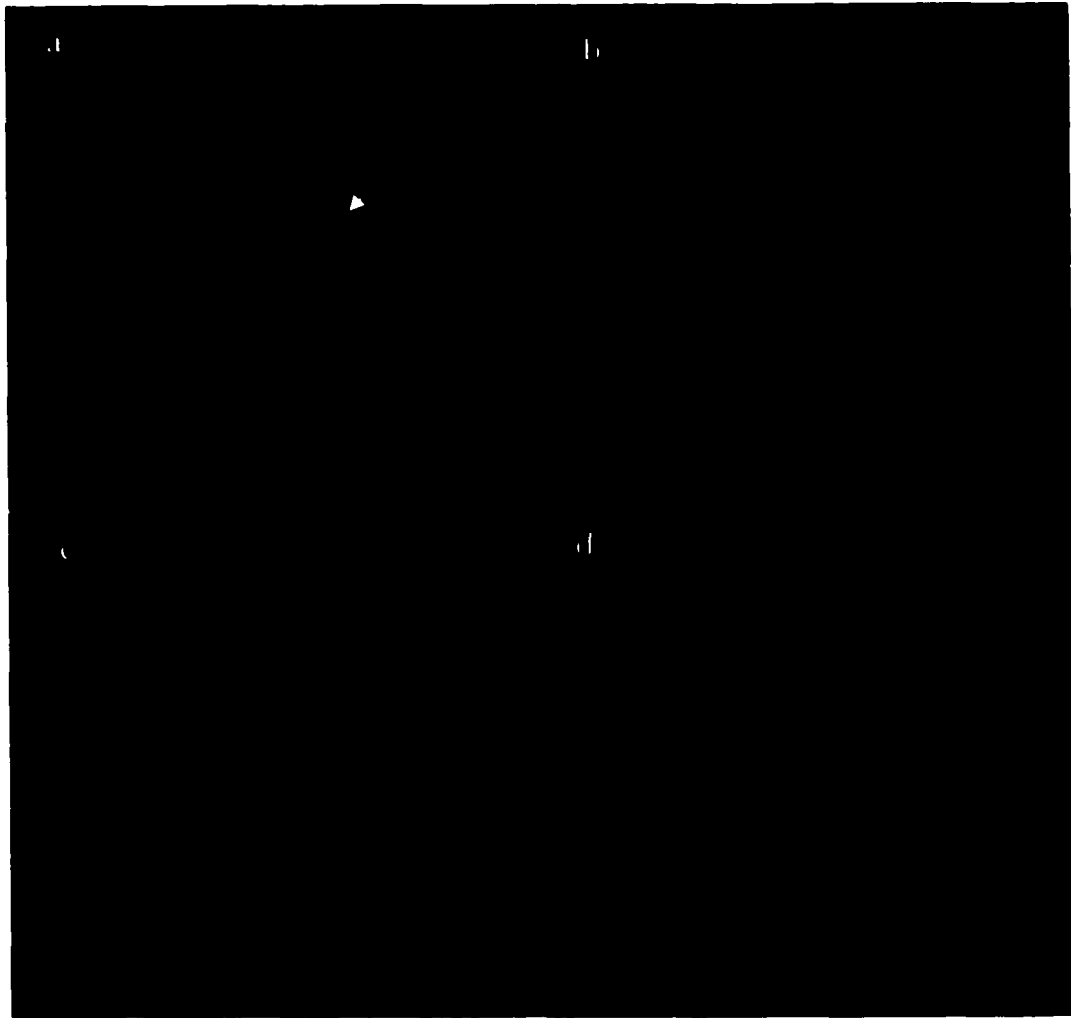


Figure 5-13. Confocal image of serum-starved AV cushion culture stained for endogenous bax. (a) DAPI staining on serum starved dissociated primary cultures of AV cushion cells showing the shrunken nucleus of an apoptotic cell (arrow) between intact nuclei. (b) Staining of the mitochondria with Mitotracker Red in the same field of view, showing the dispersed mitochondria in the intact cells, while the mitochondria in the dying cell surround the nucleus. (c) Staining for bax (green) shows distribution in the cytoplasm and nucleus of the intact cells. In the dying cell, bax staining is seen in the characteristic blebs of an apoptotic cell, and is now absent from the nucleus. (d) In the combined image, there appears to be little overlap of bax with the mitochondria. In the serum-starved cells, bax appears to overlap with the nuclei, while in the apoptotic blebbing cell, this overlap is absent. Mag. x560.

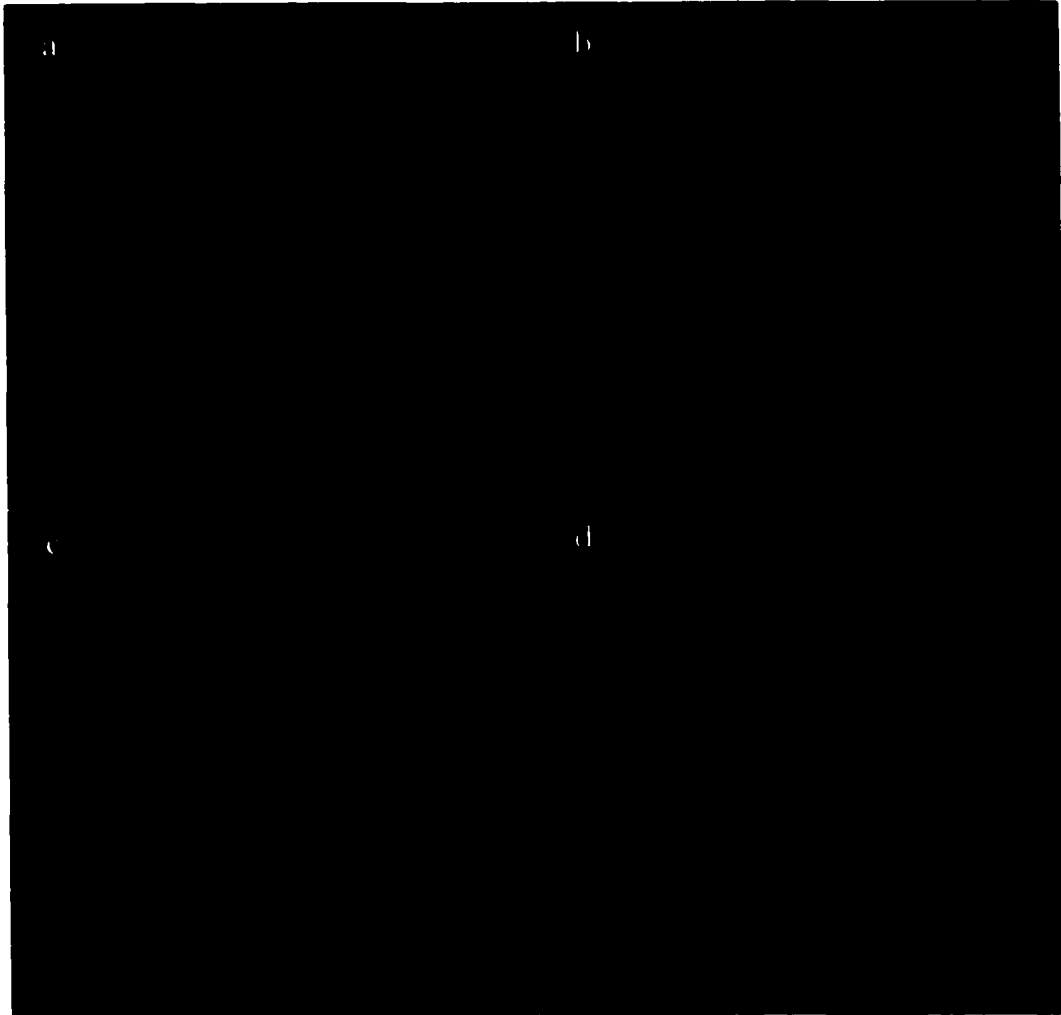


Figure 5-14. Confocal image of non-apoptotic serum-starved AV cushion culture, with a general caspase inhibitor, stained for endogenous bax. (a) DAPI staining on serum starved dissociated primary cultures of AV cushion cells showing the shrunken nuclei of a recently divided cell. (b) Staining of the mitochondria with Mitotracker Red in the same field of view showing the dispersed mitochondria. (c) Staining for bax (green) shows distribution in the cytoplasm and but is not seen in the nuclear area, similar to non-serum starved cultures.. (d) In the combined image, there appears to be no overlap of bax staining with the mitochondria or nuclei. Mag. x560.

Table 1 shows a summary of the sub-cellular distribution of bcl-2 and bax in the healthy and serum starved cushion cultures.

Figure 5-15 shows a western blot for the bax antibody used in the immunocytochemical studies, showing that the antibody recognizes the 23kDa band in AV cushion tissue and whole embryo, and that pre-absorption with the blocking peptide abolishes immunoreactivity.

Molecule	Healthy Cell	Serum Starved non-apoptotic cell	Apoptotic cell
Bcl-2	Cytoplasmic Nuclear/ER association? Some mitochondrial association	Cytoplasmic Some mitochondrial overlap Nuclear clusters absent	Cytoplasmic Nuclear overlap
With caspase inhibitor	-	Cytoplasmic Nuclear/ER association? Some mitochondrial overlap	-
Bax	Cytoplasmic No nuclear/mitochondrial overlap	Cytoplasmic Nuclear association No mitochondrial overlap	Cytoplasmic No nuclear association Apoptotic bleb association
With caspase inhibitor	-	Cytoplasmic Nuclear association absent	-

Table 5- 1. Summary of bcl-2 and bax distribution in healthy, serum starved and apoptotic cushions cells in culture. Representative cells from 3 individual cultures with each treatment are shown, with the majority of cells per treatment exhibiting the same staining patterns.

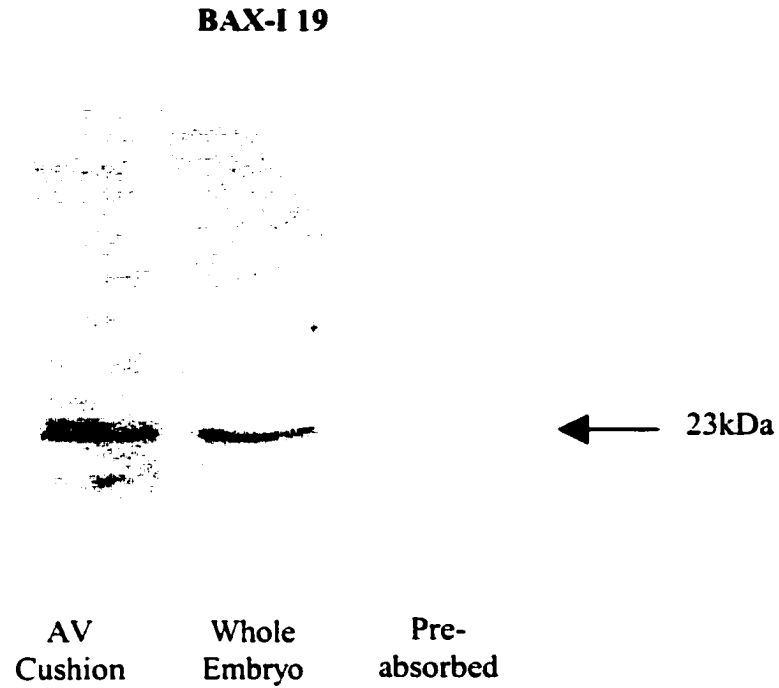


Figure 5-15. Immunoblotting with the I-19 bax polyclonal antibody. To test the antibody specificity, dissected AV tissue and a whole embryo positive control were immunoblotted with the I-19 antibody. The negative control with the antibody preabsorbed with the blocking peptide showed no bands.

CASPASE EXPRESSION AND ACTIVITY IN THE EMBRYONIC HEART

Immunoblot analysis of caspase-9 and the caspase substrate PARP

Immunoblot analysis was performed on dissected AV cushions and OT for evidence of expression and activity of the caspase family of enzymes. Initial attempts with antibodies to caspase -3 and -8 proved unsuccessful, with the antibody not recognizing any antigen in the tissue. Immunoblot analysis with a polyclonal antibody to caspase-9 recognized the 10kDa cleavage fragment of active caspase-9. Inactive caspase-9 (45kDa) is activated by cleavage into 35kDa and 10kDa fragments (Slee *et al*, 1999). In dissected AV cushions, the 10kDa cleavage fragment band was present in immunoblots from ED 5-8 with only very low levels seen in ED4 (Figure 5-16a). Immunoblots on dissected outflow tract revealed expression of the 10kDa band throughout ED 4-8 (Figure 5-16b). Densitometric analysis of the 10kDa band blots in the AV cushions revealed a low level of expression at ED 4, in comparison to similar raised levels throughout ED 5-8 (Figure 5-16c). In densitometric scans of the 10kDa band in blots on OT tissue, similar levels of caspase-9 cleavage fragment expression were seen during ED 4-8 (Figure 5-16d).

In the apoptotic signaling cascade, cellular proteins are cleaved and inactivated by active members of the caspase family of enzymes (Thornberry and Lazebnik, 1998). One such protein, poly(ADP)-ribose polymerase (PARP), a 113kDa protein, is cleaved and inactivated, resulting in cleavage fragments of 89 and 24kDa size, which are characteristic of apoptotic cells (Duriez and Shah, 1997). Dissected AV cushions and OT were immunoblotted for PARP, using a cross-reactive polyclonal antibody. In the AV cushions, the 24kDa fragment was seen at ED 7-8 (Figure 5-17a), while in the dissected

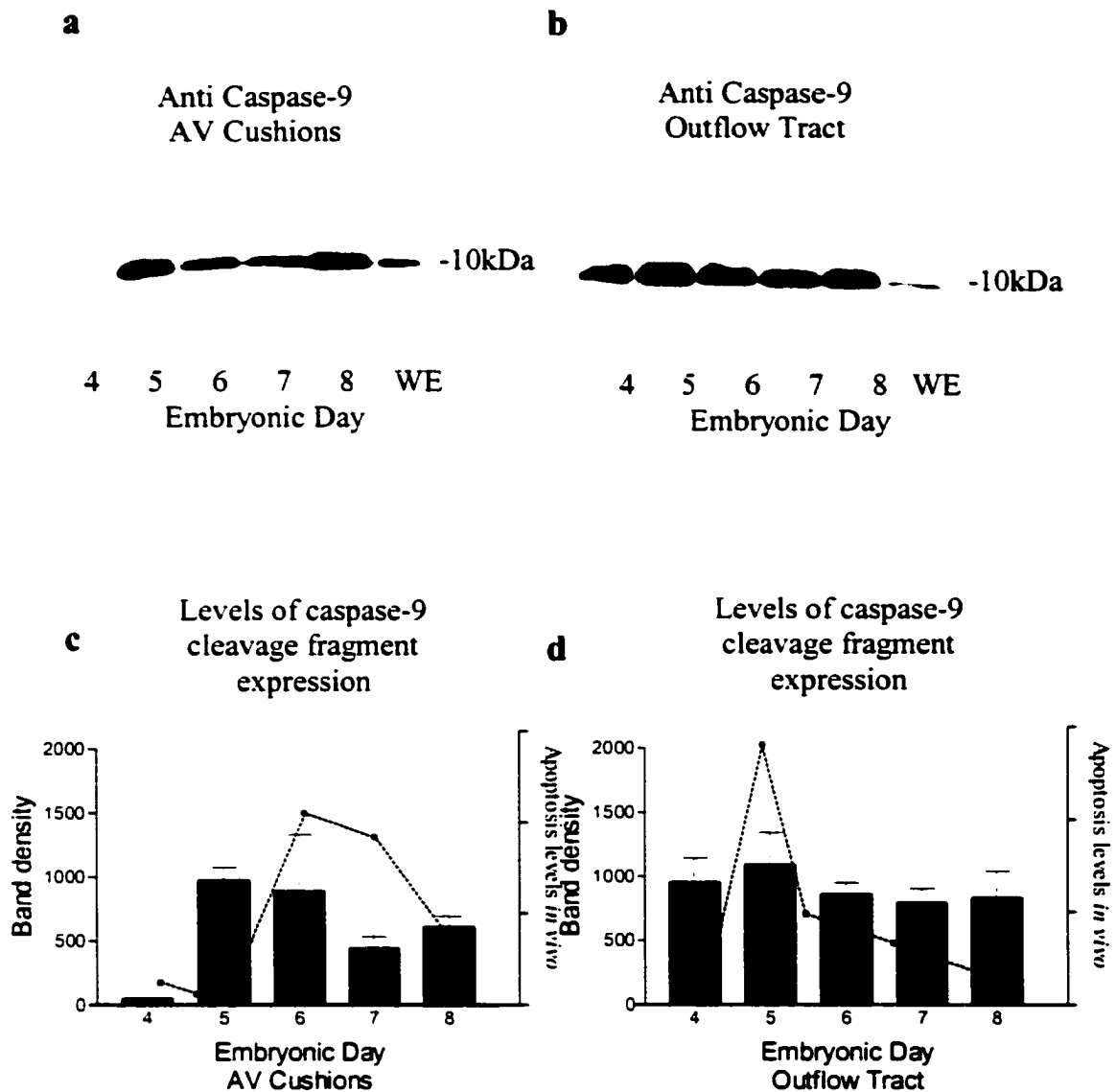


Figure 5-16. Caspase-9 cleavage fragment expression in dissected AV cushions and outflow tract. (a) Dissected atrioventricular (AV) cushions immunoblotted with a polyclonal antibody antibody to caspase-9. The 10kDa cleavage fragment band is present throughout ED 5-8 and in the whole embryo (we) positive control. (b) Dissected outflow tract immunoblotted with polyclonal caspase-9, showing the same 10kDa band throughout ED 4-8 and in the whole embryo (we) positive control. (c) Average densitometric scans for the 10kDa band in AV caspase-9 blots (n=2), showing a reduction in ED 4 expression. (d) Average densitometric scans for the 10kDa band in outflow tract caspase-9 (n=3) blots, showing similar expression throughout Ed 4-8. Data shown represents the mean band density for each day \pm SEM. The dashed lines show the pattern of apoptosis seen *in vivo*.

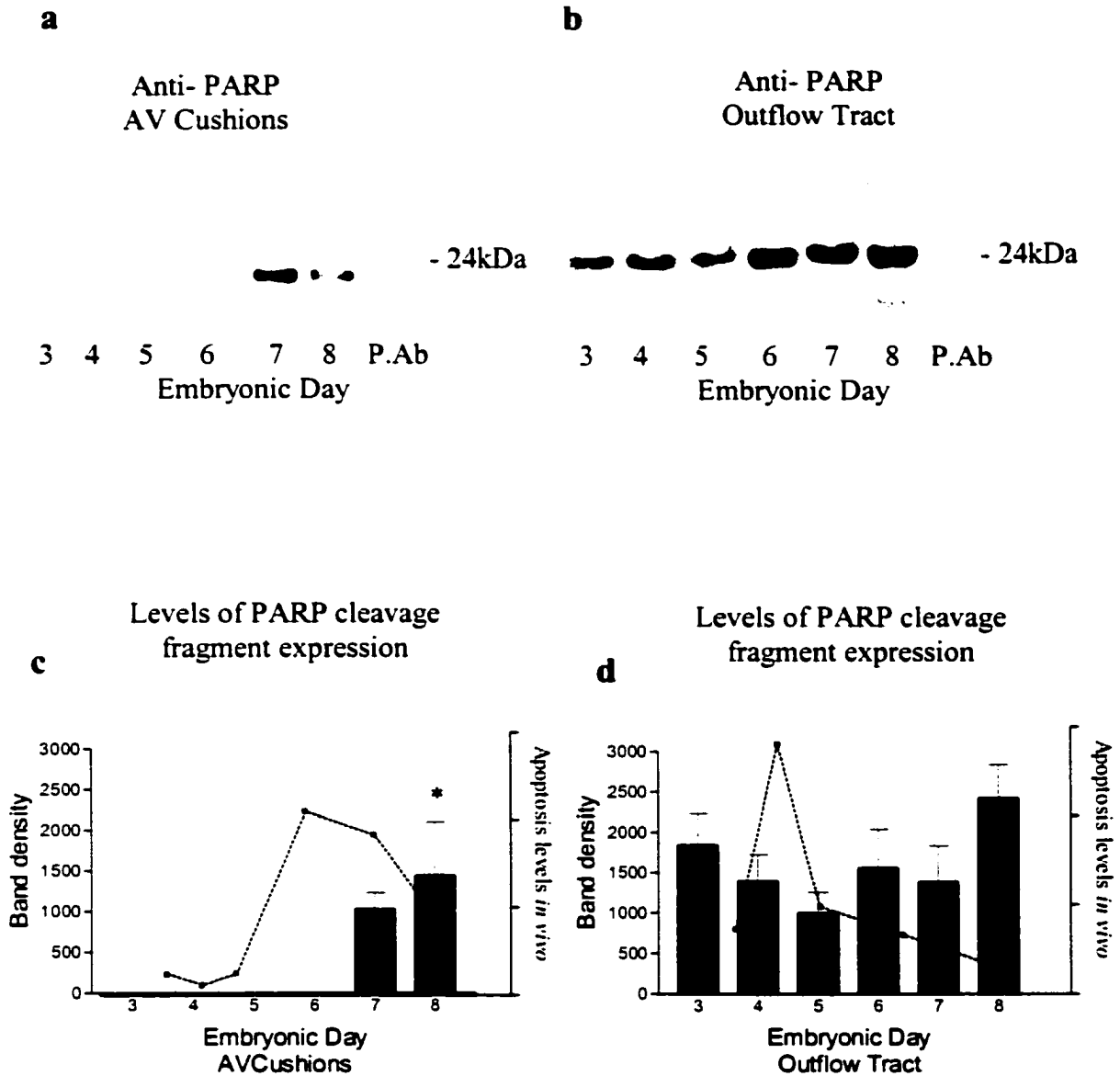


Figure 5-17. Poly (ADP)-ribose polymerase (PARP) cleavage fragment expression in dissected AV cushions and outflow tract. (a) Dissected atrioventricular (AV) cushions immunoblotted with polyclonal PARP. The 24kDa cleavage fragment band was only present in ED 7-8, and was eliminated by preabsorption (P.Ab.) with the suppliers blocking peptide. (b) Dissected outflow tract immunoblotted with polyclonal PARP, showing the same 24kDa cleavage fragment band, throughout ED 3-8, and no band with preabsorption with the blocking peptide. (c) Average densitometric scans for the 24kDa band in the AV PARP blots show that ED8 is significantly different from ED3-6 ($p < 0.05$; $n = 4$). (d) Average densitometric scans for the 24kDa band in the outflow tract blots with no significant differences ($n = 4$). Data shown represents the mean band density for each day \pm SEM, with statistical analysis by one way ANOVA and Tukey's post test. The dashed lines show the pattern of apoptosis seen *in vivo*.

OT, the cleavage fragment was seen throughout ED 3-8 (Figure 5-17b). Densitometric analysis of the 24kDa band blots in the AV cushions revealed up-regulation of expression in ED 7-8, with expression of the cleavage fragment at ED8 being significantly different from ED3-7 ($p < 0.05$; Figure 5-17c), while similar densitometric analysis of the 24kDa band in OT blots, revealed a constant level of expression throughout ED 3-8 (Figure 5-17d).

Caspase inhibitors on serum starved AV cushion cultures

Dissociated AV cushion cultures were grown and were serum starved to induce the cells to undergo apoptosis. The cultures were treated with various synthetic peptide apoptosis inhibitors and the levels of cell death were assessed. The cultures were treated with a universal caspase inhibitor, an inhibitor of caspase-3 and an inhibitor of caspase-9, and were compared to untreated controls. The cultures were stained with DAPI to stain all the nuclei (Figure 5-18a) and TUNEL to label the apoptotic nuclei (Figure 5-18b), and the total number of TUNEL-positive staining cells was counted. When the total number of TUNEL staining nuclei per culture were compared (Figure 5-18c), the effects of the universal inhibitor and the inhibitor of caspase-9 on the inhibition of apoptosis, showed a higher significance ($p < 0.01$) than the inhibitor of caspase-3 ($p < 0.05$) when compared to the untreated control.

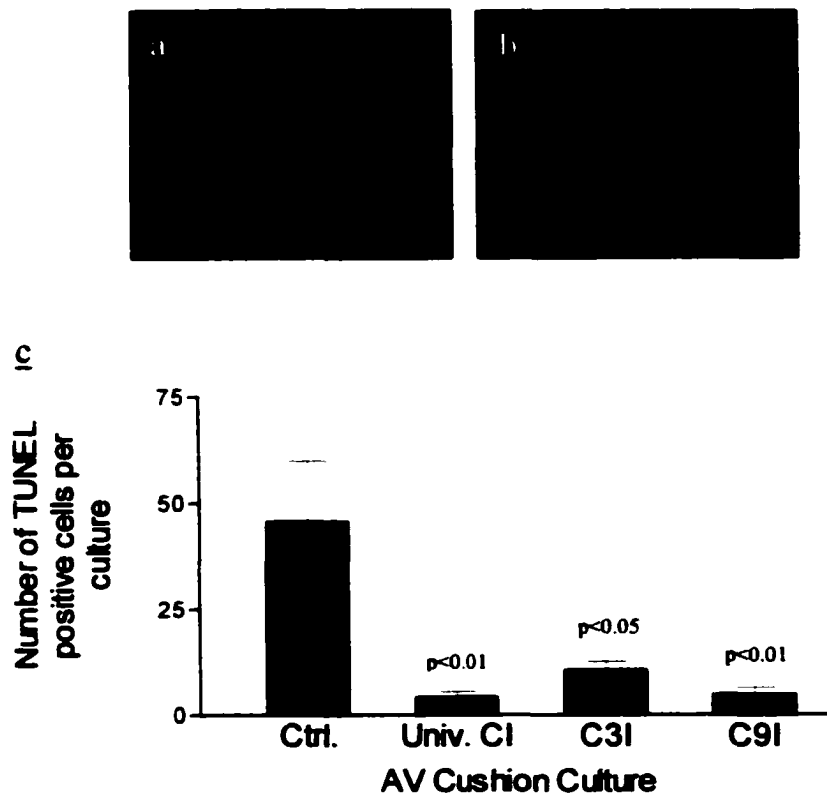


Figure 5-18. Effect of caspase inhibitors on the incidence of apoptosis in serum-starved AV cushion cultures. (a) DAPI staining on dissociated AV cushion cultures that were serum starved and treated with different caspase inhibitors. (b) TUNEL staining on the same field of view showing a TUNEL positive apoptotic cell. (c) Graph of the number of TUNEL-positive cells per culture, after no treatment (Ctrl) or after treatment with a universal caspase inhibitor (Univ. CI), an inhibitor of caspase 3 (C3I), or an inhibitor of caspase 9 (C9I). Each treatment was found to be significantly different from the control (n=5). Mag. x280, a,b.

Chapter 6

**EXPRESSION AND FUNCTION OF BONE
MORPHOGENETIC PROTEINS IN THE ENDOCARDIAL
CUSHIONS**

EXPRESSION OF BONE MORPHOGENETIC PROTEINS IN THE EMBRYONIC HEART

Previous work examining the role of BMP's in the developing heart has mostly focused on the expression patterns of mRNA at the time of epithelial-mesenchymal transformation (EMT) during endocardial cushion formation, with some speculation that the protein may play a role in apoptosis at a slightly later stage during cushion development. It was therefore decided to examine the expression pattern of two BMP proteins at a time when apoptosis is seen in the cushions.

Immunocytochemical localisation of bone morphogenetic protein 2.

To determine the localisation of bone morphogenetic protein (BMP) -2 in the heart, and to compare the distribution patterns of these proteins in the embryonic chick and mouse hearts, sections of both were immunocytochemically stained with a polyclonal antibody to BMP-2, at stages when the endocardial cushions are developing and cell death is normally seen in the chick cushions. In the chick heart, at ED 5-6, strong immunoreactivity was seen in the atrial wall and in the myocardium of the OT (Figure 6-1a). At a higher magnification of the same area (Figure 6-1b) positive staining for the protein could be seen scattered throughout the endocardial cushions of the OT. Expression was also seen throughout the ventricular myocardium (Figure 6-1d). In the AV cushions, there was positive immunoreactivity throughout the lateral and central cushions (Figure 6-1e). Negative controls, which entailed omission of the primary antibody, and incubation in serum alone, resulted in an absence of staining in all

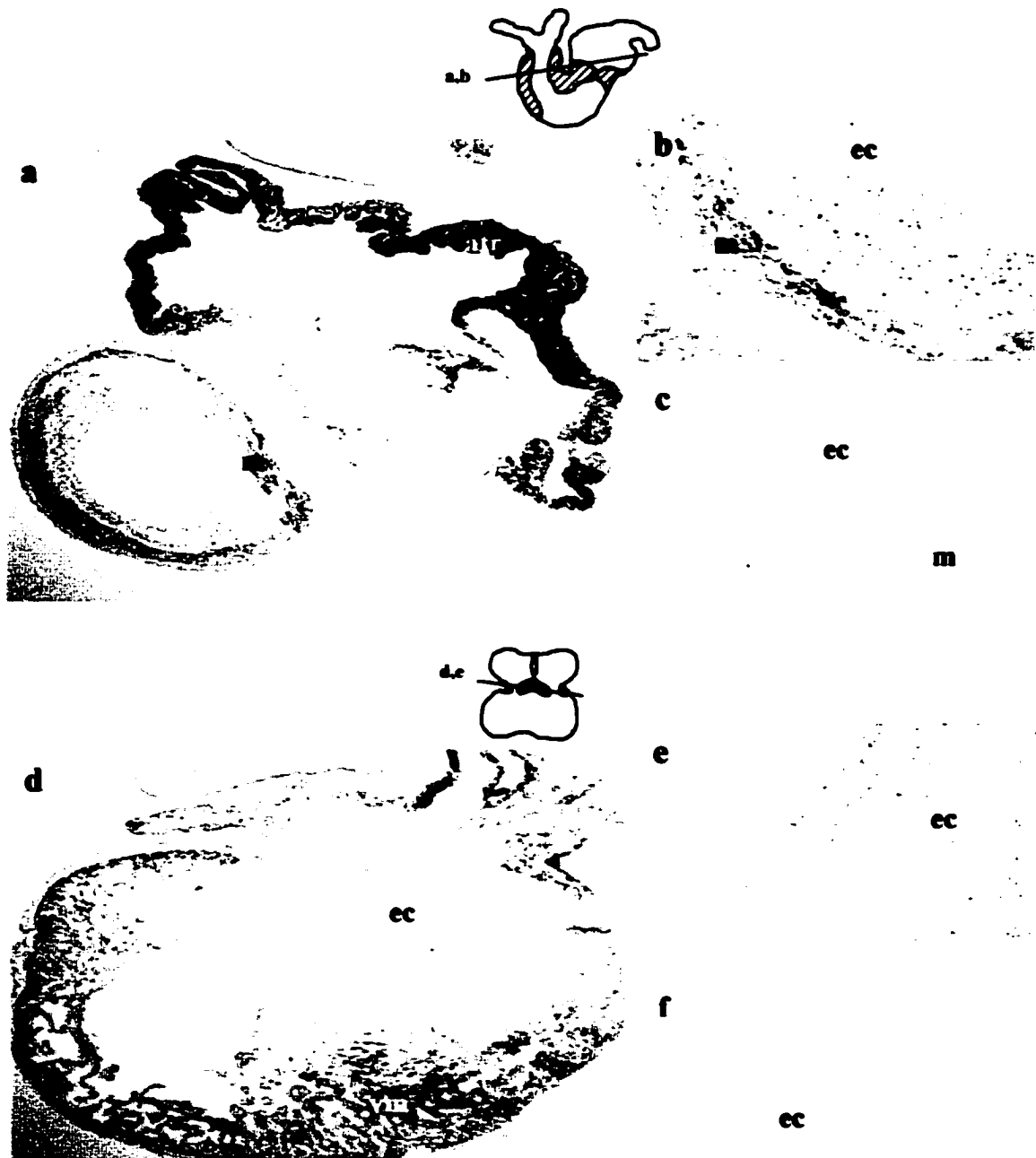


Figure 6-1. Immunocytochemical localisation of BMP2 in the ED 5-6 chick heart. (a) Sections of the chick heart stained for BMP2, show strong immunoreactivity in the atrial walls (atr) and the myocardium of the outflow tract (m). (b) At a higher magnification, staining is seen in the outflow tract endocardial cushions (ec) and in the myocardium (m). (c) Negative controls show no immunoreactivity in the OT endocardial cushions (ec) or myocardium (m). (d) Strong BMP2 immunoreactivity is also seen throughout the ventricular myocardium (vm). (e) At a higher magnification, staining can also be seen in the AV endocardial cushions (ec). (f) Negative controls show no immunoreactivity in the AV cushions (ec). Mag. x140, a,d; x280, b,c,e,f.

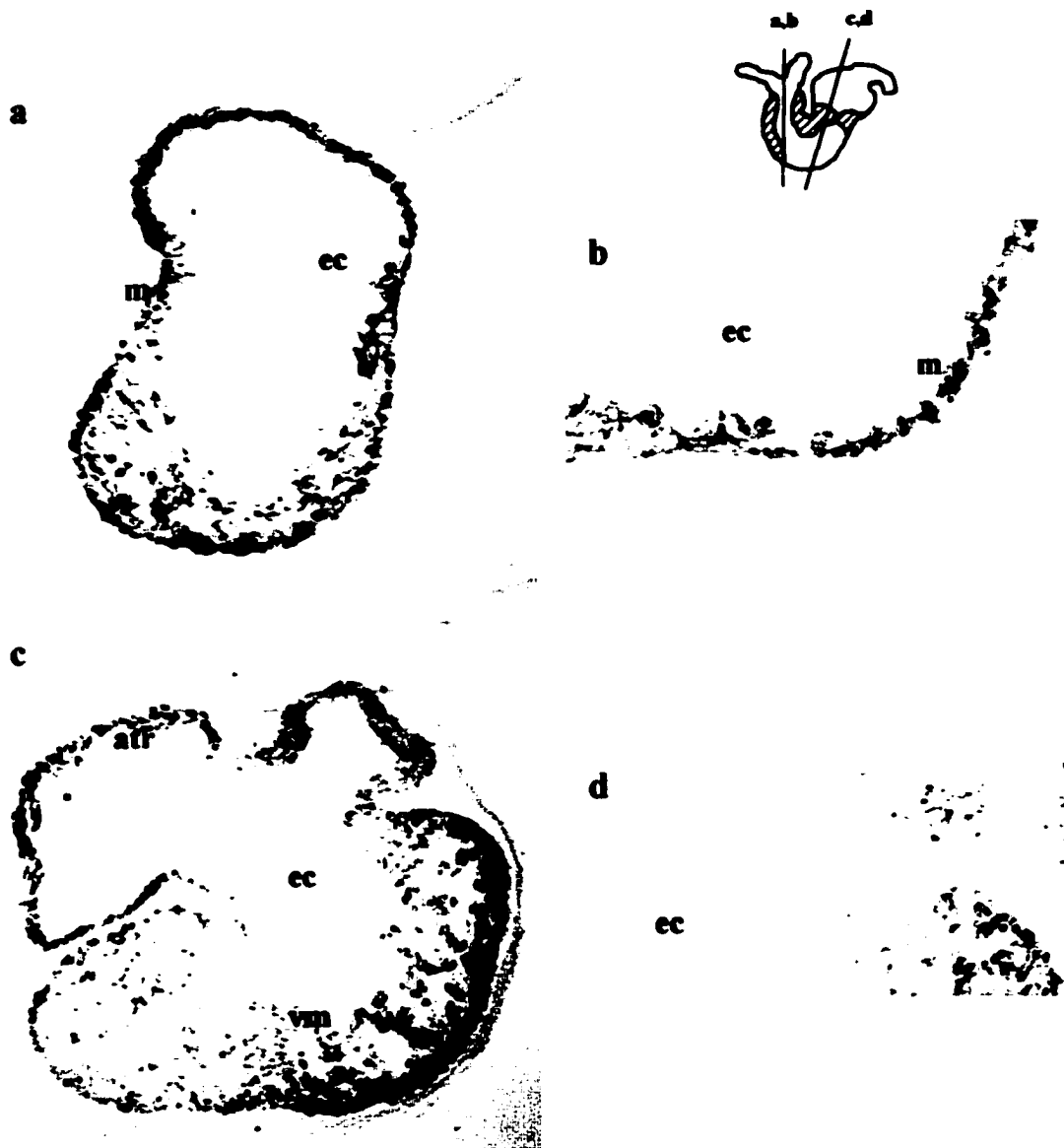


Figure 6-2. Immunocytochemical localisation of BMP2 in the ED 10.5 mouse heart. (a) Sections of the mouse heart stained for BMP2 show positive staining in the outflow tract myocardium (m) but not in the endocardial cushions of the outflow tract (ec). (b) At a higher magnification, no immunoreactivity is visible in the OT cushions (ec) (c) Strong staining is seen in the atrial wall and the ventricular myocardium (vm) but is not apparent in the atrioventricular cushions (ec). (d) At a higher magnification, no immunoreactivity is seen in the AV cushions (ec). Mag. x140, a,c; x280, b,d.



Figure 6-3. Immunocytochemical localisation of BMP2 in the ED 12.5 mouse heart. (a) Sections of the mouse heart stained for BMP2 show immunoreactivity in the myocytes of the outflow tract myocardium (m) that may be invading the endocardial cushions (ec). (b) At a higher magnification, immunoreactivity is seen in the myocardium (m) with little or none visible in the endocardial cushions of the OT (ec) (c) Staining is seen in the atrial wall (atr) and ventricular myocardium (vm), with no staining apparent in the AV cushions (avc). (d) AT a higher magnification, the immunoreactivity is absent from the AV endocardial cushions (ec). Mag. x140, a,c; x280, b,d.

immunocytochemical procedures. Representative examples are shown in figure 6-1c and f.

Staining was also performed on sections of the embryonic mouse at ED 10.5, which corresponds to a slightly earlier stage than that used in the chick. In the OT, staining was only seen in the myocardium, with no visible immunoreactivity seen in the OT cushions (Figure 6-2a and b). Staining was also widespread throughout the ventricular myocardium and the atrial walls (Figures 6-2c). In the AV endocardial cushions, again, no immunoreactivity was seen (Figure 6-2d). Staining was also performed on ED 12.5 mouse sections, at a stage when the endocardial cushions are more developed. In the OT, immunoreactivity was seen in the myocytes of the myocardium, that may be invading the endocardial cushions, but no visible immunoreactivity was seen in the OT cushions (Figures 6-3 a and b). Strong immunoreactivity was also seen in the ventricular myocardium and the atrial wall, but with no apparent staining in the AV cushions (Figure 6-3c and d). In both the chick and mouse embryos, staining was performed on sections of the entire embryo, where other regions in the embryo showing positive immunoreactivity were the chondrocytes in the developing limb (not shown).

Immunocytochemical localisation of bone morphogenetic protein 4.

Sections of the embryonic chick and mouse heart were also stained for BMP4, at similar times when the cushions are developing. In the ED 5-6 chick heart, staining in the OT was restricted to the myocardium, but no obvious immunoreactivity was apparent in the endocardial cushions (Figure 6-4a and b). In whole heart sections (Figure 6-4c), immunostaining was evident in the atrial wall, OT myocardium and the ventricular

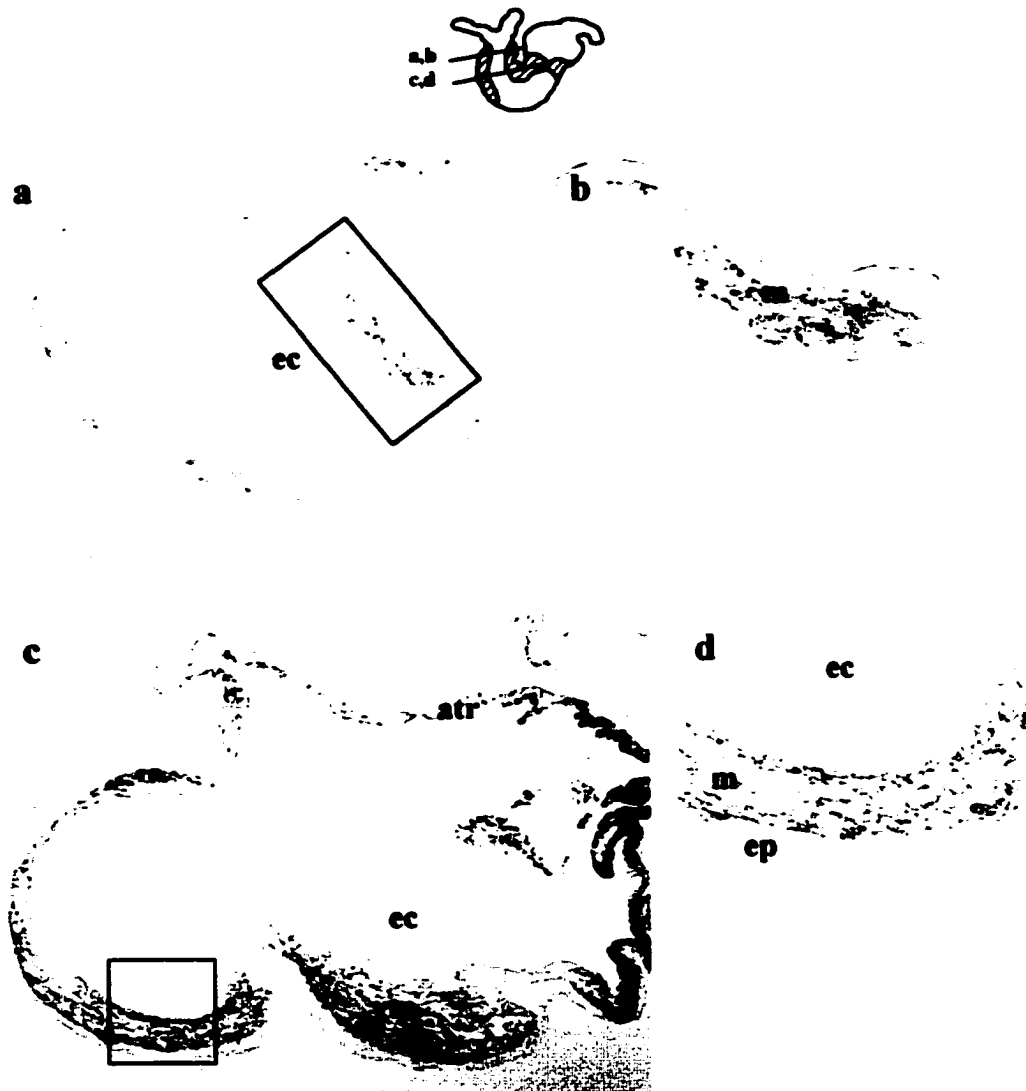


Figure 6-4. Immunocytochemical localisation of BMP4 in the ED 5-6 chick heart. (a) Sections of chick hearts stained for BMP4 show some immunoreactivity in the OT myocardium (m). (b) At a higher magnification of the boxed area, the staining is evident in the myocardium (m) but is not visible in the OT endocardial cushions (ec). (c) In whole heart sections, positive staining is seen in the atrial wall (atr) and the edge of the ventricular myocardium (vm) but with no apparent staining in the atrioventricular cushions (avc). (d) A higher magnification of the boxed area in the proximal OT shows staining in the outflow tract myocardium (otm) but not in the cushions (ec) or epicardium (ep). Mag. x140, a,c; x280, b,d.



Figure 6-5. Immunocytochemical localisation of BMP4 in the ED 10.5 mouse heart. (a) Sections of mouse heart stained for BMP4 shows strong staining in the atrial wall (atr), the right ventricular myocardium (vm) and the outflow tract (ot). (b) At a higher magnification of the OT, the staining seems to be restricted to the myocardium (m), with no apparent immunoreactivity in the endocardial cushions (ec) (c) In the AV region, strong immunoreactivity is seen in the atrial wall (atr) and the ventricular myocardium (vm). No staining is visible in the AV endocardial cushions (ec). (d) A higher magnification of the AV cushions (ec) reveals no immunoreactivity. Mag. x140, a,c; x280, b,d.

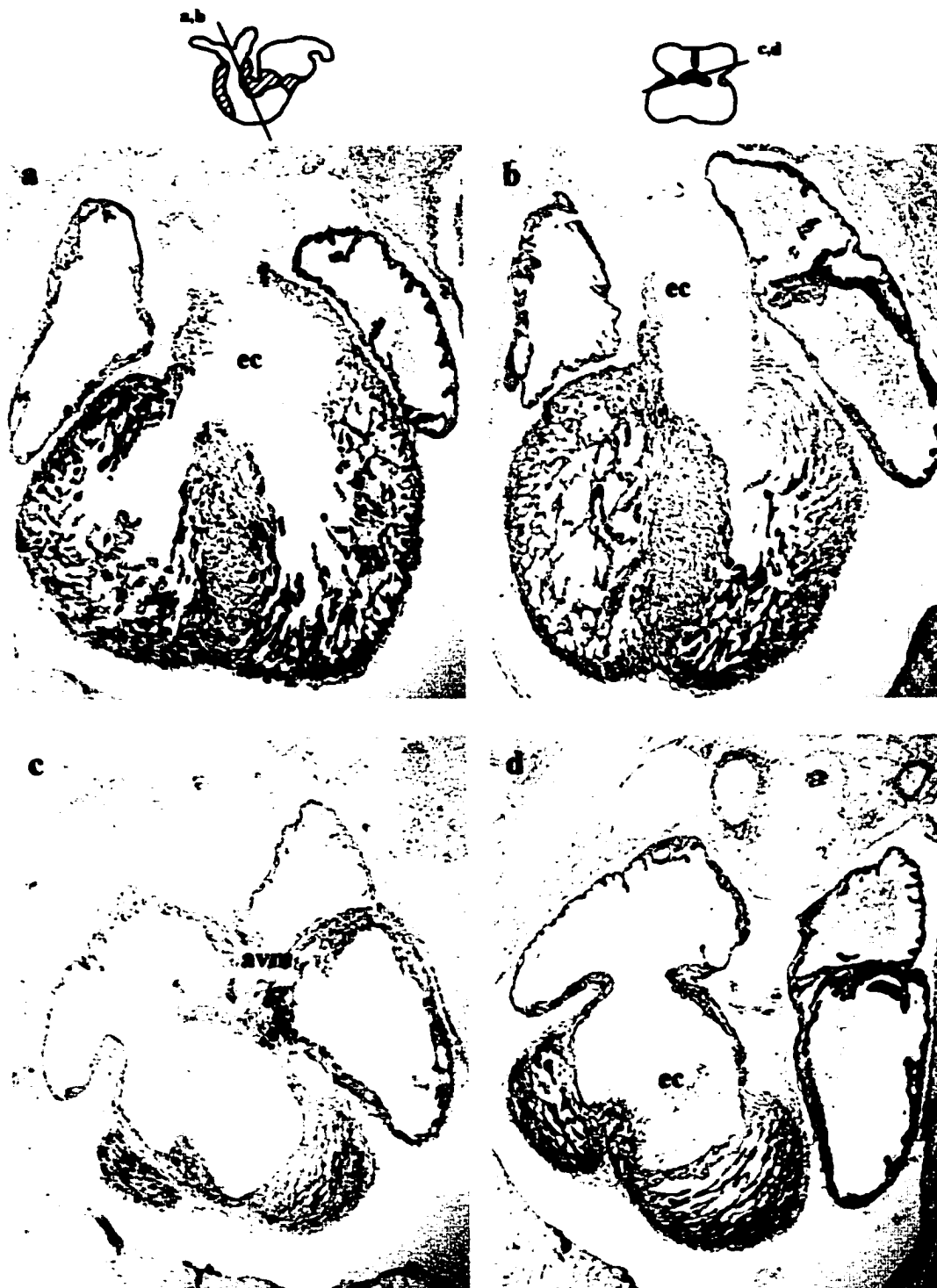


Figure 6-6. Immunocytochemical localisation on BMP4 in the ED 12.5 mouse embryonic heart. (a) Sections of the mouse heart stained for BMP4 show staining in the ventricular myocardium (vm), but no apparent immunoreactivity is seen in the endocardial cushions (ec) of the proximal OT. (b) In the slightly more distal OT endocardial cushions (ec), no staining is apparent. (c) The atrioventricular myocardial region (avm) shows a more restricted positive staining. (d) No staining is visible in the AV endocardial cushions (ec). Mag. x140.

myocardium, with no apparent staining in the AV endocardial cushions. Staining was also performed on sections of the ED 10.5 mouse heart. Strong expression was also seen in the atrial wall and ventricular myocardium (Figure 6-5a). In the OT, staining was restricted to the myocardium, with no obvious staining in the endocardial cushions (Figure 6-5b). In the AV region of the heart, strong immunoreactivity was seen in the ventricular myocardium and the atrial wall (Figure 6-5c), and again no apparent staining was visible in the AV endocardial cushions (Figures 6-5c and d). In the ED 12.5 mouse heart, the staining seemed to have a more restricted pattern. Positive staining was seen in the trabeculae of the ventricle, but was not evident in the maturing valve leaflets (Figure 6-6a and b). In the AV region, staining seemed to be restricted to a specific part of the AV myocardium (Figure 6-6c), but again, no obvious staining was seen in the AV endocardial cushions (Figures 6-6c and d).

A summary of the distribution of the immunostaining seen in both the chick and mouse heart, with BMP2 and BMP4 is shown in table 6-1.

Tissue	BMP2	BMP4
Chick		
Endocardial cushions	+	-
Atria	+++	+++
Ventricle	++	++
OT myocardium	++	++
Mouse		
Endocardial cushions	-	-
Atria	+++	++
Ventricle	+++	+++
OT myocardium	+++	++

Table 6-1. Summary of the distribution pattern for BMP2 and BMP4 immunocytochemistry in the chick and mouse heart. Immunostaining was performed on sections of chick and mouse heart, for BMP2 and BMP4. The distribution pattern and relative intensity of staining in the different areas of the heart are represented, from no visible staining (-), to minor (+) and strong immunoreactivity (+++).

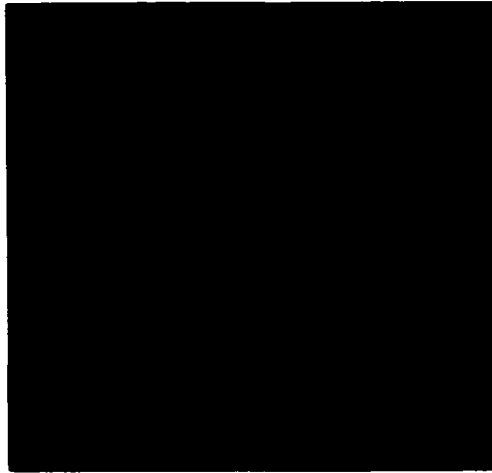
RETROVIRAL OVEREXPRESSION OF BONE MORPHOGENETIC PROTEIN RECEPTORS IN CUSHION CULTURES

As part of studies to investigate if BMP receptors are involved in apoptosis of endocardial cushion cells, dissociated cushion cultures were infected with replication-competent RCAS virus, encoding either BMP-receptor (BMPR) -1A or -1B, with constitutively-active (CA) or dominant-negative (DN) isoforms.

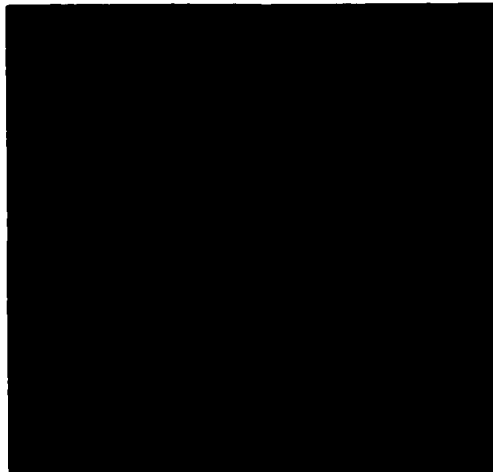
Initially, healthy cultures were grown for 4-6 days after infection, and were subsequently stained with TUNEL and DAPI. Five replicates of each treatment were performed (uninfected control; 1A, CA; 1A DN; 1B CA; 1B DN). In each case, no differences were observed in levels of apoptosis between the various treatments, with only randomly scattered individual apoptotic cells seen in each. Examples of cultures infected with the 1A and 1B DN isoforms and uninfected controls, stained with TUNEL, DAPI and an antibody to the viral coat protein are seen in Figure 6-7. To test for differences in proliferation rates, similar cultures were stained for PCNA, with five replicates of each treatment (Figure 6-8). Again, similar patterns of staining were seen between treatments in all cultures, but further experiments with statistical analysis are needed.

To test if the overexpression of the receptors was protecting the endocardial cushion cells from apoptosis, other cultures were serum-starved to induce apoptosis, and were infected with one of the four receptor isoforms, or were left uninfected as a negative control. The cultures, which each had received equal numbers of cells over a similar surface area, were stained with TUNEL and the number of positive-staining cells per culture was compared (Figure 6-9). No significant difference was observed between

Uninfected Control



BMPR 1A DN



BMPR 1B DN



Figure 6-7. Dissociated AV cushion cultures overexpressing dominant-negative BMP receptors. Dissociated AV cushion cultures were infected with RCAS virus containing transcripts for dominant-negative (DN) BMP receptors 1A and 1B, or were uninfected as a negative control. Cultures were labeled with a monoclonal anti-viral coat protein antibody (red), TUNEL (green) and DAPI (blue). No green staining is visible, as there were no TUNEL-positive cells. Mag. x560.

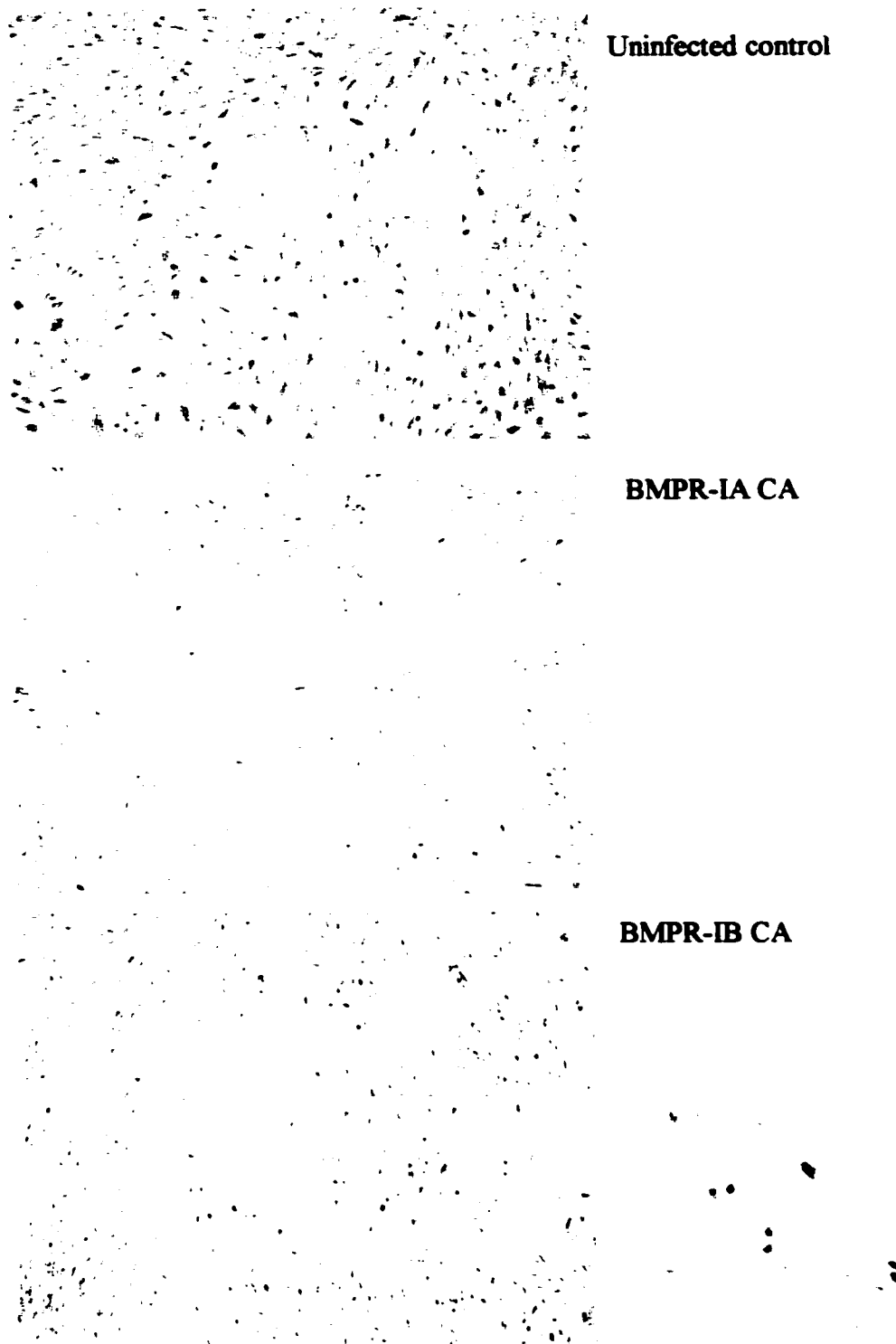


Figure 6-8. Immunocytochemistry for PCNA on AV cushion cultures overexpressing constitutively active BMP receptors. Dissociated AV cushion cultures were infected with RCAS virus containing transcripts for constitutively-active (CA) BMP receptor 1A or 1B, or were left uninfected as a negative control. Cultures were stained for PCNA, with the inset picture showing the specificity of labeling. Mag. x140. Inset, x560.

treatments, when compared to the uninfected control. However, it was observed that in cultures infected with the BMPR-1B CA-expressing virus, there was an overlap of high levels of viral staining with TUNEL positive cells (Figure 6-12), throughout replicate cultures. The intensity of the viral stain was greater than the background level seen in uninfected controls (Figure 6-10) but was similar to the level of intensity seen in BMPR-1A CA infected cells, that were not undergoing apoptosis (Figure 6-11). This suggests that at a certain threshold level, in the absence of external growth factors, BMPR-1B CA may induce apoptosis in a sub-population of cells in the endocardial cushion cultures, even though the overall level of apoptosis is not significantly changed.

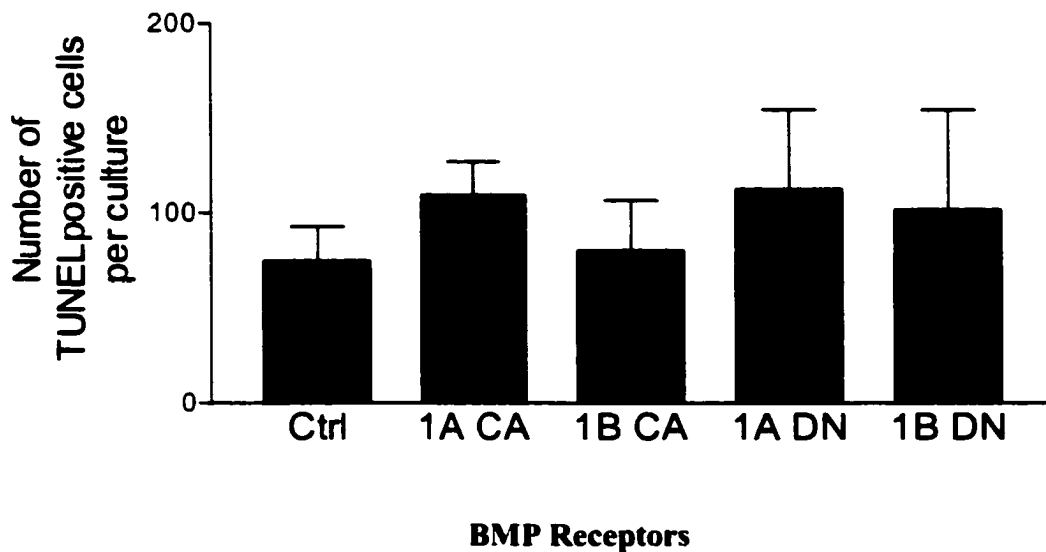


Figure 6-9. Comparison of TUNEL counts on serum starved AV cushion cultures overexpressing BMP receptors. Dissociated cushion cultures were serum starved to induce apoptosis and were infected with RCAS virus containing transcripts for BMP receptors 1A and 1B, constitutively active (CA) or dominant negative (DN). Statistical analysis using one way ANOVA and Tukey's post test showed no significant differences between treatments and the uninfected control (Ctrl) (n=5).



Figure 6-10. Uninfected control serum-starved AV cushion cultures. Dissociated AV cushion cultures were serum starved and were left uninfected as a negative control for BMPR-overexpression studies. The cultures were stained with DAPI (blue), TUNEL (green) and with a monoclonal anti-viral coat antibody (red). The background staining with the viral coat antibody has been enhanced for comparison with the infected cultures. Mag. x280.

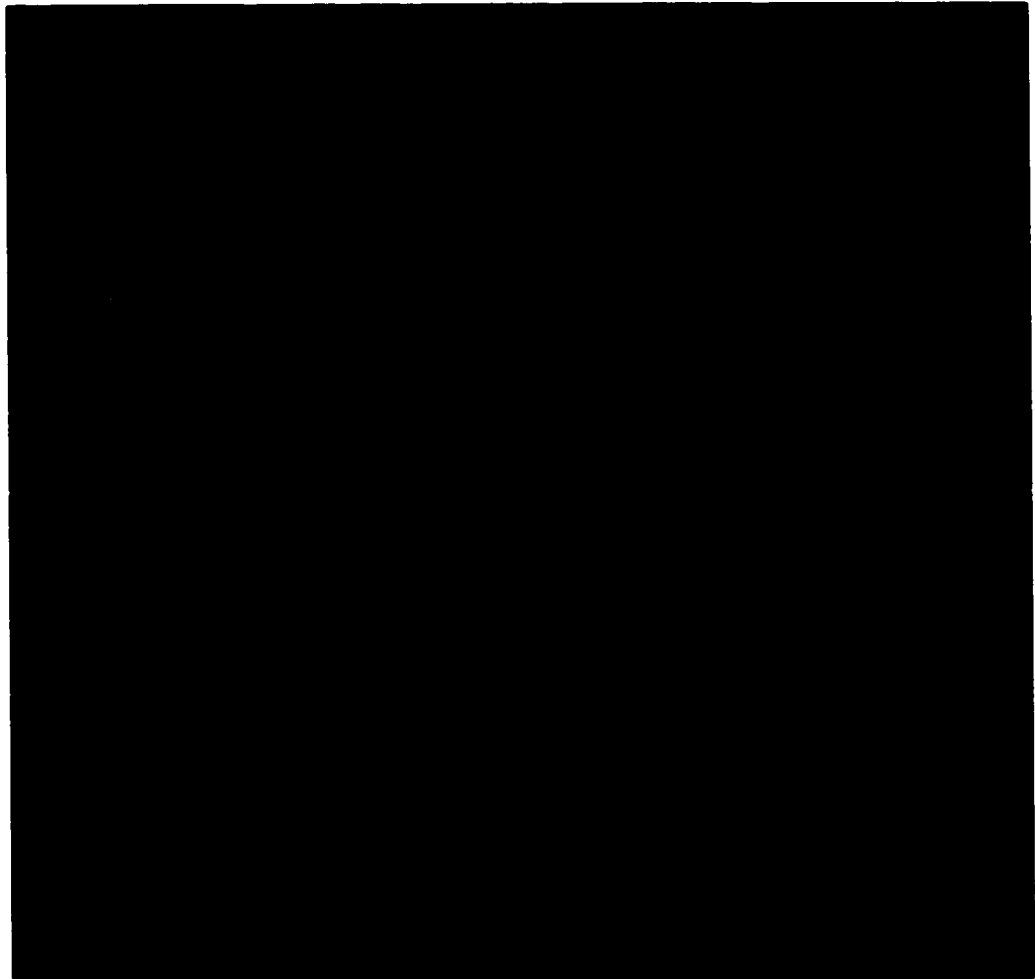


Figure 6-11. Serum starved AV cushion cultures, overexpressing constitutively-active BMP receptor 1A. Dissociated AV cushion cultures were serum starved and infected with RCAS virus containing transcripts for constitutively-active BMP receptor-1A. The cultures were stained with DAPI (blue), TUNEL (green) and with a monoclonal anti-viral coat antibody (red). Mag. x280.

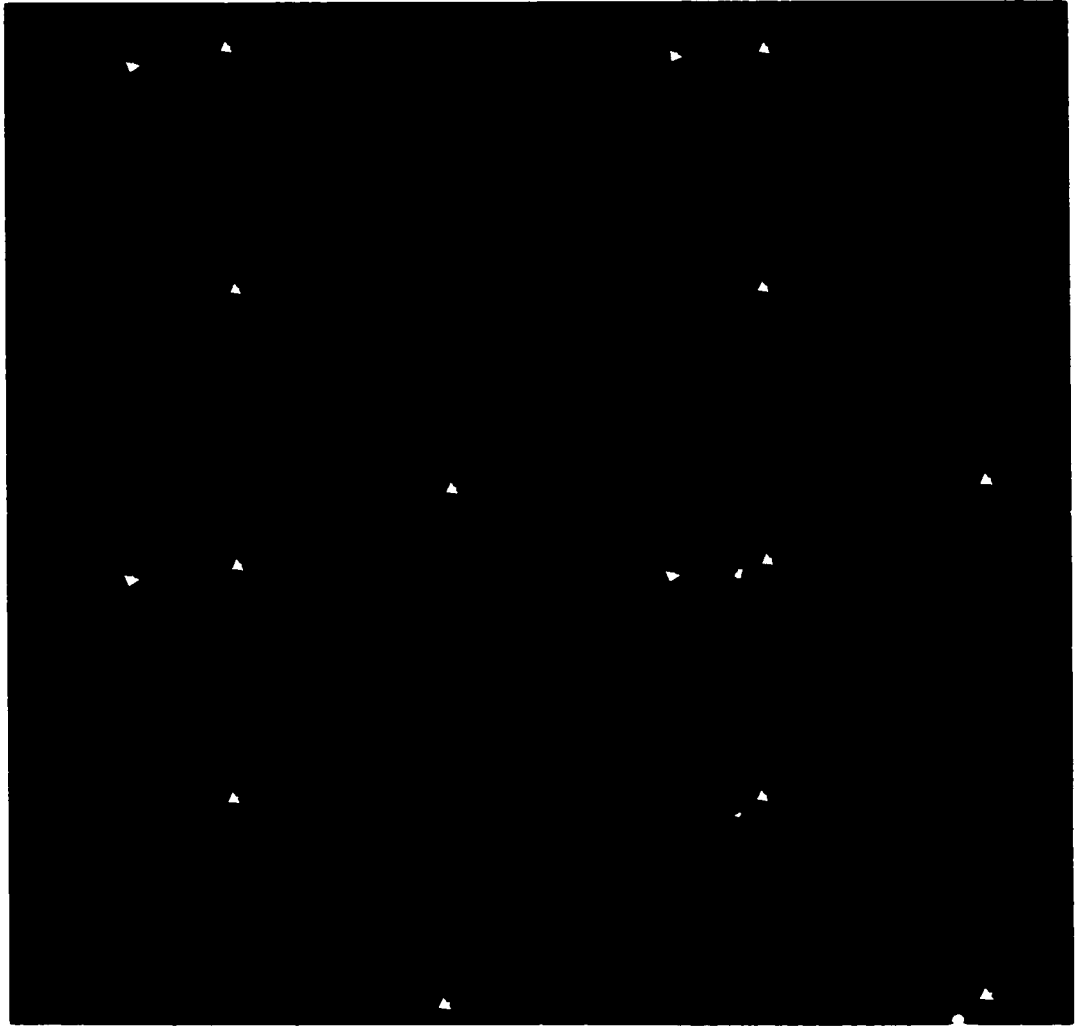


Figure 6-12. Serum starved AV cushion cultures, overexpressing constitutively-active BMP receptor 1B. Dissociated AV cushion cultures were serum starved and infected with RCAS virus containing transcripts for constitutively-active BMP receptor-1A. The cultures were stained with DAPI (blue), TUNEL (green) and with a monoclonal anti-viral coat antibody (red). Note the increased viral staining overlapping with TUNEL staining and fragmenting nuclei (arrows). Mag. x280.

Overexpression of BMP-receptors 1A and 1B in endocardial endothelial cells

Cultures were infected with RCAS viruses expressing the constitutively active and dominant negative isoforms of BMP-receptors 1A and 1B, and were compared to uninfected controls. In one experiment of five replicates, with infection of the culture with BMPR-1A CA, it was noticed that the cell morphology was changed in each of the five cultures. The cells took on the appearance of cells undergoing EMT, whereby they attained an elongated migratory appearance, which was not seen with other treatments (Figure 6-13). Treatment with BMPR-1B DN also induced some changes, but not to the same extent (Figure 6-13). It was concluded that in these cultures, endocardial endothelial cells were the dominant cell type, over the endocardial cushion cells, and that overexpression of the receptor induced EMT changes that would enable the endocardial cell to invade the cushions *in vivo*. Attempts were made at growing endocardial cell cultures from an established protocol (Runyan and Markwald, 1983), which involved another five replicates of each treatment and these cultures were infected with the virus. The outcome was the same as seen in the initial experiment, with a change in cell morphology seen. The cells with an altered appearance did not appear to have migrated further than the unaffected cells, but merely to change shape. Further experiments are necessary, but this suggests that BMPR-1A is a receptor that is involved in EMT in the initial growth stages of the endocardial cushions. It is not known which receptor subtypes are present *in vivo*.

Measurements of the cell area were made on the endocardial cell cultures that were infected with the different receptor isoforms, and were compared to the uninfected controls (Figure 6-14A). The BMPR1A-CA treated cells, with the most striking

phenotypic changes, had a significantly smaller surface area ($p < 0.01$), as did the cells infected with BMPR1A-DN ($p < 0.01$). Measurements of the aspect ratio of the cells were also compared (Figure 6-14B). This is the long axis of the cell divided by the short axis, with values closer to 1 representing rounder cells. The uninfected control cultures and the cultures infected with 1B-CA and 1A-DN all had similar results. The cultures with the observed phenotypic changes, infected with BMPR1A-CA and 1B-DN both were significantly different ($p < 0.01$) from the control.

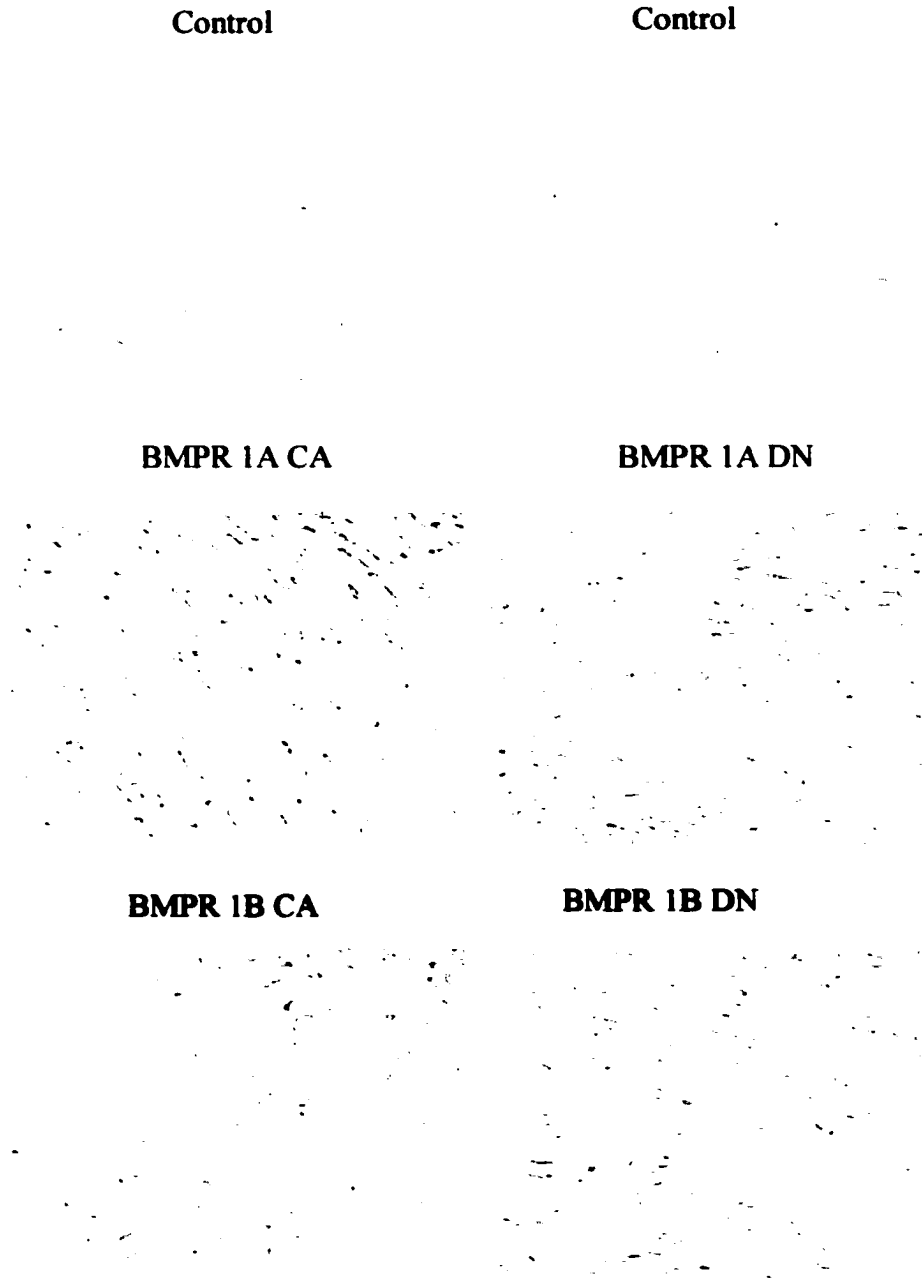


Figure 6-13. Overexpression of BMP receptors in endocardial endothelial cells. Dissociated endocardial cushion cultures were grown and infected with RCAS vectors carrying the transcripts for BMP receptors 1A and 1B, constitutively active (CA) and dominant negative (DN). Treatment with BMPR-1A-CA and 1B-DN induced cell changes characteristic of an epithelial-mesenchymal transformation, such as an elongated migratory appearance. This was not seen with the other treatments, or in untreated control cultures. Mag. x560.

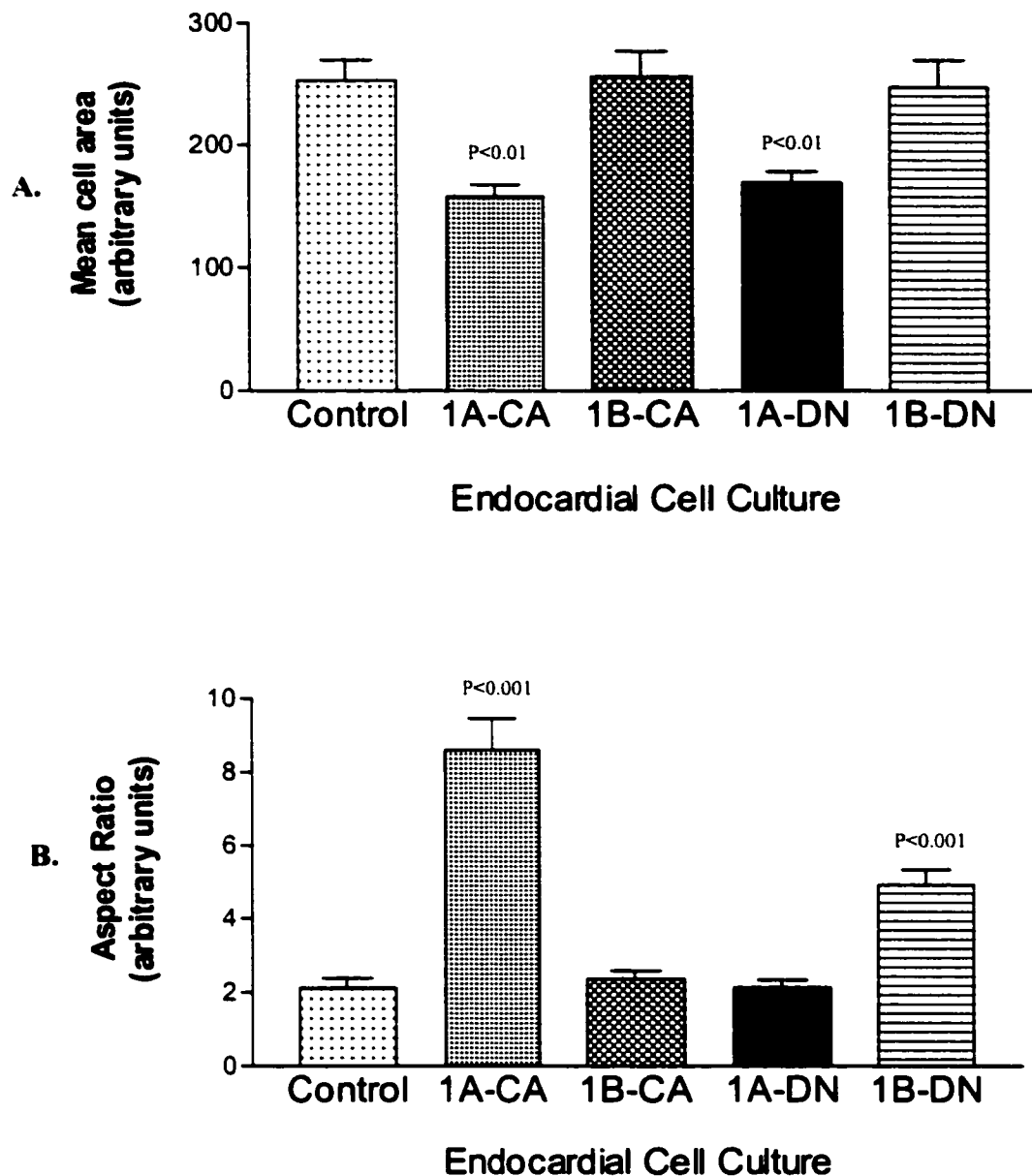


Figure 6-14. Effects of BMPR on endocardial cell cultures. Cultures were made of the endocardium lining the heart, and were infected with virus containing transcripts for the BMP-receptor, types 1A and 1B, constitutively-active (CA) or dominant-negative (DN). (A) Measurements of the cell area showed that infection with 1A-CA and 1A-DN significantly decreased the area in comparison to the uninfected controls. (B) Aspect ratio values are measurements of the long axis of the cell divided by the short axis, with values closer to 1 indicating rounder cells. Treatment with BMPR 1A-CA and 1B-DN both significantly affect the ratio. All values are calculated on an arbitrary scale, and were analyzed using one-way ANOVA and Tukey's post-test (n=10).

Chapter 7

**BCL-2 OVEREXPRESSION IN THE ENDOCARDIAL
CUSHIONS**

VIRAL-MEDIATED BCL-2 OVEREXPRESSION

A series of avian-specific replication-competent retroviral vectors has been developed by Hughes *et al* (1987). These proviral vectors are derived from the Rous sarcoma virus and have been modified so that sequences of foreign DNA, up to 2.5kb in size can be inserted, with no loss of function. A proviral vector containing the transcript for the human bcl-2 gene (pRCASBP(B)(bcl-2) and a proviral vector without a foreign sequence insert (RCASBP(B)) were obtained to attempt overexpression of the anti-apoptotic bcl-2 protein in the endocardial cushions. The proviral vectors are transfected into chick embryo fibroblasts (CEF's), which subsequently generate and release infectious virions into the medium, which can then be collected and concentrated. The CEF's are tested for viral production and bcl-2 insert stability and function. The concentrated virus can then be microinjected into the endocardial cushions, where the viral sequence, with the DNA insert, will be integrated into the genome of susceptible proliferating cells, and result in translation of the active protein.

Virus production and controls

During the generation and amplification steps of the RCAS virus, a number of controls were performed to ensure that virus was being produced after transfection of CEF's with the plasmid DNA for both pRCASBP(B) and pRCASBP(B)(bcl-2), and that the bcl-2 insert was present and producing protein. Immunocytochemistry was performed on the transfected CEF's with the monoclonal AMV-3C2 antibody, which recognizes the viral surface coat protein GAG, and with an antibody to the bcl-2 protein (Figure 7-1).

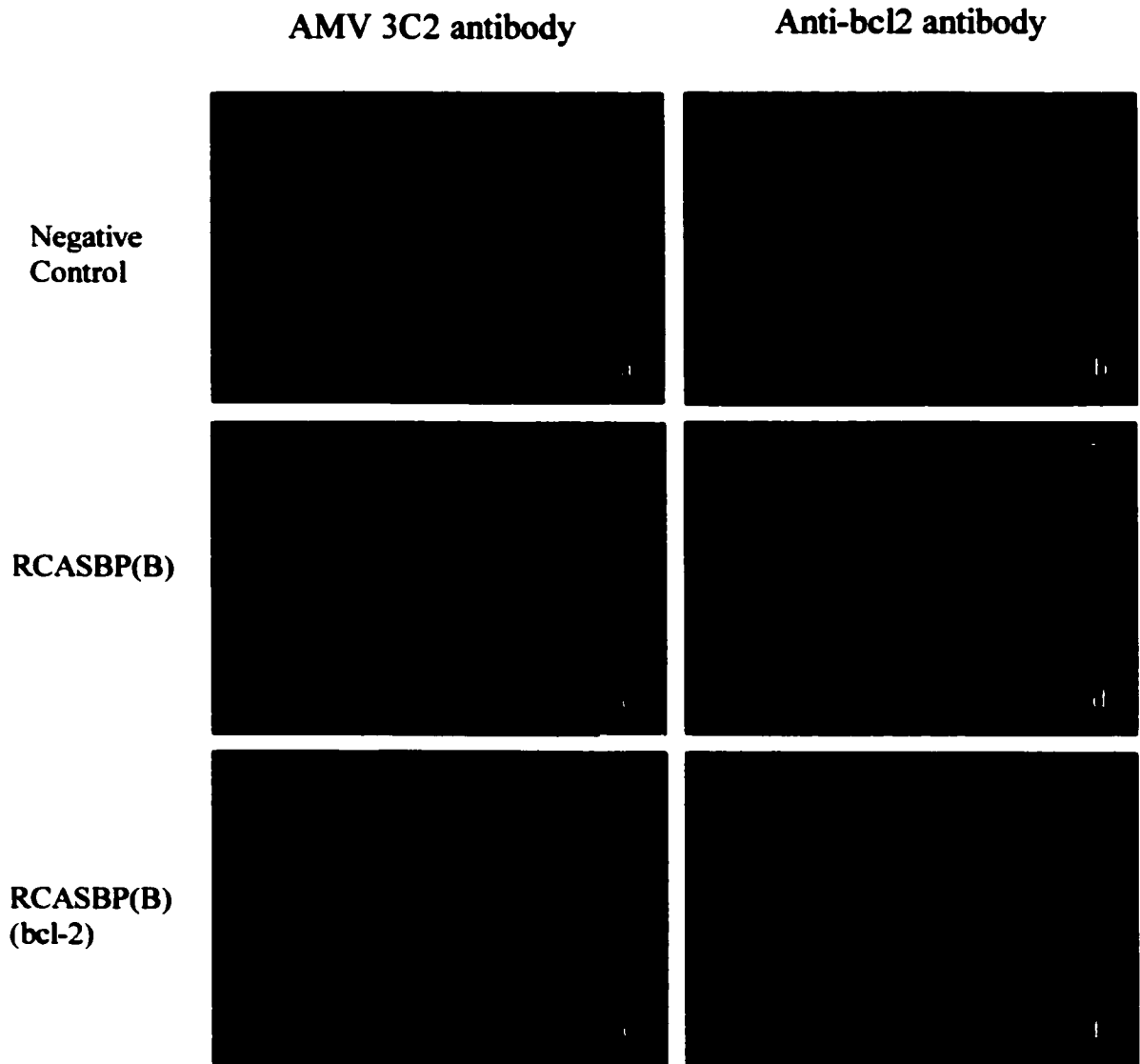


Figure 7-1. Immunocytochemical controls on RCASBP(B) transfected chick embryo fibroblasts. Untransfected negative control chick embryo fibroblasts (CEF's) and CEF's that were transfected with either RCASBP(B) only, or with RCASBP(B)(bcl-2), and each was stained with antibodies to either the viral coat protein (AMV 3C2) or to bcl-2. Mag. x560.

Anti-human bcl-2
Transfected CEF's



Figure 7-2 Immunoblotting on chick embryo fibroblasts for human bcl-2. Lane 1, untransfected CEF negative control; lane 2, RCASBP(B)-bcl-2 transfected CEF's; lane 3, RCASBP(B)/(-) transfected control; lane 4, Jurkatt cell positive control.

Immunostaining on CEF's that had not been transfected was negative for the viral coat protein (Figure 7-1a) and had low immunoreactivity for endogenous bcl-2 (Figure 7-1b). CEF's that had been transfected with RCASBP(B) with no insert were positive for the viral coat protein (Figure 7-1c) and had the same low immunoreactivity for endogenous bcl-2 (Figure 7-1d). Cells that had been transfected with RCASBP(B)(bcl-2) were strongly immunoreactive for both the viral coat protein (Figure 7-1e) and bcl-2 (Figure 7-1f). This staining confirmed that virus was being produced and that the bcl-2 insert was stable and transcribed.

CEF's were also collected and analysed by western blotting with a monoclonal antibody for the expression of the human bcl-2 protein. Samples of a non-transfected negative control and a Jurkatt cell positive control were compared to samples that had been transfected with the construct with no insert (RCASBP(B)), and samples that had been transfected with the human bcl-2 carrying construct (RCASBP(B)(bcl-2): Figure 7-2). The CEF sample that had been transfected with the human bcl-2 carrying construct was positive for the 26 kDa band for human bcl-2, as was the Jurkatt cell positive control. Both the non-transfected negative control and the samples with the no insert were negative for human bcl-2 expression.

Viral bcl-2 overexpression *in vitro*

To determine if endocardial cushion cells were susceptible to infection with the RCAS expression vectors, and to see if human bcl-2 is functional in these cells, the viral vectors were tested on primary cushion cell cultures. Primary dissociated cushion cell cultures were made as described and were serum-starved to induce the cells to undergo

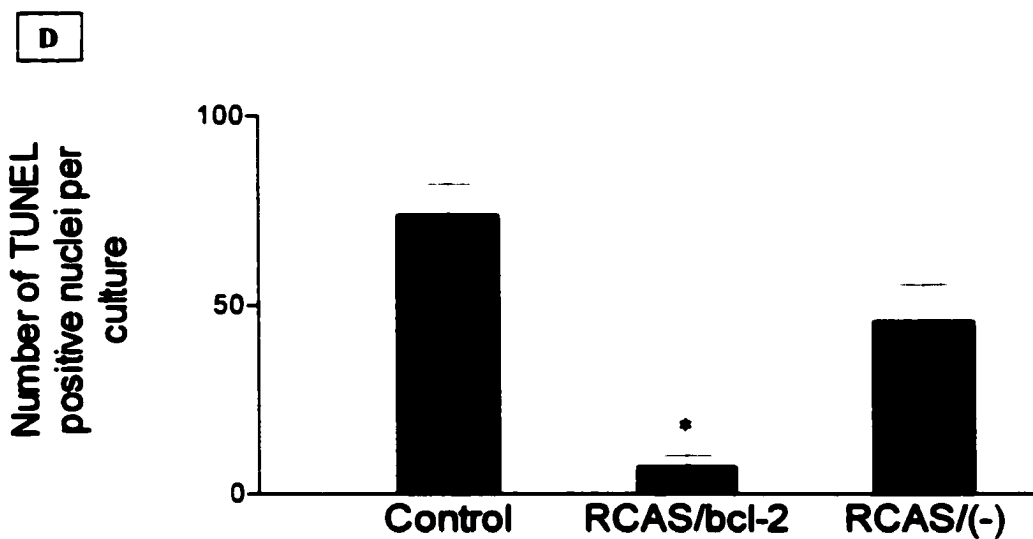
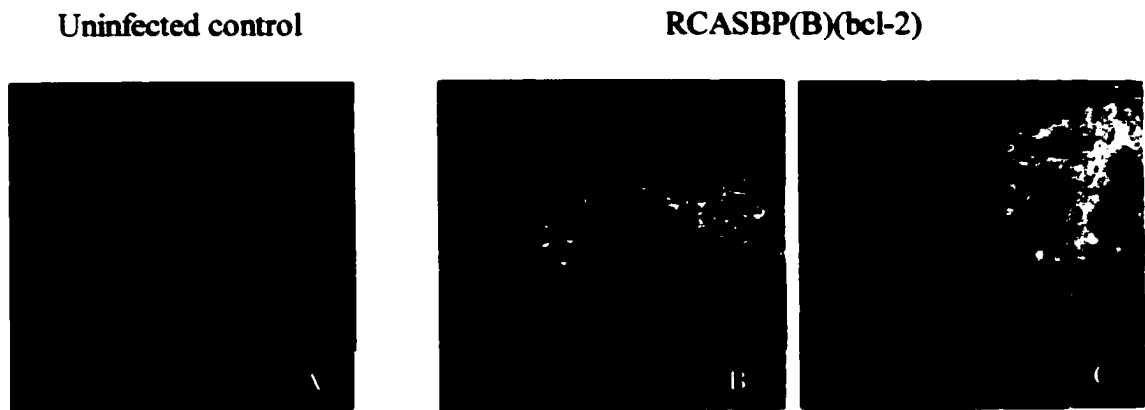


Figure 7-3. Retroviral bcl-2 overexpression in dissociated AV cushion cell cultures. Dissociated cushion cell cultures were infected with RCASBP(B)(-) or RCASBP(B)(bcl-2) or left uninfected as a control. (A) Representative immunostaining on uninfected control cultures, stained endogenous bcl-2 (green), mitochondria (red) and nuclei (blue). (B) RCASBP(B)-bcl-2 infected cultures similarly stained, showing increased levels of fluorescence for overexpressed bcl-2. (C) Infected cultures stained for viral coat (green). (D) Comparison of effects of RCASBP(B)-bcl-2 and (-) on serum starved cushion-cell cultures. Bcl-2 overexpression significantly protects the cells from apoptosis when compared to the uninfected control ($p < 0.01$) and the negative-insert control ($p < 0.05$). Results were analysed using one way ANOVA and Tukey's post-test, ($n=5$). Mag. x560, a,b,c.

apoptosis. As negative controls, the cultures were left untreated or they were infected with an aliquot of the concentrated RCASBP(B) virus. Experimental samples were infected with the virus carrying the bcl-2 insert, RCASBP(B)(bcl-2). Cultures were then incubated for a further 4-5 days. Representative cultures were stained with either the monoclonal antibody AMV 3C2, to immunolabel the viral coat protein, in order to confirm infection with the virus, or with an anti-bcl-2 antibody to test for increased expression of the bcl-2 protein as seen with increased fluorescence. Concurrent staining was performed to label the mitochondria with Mitotracker red and the nuclei with DAPI. Uninfected control cells were negative for viral coat and contained endogenous bcl-2, as reflected by faint fluorescence (Figure 7-3A). All cells in the infected cultures were positive for increased bcl-2 expression, as seen by increased levels of fluorescence (Figure 7-3B) and for viral coat protein (Figure 7-3C).

Other experimental cultures were stained with TUNEL to label the apoptotic nuclei. The total number staining positively was counted and each treatment was compared. Figure 7-3D shows the comparison of the number of TUNEL-positive cells in each treatment. Infection with the bcl-2-carrying virus was found to significantly inhibit apoptosis in comparison with the untreated control cultures and cultures infected with the negative insert control.

Viral bcl-2 overexpression *in vivo*

The aim of this work was to virally overexpress the anti-apoptotic bcl-2 protein in the embryonic chick heart in the areas that have the highest incidence of cell death, namely the AV and OT endocardial cushions, to attempt to inhibit the naturally occurring

apoptosis. If successful, this inhibition could contribute to our understanding of the natural role of this cell death. The RCAS expression system had only limited previous use in the embryonic heart, so initially, to see if it was possible to get the virus successfully into the endocardial cushions, attempts were made using only the RCASBP(B)(bcl-2) vector, without the negative control virus. If this proved adequate at infecting the areas of interest, i.e. the endocardial cushions, then subsequent attempts would make use of the negative control virus with no insert.

The endocardial cushions initially arise by an epithelial-mesenchymal transformation (EMT) from the endothelial layer, under the stimulation of the myocardium at approximately HH stage 14-16 in the chick heart (Markwald *et al.*, 1990). Retroviruses are known to infect only actively dividing cells, so the theory behind the experiment was to infect the endothelial layer during the stage when EMT was occurring, so that the cushion derivatives would be infected. We have also previously shown that there is active proliferation of the cushion cells during the timeframe that apoptosis is occurring (see Chapter 4), which should facilitate infection. Another consideration for viral injection is the 18 h needed for viral incorporation and expression of the protein of interest, so sufficient time needs to be allowed prior to cell migration from the endocardial layer.

Initial attempts at injection of the concentrated virus directly into the cushions proved technically unsuccessful, as the injection pipette pushed the heart away, and the beating of the heart also prevented accurate injection. In subsequent attempts, the pericardial sac was flooded with viral concentrate, which functioned to contain the injected solution, and maintained it in contact with the outer muscular layer of the

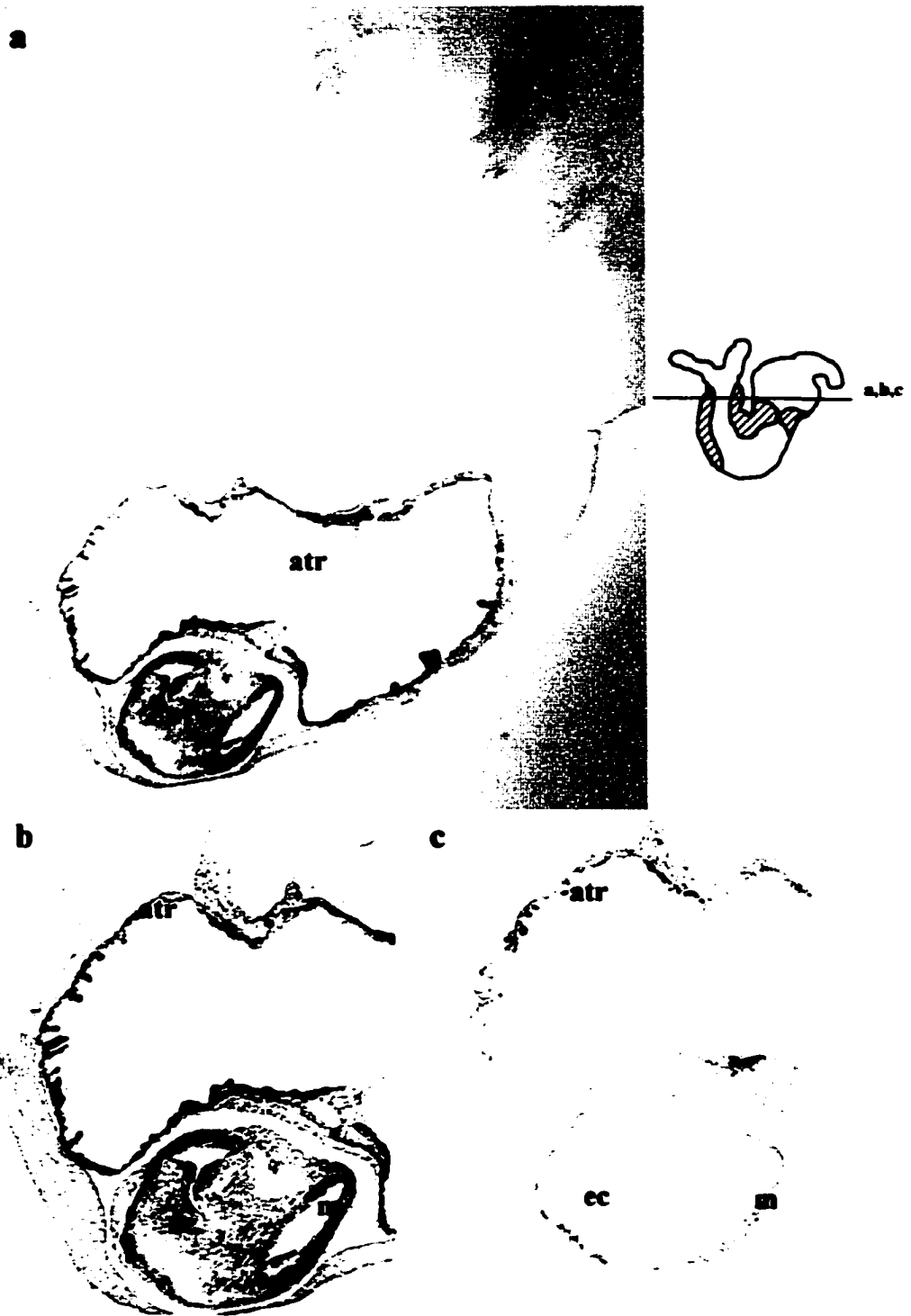


Figure 7-4. Immunocytochemistry for viral coat and human bcl-2 in RCASBP(B)-bcl-2 infected heart. (a) Immunocytochemistry for viral coat protein on embryo section, following injection of the virus into the pericardial sac. The viral spread can be seen to be limited to the heart, with immunoreactivity in the atrial walls (atr) and outflow tract (ot), with little spread throughout the rest of the body. (b) At a higher magnification of the same section, stained for the viral coat protein, viral immunoreactivity can be seen in the atrial walls (atr) and in the endocardial cushions (ec) and myocardium (m) of the OT. (c) Immunocytochemistry on an adjacent section for human bcl-2, shows a more restricted expression of the protein, in the atrial walls (atr) and myocardium (m) of the OT. Mag. x140, a; x280, b,c.

primitive heart (see Figure 3-1). The layers of the heart at this stage of injection (HH 10-14) are thin, consisting of only a few cell layers. The viral concentrate was not injected into the lumen of the heart, as the heart is already beating at this stage and the viral solution would be pumped away from the cushion region. After injection, the eggs were re-incubated for 3-5 days. The embryos were subsequently sectioned and stained with the monoclonal antibody to the viral coat protein, or with a monoclonal antibody to human bcl-2. Figure 7-4a shows a representative section of an infected embryo stained for the viral coat protein. The viral spread, following initial injection into the pericardial sac, has been maintained in the heart, with little or no spread to other tissues or regions of the embryo. At a higher magnification (Figure 7-4b), the staining for the viral coat protein shows expression in the atrial walls and in the myocardium and endocardial cushions of the OT. When an adjacent section was stained for human bcl-2 (Figure 7-4c), there was a much more restricted expression of the protein, with only parts of the atrial wall and myocardium of the OT showing immunoreactivity.

In another example of infection in the OT (Figure 7-5a), staining for the viral coat protein again showed expression throughout the muscular layers of the heart, and in the OT cushions. However, when an adjacent section was stained for human bcl-2, a more restricted pattern was observed (Figure 7-5b). Some staining was seen in the endocardial cushions, but most was observed in the muscular layers of the ventricle and OT.

In another example (Figure 7-6a), staining for the viral coat protein again revealed expression throughout the muscular layers of the atrial walls and the ventricles, along with immunoreactivity in the AV cushions. With staining for human bcl-2 in the same



Figure 7-5. Immunocytochemistry for viral coat and human bcl-2 in RCASBP(B)-bcl-2 infected heart. (a) Immunocytochemistry for viral coat protein after viral injection into the pericardial sac. Viral immunoreactivity is seen throughout the heart, in the atrial walls (atr), the ventricle (v), and in the myocardium (m) and endocardial cushions (ec) of the outflow tract. (b) Immunocytochemistry for human bcl-2 on an adjacent section, shows a more restricted expression of the protein, with immunoreactivity only seen in parts of the atrial walls (atr), ventricle (v) and the myocardium (m) and endocardial cushions (ec) of the outflow tract. Mag. x140.



Figure 7-6. Immunocytochemistry for viral coat and human bcl-2 in RCASBP(B)-bcl-2 infected heart. (a) Immunocytochemistry for viral coat protein after viral injection into the pericardial sac. Viral immunoreactivity is seen throughout the heart, in the atrial walls (atr), the ventricle (v) and throughout the central mass of AV endocardial cushions (ec). (b) Immunocytochemistry for human bcl-2 on the same heart, showing a more restricted expression of the protein, with immunoreactivity only seen in parts of the atria (atr), ventricle (v) and the AV cushions (ec). Mag. x140.

tissue (Figure 7-6b), again a more restricted pattern of expression was seen, with only some of the AV cushions having positive staining.

In summary, under the parameters tested, *bcl-2* was not sufficiently overexpressed in the endocardial cushion tissue to merit further analysis of these tissues, by measuring changes in the levels of apoptosis. The examples shown represent the best results of viral spread, after many repeats and slightly altered parameters of injections e.g. larger quantities of viral solution, increased polybrene concentration, injection into different sides of the pericardial sac. Each experiment involved injection of 24-36 embryos, with a post-injection survival rate of 50%, with 17 total experiments performed. Further attempts are needed, using different parameters, to ensure adequate and consistent infection.

DNA OVEREXPRESSION VIA ELECTROPORATION

Another more recent method for gene overexpression in the embryo is via electroporation (Swartz *et al.*, 2001). This involves the application of electric current pulses to introduce an exogenous DNA sequence of interest into a particular site in the embryo. Two electrodes are placed either side of the tissue of interest, in this case the heart, and the DNA is microinjected into the tissue. As the DNA is negatively charged, the application of the electrical current results in the DNA moving towards the cathode of the electrodes. At the same time, the current disrupts the cell membranes, resulting in the formation of pores in the cells. The migrating DNA can then enter the cells through the disrupted membrane. After cessation of the electric current, the cell membrane returns to normal, providing the correct voltage parameters have been met. In this work, attempts

were made to overexpress human bcl-2 DNA and green fluorescent protein (GFP) in the endocardial cushions of the AV and OT by means of electroporation.

Bcl-2 and GFP DNA Electroporation

There has only been a little work done with electroporation into cardiac tissue (Harrison *et al*, 1998), so various modifications were made in each attempt in these experiments. Two of the main parameters to be considered in electroporation are the site of injection of the DNA, and the frequency and strength of the current pulses applied. In addressing the first parameter, the endocardial cushions were the target tissues for electroporation, so the DNA solution was injected as close to the target tissue as possible. In the heart, this involved injection of the DNA into the lumen of the heart, to lie adjacent to the endothelial layer lining the developing cushions (see Figure 3-2), in the expectation that during the pulsing process, the DNA would enter the endothelial cell layer, or pass directly into the cushions.

The DNA samples used were the proviral DNA constructs RCASBP(B)(gfp) and RCASBP(B)(bcl-2). A summary of the experimental parameters and results are shown in Table 7-1.

Initially, small amounts of concentrated DNA (either GFP or bcl-2) were injected into the lumen of the heart of HH 14-17 embryos (total 68), and these were pulsed for 5 x 25 ms at 25V. The following day, the GFP injected embryos were examined using fluorescent wholemount microscopy, but no fluorescence was seen. A second set of electroporations used the same parameters (total 108), but with larger amounts of DNA, and again no fluorescence was seen. For both sets of injections, the combined survival

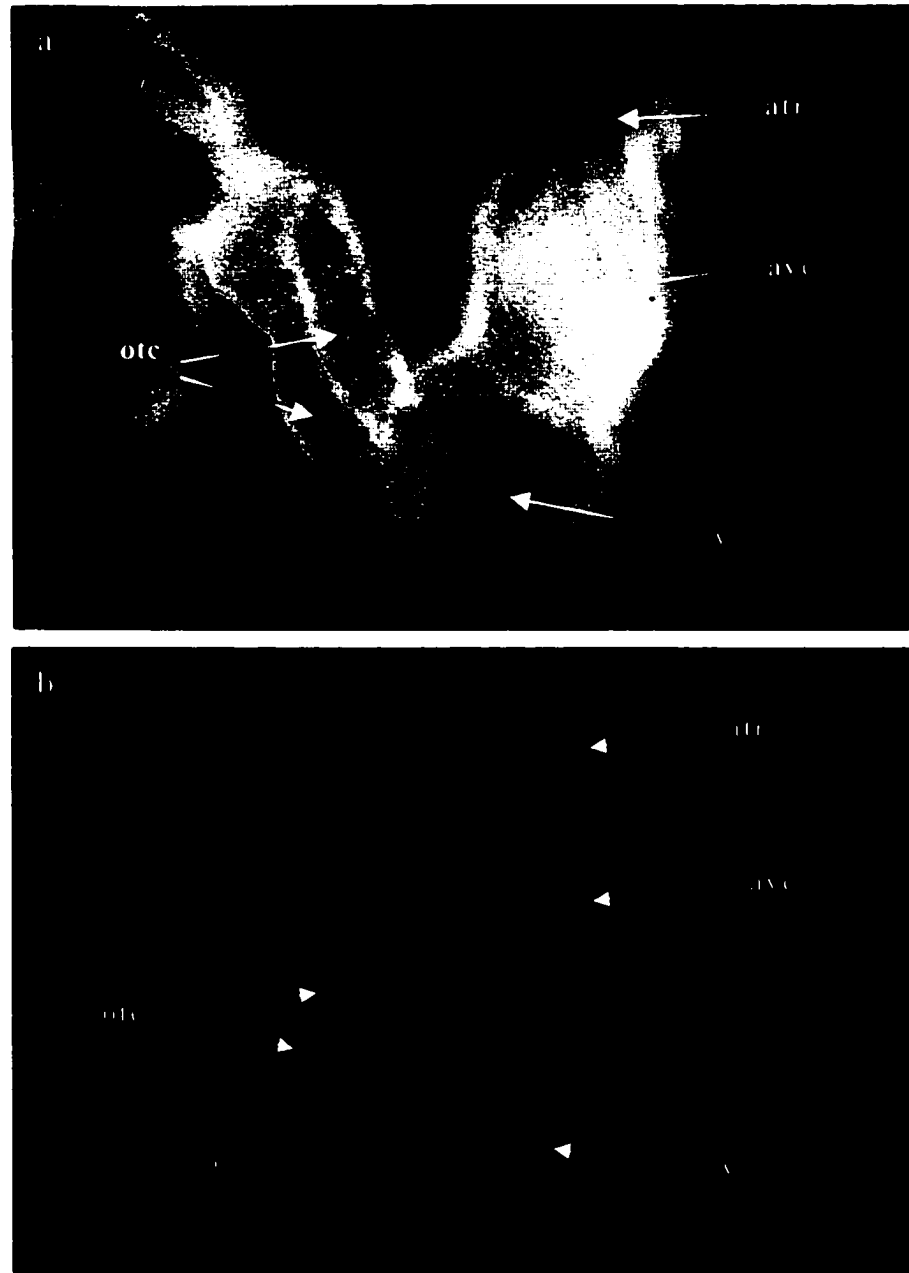


Figure 7-7. Brightfield and fluorescence views of embryonic heart following GFP electroporation. (a) Bright field whole mount of ED 3 heart, showing the different regions: atria (atr), AV cushions (avc), ventricle (v) and OT cushions (otc). Note that both ridges of the OT cushions are visible in the outflow tract. (b) Fluorescence view of the same heart showing some GFP expression at the base of both ridges of the OT cushions and in the region of the AV cushions, following GFP-DNA electroporation.

was about 65%. For a third set of injections, HH 11-14 embryos (total 79) were injected with larger amounts of DNA and 10 x 50 ms pulses, 25V were used. The extra pulses proved more deleterious to the embryos, with a combined survival of about 40%. Some of the GFP injected embryos were examined under fluorescence wholemount after 18-24 hours. Some fluorescence was seen in a few of these embryos, but not consistently in the same area, or with the same intensity. An example is seen in Figure 7-7. Under brightfield view, the two ridges of the OT cushions are visible, as are the swellings of the AV cushions and the boundaries of the atria and single ventricle (Figure 7-7a). In the same heart (Figure 7-7b), fluorescence can be seen at the base of each OT cushion ridge and in the area of the AV cushions.

On the next attempt at electroporation, the heart was stopped temporarily while the DNA was injected, in the hope that this would prevent the DNA being removed by the beating heart and circulation. For this, ice-cold Ringer's saline was added to the embryo immediately prior to DNA injection and electroporation. An increased volume of DNA was again used and the pulses reduced to 8 x 25 ms, 25V, or 10 x 25 ms, 25V. However, the survival rate remained about 40%, presumably with the increased volume in the circulation being fatal to the embryos. After 24 hours, some of the GFP-injected embryos were examined for fluorescence. Figure 7-8a shows a representative embryo with some green fluorescence in the heart, but it is not seen elsewhere in the embryo. At a higher magnification, when the heart was removed from the body (Figure 7-8b), the fluorescence can be seen in the apex of the ventricle and around the base of one of the OT cushion ridges. In another example (Figure 7-8c), fluorescence can be seen in the common ventricle, but not in the endocardial cushions.

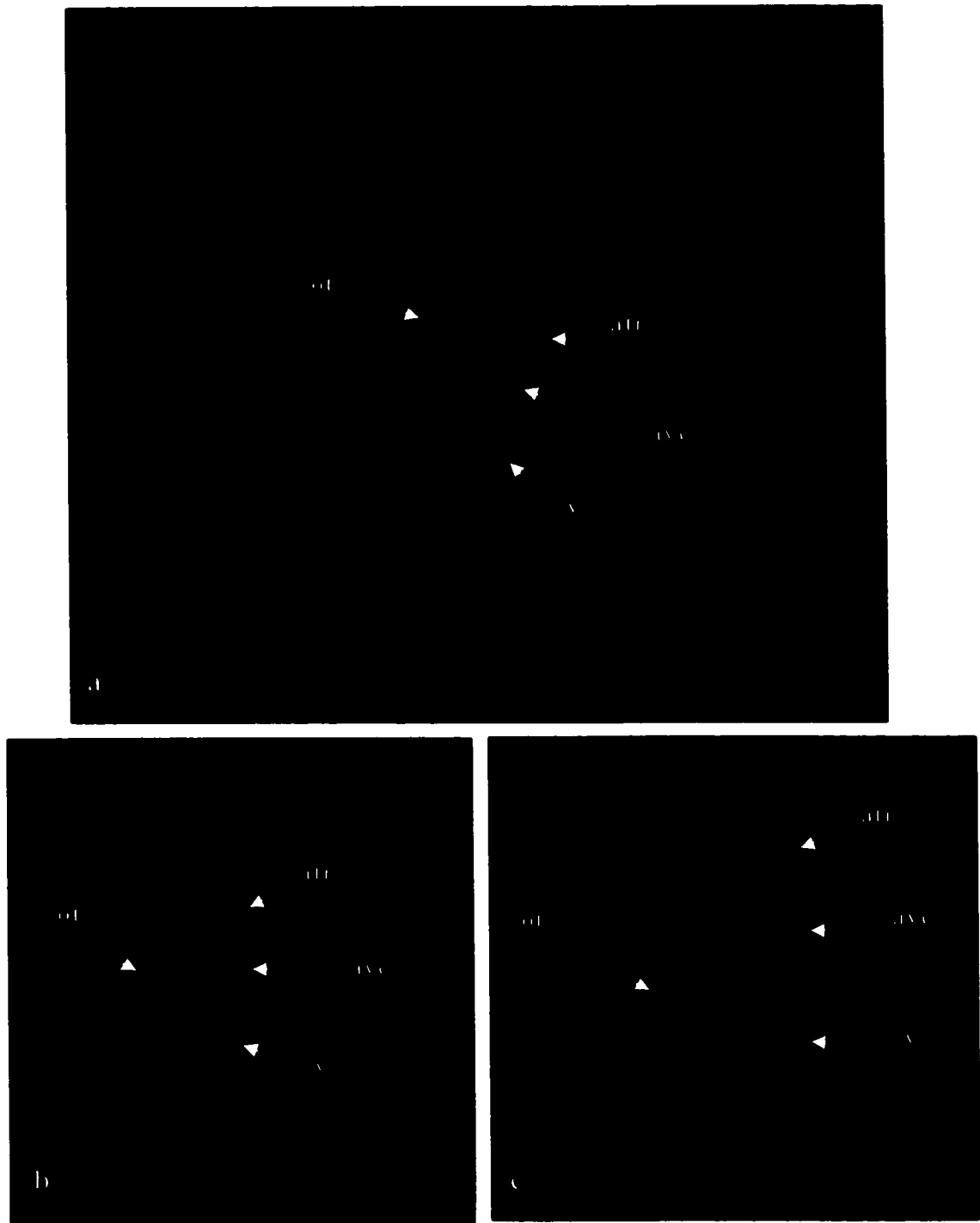


Figure 7-8. Examples of green fluorescent protein in the embryonic chick heart following electroporation. (a) Electroporation of GFP-DNA in the heart resulted in limited GFP expression in the heart, but nowhere else in the embryo. Regions of the heart are clearly distinguishable, showing, in each picture, the atrium (atr), AV cushions (AVC), ventricle (V) and outflow tract (OT). (b) In the same heart, green fluorescence is expressed in the apex of the ventricle. (c) In another example, green fluorescence is seen again in the ventricle wall, and also around the regions of the OT cushions.

Other attempts at electroporation were made to assess the quality of injection and construct integrity. These entailed electroporation of either the anterior or posterior neural tube of 10-15 embryos with GFP and subsequent analysis for protein expression. With each surviving embryo (about 40% survival), positive staining was seen in the tissue that had been on the cathode side of the electrode, and not on the other (not shown).

Similar experimental embryos were electroporated in the heart with DNA encoding human bcl-2, under each of the above conditions. These were subsequently processed for immunohistochemistry and stained with a monoclonal antibody to human bcl-2. Positive staining was found in only 4-5 individual embryos. Figure 7-9a shows an example of positive staining in the OT, with human bcl-2 expressed on one side of the OT, and in the atrial wall. At a higher magnification of the OT (Figure 7-9b), the immunoreactivity can be seen in the myocardium of the OT, and to a lesser extent in the endocardial cushions. In another example (Figure 7-10), immunoreactivity for human bcl-2 can be seen in the interventricular septum and apex of the ventricle, but not in the AV cushions.

In summary, under the parameters tested, bcl-2 or GFP were not sufficiently overexpressed in the endocardial cushion tissue to merit further analysis of these tissues, by measuring changes in the levels of apoptosis. Further attempts will be needed, using different parameters, to ensure adequate and consistent infection.

Future approaches: TIMP-2 / TAT studies

One potential future method of targeting the endocardial cushions might be to make use of the developing technology utilizing TAT-mediated protein transduction

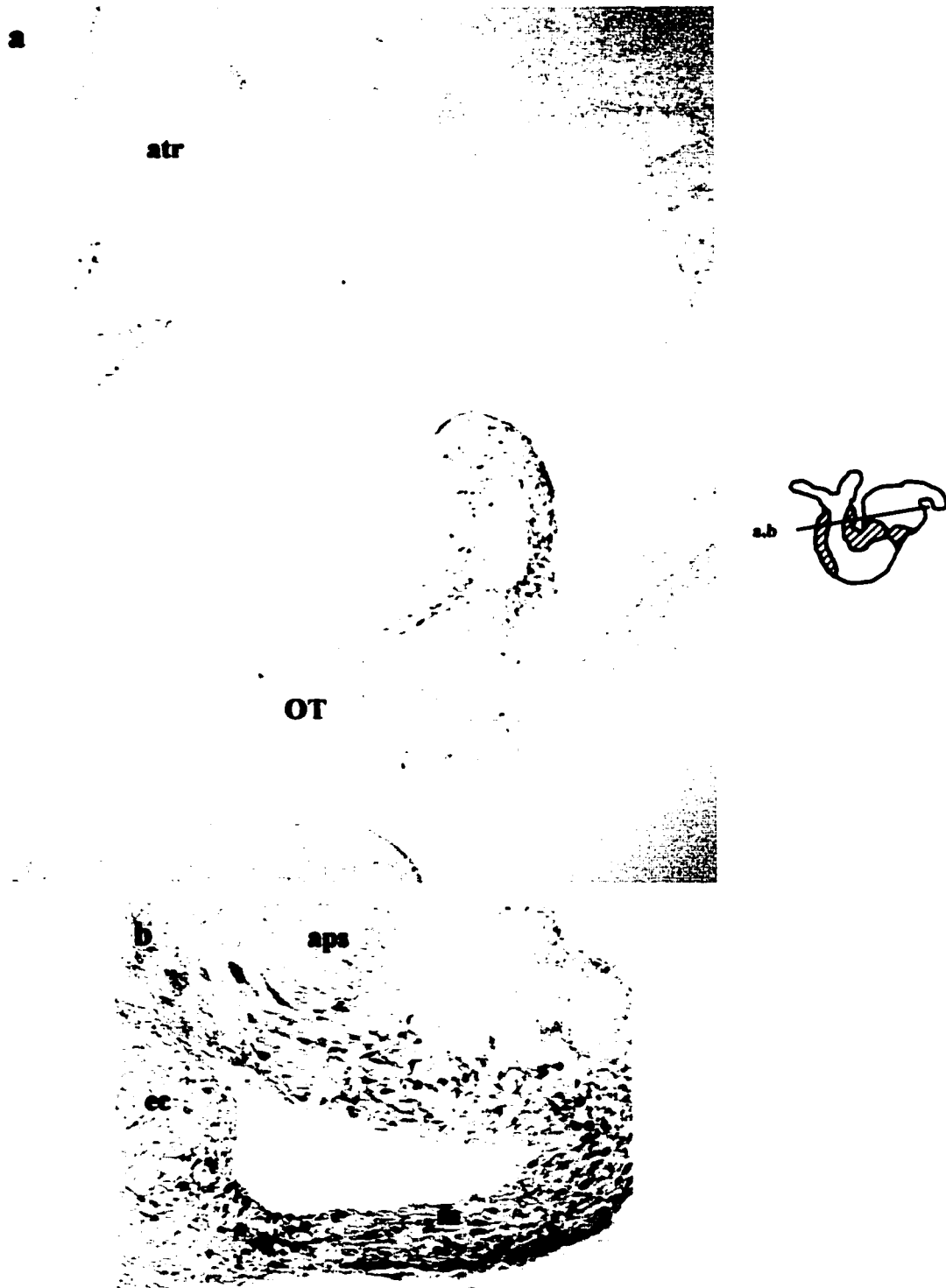


Figure 7-9. Immunostaining for human bcl-2 following electroporation of RCASBP(B)-bcl-2 into the embryonic chick heart. (a) Human bcl-2 expression is seen only on one side of the outflow tract (OT) and the atrial wall (atr). Mag. x140. (b) At a higher magnification of the same heart, bcl-2 expression can be seen in the myocardium (m) and endocardial cushions (ec) of the OT, with only a few individual cells on the edge of the AP septum (aps) staining positively. Mag. x280.

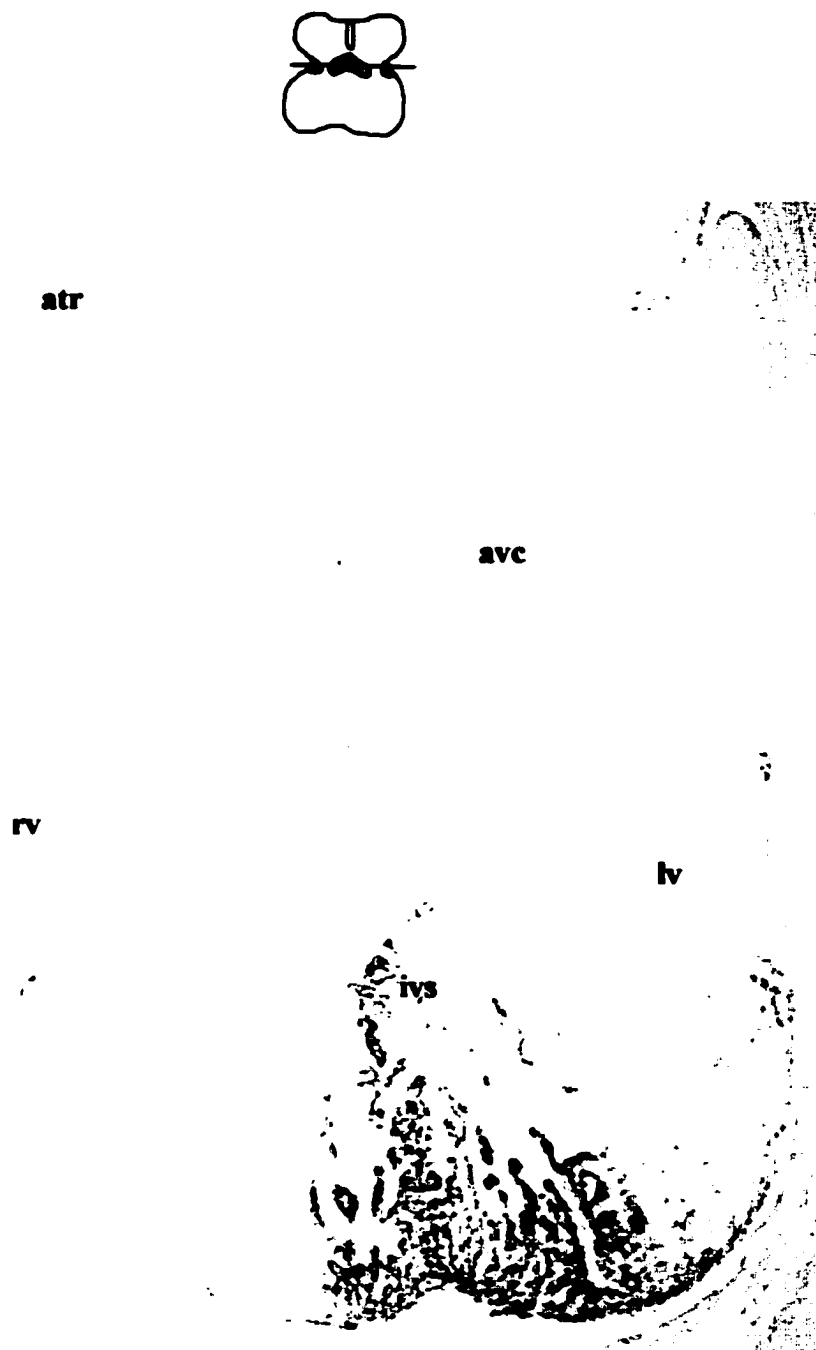


Figure 7-10. Immunostaining for human bcl-2 following electroporation of RCASBP(B)-bcl-2 into the embryonic chick heart. The various regions of the heart are visible, namely the atria (atr), the AV cushions (avc), and the left and right ventricles (lv and rv). Immunoreactivity for the human bcl-2 protein is only seen in the interventricular septum (ivs) and some trabeculae at the apex of the heart. Mag. x140.

Treatment	Parameters	Stage injected (HH)	No. injected		Survival (no. embryos)		% Survival		# GFP positive	# Bcl-2 positive
			GFP	Bcl-2	GFP	Bcl-2	GFP	Bcl-2		
1	5x25ms, 25V	14-17	38	30	25	19	65	63	0	0
2	5x25ms, 25V	14-17	49	59	30	41	61	69	0	0
3	10-15x 50ms, 25V	11-14	38	41	19	12	50	29	2	0
4	8x25ms, 25V	14-17	39	59	10	34	26	58	3	2
5	10x25ms, 25V	14-17	42	31	12	9	29	29	2	2

Table 7-1. Summary of electroporation experiments, for RCASBP(B)-gfp and RCASBP(B)-bcl-2.

(Fawell *et al*, 1994). This method allows for the introduction of full-length proteins into primary cells and tissue. Belonging to the human immuno-deficiency virus (HIV), the HIV-Tat protein was found to be able to cross cell membranes. The technology involves linking a protein of interest to the TAT molecule (the protein transduction domain of Tat), forming a fusion-protein. When added to cell culture or injected into mice, the TAT-domain transduces the entire fusion-protein of interest into every cell in the population, in a concentration-dependant manner, although the exact mechanisms of transduction remain unclear (Schwarze *et al*, 1999; Becker-Hapak *et al*, 2001).

When β -galactosidase-TAT-fusion proteins were injected intraperitoneally into 4-8-week old mice, the biologically active fusion protein was seen in all tissues, including the brain (Schwarze *et al*, 1999), reaching maximal intracellular concentrations within 15 minutes. As part of preliminary investigations into the potential use of this technology, in collaboration with Dr. C. Fernandez-Patron, University of Alberta, the effectiveness of TAT-mediated transduction into the chick embryo was examined. In work performed here, TAT linked to tissue inhibitor of metalloproteinase-2 (TIMP-2) was added to primary cushion cell cultures or was injected into the lumen of the chick heart *in vivo*. Although the work was very preliminary and raises more questions than answers, the results are promising, for developing and utilizing this technique as a tool for embryologists. When added to primary dissociated cushion cultures, TIMP-2 –TAT with FITC attached was seen to enter the cells in a concentration-dependant manner (Figure 7-11). The fusion-protein was also injected into the circulation of the chick embryo. An initial experiment involved injection of equal volumes of TIMP-2-TAT, GFP-TAT or

PBS control to 3 x 48-hour embryos, with reincubation for another 24 hours. As seen in figure 7-12, in comparison to the PBS control, the TIMP-2-TAT injected embryo had under-developed endocardial cushions and ventricular and atrial -musculature. The GFP-TAT injected embryo appeared normal, similar to the control (not shown). The initial invasion of the endocardial cushion cells is known to involve matrix-metalloproteinases (MMP's; Song *et al*, 2000), which are inhibited by TIMP's. The disruption of the endocardial cushions may be due to the impairment of the initial EMT by the transduced TIMP-2-TAT. When the experiment was repeated with twice the initial volume of TIMP-2-TAT, again in 3 embryos for each treatment, the TIMP-2-TAT embryos could not be sectioned as the embryos disintegrated during the sectioning process, which did not happen in the controls. Although many further experiments are needed, this technology raises the possibility of targeting the developing endocardial cushions with anti-apoptotic-TAT conjugated proteins. Transduction of a modified TAT-caspase-3 has already been demonstrated to induce apoptosis in HIV-infected cells (Vocero-Akbani *et al*, 1999).

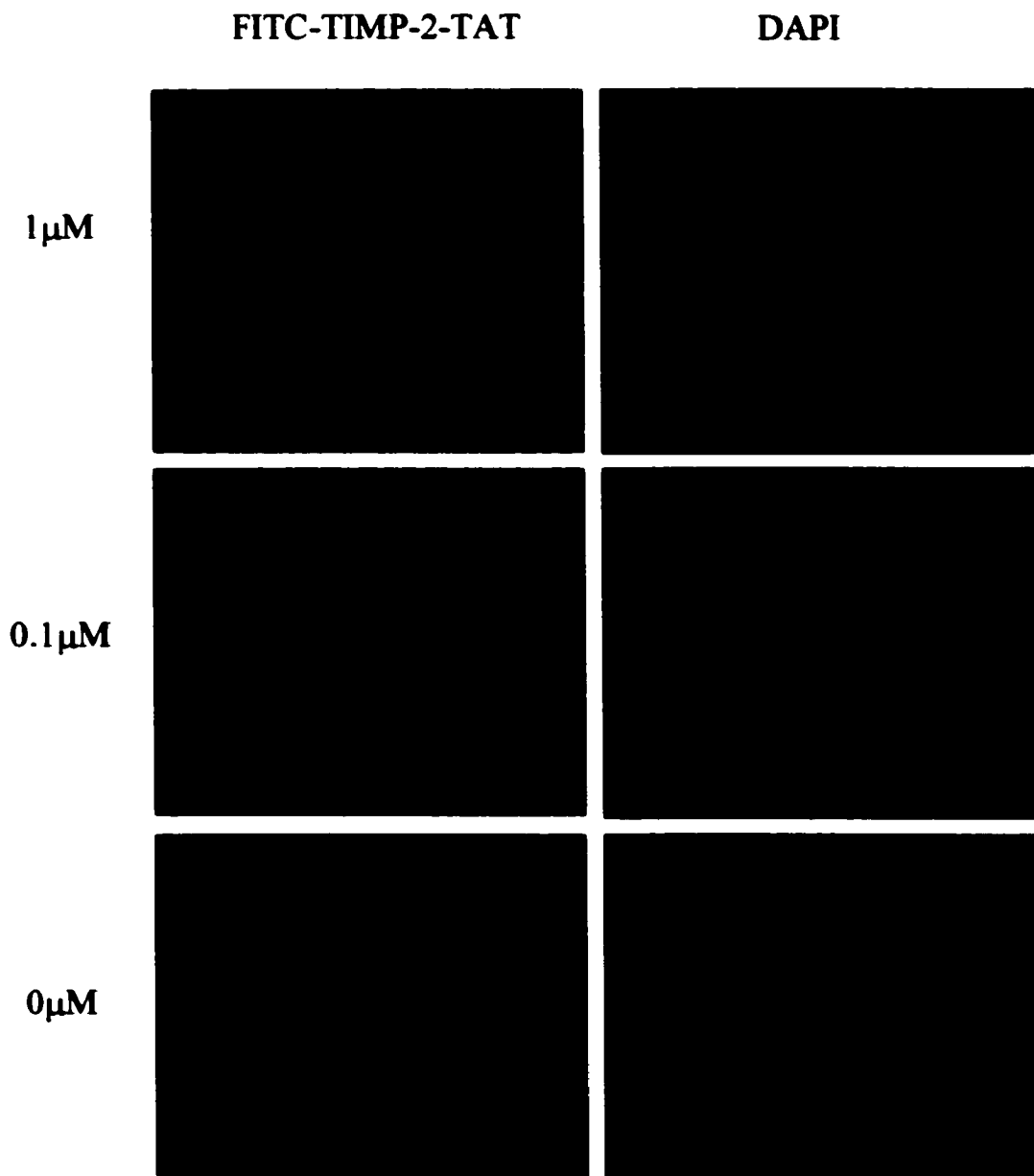


Figure 7-11. TIMP-2-TAT-FITC transduces into primary cultures of endocardial cushion cells in a concentration-dependant manner. Addition of TIMP-2-TAT fusion protein conjugated to FITC appears to enter primary cultures of endocardial cushion cells in a concentration dependant manner. Counterstaining with DAPI shows the cell nuclei. Mag. x560.

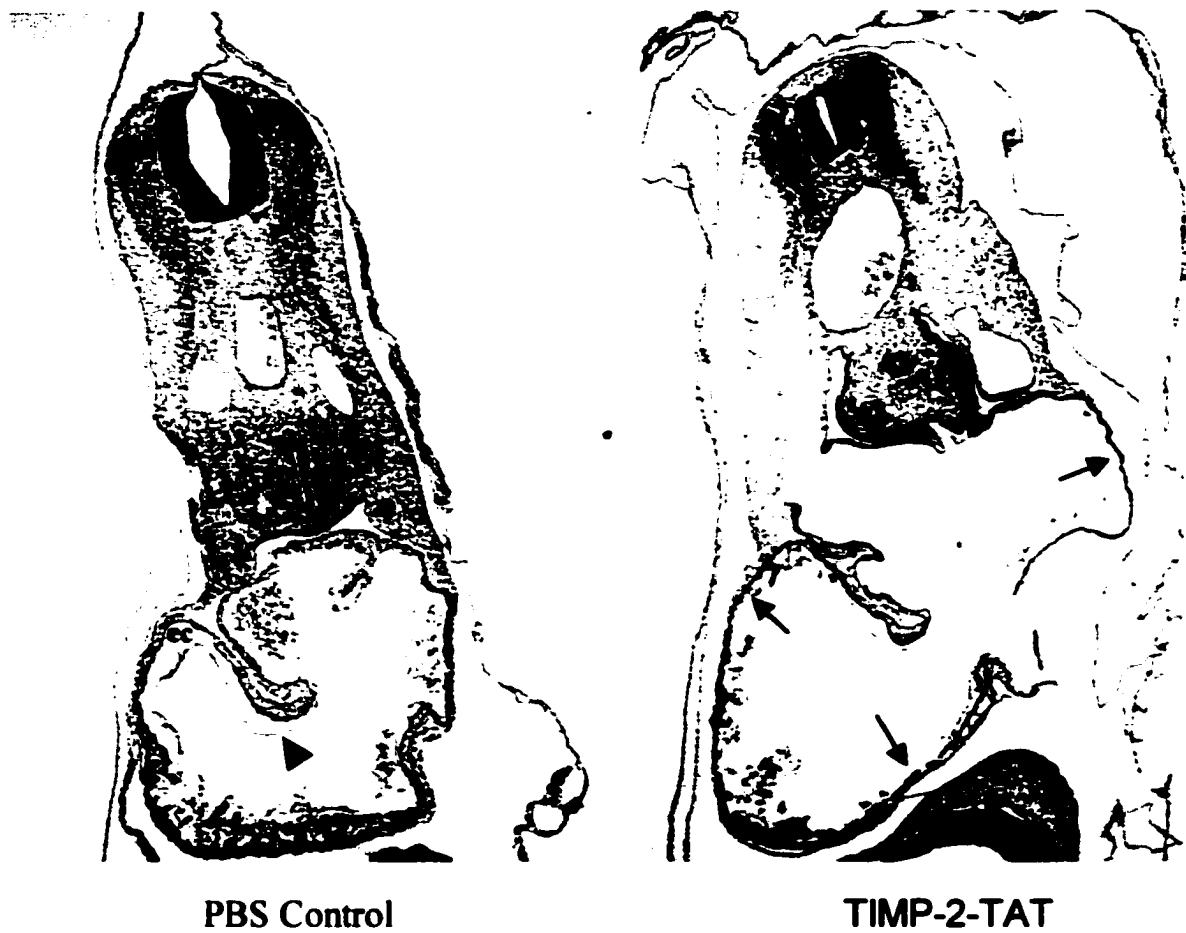


Figure 7-12. Injection of TIMP-2-TAT into the circulation of the chick embryo. Chick embryos (ED2) were injected with equal volumes of Timp-2-TAT, and a PBS control. The embryo receiving the fusion-protein showed obvious impaired heart structure, with thinner musculature (arrows), no visible endocardial layer (arrowhead), and no initial seeding of the endocardial cushions (ec). Mag. x55.

Chapter 8
DISCUSSION

Discussion

The interest in apoptosis in heart development has dramatically increased since the current research program began (Fisher *et al*, 2000; Poelmann *et al*, 2000; van den Hoff *et al*, 2000). Much of this recent work has concentrated on the distribution and occurrence of apoptosis in the developing heart, with a reassessment of the detailed work of Pexieder (1975), using more modern techniques. These techniques seem to be pointing to a more localized distribution of dying cells than previously thought, with a smaller number of main foci of cell death. Atrial and ventricular tissue seem to have little cell death in very early development, while the AV and the OT cushions seem to be the principle foci with the largest numbers of dying cells (Poelmann *et al*, 1998; Keyes and Sanders, 1999). Outflow tract myocytes have also been shown to be eliminated in large numbers (Watanabe *et al*, 1998) and some neural crest cells undergo apoptosis in the AV region after entering the heart through the venous pole of the heart (Poelmann and Gittenberger-de Groot, 1999). A large number of dying cells are also reportedly seen in the superior aspect of the interventricular septum, at the site of its fusion with the atrial septum and OT septum (Fisher *et al*, 2000; van den Hoff *et al*, 2000). However, the knowledge of the regulation of the process or the exact role of the cell death is far from conclusive.

The work presented here had a number of aims. Firstly, to help elucidate the distribution patterns of apoptotic cells during heart development, using techniques specific for programmed cell death. Secondly, to unravel some of the mechanisms involved in this cell death, concentrating on the better-known regulators of the apoptotic pathway and on some of the suspected stimuli for cell death. And thirdly, attempts were

made to understand the role of this cell death, by inhibition of the normal pattern of apoptosis with overexpression studies.

Are members of the bcl-2 family involved in the regulation of apoptosis in the endocardial cushions?

To date little work has been done to characterize the factors involved in the apoptosis of cushion cells. The suggested involvement of the bcl-2 family of cell death regulators arises from inconclusive results using knockout mice or mRNA localization in heart extracts (reviewed by van den Hoff *et al.*, 2000). The *bcl-2* gene has been shown to be present in the heart of the chick embryo (Eguchi *et al.*, 1992). The results presented here show for the first time that anti-apoptotic bcl-2 and pro-apoptotic bax and bak are present and developmentally regulated in the endocardial cushions of the heart. Immunoblotting studies show that bcl-2 itself is present throughout the main phase of apoptosis (ED4-8) with a transient downregulation of the protein seen at day 4 in the OT cushions and at day 5 in the AV cushions. Bcl-2 acts in a cytoprotective manner in cells, by interacting with and hindering the function of pro-apoptotic stimuli. That fact that there is a downregulation of protein level may suggest interplay of other factors or signaling molecules. Levels of the pro-apoptotic bax protein appear to remain constant throughout the time course examined, while the pro-apoptotic molecule bak appears to be upregulated at the time of the highest incidences of cell death in the cushions, further implicating members of this family in regulating cell death in these areas. When compared to the distribution and timeline of TUNEL staining in heart sections, there is little direct overlap between increases in pro-apoptotic proteins and decreases in anti-

apoptotic bcl-2. This obviously implies that there are complex signaling pathways in effect in these tissues, with other family members probably being involved. Only further analysis of other family members will lead to more conclusive results. Both pro- and anti-apoptotic members of the bcl-2 family seemed to strongly associate with the prongs of the aorticopulmonary septum, but were also seen in individual cells throughout the endocardial cushions. However, immunoblotting for these proteins does not reflect the distribution patterns, but merely the levels seen in the tissue extracts.

Using the cushion-culture model, the sub-cellular distribution of bcl-2 and bax was examined in the presence of normal- and reduced-serum conditions. Anti-apoptotic bcl-2 was seen to associate with the mitochondria when the serum was removed, which is a signal for apoptosis in many cell types. Bcl-2 normally protects the cell via interaction with, and inhibition of, the function of pro-apoptotic family members, but when conditions become too stressful for the cell, the apoptotic pathway is initiated. In the same culture model, pro-apoptotic bax was not observed to associate with the mitochondria under apoptosis-inducing situations, but was seen to associate with the nucleus. This may imply that other pro-apoptotic molecules may be interacting with bcl-2 at the mitochondrial membrane, resulting in activation of apoptosis. Pro-apoptotic bak is shown to be upregulated *in vivo* at the time when cell death is seen, and it too is known to translocate to the mitochondrial membrane under apoptotic conditions and to interact with bcl-2. It would be interesting to investigate the sub-cellular distribution of bak, or other pro-apoptotic molecules under similar conditions in the cushion-culture model.

In each case, the apparent sub-cellular translocation of bcl-2 and bax under apoptosis-inducing conditions was seen to be inhibited by a general caspase inhibitor.

The general caspase inhibitor used here was also shown in this work to significantly protect these cells from apoptosis, so it is known to be functional in these cells. Both bax and bcl-2 have been shown to be cleaved by caspases (Gross *et al*, 1999), and inhibition by a caspase inhibitor would implicate the bcl-2 family downstream of caspase activity, and not at the beginning of the cascade.

Both bcl-2 and bax have also been shown to associate with the nuclear matrix (Wang *et al*, 1999), which has been shown to be the site of initiation of DNA-fragmentation during apoptosis (Walker and Sikorska, 1997). Bax-antisense oligonucleotides have also been shown to inhibit cleavage of the nuclear lamins, which are involved in maintenance of the nuclear scaffold, and are cleaved during apoptosis (Robertson *et al*, 2000). Interestingly, PARP cleavage is not inhibited by bax antisense oligonucleotides, implying specific roles for bax in the nucleus.

In addition to showing that bcl-2 is present in the endocardial cushions, it is shown that this molecule can also protect primary cultures of the cushions from serum-starvation induced apoptosis. Bcl-2 has been shown to protect numerous cell types from a variety of insults. It would be interesting to identify the cell types predominating in our cushion cultures, but as yet, there are no specific antibodies to distinguish endocardially derived cushion cells from the neural crest cells. One interesting observation in this culture model was the fact that under serum-starved conditions, when the cells were stained using the TUNEL technique, only 3-5% of the cultures were ever apoptotic at any one time, which may suggest that a specific population of cells is dying. However, bcl-2 seems to be functional in the majority of the heterogeneous population of cells in the culture model.

In tissue sections, the pro-apoptotic bcl-2 family members bax and bak appear to predominantly associate with the prongs of the AP septum. However, the previously shown distribution patterns of apoptotic cells appear not to overlap exactly with the pattern of these pro-apoptotic molecules. One possible explanation for this is that the pro-apoptotic members may not yet be active. Bax and bak are often normally found to reside in the cytoplasm of healthy cells, and on receiving a necessary signal, these molecules are activated and translocate to the mitochondria and nucleus where they contribute to the downstream apoptotic-signaling pathway (Gross *et al*, 1999). As the antibodies used in the current study do not distinguish between the inactive and active forms, it is possible that the NC cells contain the inactive pro-apoptotic molecules during migration and invasion of the different regions of the heart, especially in the endocardial cushions. On reaching a certain site, probably associated with remodeling, the NC cells may receive an activation signal that brings about translocation of the pro-apoptotic molecules. Another explanation is that other pro-apoptotic bcl-2 family members may be present and active in the apoptotic cells, with a pattern of direct overlap with TUNEL distribution, or even that other non-bcl-2 family regulators of apoptosis are involved.

Are members of the caspase family of enzymes involved in apoptosis in the endocardial cushions?

Some evidence for caspase involvement in heart development has been demonstrated. Homogenous disruption of the caspase-8 gene in mice results in, amongst other features, impaired ventricular musculature (Varfolomeev *et al.*, 1998). Disruption of the upstream receptor linked to caspase-8, FADD/MORT1 (Yeh *et al.*, 1998; Zhang *et*

al., 1998) results in a similar phenotype, as does inactivation of casper (c-FLIP), the upstream inhibitor of this pathway (Yeh *et al.*, 2000). These gene knockouts do not however, appear to affect cushion development and the hypothesis has been suggested that these molecules may act in a cell death independent manner (Yeh *et al.*, 2000). Also, some evidence for caspase-3 activity has been found by Watanabe *et al.* (1998), who showed enzyme activity in homogenates of whole chick OT. Immunoblotting of the dissected AV cushions and the OT provide evidence of caspase activation in these tissues. The caspase family of enzymes are the downstream effectors of cell death, that bring about the demise of the cell by cleaving and inactivating cellular proteins necessary to maintain cellular homeostasis, or by activating other cellular destruction proteins (Thornberry and Lazebnik, 1998). Different pathways of caspase activation may be present, with simplified processes being either receptor-mediated or mitochondrial-initiated. Here we show evidence of activation of one of the upstream mitochondrial-associated enzymes. Caspase 9 normally resides in an inactive state in the cytoplasm and is activated via the release of cytochrome c from the mitochondria. Activation results in cleavage of pro-caspase 9 by a cytochrome c / Apaf-1 complex (Li *et al.*, 1997) which then activates the downstream caspases (Slee *et al.*, 1999). The antibody used in this study recognized the smaller cleavage fragment of the active enzyme, and showed the presence of the activated enzyme at times when apoptosis is occurring *in vivo*. Caspase-9 cleavage was seen to begin a day later in AV cushion tissue (ED5) than in the OT (ED4), which resembles the pattern of peak apoptosis in the cushions *in vivo*, thus implicating the caspase-9 enzyme. Attempts at immunoblotting with antibodies to caspase-8 and -3 were unsuccessful, with the antibodies not recognizing any antigen in the tissue. However,

evidence for caspase-3 activity has been shown in homogenates of the entire OT, throughout the timecourse that apoptosis is seen in the OT cushions (Watanabe *et al*, 1998).

Further evidence of caspase activity in endocardial cushion cells is presented here in the *in vitro* studies on primary cultures of dissociated cushions. An inhibitor of the upstream mitochondrial pathway associated caspase-9 was as effective as a universal inhibitor, while an inhibitor of the downstream caspase-3 was slightly less effective, but still significant.

Another hallmark of programmed cell death and usually of caspase activity is the cleavage of PARP, a DNA repair enzyme. In dying cells this protein is cleaved and inactivated from a 113 kDa isoform to 89 and 24 kDa cleavage products (Duriez and Shah, 1997). PARP cleavage is seen throughout ED3-8 in the OT, which may reflect the prolonged timecourse of apoptosis in the OT myocardium (van den Hoff, 1998) as well as the slightly earlier phase in the cushions. In the dissected AV cushions, PARP was repeatedly seen to be cleaved during ED7-8, which seems to slightly succeed the phase of peak cell death.

There is discrepancy between the timing of caspase-9 activation and PARP cleavage, as seen with immunoblotting on dissected tissues. As mentioned, caspase-9 is seen to be cleaved throughout the timecourse of apoptosis, but in the AV cushions, PARP cleavage is only seen during ED7-8, a time later than peak apoptosis level are observed. There are a number of different possible explanations for this. First, that PARP is cleaved by another caspase family member that may or may not reside downstream of caspase-9 activation. Caspase-9 is known to activate caspases-3 and -7, both of which are known to

cleave PARP (Slee *et al*, 1999). It would be interesting to see if either protein has a differential expression pattern in the endocardial cushions. Results presented here on the effect of caspase-inhibitors on the levels of cell death in cushion-cell cultures show that a universal inhibitor is more effective at blocking apoptosis than an inhibitor of caspase-3, which may suggest a caspase-3-independent pathway. Second, receptor-mediated caspase-8 activation may be involved in PARP cleavage. Although the work presented here shows no evidence for caspase-8 activity, as mentioned earlier caspase-8 knockout mice die as a result of severe cardiac defects (Varfolomeev *et al.*, 1998). In these studies, no mention is made of endocardial cushion defects, and the main defect observed is impaired ventricular musculature. The inference here is that caspases may have activity at other times in apoptosis in the ventricle and myocardial layers in the heart. In the postnatal heart, there is a surge in levels of apoptosis in the ventricle and in the conduction system of the heart, in both human and mice hearts (James, 1998; Fernandez *et al*, 2001). The findings in the work presented here that *bax* is constitutively expressed in the ventricle may lend support to this view. Other emerging views are that these molecules may be acting in a cell death-independent manner (Yeh *et al*, 2000). Third, PARP cleavage may occur in a caspase-independent manner, via cleavage by the enzyme calpain. This cysteine protease is activated in certain types of apoptosis, and in necrosis, and has been shown to cleave PARP and even caspase-3 (McGinnis *et al*, 1999).

What is the cell type dying in the endocardial cushions?

The pattern of apoptotic cells seen in the work presented here does not appear to be associated with any identifiable cell type. The pattern does not overlap with the known

distribution of neural crest cells. The dying cells do not seem to lie to one side of the cushion tissue. As no cell-specific marker of the apoptotic cells is known, the type of cells which are dying can only be inferred. As discussed below, the evidence seems to suggest that some, but not all, of the apoptotic cells are neural crest in origin.

The dying cells may also be myocardial in origin, after migrating from the inner curvature of the earlier stage looping heart. During the looping of the heart tube, the posterior wall of the conal OT and the anterior wall of the AV canal fuse to form a common wall between the two areas, consisting of myocytes on the outside and cushions cells on the inside of the inner curvature area (see Figure 2-1). The non-proliferating myocytes from this area migrate into the endocardial cushions of the AV and OT regions, in a process called myocardialization (Mjaatvedt *et al*, 1999). This is an earlier process of "myocardialization" than is discussed elsewhere (see "*what is the role of apoptosis in the endocardial cushions?*"), when at a later stage, during valve maturation, ingression of myocytes from the adjacent myocardium is also seen. The timing of migration here is after HH stage 24, which is consistent with the timing of apoptosis. It is thought that the developing cushions may induce the migration of the myocytes from the inner curvature, through the putative interactions of homeobox genes expressed in the area, including *Msx-1* (Chan-Thomas *et al*, 1993), *Mox-1* (Candia *et al*, 1992), *Prx-1* and *Prx-2* (Leussink *et al*, 1995). These genes are upregulated in cushion mesenchyme following the EMT of the endocardial layer, and are thought to induce differentiation and maturation of cushion mesenchyme, which subsequently induces migration of the adjacent myocytes (Mjaatvedt *et al*, 1999).

Are similar processes of cell death in effect in both sets of cushions?

The derivation of the endocardial cushions in both the AV and OT regions appears to be similar (Nakajima *et al*, 2000), but no work has commented on mechanisms of apoptosis. A number of the findings presented here suggest a similar pathway is in effect in both sets of cushions. Bcl-2 appears to be down regulated at the onset times of peak cell death in both areas, whereas the pro-apoptotic bak appears to be up regulated in each area. Immunoblotting also shows the cleavage fragment of active caspase 9 in both sets of cushions. Evidence of PARP cleavage in the AV cushions and the OT further support the idea that it is indeed apoptosis that is occurring in the cushions of the heart, and that similar processes are in effect in both regions.

Are the dying cells neural crest in origin?

There is debate as to whether or not the apoptotic cells in heart development are of neural crest origin. Retroviral and TUNEL labeling of neural crest cells (Poelmann *et al*, 1998) suggests that some of the apoptotic cells in the conal cushions of the outflow tract may be crest derived. However, quail-chick chimeras imply a fate of differentiation as opposed to apoptosis for most neural crest cells (Waldo *et al*, 1998; van den Hoff *et al*, 1999). Furthermore, the mismatch of timing of invasion and arrival at their final destination of migrating neural crest cells, with the distribution and numbers of apoptotic cells further adds to the complexity. Probably, some neural crest cells are eliminated by apoptosis (Poelmann *et al*, 1998) but whether or not it is the final fate of the majority of them remains to be shown conclusively.

The work presented here shows some evidence of NC cells in the OT cushions and the prongs of the AP septum undergoing apoptosis. The overlap of DiI labeling with the fragmenting nuclei, characteristic of apoptotic cells, suggests that for at least some NC cells, cell death is the final fate. This is further supported by the apparent association of the pro-apoptotic bcl-2 family members bax and bak with the prongs of the AP septum, the neural crest derived mesenchyme that invades the endocardial cushions, with staining seemingly absent from the condensed mesenchyme. The significance of this is uncertain, but it is known that the prongs of the AP septum are located in an area that will become muscularized, as opposed to the condensed mesenchyme of the septum, which remains mesenchymal (Poelmann *et al.*, 2000). Poelmann *et al.* (1999) contend that only a subpopulation of neural crest cells in the distal tips of the prongs undergoes apoptosis. It is this hypothesis that best fits the results presented here. However, the patterns of apoptosis shown by TUNEL labeling in this work do not exactly overlap with neural crest distribution. This would suggest an even more complex process, with other cell populations in the cushions dying also. In neural crest ablated embryos, the cushions of the outflow tract fail to fuse, resulting in a heart defect known as persistent truncus arteriosus (PTA) (Waldo *et al.*, 1998; Kirby *et al.*, 1985), amongst other phenotypic changes, depending on the completeness of ablation. However, it remains to be seen if levels of apoptosis in the cushions of the developing heart are affected in neural crest ablated embryos. In the cardiac conduction system, it is speculated that the apoptosis of neural crest cells that target the prospective cardiac conduction, play a role in the final phase of differentiation of the cells of the conduction system, due to the overlap of timing of arrival of the migrating cells and a change in the electrophysiological activity of the

heart (Poelmann and Gittenberger-de-Groot, 1999). Alternatively, the apoptosis of the cells aids in separating the central conduction system from the working myocardium. A large number of dying cells are also supposedly seen in the superior aspect of the interventricular septum, at the site of its fusion with the atrial septum and OT septum (Fisher *et al*, 2000; van den Hoff *et al*, 2000). This area includes the sites of formation of the AV node, the bundle of His and the left and right bundle branches, and is also the final destination of some of the cardiac neural crest cells. Probably many cardiac neural crest cells undergo apoptosis, but regarding the cushion-targeted neural crest cells, the situation remains unclear. Evidence here and elsewhere suggests that some cushion-neural crest cells do die, but that these are in the minority.

What are the species differences in the distribution of apoptosis?

In his initial studies, Pexieder (1975) compared chick, human and rat hearts, although he admits that only poor-quality human samples were available. However, that study pointed to species differences, with fewer foci of cell death seen in the rodent and human hearts when compared to the avian model. Despite the differences in incidence, there were areas common to each species that contained large numbers of dying cells, which included the OT and AV endocardial cushions. Much of the recent work on cell death in the heart has used the chick as a model, with some work performed on mouse and rat hearts. The distribution of apoptotic cells in each species seems similar, with each having cell death in the AV and OT cushions. However, in the mouse and the rat hearts, the number of apoptotic cells, as seen by TUNEL labeling seems to be much lower than

in the chick (Takeda *et al.*, 1996; Abdelwahid *et al.*, 2001a). In this study, attempts were made to label the mouse embryonic heart using TUNEL, but did not prove successful in identifying more than individual isolated cells, and the attempts were abandoned. Because the TUNEL technique is now known to label only a fraction of the total number of dying cells at any one time, due to the rapid clearance of the cell fragments, it was probably a mistake not to pay more attention to the individual cells, which may have represented smaller foci. However, it is still correct to say, based on Pexieders work, and the more recent studies, that the chick appears to have a higher incidence of cell death than mammalian species (van den Hoff *et al.*, 2000). Studies on human embryos have not progressed much beyond Pexieder's initial assessment on poor-quality tissue samples from human embryos, with a description of 16 foci of cell death (Pexieder, 1975). Again, in my study, attempts were made to obtain suitable human embryonic tissue for TUNEL labeling, from the Canadian Embryo and Fetal Tissue Bank, University of Alberta. However, due to the very early stage required, only one embryo was obtained that was at a stage with endocardial cushion tissue. This sample had been in fixative for a long period of time, which is a hindrance to TUNEL labeling, and again, only a few isolated individual cells in the late-stage AV cushions stained positively with the test. So, the conclusion seems to be that apoptosis is seen in at least the AV and OT cushions of each species examined, but that the chick may have the highest incidence of cell death.

Why is there a more limited distribution of apoptotic cells than initially described?

In his initial studies, Pexieder (1972; 1975) described 31 different foci of cell death in the chick heart. More recent studies seem to point to a lower number of foci at the same stages. There may be a number of reasons for this. Firstly, Pexieder performed his analysis using vital dyes and cell morphological assessment. Although these are accurate methods of identifying dying cells, they are not as specific as the TUNEL technique for quantitative descriptive accounts in localizing studies. Pexieder also included macrophages containing cell debris in his counts of dying cells. Secondly, in his studies, Pexieder mostly worked on isolated hearts and squashed samples in counting dying cells. In my study, it was found that dissecting the heart from the embryo resulted in damage to the tissue that subsequently gave false-positive results. Subsequently, whole embryo sections were stained in the present work, with no direct contact made with cardiac tissue, thus making it possible that Pexieder may also have had damaged tissue-staining in his work. Thirdly, in his detailed analysis of the regions of cell death in the heart, Pexieder was much more thorough in his identification of specific areas than the more recent studies. For example, in that work, cell death was described in the left and right, proximal and distal bulbar cushions and in the bulboventricular groove as five different areas, whereas more recent work has grouped these areas together under general all-encompassing headings, such as "the OT". Finally, whereas Pexieder's work included individual dying cells, or scattered individual cells as specific foci, my study tended to view these as background cell death, and does not include them, even though scattered TUNEL positive cells were seen in other regions such as the ventricle and atrial walls.

What is the stimulus for the cells to die?

There are many different signals that are known to instruct cells to undergo apoptosis. It has been postulated that apoptosis is the default state of all metazoan cells, which die if they are deprived of certain survival signals (Raff, 1992). Different cell types require different survival signals that are only available in their own environment, such as cell-cell interactions, cell-matrix interactions, soluble cytokines and hormones, or synaptic connections. Then, in differentiated cells, should they stray from their correct environment, the default cell death pathway is activated. Apoptotic cells may also receive inductive signals in the form of secreted growth factors, triggering the apoptotic pathway. The transforming growth factor-beta family of growth factors, and the bone morphogenetic protein subfamily are likely candidates as inducers of apoptosis in the endocardial cushions.

The initial culture work presented here on cushion explants suggests that some factor present in the cushions may induce apoptosis. The timecourse of the increase in levels of apoptosis precedes that seen *in vivo* by 24 h, suggesting that some factor present in the degrading explant may be inducing cell death in the outgrowing explant.

Also presented here, treatment of endocardial cushion cultures with conditioned medium from various regions of the heart showed that both AV and OT cushion-cell apoptosis was increased by addition of conditioned medium from the cushions themselves, and in the OT, also from the ventricle. Attempts at immunoblotting the conditioned medium samples for BMP4 proved unsuccessful. However, the areas of the heart that were shown to increase levels of cell death are known to contain the message for BMP's and TGF- β . The work presented here describes the presence of BMP2 protein

in the endocardial cushions of both the AV and OT regions. As described, BMP2 has also been shown to induce apoptosis in some cell populations (Kimura *et al*, 2000). It would be interesting to examine the cushion conditioned medium for the presence of BMP2 protein, or attempt to inhibit the apoptosis-inducing effects of the medium with function-blocking anti BMP2 antibodies. As also described, overexpression of the constitutively-active BMP-1B receptor was shown to induce apoptosis in some of the endocardial cushion cells in culture. This receptor is known to transduce BMP signals in the absence of protein. Addition of the dominant-negative BMP receptor may also block the apoptosis-inducing effects of the cushion-conditioned medium, if it is indeed BMP2 protein that is the inductive signal.

As described, there is a differential distribution of the message for various BMP family members prior to and during endocardial cushion development (Nakajima *et al*, 2000). However, most of this work has been descriptive in nature, localizing the message to the myocardium, and recently in the mouse cushions. The work presented here shows that with immunocytochemistry, BMP2 protein is actually seen in the cushions, and that this expression may be different between the chick and the mouse. The expression for BMP4 protein correlates with the previous descriptions of mRNA expression, with protein expression seen in the musculature of the heart. Bone morphogenetic protein-4 has been shown to induce cell death in the tissue culture explants of the endocardial cushions of the OT and AV regions (Zhao and Rivkees, 2000), as well as in other developmental tissues, such as the limb (Yokouchi *et al*. 1996) and the paraxial and lateral plate mesoderm (Schmidt *et al*, 1998). The findings of the work presented here implicates the BMP receptor 1B in apoptosis of some cells in cushion cultures, possibly

acting in a concentration-dependent manner. The RCAS expression system is known to act in a concentration-dependent manner (Morgan and Fekete, 1996) and viral mediated overexpression of constitutively-active BMP receptor-1A has previously been shown to act in a threshold-dependent manner in primary cultures (Varley *et al*, 1998). Some recent reports (Abdelwahid *et al*, 2001b; Allen *et al*, 2001; Kim *et al*, 2001) further examine the involvement of the BMP's in apoptosis during cushion development. The message for BMP2 and 4 and the homeobox gene *msx-2* were suggested to overlap with areas of apoptosis in the mouse endocardial cushions. Kim *et al* (2001) examined apoptotic levels in BMP6:BMP7 double mutant mice, and found no difference in the levels of cell death in the myocytes compared to the wild-type control. However, they observed no apoptosis in the endocardial cushions of either wild type or mutants, which may exclude these factors from apoptosis in the heart, or may further support the possibility of species differences. Allen *et al* (2001) inhibited BMP-2/4 via retroviral *noggin* overexpression, and mention that no increase in apoptosis was seen in the cushions. However, if BMP signaling is implicated in triggering apoptosis, then its inhibition will not increase levels. It would be interesting to know if any decrease in levels of cell death was observed in these mice. Also, from their results, it would appear that the endocardial cushions were not adequately infected with the virus, so perhaps no inference on cushion cell death can be made. Interestingly, knockout mice for the intracellular BMP-signaling molecule Smad-6 develop severe cardiac defects, with hyperplasia of the cardiac valves, and defects of septation in the OT (Galvin *et al*, 2000). Taken together, the outlined work points to a potential role of BMP's in apoptosis in the endocardial cushions of the developing heart.

What is the role of apoptosis in the endocardial cushions?

It has been suggested that the dying cells in the cushions play a role in the subsequent myocardialization of the cushions (Poelmann and Gittenberger-de Groot, 1999). It has also been suggested that these myocardializing apoptotic cells are neural crest derived (Poelmann *et al.*, 1998). So far, the emphasis of the role of apoptosis in the cushions seems to be on the muscularization of the cushions during development of the valve leaflets. At later stages of cushion development, myocardial cells invade the mesenchymal tissues by migration from the adjacent muscle layer (Ya *et al.*, 1998; van den Hoff *et al.*, 1999). In the OT, this process has been shown to be stimulated by the mesenchymal tissue of the distal OT. The timing of this migration follows the period of peak cell death in the cushions, and corresponds with the timing of invasion of NC cells. Poelmann and Gittenberger-de Groot (1999) postulate that apoptotic NC cells may release “molecules” that stimulate myocardialization of the septa. So far however, there is little evidence of apoptotic cells acting as in such a signaling manner. Specific roles have also been postulated for some of the other apoptotic populations of cells in the heart. Cell death in the neural crest cells that enter the heart via the venous pole are thought to induce the final differentiation of cardiomyocytes into the specialized conduction system. (Poelmann and Gittenberger-de Groot, 1999). Apoptosis of the OT myocytes have been suggested to be involved in the shortening of the OT, which changes from a relatively long and separate tubular structure, to a compact ring of tissue incorporated into the heart (Watanabe *et al.*, 1998). This remodeling and shortening of the OT facilitates correct alignment of the ventricles with the aorta and the pulmonary artery (Watanabe *et al.*, 1998). To address the role of apoptosis in the cushions, in the current study attempts were

made at *in vivo* bcl-2 overexpression via retroviral microinjection and DNA electroporation. It was hypothesized that if cell death could be specifically inhibited, perhaps the resulting phenotype could aid in attributing a role to the cell death. It would be interesting to see if the invasion of myocytes during muscularization is inhibited, or if valve structure is impaired. If a significant portion of NC cells are indeed dying, inhibition of apoptosis should reflect this perhaps by impaired septation or fusion of the cushions.

What are the possible reasons for lack of viral infection?

There are a number of reasons why the virus may not have infected the endocardial cushions adequately. The most probable is that the viral titer used was too low. Morgan and Fekete (1996) report that a viral titer below 5×10^7 would not be considered useful, and that routinely, stocks of a minimum of 10^8 infectious units (IU)/ml are needed. The stock used in this work (5×10^7 IU/ml) was probably below the level of optimal infection efficiency and only further experiments with a higher titer virus will provide more answers.

The RCAS virus expression system is known only to infect actively dividing cells. The PCNA staining shown here indicates that the myocardial layer of the heart contains many proliferating cells by the stage that apoptosis is seen in the cushions, while the endocardial cushions contain proliferating cells initially in the area adjacent to the endocardium, but at later stages, proliferating cells are seen throughout the cushions. This supports the feasibility of infecting the endocardium with virus prior to and during the stages of EMT during cushion development. Addition of the virus to the outer myocardial

layer may not have achieved this, whereas injection of the virus into the lumen of the heart would have resulted in the viral solution being removed by the bloodflow.

The RCAS virus has been shown to require an infection period of approximately 18 hours before maximal viral expression (Homburger and Fekete, 1996). In the work presented here, the virus was added to the pericardial sac, with the aim of infecting the outer and inner layers of the heart. It is possible that the rate of infection and incorporation of the proviral insert was approximately equal to the rate of proliferation of the outer myocardium of the heart, such that the viral spread only infected the growing myocardium, and only minor secondary infection reached some parts of the endocardial cushions. This however, would not account for the apparent viral staining in the cushions, without the accompanying pattern of human *bcl-2* expression. Preliminary attempts in this study were made to infect the precardiac mesoderm, prior to formation of the heart tube. This proved fatal to embryo in each of the initial attempts, so this approach was abandoned in favour of injection into the heart itself. However, the approach of labeling the mesoderm was used in recent studies that also used the RCAS expression vector to overexpress *noggin* in the developing heart (Allen *et al*, 2001). In this study, the precardiac mesoderm was flooded with a high concentration viral solution, and the embryos reincubated. Although the endocardial cushions were not the main focus of that work, the pattern of viral expression seen in the cushions is similar to that shown here. Also, a higher viral titer was used in that work, and it still did not adequately infect the cushions. Taken together, the results seem to suggest that there may be some cell-specific factor, intrinsic to cushion development, preventing viral infection.

The same viral DNA construct was used in the electroporation studies, in an attempt to incorporate the DNA sequence of interest into the developing cushions. Although the extent of proviral incorporation and secondary infection by virus is not known, use of the proviral DNA constructs as a reagent for electroporation is known to be adequate at infecting embryonic cells, as seen with infection of the neural tube with GFP constructs (not shown). In the work outlined here, some limited expression of green fluorescent protein and bcl-2 was seen in the heart tissues, which suggests that the tissue is susceptible to incorporation of the DNA inserts. As outlined, the initial attempts at electroporation involved small amounts of DNA, and the beating heart probably pumped the solution away from the heart. Attempts were then made at stopping the heart with ice-cold saline while the DNA solution was injected. This resulted in only a few examples of protein expression. However, even when the heart was stopped prior to injection, the pulses of current applied immediately reactivated and increased the heartbeat, which presumably removed most of the DNA present.

Future attempts at retroviral bcl-2 overexpression in the heart may take a number of approaches. Initially, similar injections with a high-titer virus will be needed, to assess if a similar pattern of exogenous bcl-2 protein is seen. Further attempts at injection of the precardiac mesoderm should also be attempted with a high concentration virus, to attempt to infect the endocardial layer prior to the EMT. Other attempts could target specific populations of cardiac cells. Electroporation of neural crest cells prior to their migration from the neural tube would be a very interesting experiment. As outlined here and elsewhere, a sub-population of the cardiac neural crest cells undergoes apoptosis in the heart environment. Inhibition of this process may help define the role of at least some of

the neural crest cells in the heart. Viral infection of the myocytes of the inner curvature of the heart may also prove interesting, if these cells do indeed invade the endocardial cushions and undergo apoptosis. Concomitant staining with muscle-specific markers could also be performed.

In conclusion, these results provide a better understanding of apoptosis as a natural process during early heart development. Labeling of apoptotic cells using the TUNEL technique has shown that the highest incidence of apoptosis occurs during the development and morphogenesis of the endocardial cushions. Fluorescent labeling of neural crest cells show that some, but probably not all, of these dying cells are neural crest-derived. Analysis of the *bcl-2* and caspase families of apoptosis regulators and effectors shows expression patterns of *bcl-2*, *bax* and *bak* suggestive of roles in the regulation of apoptosis, while evidence of caspase-9 activity and caspase inhibitors on cell cultures suggests that these molecules may also be active *in vivo*. Immunocytochemistry for bone morphogenetic proteins -2 and -4 displays different expression patterns, with a novel finding of BMP-2 protein in the endocardial cushions. Preliminary studies with BMP receptor overexpression implicate BMPR-1A in the epithelial-mesenchymal transformation that occurs during cushion formation, with BMPR-1B possibly having a role in apoptosis of some cells in the cushions. Further attempts to inhibit the normal pattern of apoptosis using retroviral and DNA overexpression techniques will contribute to the understanding of the functional role of apoptosis in these regions.

FUTURE DIRECTIONS

The majority of the work outlined here is descriptive in nature, describing the patterns of distribution of dying cells and some of the main factors involved in this process. Attempts were also made at functional studies of the role of apoptosis, via inhibition of the naturally occurring process. Future functional studies to consolidate this work could take a number of directions. As described, inhibition of cell death in specific populations of cells in the endocardial cushions could provide information on the roles of these cells. Premigratory neural crest cells or cardiac myocytes could be infected with *bcl-2* before they enter the endocardial cushions. Further analysis of the cell types dying in the cushions should be made, possibly with cell-type specific markers of myocytes and endocardial cells as they become available. Preliminary studies have been described here that suggest specific roles for members of the BMP family, and some of their receptors. Using the culture model, further analysis of the functions of the receptor subtypes under more defined conditions, such as varying viral concentrations and functional receptor expression assessment could be performed. To identify the receptor subtypes present *in vivo*, *in situ hybridisation* studies could be performed to localise the receptors in the developing heart. Functional studies with BMP's or their inhibitor *noggin*, could be performed *in ovo*, by implanting beads soaked in the protein into the developing heart, which would enable specific regions of the heart to be targeted at specific times, with the subsequent assessment of apoptosis levels and morphological development of the valves. The analysis of the involvement of the *bcl-2* and caspase family could be continued, as evidenced by the lack of direct overlap between apoptosis and the levels and distribution of the main apoptotic regulators. As the mechanism of apoptosis involves an ever-

increasing number of factors, further analysis of the bcl-2 and caspase pathways, as well as other apoptotic pathways will be needed.

REFERENCES

- Abdelwahid, E., Eriksson, M., Pelliniemi, L. J. and Jokinen, E. (2001a) Heat shock proteins, HSP25 and HSP70, and apoptosis in developing endocardial cushion of the mouse heart. *Histochem Cell Biol* **115**:95-104
- Abdelwahid, E., Pelliniemi, L. J., Niinikoski, H., Simell, O., Tuominen, J., Rahkonen, O. and Jokinen, E. (1999) Apoptosis in the pattern formation of the ventricular wall during mouse heart organogenesis. *Anat Rec* **256**:208-217
- Abdelwahid, E., Rice, D., Pelliniemi, L. J. and Jokinen, E. (2001b) Overlapping and differential localization of Bmp-2, Bmp-4, Msx-2 and apoptosis in the endocardial cushion and adjacent tissues of the developing mouse heart. *Cell Tissue Res* **305**:67-78
- Adams, J. M. and Cory, S. (1998) The Bcl-2 protein family: arbiters of cell survival. *Science* **281**:1322-1326
- Akhurst, R. J., Lehnert, S. A., Faissner, A. and Duffie, E. (1990) TGF beta in murine morphogenetic processes: the early embryo and cardiogenesis. *Development* **108**:645-656
- Allen, R. T., Hunter, W. J. 3rd and Agrawal, D. K. (1997) Morphological and biochemical characterization and analysis of apoptosis. *J Pharmacol Toxicol Methods* **37**:215-228
- Allen, S. P., Bogardi, J. P., Barlow, A. J., Mir, S. A., Qayyum, S. R., Verbeek, F. J., Anderson, R. H., Francis-West, P. H., Brown, N. A. and Richardson, M. K. (2001) Misexpression of noggin leads to septal defects in the outflow tract of the chick heart. *Dev Biol* **235**:98-109
- Alnemri, E. S., Livingston, D. J., Nicholson, D. W., Salvesen, G., Thornberry, N. A., Wong, W. W. and Yuan, J. (1996) Human ICE/CED-3 protease nomenclature. *Cell* **18**:171
- Antonsson, B., Montessuit, S., Lauper, S., Eskes, R. and Martinou, J. C. (2000) Bax oligomerization is required for channel-forming activity in liposomes and to trigger cytochrome c release from. *Biochem J* **345**:271-278
- Bagnali, K. M. (1992) The migration and distribution of somite cells after labelling with the carbocyanine dye, DiI: the relationship of this distribution to segmentation in

the vertebrate body. *Anat. Embryol.* **185**:317-324

Bao, Z. Z., Bruneau, B. G., Seidman, J. G., Seidman, C. E. and Cepko, C. L. (1999) Regulation of chamber-specific gene expression in the developing heart by *Irx4*. *Science* **283**:1161-1164

Barde, Y. A. (1989) Trophic factors and neuronal survival. *Neuron* **2**:1525-1534

Barinaga, M. (1998) Stroke-damaged neurons may commit cellular suicide. *Science* **281**:1302-1303

Bartelings, M. M. and Gittenberger-de Groot, A. C. (1989) The outflow tract of the heart-embryologic and morphologic correlations. *Int J Cardiol* **22**:289-300

Becker-Hapak, M., McAllister, S. S. and Dowdy, S. F. (2001) TAT-mediated protein transduction into mammalian cells. *Methods* **24**:247-256

Bernanke, D. H. and Markwald, R. R. (1982) Migratory behavior of cardiac cushion tissue cells in a collagen-lattice culture system. *Dev Biol* **91**:235-245

Boise, L. H., Minn, A. J., Noel, P. J., June, C. H., Accavitti, M. A., Lindsten, T. and Thompson, C. B. (1995) CD28 costimulation can promote T cell survival by enhancing the expression of Bcl-XL. *Immunity* **3**:87-98

Bolender, D. L. and Markwald, R. R. (1979) Epithelial-mesenchymal transformation in chick atrioventricular cushion morphogenesis. *SEM III*:313-322

Bollag, R. J., Siegfried, Z., Cebra-Thomas, J. A., Garvey, N., Davison, E. M. and Silver, L. M. (1994) An ancient family of embryonically expressed mouse genes sharing a conserved protein motif with the T locus. *Nat Genet* **7**:383-389

Boyer, A. S., Ayerinkas, I. I., Vincent, E. B., McKinney, L. A., Weeks, D. L. and Runyan, R. B. (1999) TGFbeta2 and TGFbeta3 have separate and sequential activities during epithelial-mesenchymal cell transformation in the embryonic heart. *Dev Biol* **208**:530-545

Bruneau, B. G., Logan, M., Davis, N., Levi, T., Tabin, C. J., Seidman, J. G. and Seidman,

- C. E. (1999) Chamber-specific cardiac expression of Tbx5 and heart defects in Holt-Oram syndrome. *Dev Biol* **211**:100-108
- Bruneau, B. G., Nemer, G., Schmitt, J. P., Charron, F., Robitaille, L., Caron, S., Conner, D. A., Gessler, M., Nemer, M., Seidman, C. E. and Seidman, J. G. (2001) A murine model of Holt-Oram syndrome defines roles of the T-box transcription factor Tbx5 in cardiogenesis and disease. *Cell* **106**:709-721
- Budihardjo, I., Oliver, H., Lutter, M., Luo, X. and Wang, X. (1999) Biochemical pathways of caspase activation during apoptosis. *Annu. rev. Cell. Dev. Biol.* **15**:269-290
- Candia, A. F., Hu, J., Crosby, J., Lalley, P. A., Noden, D., Nadeau, J. H. and Wright, C. V. (1992) Mox-1 and Mox-2 define a novel homeobox gene subfamily and are differentially expressed during early mesodermal patterning in mouse embryos. *Development* **116**:1123-1136
- Chan-Thomas, P. S., Thompson, R. P., Robert, B., Yacoub, M. H. and Barton, P. J. (1993) Expression of homeobox genes Msx-1 (Hox-7) and Msx-2 (Hox-8) during cardiac development in the chick. *Dev Dyn* **197**:203-216
- Cheng, E. H. Y., Kirsch, D. G., Clem, R. J., Ravi, R., Kastan, M. B., Bedi, A., Ueno, K. and Hardwick, J. M. (1997) Conversion of Bcl-2 to a Bax-like death effector by caspases. *Science* **278**:1966-1968
- Cheng, E. H., Wei, M. C., Weiler, S., Flavell, R. A., Mak, T. W., Lindsten, T. and Korsmeyer, S. J. (2001) Bcl-2, bcl-x(l) sequester bh3 domain-only molecules preventing bax- and bak-mediated mitochondrial apoptosis. *Mol Cell* **8**:705-711
- Chittendon, T., Harrington, E. A., O'Connor, R., Flemington, C., Lutz, R. J., Evan, G. I. and Guild, B. C. (1995) Induction of apoptosis by the Bcl-2 homologue Bak. *Nature* **374**:733-736
- Chou, J. J., Matsuo, H., Duan, H. and Wagner, G. (1998) Solution structure of the RAIDD CARD and model for CARD/CARD interaction in caspase-2 and caspase-9 recruitment. *Cell* **94**:171-180
- Christoffels, V. M., Habets, P. E. M. H., Franco, D., Campione, M., de Jong, F., Lamers, W. H., Bao, Z., Palmer, S., Biben, C., Harvey, R. P. and Moorman, A. F. M.

(2000) Chamber formation and morphogenesis in the developing mammalian heart. *Dev. Biol.* **223**:266-278

Clarke, P. G. H. (1990) Developmental cell death: morphological diversity and multiple mechanisms. *Anat. Embryol.* **181**:195-213

Clarke, P. G. and Clarke, S. (1996) Nineteenth century research on naturally occurring cell death and related phenomena. *Anat Embryol* **193**:81-99

Conradt, B. and Horvitz, H. R. (1998) The *C. elegans* protein EGL-1 is required for programmed cell death and interacts with the Bcl-2-like protein CED-9. *Cell* **93**:519-529

Creazzo, T. L., Godt, R. E., Leatherbury, L., Conway, S. J. and Kirby, M. L. (1998) Role of cardiac neural crest cells in cardiovascular development. *Annu. Rev. Physiol.* **60**:267-286

Crossin, K. L. and Hoffman, S. (1991) Expression of adhesion molecules during the formation and differentiation of the avian endocardial cushion tissue. *Dev Biol* **145**:277-286

Daniel, P. T., Wieder, T, Sturm, I. and Schulze-Osthoff, K. (2001) The kiss of death: promises and failures of death receptors and ligands in cancer therapy. *Leukemia* **15**:1022-1032

De La Cruz, M., Gimenez-Ribotta, M., Saravalli, O. and Cayre, R. (1983) The contribution of the inferior endocardial cushion of the atrioventricular canal to cardiac septation and to the development of the atrioventricular valves: study in the chick embryo. *Am. J. Anat.* **166**:63-72

de la Pompa, J. L., Timmerman, L. A., Takimoto, H., Yoshida, H., Elia, A. J., Samper, E., Potter, J., Wakeham, A., Marengere, L., Langille, B. L., Crabtree, G. R. and Mak, T. W. (1998) Role of the NF-ATc transcription factor in morphogenesis of cardiac valves and septum. *Nature* **392**:182-6

Dickson, M. C., Slager, H. G., Duffie, E., Mummery, C. L. and Akhurst, R. J. (1993) RNA and protein localisations of TGF beta 2 in the early mouse embryo suggest an involvement in cardiac development. *Development* **117**:625-639

- Duan, H. and Dixit, V. M. (1997) RAIDD is a new 'death' adaptor molecule. *Nature* **385**:86-89
- Dudley, A. T. and Robertson, E. J. (1997) Overlapping expression domains of bone morphogenetic protein family members potentially account for limited tissue defects in BMP7 deficient embryos. *Dev Dyn* **208**:349-362
- Duriez, P. J. and Shah, G. M. (1997) Cleavage of poly(ADP-ribose) polymerase: a sensitive parameter to study cell death. *Biochem Cell Biol* **75**:337-349
- Earnshaw, W. C., Martins, L. M. and Kaufmann, S. H. (1999) Mammalian caspases: Structure, activation, substrates, and functions during apoptosis. *Annu Rev Biochem* **68**:383-424
- Eguchi, K. (2001) Apoptosis in autoimmune diseases. *Intern Med* **40**:275-284
- Eguchi, Y., Ewert, D. L. and Tsujimoto, Y. (1992) Isolation and characterization of the chicken bcl-2 gene: expression in a variety of tissues including lymphoid and neuronal organs in adult and embryo. *Nucleic Acids Res* **20**:4187-4192
- Ehrman, L. A. and Yutzey, K. E. (1999) Lack of regulation in the heart forming region of avian embryos. *Dev Biol* **207**:163-175
- Eisenberg, L. M. and Markwald, R. R. (1995) Molecular regulation of atrioventricular valvuloseptal morphogenesis. *Circ. Res.* **77**:1-6
- Ellis, H. M. and Horvitz, H. R. (1986) Genetic control of programmed cell death in the nematode *C. elegans*. *Cell* **44**:817-829
- Ellis, L. C. and Youson, J. H. (1990) Pronephric regression during larval life in the sea lamprey, *Petromyzon marinus* L. A histochemical and ultrastructural study. *Anat Embryol* **182**:41-52
- Enari, M., Sakahira, H., Yokoyama, H., Okawa, K., Iwamatsu, A. and Nagata, S. (1998) A caspase-activated DNase that degrades DNA during apoptosis, and its inhibitor ICAD. *Nature* **391**:43-50

- Fadok, V. A., Bratton, D. L., Frasch, S. C., Warner, M. L. and Henson, P. M. (1998) The role of phosphatidylserine in recognition of apoptotic cells by phagocytes. *Cell Death Differ* **5**:551-562
- Fadok, V. A., Voelker, D. R., Campbell, P. A., Cohen, J. J., Bratton, D. L. and Henson, P. M. (1992) Exposure of phosphatidylserine on the surface of apoptotic lymphocytes triggers specific recognition and removal by macrophages. *J Immunol* **148**:2207-2216
- Fawell, S., Seery, J., Daikh, Y., Moore, C., Chen, L. L., Pepinsky, B. and Barsoum, J. (1994) Tat-mediated delivery of heterologous proteins into cells. *Proc Natl Acad Sci U S A* **91**:664-668
- Fernandez, E., Siddiquee, Z. and Shoheit, R. V. (2001) Apoptosis and proliferation in the neonatal murine heart. *Dev Dyn* **221**:302-310
- Fisher, S. A., Lowell Langille, B. and Srivastava, D. (2000) Apoptosis during cardiovascular development. *Circ. Res.* **87**:856-864
- Fishman, M. C. and Chien, K. R. (1997) Fashioning the vertebrate heart: Earliest embryonic decisions. *Development* **124**:2099-2117
- Fitzharris, T. P. (1981) Origin and migration of cushion tissue in the developing heart. *Scanning Electron Microscopy II*:255-260
- Flanders, K. C., Kim, E. S. and Roberts, A. B. (2001) Immunohistochemical expression of Smads 1-6 in the 15-day gestation mouse embryo: signaling by BMPs and TGF-betas. *Dev Dyn* **220**:141-154
- Foyouzi-Youssefi, R., Arnaudeau, S., Borner, C., Kelley, W. L., Tschopp, J., Lew, D. P., Demaurex, N. and Krause, K. H. (2000) Bcl-2 decreases the free Ca²⁺ concentration within the endoplasmic reticulum. *Proc Natl Acad Sci U S A* **97**:5723-5728
- Frisch, S. M. and Ruoslahti, E. (1997) Integrins and anoikis. *Curr Opin Cell Biol* **9**:701-706

- Frisch, S. M. and Screaton, R. A. (2001) Anoikis mechanisms. *Curr Opin Cell Biol* **13**:555-562
- Gajkowska, B., Motyl, T., Olszewska-Badarczuk, H. and Godlewski, M. M. (2001) Expression of BAX in cell nucleus after experimentally induced apoptosis revealed by immunogold and embedment-free electron microscopy. *Cell Biol Int* **25**:725-733
- Galvin, K. M., Donovan, M. J., Lynch, C. A., Meyer, R. I., Paul, R. J., Lorenz, J. N., Fairchild-Huntress, V., Dixon, K. L., Dunmore, J. H., Gimbrone, M. A. Jr, Falb, D. and Huszar, D. (2000) A role for smad6 in development and homeostasis of the cardiovascular system. *Nat Genet* **24**:171-174
- Garcia-Martinez, V., Macias, D., Ganan, Y., Garcia-Lobo, M. V., Fernandez-Teran, M. A. and Hurle, J. M. (1993) Internucleosomal DNA fragmentation and programmed cell death (apoptosis) in the interdigital tissue of the embryonic chick leg bud. *J. Cell Sci.* **106**:201-208
- Gavrieli, Y., Sherman, Y. and Ben-Sasson, S. A. (1992) Identification of programmed cell death in situ via specific labeling of nuclear DNA fragmentation. *J. Cell Biol.* **119**:493-501
- Gilmore, A. P., Metcalfe, A. D., Romer, L. H. and Streuli, C. H. (2000) Integrin-mediated survival signals regulate the apoptotic function of Bax through its conformation and subcellular. *J Cell Biol* **149**:431-445
- Glucksmann, A. (1951) Cell deaths in normal vertebrate ontogeny. *Biol Rev Cambridge Philos Soc* **26**:59-86
- Gomes, W. A. and Kessler, J. A. (2001) Msx-2 and p21 mediate the pro-apoptotic but not the anti-proliferative effects of BMP4 on cultured sympathetic neuroblasts. *Dev Biol* **237**:212-221
- Graham, A., Francis-West, P., Brickell, P. and Lumsden, A. (1994) The signalling molecule BMP4 mediates apoptosis in the rhombencephalic neural crest. *Nature* **372**:684-686
- Green, D. R. (1998) Apoptotic pathways: the roads to ruin. *Cell* **94**:695-698

- Green, D. R. and Reed, J. C. (1998) Mitochondria and apoptosis. *Science* **281**:1309-1312
- Greidinger, E. L., Miller, D. K., Yamin, T. T., Casciola-Rosen, L. and Rosen, A. (1996) Sequential activation of three distinct ICE-like activities in Fas-ligated Jurkat cells. *FEBS Lett* **390** :299-303
- Griffiths, G. J., Dubrez, L., Morgan, C. P., Jones, N. A., Whitehouse, J., Corfe, B. M., Dive, C. and Hickman, J. A. (1999) Cell damage-induced conformational changes of the pro-apoptotic protein bak in vivo precede the onset of apoptosis. *J Cell Biol* **144**:903-914
- Gross, A., Jockel, J., Wei, M. C. and Korsmeyer, S. J. (1998) Enforced dimerization of BAX results in its translocation, mitochondrial dysfunction and apoptosis. *EMBO J* **17**:3878-3885
- Gross, A., McDonnell, J. M. and Korsmeyer, S. J. (1999) BCL-2 family members and the mitochondria in apoptosis. *Genes Dev.* **13**:1899-1911
- Gruber, P. J., Kubalak, S. W., Pexieder, T., Sucov, H. M., Evans, R. M. and Chien, K. R. (1996) RXR alpha deficiency confers genetic susceptibility for aortic sac, conotruncal, atrioventricular cushion, and ventricular muscle defects in mice. *J Clin Invest* **98**:1332-1343
- Hacki, J., Egger, L., Monney, L., Conus, S., Rosse, T., Fellay, I. and Borner, C. (2000) Apoptotic crosstalk between the endoplasmic reticulum and mitochondria controlled by Bcl-2. *Oncogene* **19**:2286-2295
- Hamburger, V. and Hamilton, J. L. (1951) A series of normal stages in the development of the chick embryo. *J. Morphol.* **88**:49-92
- Harrison, R. L., Byrne, B. J. and Tung, L. (1998) Electroporation-mediated gene transfer in cardiac tissue. *FEBS Lett* **435**:1-5
- Hay, D. A. and Low, F. N. (1972) The fusion of the dorsal and ventral endocardial cushions in the embryonic chick heart: a study in fine structure. *Am. J. Anat.* **133**:1-24

- Hay, D. A., Markwald, R. R. and Fitzharris, T. P. (1984) Selected views of early heart development by scanning electron microscopy. *Scan Electron Microsc* :1983-1993
- Hay, E., Lemonnier, J., Fromigue, O. and Marie, P. J. (2001) Bone morphogenetic protein-2 promotes osteoblast apoptosis through a Smad-independent, protein kinase C-dependent signaling pathway. *J Biol Chem* **276**:29028-29036
- Heine, U. I., Roberts, A. B., Munoz, E. F., Roche, N. S. and Sporn, M. B. (1985) Effects of retinoid deficiency on the development of the heart and vascular system of the quail embryo. *Virchows Arch B Cell Pathol Incl Mol Pathol* **50**:135-152
- Hengartner, M. O. (2000) The biochemistry of apoptosis. *Nature* **407**:770-776
- Hengartner, M. O. and Horvitz, H. R. (1994) *C. elegans* cell survival gene *ced-9* encodes a functional homolog of the mammalian proto-oncogene *bcl-2*. *Cell* **76**:665-676
- Hirata, M. and Hall, B. K. (2000) Temporospatial patterns of apoptosis in chick embryos during the morphogenetic period of development. *Int J Dev Biol* **44**:757-768
- Ho, Y. S., Lee, H. M., Chang, C. R. and Lin, J. K. (1999) Induction of Bax protein and degradation of lamin A during p53-dependent apoptosis induced by chemotherapeutic agents in human cancer cell lines. *Biochem Pharmacol* **57**:143-154
- Hockenbery, D., Nunez, G., Milliman, C., Schreiber, R. D. and Korsmeyer, S. J. (1990) Bcl-2 is an inner mitochondrial membrane protein that blocks programmed cell death. *Nature* **348**:334-336
- Hofmann, K., Bucher, P. and Tschopp, J. (1997) The CARD domain: a new apoptotic signalling motif. *Trends Biochem Sci* **22**:155-156
- Hogan, B. L. (1996) Bone morphogenetic proteins: multifunctional regulators of vertebrate development. *Genes Dev* **10**:1580-1594
- Homburger, S. A. and Fekete, D. M. (1996) High efficiency gene transfer into the embryonic chicken CNS using B-subgroup retroviruses. *Dev Dyn* **206**:112-120

- Horvitz, H. R. (1999) Genetic control of programmed cell death in the nematode *Caenorhabditis elegans*. *Cancer Res* **59**:1701s-1706s
- Hsu, H., Xiong, J. and Goeddel, D. V. (1995) The TNF receptor-1 associated protein TRADD signals cell death and NF-kappa B activation. *Cell* **19**:495-504
- Hu, Y., Benedict, M. A., Wu, D., Inohara, N. and Nunez, G. (1998) Bcl-XL interacts with Apaf-1 and inhibits Apaf-1-dependent caspase-9 activation. *Proc Natl Acad Sci U S A* **95**:4386-4391
- Hughes, S. H., Kosik, E., Fadly, A. M., Salter, D. W. and Crittenden, L. B. (1986) Design of retroviral vectors for the insertion of foreign deoxyribonucleic acid sequences into the avian germ line. *Poult Sci* **65**:1459-1467
- Hurle, J. M., Icardo, J. M. and Ojeda, J. L. (1980) Compositional and structural heterogeneity of the cardiac jelly of the chick embryo tubular heart: a TEM, SEM and histochemical study. *J Embryol Exp Morphol* **56**:211-223
- Icardo, J. M. (1996) Developmental biology of the vertebrate heart. *J. Exp. Zool.* **275**:144-161
- Icardo, J. M. and Fernandez-Teran, A. (1987) Morphologic study of ventricular trabeculation in the embryonic chick heart. *Acta Anat* **130**:264-274
- Ichimiya, M., Chang, S. H., Liu, H., Berezsky, I. K., Trump, B. F. and Amstad, P. A. (1998) Effect of Bcl-2 on oxidant-induced cell death and intracellular Ca²⁺ mobilization. *Am J Physiol* **275**:C832-839
- Ikeda, T., Takahashi, H., Suzuki, A., Ueno, N., Yokose, S., Yamaguchi, A. and Yoshiki, S. (1996) Cloning of rat type I receptor cDNA for bone morphogenetic protein-2 and bone morphogenetic protein-4, and the localization compared with that of the ligands. *Dev Dyn* **206**:318-329
- Izumi, M., Fujio, Y., Kunisada, K., Negoro, S., Tone, E., Funamoto, M., Osugi, T., Oshima, Y., Nakaoka, Y., Kishimoto, T., Yamauchi-Takahara, K. and Hirota, H. (2001) Bone morphogenetic protein-2 inhibits serum deprivation-induced apoptosis of neonatal cardiac myocytes through activation of the Smad1 pathway.

- Jacobson, M. D., Weil, M. and Raff, M. C. (1997) Programmed cell death in animal development. *Cell* **88**:347-354
- James, T. N. (1997) Apoptosis in congenital heart disease. *Coronary Artery Dis* **8**:599-616
- James, T. N. (1998) Normal and abnormal consequences of apoptosis in the human heart. *Annu Rev Physiol* **60**:309-25
- Jiang, X., Rowitch, D. H., Soriano, P., McMahon, A. P. and Sucov, H. M. (2000) Fate of the mammalian cardiac neural crest. *Development* **127**:1607-1616
- Jones, C. M., Lyons, K. M. and Hogan, B. L. (1991) Involvement of Bone Morphogenetic Protein-4 (BMP-4) and Vgr-1 in morphogenesis and neurogenesis in the mouse. *Development* **111**:531-542
- Jurgensmeier, J. M., Xie, Z., Deveraux, Q., Ellerby, L., Bredesen, D. and Reed, J. C. (1998) Bax directly induces release of cytochrome c from isolated mitochondria. *Proc Natl Acad Sci U S A* **95**:4997-5002
- Kamada, S., Kusano, H., Fujita, H., Ohtsu, M., Koya, R. C., Kuzumaki, N. and Tsujimoto, Y. (1998) A cloning method for caspase substrates that uses the yeast two-hybrid system: Cloning of the antiapoptotic gene gelsolin. *Proc Natl Acad Sci USA* **95**:8532-8537
- Kang, P. M. and Izumo, S. (2000) Apoptosis and heart failure - A critical review of the literature. *Circ Res* **86**:1107-1113
- Kaufmann, S. H. (1989) Induction of endonucleolytic DNA cleavage in human acute myelogenous leukemia cells by etoposide, camptothecin, and other cytotoxic anticancer drugs: a cautionary note. *Cancer Res* **49**:5870-5878
- Kelekar, A. and Thompson, C. B. (1998) Bcl-2-family proteins: the role of the BH3 domain in apoptosis. *Trends Cell Biol* **8**:324-330

- Kerr, J. F. R. (1971) Shrinkage necrosis: a distinct mode of cellular death. *J Path* **105**:13-20
- Kerr, J. F., Wyllie, A. H. and Currie, A. R. (1972) Apoptosis: a basic biological phenomenon with wide-ranging implications in tissue kinetics. *Br J Cancer* **26**:239-257
- Keyes, W. M. and Sanders, E. J. (1999) Cell death in the endocardial cushions of the developing heart. *J Mol Cell Cardiol* **31**:1015-1023
- Khaled, A. R., Kim, K., Hofmeister, R., Muegge, K. and Durum, S. K. (1999) Withdrawal of IL-7 induces Bax translocation from cytosol to mitochondria through a rise in intracellular pH. *Proc Natl Acad Sci U S A* **96**:14476-14481
- Kiefer, M. C., Brauer, M. J., Powers, V. C., Wu, J. J., Umansky, S. R., Tomei, L. D. and Barr, P. J. (1995) Modulation of apoptosis by the widely distributed Bcl-2 homologue Bak. *Nature* **374**:736-739
- Kim, R. Y., Robertson, E. J. and Solloway, M. J. (2001) Bmp6 and Bmp7 are required for cushion formation and septation in the developing mouse heart. *Dev Biol* **235**:449-466
- Kimura, N., Matsuo, R., Shibuya, H., Nakashima, K. and Taga, T. (2000) BMP2-induced apoptosis is mediated by activation of the TAK1-p38 kinase pathway that is negatively regulated by Smad6. *J Biol Chem* **275**:17647-17652
- Kirby, M. L. (1999) Contribution of Neural Crest to Heart and Vessel Morphology. *Heart Development, Academic Press, editors R.P. Harvey and N. Rosenthal* :p179-193
- Kirby, M. L. (1997) The Heart. *Embryos, Genes and Birth Defects. Wiley and Sons Ltd. Edited by P. Thorogood*
- Kirby, M. L. (1989) Plasticity and predetermination of mesencephalic and trunk neural crest transplanted into the region of the cardiac neural crest. *Dev Biol* **134**:402-412
- Kirby, M. L., Gale, T. F. and Stewart, D. E. (1983) Neural crest cells contribute to aorticpulmonary septation. *Science* **220**:1059-1061

- Kirby, M. L., Turnage, K. L. and Hays, B. M. (1985) Characterization of conotruncal malformations following ablation of "cardiac" neural crest. *Anat. Rec.* **213**:87-93
- Kirby, M. L. and Waldo, K. L. (1995) Neural crest and cardiovascular patterning. *Circ. Res.* **77**:211-215
- Kirby, M. L. and Waldo, K. L. (1990) Role of neural crest in congenital heart disease. *Circulation* **82**:332-430
- Knudson, C. M., Tung, K. S., Tourtellotte, W. G., Brown, G. A. and Korsmeyer, S. J. (1995) Bax-deficient mice with lymphoid hyperplasia and male germ cell death. *Science* **270**:96-99
- Krajewski, S., Tanaka, S., Takayama, S., Schibler, M. J., Fenton, W. and Reed, J. C. (1993) Investigation of the subcellular distribution of the bcl-2 oncoprotein: residence in the nuclear envelope, endoplasmic reticulum, and outer mitochondrial membranes. *Cancer Res* **53** :4701-4714
- Krammer, P. H. (2000) CD95's deadly mission in the immune system. *Nature* **407**:789-795
- Kroemer, G., Zamzami, N. and Susin, S. A. (1997) Mitochondrial control of apoptosis. *Immunol Today* **18**:44-51
- Krug, E. L., Runyan, R. B. and Markwald, R. R. (1985) Protein extracts from early embryonic hearts initiate cardiac endothelial cytodifferentiation. *Dev Biol* **112**:414-426
- Kubalak, S. W. and Sucov, H. M. (1999) Retinoids in Heart Development. *Heart Development, Academic Press, editors R.P. Harvey and N. Rosenthal* :209-219
- Kuida, K., Haydar, T. F., Kuan, C. Y., Gu, Y., Taya, C., Karasuyama, H., Su, M. S., Rakic, P. and Flavell, R. A. (1998) Reduced apoptosis and cytochrome c-mediated caspase activation in mice lacking caspase 9. *Cell* **94**:325-337
- Kuo, C. T., Morrissey, E. E., Anandappa, R., Sigrist, K., Lu, M. M., Parmacek, M. S.,

- Soudais, C. and Leiden, J. M. (1997) GATA4 transcription factor is required for ventral morphogenesis and heart tube formation. *Genes Dev* **11**:1048-1060
- Lamers, W.H. , Viragh, S., Wessels, A., Moorman, A. F. M. and Anderson, R. H. (1995) Formation of the tricuspid valve in the human heart. *Circ.* **91**:111-121
- Le Lievre, C. S. and Le Douarin, N. M. (1975) Mesenchymal derivatives of the neural crest: analysis of chimaeric quail and chick embryos. *J Embryol Exp Morphol* **34**:125-154
- Leussink, B., Brouwer, A., el Khattabi, M., Poelmann, R. E., Gittenberger-de Groot, A. C. and Meijlink, F. (1995) Expression patterns of the paired-related homeobox genes MHOX/Prx1 and S8/Prx2 suggest roles in development of the heart and the forebrain. *Mech Dev* **52**:51-64
- Levin, M., Johnson, R. L., Stern, C. D., Kuehn, M. and Tabin, C. (1995) A molecular pathway determining left-right asymmetry in chick embryogenesis. *Cell* **82**:803-814
- Li, H., Zhu, H., Xu, C. J. and Yuan, J. (1998) Cleavage of BID by caspase 8 mediates the mitochondrial damage in the Fas pathway of apoptosis. *Cell* **94**:491-501
- Li, Q. Y., Newbury-Ecob, R. A., Terrett, J. A., Wilson, D. I., Curtis, A. R., Yi, C. H., Gebuhr, T., Bullen, P. J., Robson, S. C., Strachan, T., Bonnet, D., Lyonnet, S., Young, I. D., Raeburn, J. A., Buckler, A. J., Law, D. J. and Brook, J. D. (1997) Holt-Oram syndrome is caused by mutations in TBX5, a member of the Brachyury (T) gene family. *Nat Genet* **15**:21-29
- Lin, Q., Schwarz, J., Bucana, C. and Olson, E. N. (1997) Control of mouse cardiac morphogenesis and myogenesis by transcription factor MEF2C. *Science* **276**:1404-1407
- Lincz, L. F. (1998) Deciphering the apoptotic pathway: All roads lead to death. *Immunol Cell Biol* **76**:1-19
- Lindahl, T. (1995) Recognition and processing of damaged DNA. *J Cell Sci Suppl* **19**:73-77.

- Lints, T. J., Parsons, L. M., Hartley, L., Lyons, I. and Harvey, R. P. (1993) Nkx-2.5: a novel murine homeobox gene expressed in early heart progenitor cells and their myogenic descendants. *Development* **119**:419-431
- Little, C. D., Piquet, D. M., Davis, L. A., Walters, L. and Drake, C. J. (1989) Distribution of laminin, collagen type IV, collagen type I, and fibronectin in chicken cardiac jelly/basement membrane. *Anat Rec* **224**:417-425
- Liu, X., Kim, C. N., Yang, J., Jemmerson, R. and Wang, X. (1996) Induction of apoptotic program in cell-free extracts: requirement for dATP and cytochrome c. *Cell* **12**:147-157
- Liu, X., Zou, H., Slaughter, C. and Wang, X. (1997) DFF, a heterodimeric protein that functions downstream of caspase-3 to trigger DNA fragmentation during apoptosis. *Cell* **89**
- Loeber, C. P. and Runyan, R. B. (1990) A comparison of fibronectin, laminin, and galactosyltransferase adhesion mechanisms during embryonic cardiac mesenchymal cell migration in vitro. *Dev Biol* **140**:401-412
- Logan, C. and Francis-West, P. (1999) Gene transfer in avian embryos using replication-competent retroviruses. *Methods Mol. Biol.* **97**:539-551
- Lorenz, H. M., Herrmann, M., Winkler, T., Gaipl, U. and Kalden, J. R. (2000) Role of apoptosis in autoimmunity. *Apoptosis* **5**:443-449
- Lyons, K. M., Pelton, R. W. and Hogan, B. L. (1990) Organogenesis and pattern formation in the mouse: RNA distribution patterns suggest a role for bone morphogenetic protein-2A (BMP-2A). *Development* **109**:833-844
- Majumder, K. and Overbeek, P. A. (1999) Left-Right Asymmetry and Cardiac Looping. *Heart Development, Academic Press, editors R.P. Harvey and N. Rosenthal* :391-402
- Manner, J. (2000) Cardiac looping in the chick embryo: a morphological review with special reference to terminological and biomechanical aspects of the looping process. *Anat Rec* **259**:248-262

- Markwald, R. R., Fitzharris, T. P. and Manasek, F. J. (1977) Structural development of endocardial cushions. *Am J Anat* **148**:85-119
- Markwald, R. R., Mjaatvedt, C. H., Krug, E. L. and Sinning, A. R. (1990) Inductive interactions in heart development. *Ann. N.Y. Acad. Sci.* **588**:13-25
- Martinez-Alvarez, C., Tudela, C., Perez-Miguelsanz, J., O'Kane, S., Puerta, J. and Ferguson, M. W. (2000) Medial edge epithelial cell fate during palatal fusion. *Dev Biol* **220**:343-357
- Martins, L. M. and Earnshaw, W. C. (1997) Apoptosis: Alive and kicking in 1997. *Trends Cell Biol* **7**:111-114
- Massague, J. (1996) TGFbeta signaling: receptors, transducers, and Mad proteins. *Cell* **85**:947-50
- Massague, J. and Weis-Garcia, F. (1996) Serine/threonine kinase receptors: mediators of transforming growth factor beta family signals. *Cancer Surv* **27**:41-64
- Mattson, M. P. (2000) Apoptosis in neurodegenerative disorders. *Nat Rev Mol Cell Biol* **1**:120-129
- Mattson, M. P., Duan, W., Pederson, W. A. and Culmsee, C. (2001) Neurodegenerative disorders and ischemic brain diseases. *Apoptosis* **6**:69-81
- McDonnell, J. M., Fushman, D., Milliman, C. L., Korsmeyer, S. J. and Cowburn, D. (1999) Solution structure of the proapoptotic molecule BID: a structural basis for apoptotic agonists and antagonists. *Cell* **96**:625-634
- McGinnis, K. M., Gnegy, M. E., Park, Y. H., Mukerjee, N. and Wang, K. K. (1999) Procaspase-3 and poly(ADP)ribose polymerase (PARP) are calpain substrates. *Biochem Biophys Res Commun* **263**:94-99
- Meier, P., Finch, A. and Evan, G. (2000) Apoptosis in development. *Nature* **407**:796-801
- Mikawa, T. (1999) Cardiac Lineages. *Heart Development, Academic Press, editors R.P. Harvey and N. Rosenthal* :p19-33

- Millan, F. A., Denhez, F., Kondaiiah, P. and Akhurst, R. J. (1991) Embryonic gene expression patterns of TGF beta 1, beta 2 and beta 3 suggest different developmental functions in vivo. *Development* **111**:131-143
- Miyashita, T. and Reed, J. C. (1995) Tumor suppressor p53 is a direct transcriptional activator of the human bax gene. *Cell* **80**:293-299
- Mjaatvedt, C. H., Nakaoka, T., Moreno-Rodriguez, R., Norris, R. A., Kern, M. J., Eisenberg, C. A., Turner, D. and Markwald, R. R. (2001) The outflow tract of the heart is recruited from a novel heart-forming field. *Dev Biol* **238**:97-109
- Mjaatvedt, C. H., Yamamura, H., Wessels, A., Ramsdell, A., Turner, D. and Markwald, R. R. (1999) Mechanisms of Segmentation, Septation, and Remodeling of the Tubular Heart: Endocardial Cushion Fate and Cardiac Looping. *Heart Development, Academic Press, editors R.P. Harvey and N. Rosenthal p159-177*
- Molkentin, J. D., Lin, Q., Duncan, S. A. and Olson, E. N. (1997) Requirement of the transcription factor GATA4 for heart tube formation and ventral morphogenesis. *Genes Dev* **11**:1061-1072
- Montero, J. A., Ganan, Y., Macias, D., Rodriguez-Leon, J., Sanz-Ezquerro, J. J., Merino, R., Chimal-Monroy, J., Nieto, M. A. and Hurler, J. M. (2001) Role of FGFs in the control of programmed cell death during limb development. *Development* **128**:2075-2084
- Morgan, B. A. and Fekete, D. M. (1996) Manipulating gene expression with replication-competent retroviruses. *Methods Cell Biol* **51**:185-218
- Motoyama, N., Wang, F., Roth, K. A., Sawa, H., Nakayama, K., Nakayama, K., Negishi, I., Senju, S., Zhang, Q., Fujii, S. and et, a. I. (1995) Massive cell death of immature hematopoietic cells and neurons in Bcl-x-deficient mice. *Science* **267**:1506-1510
- Muchmore, S. W., Sattler, M., Liang, H., Meadows, R. P., Harlan, J. E., Yoon, H. S., Nettesheim, D., Chang, B. S., Thompson, C. B., Wong, S. L., Ng, S. L. and Fesik, S. W. (1996) X-ray and NMR structure of human Bcl-xL, an inhibitor of programmed cell death. *Nature* **381**:335-341

- Muhlenbeck, F., Haas, E., Schwenger, R., Schubert, G., Grell, M., Smith, C., Scheurich, P. and Wajant, H. (1998) TRAIL/Apo2L activates c-Jun NH2-terminal kinase (JNK) via caspase-dependent and caspase-independent pathways. *J. Biol. Chem.* **273**:33091-33098
- Muzio, M., Chinnaiyan, A. M., Kischkel, F. C., O'Rourke, K., Shevchenko, A., Ni, J., Scaffidi, C., Bretz, J. D., Zhang, M., Gentz, R., Mann, M., Krammer, P. H., Peter, M. E. and Dixit, V. M. (1996) FLICE, a novel FADD-homologous ICE/CED-3-like protease, is recruited to the CD95 (Fas/APO-1) death--inducing signaling complex. *Cell* **85**:817-827
- Muzio, M., Stockwell, B. R., Stennicke, H. R., Salvesen, G. S. and Dixit, V. M. (1998) An induced proximity model for caspase-8 activation. *J Biol Chem* **273**:2926-2930
- Nakajima, Y., Morishima, M., Nakazawa, M. and Momma, K. (1996) Inhibition of outflow cushion mesenchyme formation in retinoic acid-induced complete transposition of the great arteries. *Cardiovasc Res* **31**:E77-85
- Nakajima, Y., Yamagishi, T., Hokari, S. and Nakamura, H. (2000) Mechanisms involved in valvuloseptal endocardial cushion formation in early cardiogenesis: Roles of transforming growth factor (TGF)-beta and bone morphogenetic protein (BMP). *Anat Rec* **258**:119-127
- Nakajima, Y., Yamagishi, T., Nakamura, H., Markwald, R. R. and Krug, E. L. (1998) An autocrine function for transforming growth factor beta3 in the atrioventricular endocardial cushion tissue. *Ann NY Acad Sci* :857:272-275
- Nakamura, A. and Manasek, F. J. (1981) An experimental study of the relation of cardiac jelly to the shape of the early chick embryonic heart. *J Embryol Exp Morphol* **65**:235-256
- Nechushtan, A., Smith, C. L., Lamensdorf, I., Yoon, S. H. and Youle, R. J. (2001) Bax and Bak coalesce into novel mitochondria-associated clusters during apoptosis. *J Cell Biol* **153**:1265-1276
- Neuhaus, H., Rosen, V. and Thies, R. S. (1999) Heart specific expression of mouse BMP-10 a novel member of the TGF-beta superfamily. *Mech Dev* **80**:181-184

- Nijhawan, D., Honarpour, N. and Wang, X. (2000) Apoptosis in neural development and disease. *Annu Rev Neurosci* **23**:73-87
- Ohtsu, M., Sakai, N., Fujita, H., Kashiwagi, M., Gasa, S., Shimizu, S., Eguchi, Y., Tsujimoto, Y., Sakiyama, Y., Kobayashi, K. and Kuzumaki, N. (1997) Inhibition of apoptosis by the actin-regulatory protein gelsolin. *EMBO J* **16**:4650-4656
- Olson, E. and Srivastava, D. (1996) Molecular pathways controlling heart development. *Science* **272**:671-676
- Oppenheim, R. W. (1991) Cell death during development of the nervous system. *Annu Rev Neurosci* **14**:453-4501
- Orth, K., Chinnaiyan, A. M., Garg, M., Froelich, C. J. and Dixit, V. M. (1996) The CED/ICE-like protease Mch2 is activated during apoptosis, and cleaves the death substrate lamin A. *J.B.C.* **271**:16443-16446
- Parton, M., Dowsett, M. and Smith, I. (2001) Studies of apoptosis in breast cancer. *BMJ* **322**:1528-1532
- Pexieder, T (1975) Cell death in the morphogenesis and teratogenesis of the heart. *Adv. Anat. Embryol. Cell Biol.* **51**:1-100
- Pexieder, T (1972) The tissue dynamics of heart morphogenesis I. The phenomena of cell death A. Identification and morphology. *Z. Anat. Entwickl.-Gesch.* **137**:270-284
- Poelmann, R. E. and Gittenberger-de-Groot, A. C (1999) A subpopulation of apoptosis-prone cardiac neural crest cells targets to the venous pole: multiple functions in heart development? *Dev. Biol.* **207**:271-286
- Poelmann, R. E., Mikawa, T. and Gittenberger-De Groot, A. C. (1998) Neural crest cells in outflow tract septation of the embryonic chicken heart: Differentiation and apoptosis. *Dev Dyn* **212**:373-384
- Poelmann, R. E., Molin, D., Wisse, L. J. and Gittenberger-de Groot, A. C. (2000) Apoptosis in cardiac development. *Cell Tissue Res.* **301**:43-52

- Potts, J. D., Dagle, J. M., Walder, J. A., Weeks, D. L. and Runyan, R. B. (1991) Epithelial-mesenchymal transformation of embryonic cardiac endothelial cells is inhibited by a modified antisense oligodeoxynucleotide to transforming growth factor beta 3. *Proc Natl Acad Sci U S A* **88**:1516-1520
- Pugazhenthii, S., Nesterova, A., Sable, C., Heidenreich, K. A., Boxer, L. M., Heasley, L. E. and Reusch, J. E. (2000) Akt/protein kinase B up-regulates Bcl-2 expression through cAMP-response element-binding protein. *J Biol Chem* **275**:10761-10766
- Raff, M. C. (1992) Social controls on cell survival and cell death. *Nature* **356**:397-400
- Ramsdell, A. F. and Markwald, R. R. (1997) Induction of endocardial cushion tissue in the avian heart is regulated, in part, by TGF β -3-mediated autocrine signaling. *Dev. Biol.* **188**:64-74
- Ranganath, R. M. and Nagashree, N. R. (2001) Role of programmed cell death in development. *Int Rev Cytol* **202**:159-242
- Ranger, A. M., Grusby, M. J., Hodge, M. R., Gravallesse, E. M., de la Brousse, F. C., Hoey, T., Mickanin, C., Baldwin, H. S. and Glimcher, L. H. (1998) The transcription factor NF-ATc is essential for cardiac valve formation. *Nature* **392**:186-190
- Reed, J. C. (1997) Double identity for proteins of the Bcl-2 family. *Nature* **387**:773-776
- Renehan, A. G., Bach, S. P. and Potten, C. S. (2001) The relevance of apoptosis for cellular homeostasis and tumorigenesis in the intestine. *Can J Gastroenterol* **15**:166-76
- Robertson, J. D., Orrenius, S. and Zhivotovsky, B. (2000) Review: nuclear events in apoptosis. *J Struct Biol* **129**:346-58. 346-58.
- Romanoff, A. L. (1960) "*The Avian Embryo - Structural and Functional Development*" The Macmillan Company. Chapter 9
- Rongish, B. J., Drake, C. J., Argraves, W. S. and Little, C. D. (1998) Identification of the developmental marker, JB3-antigen, as fibrillin-2 and its de novo organization into embryonic microfibrillar arrays. *Dev Dyn* **212**:461-471

- Rosenquist, G. C. and DeHaan, R. L. (1966) Migration of precardiac cells in the chick embryo. *Carnegie Inst. Wash. Contrib. Embryol.* **38**:111-121
- Ross, A. J., Waymire, K. G., Moss, J. E., Parlow, A. F., Skinner, M. K., Russell, L. D. and MacGregor, G. R. (1998) Testicular degeneration in Bclw-deficient mice. *Nat Genet* **18**:251-256
- Runyan, R. B. and Markwald, R. R. (1983) Invasion of mesenchyme into three-dimensional collagen gels: a regional and temporal analysis of interaction in embryonic heart tissue. *Dev Biol* **95**:108-114
- Sachs, L. M., Abdallah, B., Hassan, A., Levi, G., De Luze, A., Reed, J. C. and Demeneix, B. A. (1997) Apoptosis in *Xenopus* tadpole tail muscles involves Bax-dependent pathways. *FASEB J* **11**:801-808
- Salvesen, G. S. and Dixit, V. M. (1999) Caspase activation: The induced-proximity model. *Proc Natl Acad Sci USA* **96**:10964-10967
- Sanders, E. J. and Wride, M. A. (1995) Programmed cell death in development. *Int. Rev. Cytol.* **163**:105-173
- Satoh, M. S. and Lindahl, T. (1992) Role of poly(ADP-ribose) formation in DNA repair. *Nature* **356**:356-358
- Sattler, M., Liang, H., Nettesheim, D., Meadows, R. P., Harlan, J. E., Eberstadt, M., Yoon, H. S., Shuker, S. B., Chang, B. S., Minn, A. J., Thompson, C. B. and Fesik, S. W. (1997) Structure of Bcl-xL-Bak peptide complex: recognition between regulators of apoptosis. *Science* **275**:983-986
- Saunders, J. W. Jr (1966) Death in embryonic systems. *Science* **154**:604-612
- Savill, J. and Fadok, V. (2000) Corpse clearance defines the meaning of cell death. *Nature* **407**:784-788
- Schmidt, C., Christ, B., Patel, K. and Brand-Saberi, B. (1998) Experimental induction of BMP-4 expression leads to apoptosis in the paraxial and lateral plate mesoderm.

- Schmitz, I., Kirchoff, S. and Krammer, P. H. (2000) Regulation of death receptor-mediated apoptosis pathways. *Int J Biochem Cell Biol* **32**:1123-1136
- Schultheiss, T. M., Burch, J. B. and Lassar, A. B. (1997) A role for bone morphogenetic proteins in the induction of cardiac myogenesis. *Genes Dev* **11**:451-462
- Schultheiss, T. M. and Lassar, A. B. (1997) Induction of chick cardiac myogenesis by bone morphogenetic proteins. *Cold Spring Harb Symp Quant Biol* **62**:413-419
- Schultheiss, T. M. and Lassar, A. B. (1999) Vertebrate Heart Induction. *Heart Development, Academic Press, editors R.P. Harvey and N. Rosenthal* :p52-62
- Schultheiss, T. M., Xydas, S. and Lassar, A. B. (1995) Induction of avian cardiac myogenesis by anterior endoderm. *Development* **121**:4203-4214
- Schwarze, S. R., Ho, A., Vocero-Akbani, A. and Dowdy, S. F. (1999) In vivo protein transduction: delivery of a biologically active protein into the mouse. *Science* **285**:1569-1572
- Sedmera, D., Pexieder, T., Hu, N. and Clark, E. B. (1997) Developmental changes in the myocardial architecture of the chick. *Anat Rec* **248**:421-432
- Shimizu, S., Ide, T., Yanagida, T. and Tsujimoto, Y. (2000) Electrophysiological study of a novel large pore formed by Bax and the voltage-dependent anion channel that is permeable to cytochrome C. *J. Biol. Chem.* **275**:12321-12325
- Shimizu, S., Narita, M. and Tsujimoto, Y. (1999) Bcl-2 family proteins regulate the release of apoptogenic cytochrome c by the mitochondrial channel VDAC. *Nature* **399**:483-487
- Shimizu, S. and Tsujimoto, Y. (2000) Proapoptotic BH3-only Bcl-2 family members induce cytochrome c release, but not mitochondrial membrane potential loss, and do not directly modulate voltage-dependent anion channel activity. *Proc Natl Acad Sci USA* **97**:577-582

- Slee, E. A., Harte, M. T., Kluck, R. M., Wolf, B. B., Casiano, C. A., Newmeyer, D. D., Wang, H. G., Reed, J. C., Nicholson, D. W., Alnemri, E. S., Green, D. R. and Martin, S. J. (1999) Ordering the cytochrome c-initiated caspase cascade: Hierarchical activation of caspases-2, -3, -6, -7, -8, and -10 in a caspase-9-dependent manner. *J Cell Biol* **144**:281-292
- Song, Q., Lees-Miller, S. P., Kumar, S., Zhang, Z., Chan, D. W., Smith, G. C., Jackson, S. P., Alnemri, E. S., Litwack, G., Khanna, K. K. and Lavin, M. F. (1996) DNA-dependent protein kinase catalytic subunit: a target for an ICE-like protease in apoptosis. *EMBO J* **1**:3238-3246
- Song, W., Jackson, K. and McGuire, P. G. (2000) Degradation of type IV collagen by matrix metalloproteinases is an important step in the epithelial-mesenchymal transformation of the endocardial cushions. *Dev Biol* **227**:606-617
- Spence, S. G., Argraves, W. S., Walters, L., Hungerford, J. E. and Little, C. D. (1992) Fibulin is localized at sites of epithelial-mesenchymal transitions in the early avian embryo. *Dev Biol* **151**:473-484
- Srivastava, D. and Olson, E. N. (2000) A genetic blueprint for cardiac development. *Nature* **407**:221-226
- Srivastava, D., Thomas, T., Lin, Q., Kirby, M. L., Brown, D. and Olson, E. N. (1997) Regulation of cardiac mesodermal and neural crest development by the bHLH transcription factor, dHAND. *Nat Genet* **16**:154-160
- Susin, S. A., Zamzami, N. and Kroemer, G. (1998) Mitochondria as regulators of apoptosis: doubt no more. *Biochim Biophys Acta Bio-Energetics* **1366**:151-165
- Swartz, M., Eberhart, J., Mastick, G. S. and Krull, C. E. (2001) Sparking new frontiers: using in vivo electroporation for genetic manipulations. *Dev Biol* **233**:13-21
- Takahashi, A., Alnemri, E. S., Lazebnik, Y. A., Fernandes-Alnemri, T., Litwack, G., Moir, R. D., Goldman, R. D., Poirier, G. G., Kaufmann, S. H. and Earnshaw, W. C. (1996) Cleavage of lamin A by Mch2 alpha but not CPP32: multiple interleukin 1 beta-converting enzyme-related proteases with distinct substrate recognition properties are active in apoptosis. *Proc Natl Acad Sci U S A* **93**:8395-400

- Takeda, K., Yu, Z. X., Nishikawa, T., Tanaka, M., Hosoda, S., Ferrans, V. J. and Kasajima, T. (1996) Apoptosis and DNA fragmentation in the bulbus cordis of the developing rat heart. *J Mol Cell Cardiol* **28**:209-215
- Tang, D. and Kidd, V. J. (1998) Cleavage of DFF-45/ICAD by multiple caspases is essential for its function during apoptosis. *J Biol Chem* **273**:28549-28552
- Tewari, M., Quan, L. T., O'Rourke, K., Desnoyers, S., Zeng, Z., Beidler, D. R., Poirier, G. G., Salvesen, G. S. and Dixit, V. M. (1995) Yama/CPP32 beta, a mammalian homolog of CED-3, is a CrmA-inhibitable protease that cleaves the death substrate poly(ADP-ribose) polymerase. *Cell* **2**:801-809
- Thornberry, N. A. and Lazebnik, Y. (1998) Caspases: Enemies within. *Science* **281**:1312-1316
- Thornberry, N. A., Ranon, T. A., Pieterse, E. P., Rasper, D. M., Timkey, T., Garcia-Calvo, M., Houtzager, V. M., Nordstrom, P. A., Roy, S., Vaillancourt, J. P., Chapman, K. T. and Nicholson, D. W. (1997) A combinatorial approach defines specificities of members of the caspase family and granzyme B - Functional relationships established for. *J Biol Chem* **272**:17907-17911
- Todd, J. L., Silverman, M. E., Kirby, M. L., Gray, S. W. and Skandalakis, J. E. (1994) Chapter 26; The Heart. *Embryology for Surgeons: Baltimore Press, Williams and Wilkins*
- Tone, S., Tanaka, S., Minatogawa, Y. and Kido, R. (1994) DNA fragmentation during the programmed cell death in the chick limb buds. *Exp. Cell Res.* **215**:234-236
- Tsuda, T., Wang, H., Timpl, R. and Chu, M. L. (2001) Fibulin-2 expression marks transformed mesenchymal cells in developing cardiac valves, aortic arch vessels, and coronary vessels. *Dev Dyn* **222**:89-100
- Tsujimoto, Y. and Croce, C. M. (1986) Analysis of the structure, transcripts, and protein products of bcl-2, the gene involved in human follicular lymphoma. *Proc. Natl. Acad. Sci. USA.* **83**:5214-5218
- Tsujimoto, Y. and Shimizu, S. (2000a) Bcl-2 family: Life-or-death switch. *FEBS Lett* **466**:6-10

- Tsujimoto, Y. and Shimizu, S. (2000b) VDAC regulation by the Bcl-2 family of proteins. *Cell Death Differ* **7**:1174-1181
- Van den Hoff, M. J. B., Moorman, A. F. M., Ruijter, J. M., Lamers, W. H., Bennington, R. W., Markwald, R. R. and Wessels, A. (1999) Myocardialization of the cardiac outflow tract. *Dev Biol* **212**:477-490
- Van den Hoff, M. J. B., Van den Eijnde, S. M., Viragh, S. and Moorman, A. F. M. (2000) Programmed cell death in the developing heart. *Cardiovasc Res* **45**:603-620
- Varfolomeev, E. E., Schuchmann, M., Luria, V., Chiannikulchai, N., Beckmann, J. S., Mett, I. L., Rebrikov, D., Brodianski, V. M., Kemper, O. C., Kollet, O., Lapidot, T., Soffer, D., Sobe, T., Avraham, K. B., Goncharov, T., Holtmann, H., Lonai, P. and Wallach, D. (1998) Targeted disruption of the mouse Caspase 8 gene ablates cell death induction by the TNF receptors, Fas/Apo1, and DR3 and is lethal prenatally. *Immunity* **9**:267-276
- Varley, J. E., McPherson, C. E., Zou, H., Niswander, L. and Maxwell, G. D. (1998) Expression of a constitutively active type I BMP receptor using a retroviral vector promotes the development of adrenergic cells in neural crest cultures. *Dev Biol* **196**:107-118
- Vaux, D. L. and Korsmeyer, S. J. (1999) Cell death in development. *Cell* **96**:245-254
- Veis, D. J., Sorenson, C. M., Shutter, J. R. and Korsmeyer, S. J. (1993) Bcl-2-deficient mice demonstrate fulminant lymphoid apoptosis, polycystic kidneys, and hypopigmented hair. *Cell* **75**:229-240
- Velkey, J. M. and Bernanke, D. H. (2001) Apoptosis during coronary artery orifice development in the chick embryo. *Anat Rec* **262**:310-317
- Vermes, I., Haanen, C., Steffens-Nakken, H. and Reutelingsperger, C. (1995) A novel assay for apoptosis. Flow cytometric detection of phosphatidylserine expression on early apoptotic cells using fluorescein labelled Annexin V. *J Immunol Methods* **184**:39-51
- Villa, P., Kaufmann, S. H. and Earnshaw, W. C. (1997) Caspases and caspase inhibitors. *Trends Biochem Sci* **22**:388-393

- Waldo, K., Miyagawa-Tomita, S., Kumiski, D. and Kirby, M. L. (1998) Cardiac neural crest cells provide new insight into septation of the cardiac outflow tract: aortic sac to ventricular septal closure. *Dev. Biol.* **196**:129-144
- Walker, N. I., Harmon, B. V., Gobe, G. C. and Kerr, J. F. (1988) Patterns of cell death. *Methods Achiev Exp Pathol* **13**:18-54
- Walker, P. R. and Sikorska, M. (1997) New aspects of the mechanism of DNA fragmentation in apoptosis. *Biochem Cell Biol* **75**:287-299
- Wallach, D. (1997) Cell death induction by TNF: a matter of self control. *TIBS* **22**:107-109
- Wang, J. and Lenardo, M. J. (2000) Roles of caspases in apoptosis, development, and cytokine maturation revealed by homozygous gene deficiencies. *J Cell Sci* **113**:753-757
- Wang, X., Zelenski, N. G., Yang, J., Sakai, J., Brown, M. S. and Goldstein, J. L. (1996) Cleavage of sterol regulatory element binding proteins (SREBPs) by CPP32 during apoptosis. *EMBO J.* **15**:1012-1020
- Wang, Z. H., Ding, M. X., Chew-Cheng, S. B., Yun, J. P. and Chew, E. C. (1999) Bcl-2 and Bax proteins are nuclear matrix associated proteins. *Anticancer Res* **19**:5445-5449
- Wang, Z. Q., Auer, B., Stingl, L., Berghammer, H., Haidacher, D., Schweiger, M. and Wagner, E. F. (1995) Mice lacking ADPRT and poly(ADP-ribosylation) develop normally but are susceptible to skin disease. *Genes Dev* **9**:509-520
- Watanabe, M., Choudhry, A., Berlan, M., Singal, A., Siwik, E., Mohr, S. and Fisher, S. A. (1998) Developmental remodeling and shortening of the cardiac outflow tract involves myocyte programmed cell death. *Development* **125**:3809-3820
- Webb, S., Brown, N. A. and Anderson, R. H. (1998) Formation of the atrioventricular septal structures in the normal mouse. *Circ. Res.* **82**:645-656

- Weil, M., Jacobson, M. D., Coles, H. S., Davies, T. J., Gardner, R. L., Raff, K. D. and Raff, M. C. (1996) Constitutive expression of the machinery for programmed cell death. *J Cell Biol* **133** :1053-1059
- Weil, M., Jacobson, M. D. and Raff, M. C. (1997) Is Programmed cell Death Required for Neural Tube Closure? *Curr. Biol.* **7**:281-284
- Wessels, A., Markman, M. W. M., Vermeulen, J. L. M., Anderson, R. H., Moorman, A. F. M. and Lamers, W. H. (1996) The development of the atrioventricular junction in the human heart. *Circ. Res.* **78**:110-117
- White, M. K. and McCubrey, J. A. (2001) Suppression of apoptosis: role in cell growth and neoplasia. *Leukemia* **15**:1011-1021
- Wolter, K. G., Hsu, Y. T., Smith, C. L., Nechushtan, A., Xi, X. G. and Youle, R. J. (1997) Movement of Bax from the cytosol to mitochondria during apoptosis. *J Cell Biol* **139**:1281-1292
- Wride, M. A., Parker, E. and Sanders, E. J. (1999) Members of the bcl-2 and caspase families regulate nuclear degeneration during chick lens fibre differentiation. *Dev Biol* **213**:142-156
- Wunsch, A. M., Little, C. D. and Markwald, R. R. (1994) Cardiac endothelial heterogeneity defines valvular development as demonstrated by the diverse expression of JB3, an antigen of the endocardial cushion tissue. *Dev. Biol.* **165**:585-601
- Wyllie, A. H. (1980) Glucocorticoid-induced thymocyte apoptosis is associated with endogenous endonuclease activation. *Nature* **284**:555-556
- Wyllie, A. H., Beattie, G. J. and Hargreaves, A. D. (1981) Chromatin changes in apoptosis. *Histochem J.* **13**:681-692
- Wyllie, A. H., Kerr, J. F. R. and Currie, A. R. (1980) Cell death: the significance of apoptosis. *Int. Rev. Cytol.* **68**:251-305
- Ya, J., van den Hoff, M. J. B., de Boer, P. A. J., Tesink-Taekema, S., Franco, D., Moorman, A. F. M. and Lamers, W. H. (1998) Normal development of the

outflow tract in the rat. *Circ. Res.* **82**:464-472

- Yamada, M., Revelli, J. P., Eichele, G., Barron, M. and Schwartz, R. J. (2000) Expression of chick Tbx-2, Tbx-3, and Tbx-5 genes during early heart development: evidence for BMP2 induction of Tbx2. *Dev Biol* **228**:95-105
- Yamagishi, T., Nakajima, Y., Miyazono, K. and Nakamura, H. (1999b) Bone morphogenetic protein-2 acts synergistically with transforming growth factor-beta3 during endothelial-mesenchymal transformation in the developing chick heart. *J Cell Physiol* **180**:35-45
- Yamagishi, T., Nakajima, Y. and Nakamura, H. (1999a) Expression of TGFbeta3 RNA during chick embryogenesis: a possible important role in cardiovascular development. *Cell Tissue Res* **298**:85-93
- Yamagishi, T., Nakajima, Y., Sampath, T. K., Miyazono, K. and Nakamura, H. (1998) Bone morphogenetic protein 2 acts synergistically with transforming growth factor beta 3 in endothelial-mesenchymal cell transformation during chick heart development. *Ann N Y Acad Sci* **857** :276-278
- Yang, J., Liu, X. S., Bhalla, K., Kim, C. N., Ibrado, A. M., Cai, J. Y., Peng, T. I., Jones, D. P. and Wang, X. D. (1997) Prevention of apoptosis by Bcl-2: Release of cytochrome c from mitochondria blocked. *Science* **275**:1129-1132
- Yatskievych, T. A., Ladd, A. N. and Antin, P. B. (1997) Induction of cardiac myogenesis in avian pregastrula epiblast: The role of the hypoblast and activin. *Development* **124**:2561-2570
- Yeh, W. C., De la Pompa, J. L., McCurrach, M. E., Shu, H. B., Elia, A. J., Shahinian, A., Ng, M., Wakeham, A., Khoo, W., Mitchell, K., El-Deiry, W. S., Lowe, S. W., Goeddel, D. V. and Mak, T. W. (1998) FADD: Essential for embryo development and signaling from some, but not all, inducers of apoptosis. *Science* **279**:1954-1958
- Yeh, W. C., Itie, A., Elia, A. J., Ng, M., Shu, H. B., Wakeham, A., Mirtsos, C., Suzuki, N., Bonnard, M., Goeddel, D. V. and Mak, T. W. (2000) Requirement for Casper (c-FLIP) in Regulation of death receptor-induced apoptosis and embryonic development. *Immunity* **12**:633-642

Yokouchi, Y., Sakiyama, J., Kameda, T., Iba, H., Suzuki, A., Ueno, N. and Kuroiwa, A. (1996) BMP-2/-4 mediate programmed cell death in chicken limb buds. *Development* **122**:3725-3734

Yoshida, H., Kong, Y. Y., Yoshida, R., Elia, A. J., Hakem, A., Hakem, R., Penninger, J. M. and Mak, T. W. (1998) Apaf1 is required for mitochondrial pathways of apoptosis and brain development. *Cell* **94**:739-750

Yuan, J. and Horvitz, H. R. (1992) The *Caenorhabditis elegans* cell death gene *ced-4* encodes a novel protein and is expressed during the period of extensive programmed cell death. *Development* **116**:309-320

Yuan, J., Shaham, S., Ledoux, S., Ellis, H. M. and Horvitz, H. R. (1993) The *C. elegans* cell death gene *ced-3* encodes a protein similar to mammalian interleukin-1 beta-converting enzyme. *Cell* **75**:641-652

Yutzey, K. E. and Bader, D. (1995) Diversification of cardiomyogenic cell lineages during early heart development. *Circ. Res.* **77**:216-219

Zha, J., Harada, H., Osipov, K., Jockel, J., Waksman, G. and Korsmeyer, S. J. (1997) BH3 domain of BAD is required for heterodimerization with BCL-XL and proapoptotic activity. *J Biol Chem* **272**:24101-24104

Zha, J., Harada, H., Yang, E., Jockel, J. and Korsmeyer, S. J. (1996) Serine phosphorylation of death agonist BAD in response to survival factor results in binding to 14-3-3 not BCL-X(L). *Cell* **87**:619-628

Zhang, H. Y., Chu, M. L., Pan, T. C., Sasaki, T., Timpl, R. and Ekblom, P. (1995) Extracellular matrix protein fibulin-2 is expressed in the embryonic endocardial cushion tissue and is a prominent component of valves in adult heart. *Dev Biol* **167**:18-26

Zhang, H. and Bradley, A. (1996) Mice deficient for BMP2 are nonviable and have defects in amnion/chorion and cardiac development. *Development* **122**:2977-2986

Zhang, J. H. and Xu, M. (2000) DNA fragmentation in apoptosis. *Cell Res* **10**:205-11

Zhang, J., Cado, D., Chen, A., Kabra, N. H. and Winoto, A. (1998) Fas-mediated

apoptosis and activation-induced T-cell proliferation are defective in mice lacking FADD/Mort1. *Nature* **392**:296-300

Zhang, Z., Yu, X., Zhang, Y., Geronimo, B., Lovlie, A., Fromm, S. H. and Chen, Y. (2000) Targeted misexpression of constitutively active BMP receptor-IB causes bifurcation, duplication, and posterior transformation of digit in mouse limb. *Dev Biol* **220**:154-167

Zhao, Z. Y. and Rivkees, S. A. (2000) Programmed cell death in the developing heart: Regulation by BMP4 and FGF2. *Dev Dyn* **217**:388-400

Zou, H., Henzel, W. J., Liu, X., Lutschg, A. and Wang, X. (1997) Apaf-1, a human protein homologous to *C.elegans* CED-4, participates in cytochrome c-dependent activation of caspase-3. *Cell* **90**:405-413

Zou, H., Li, Y. C., Liu, H. S. and Wang, X. D. (1999) An APAF-1 cytochrome c multimeric complex is a functional apoptosome that activates procaspase-9. *J Biol Chem* **274**:11549-11556

Zou, H. and Niswander, L. (1996) Requirement for BMP signaling in interdigital apoptosis and scale formation. *Science* **272**:738-741

Zou, H., Wieser, R., Massague, J. and Niswander, L. (1997) Distinct roles of type I bone morphogenetic protein receptors in the formation and differentiation of cartilage. *Genes Dev* **11**:2191-2203